Synthesis and Circularly Polarised Luminescence of Helically Chiral 4,4-difluoro-4-bora-3a,4a-diaza-s-indacenes (BODIPYs)

by

Rebecca Grace Clarke

A thesis submitted in partial fulfilment of the requirements for the degree of

Doctor of Philosophy

Newcastle University

February 2020

Firstly I would like to thank my PhD supervisor Dr Michael Hall. It is difficult to accurately summarise all of the ways in which he has helped to shape me into the researcher that I am, but to put it briefly, I have been set an excellent example to follow. It is needless to say that without his guidance, patience and support this thesis would not have been written. I consider myself to be very fortunate to have worked under his supervision, and I would like to thank him for giving me this opportunity.

I would also like to thank all MJH group members past and present who have worked alongside me. Particularly I would like to thank Dr Andrew Tyler, who must have answered the question: 'which column should I use for this?' at least daily when I first joined the group. So thank you Andrew, for your patience and friendship. My thanks is also extended to those who have worked in the Johnston Lab over the course of the last four years, for creating such an enjoyable working environment.

There are a number of collaborators who have made a direct contribution to this work, including: Professor Wouter Herrebout and Jonathan Bogaerts who have performed the ECD spectroscopy and associated calculations; Dr Robert Pal and Dr Lewis Mackenzie who have performed the CPL spectroscopy; Dr Thomas Penfold who has performed all of the theoretical calculations; Dr Julian Knight for the use of his chiral HPLC columns and guidance during my project, and finally Dr Corinne Wills and Professor William McFarlane for their knowledge and assistance with NMR spectroscopy.

On a personal note I would like to acknowledge the support I have received from my friends and family, without which I certainly would not have completed this work. In particular to Marina Santana Vega and Nathan Potts, who have been here with me since the start of my PhD, thank you for your friendship and understanding. I can only hope that our friendship has been as valuable to you as it has been to me.

Finally I would like to thank my parents, who have always been an important source of wisdom, comfort, and often financial support. Thank you for your part in determining where and who I am today.

ABSTRACT

The differential emission of left- or right-handed circularly polarised light is termed circularly polarised luminescence (CPL).[1,2] CPL emission has promising applications in a wide range of fields, such as the development of CPL microscopes.[3,4] Commonly chiral lanthanide complexes are employed in CPL-related studies, due to their high luminescence dissymmetry factors (g_{lum}).[5-7] However these systems are limited by their typically low fluorescence quantum yields (ϕ_F), leading to low overall CPL efficiencies ($|g_{lum}|\cdot\phi_F$). Therefore there is considerable interest in the development of small organic molecules capable of CPL emission (CPL-SOMs).

The 4,4'-difluoro-4-bora-3a,4a-diaza-*s*-indacene (BODIPY) dyes are a class of organic fluorophores which have desirable photophysical properties, including typically high fluorescence quantum yields. Furthermore BODIPYs have highly tuneable absorption and emission bands which can be modulated through varied and robust synthetic transformations. In this work, we have focused on the development of helically chiral BODIPY dyes for use as CPL-SOMs.

Herein we describe the synthesis and chiroptical characterisation of a novel, helically chiral *N,N,O,C*-BODIPY, which we have shown is capable of CPL emission upon irradiation in solution (g_{lum} = 3.7×10^{-3}, figure A.1).[8] Subsequent mechanistic investigation has allowed us to identify an improved synthetic route to the *N,N,O,C*-BODIPYs, and thus the expansion of the *N,N,O,C*-BODIPY series. Study of the chiroptical properties of the *N,N,O,C*-BODIPYs has revealed that this architecture is amenable to the addition of functional groups, without detriment to CPL-emission. This opens up the possibility of introducing more complex functionality to this architecture, whilst retaining the desired chiroptical activity.
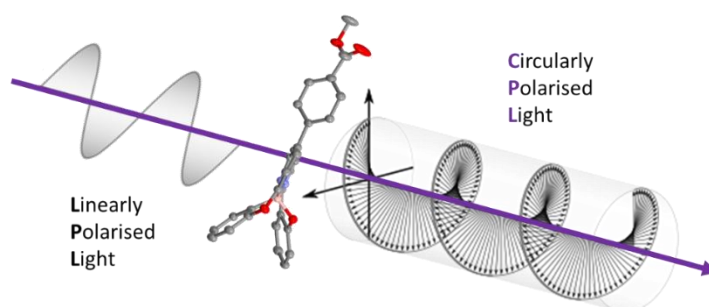

Figure A.1: Schematic representation of CPL emission from an *N,N,O,C*-BODIPY.

Furthermore our investigations into the fundamental molecular properties of the *N,N,O,C*-BODIPY system has given us insight into design strategies towards development of BODIPY CPL-SOMs with increased g_{lum}. We describe our attempts towards the synthesis of helically chiral BODIPYs containing sulfur atoms, and the synthesis of a π-extended helically chiral *N,N,O,O*-BODIPY system. Through these syntheses, we have made a preliminary assessment of the validity of these design strategies.

BINOL	1,1'-bi-2-naphthol
DDQ	2,3-dichloro-5,6-dicyano-1,4-benzoquinone
MeCN	acetonitrile
app.	apparent
BODIPY	4,4-difluoro-4-bora-3a,4a-diaza-s-indacene
br	broad
calcd	calculated
CPL	circularly polarised light / luminescence
CPL-SOM	CPL-active small organic molecule
DCM	dichloromethane
DMF	dimethylformamide
ddd	double double doublet
dd	double doublet
dt	double triplet
d	doublet
ECD	electronic circular dichroism
eq.	equivalents
EtOH	ethanol
EtOAc	ethyl acetate
TMSE	ethyltrimethylsilane
g	gram
HMBC	heteronuclear multiple bond correlation
HMQC	heteronuclear multiple-quantum correlation
HSQC	heteronuclear single quantum coherence
HPLC	high performace liquid chromatography
HRMS	high resolution mass spectrometry
h	hour
IR	infrared
lit.	literature
Mp	melting point
MeOH	methanol
μL	microlitre
mg	miligram
mL	mililitre

mmol	millimole
min	minute
M	molar
m	multiplet
nm	nanometre
NBS	*N*-bromosuccinimide
NCS	*N*-chlorosuccinimide
NIS	*N*-iodosuccinimide
NMR	nuclear magnetic resonance
ppm	parts per million
Ph	phenyl
quant.	quantitative
R.T.	room temperature
ROESY	rotating-frame overhauser spectroscopy
s	singlet
Boc	*tert*-butyloxycarbonyl
p-chloranil	tetrachloro-1,4-benzoquinone
THF	tetrahydrofuran
TLC	thin layer chromatography
TFA	trifluoroacetic acid
TMSCl	trimethylsilyl chloride
TMSOTf	trimethylsilyl trifluoromethanesulfonate
td	triple doublet
UV/Vis	ultraviolet / visible spectrophotometry

Chapter 1. Introduction

This thesis describes investigations into the synthesis of novel, chiral fluorophores which are capable of circularly polarised light emission upon irradiation with visible light in solution. In particular this work was focused on the synthesis of chiral 4,4'-difluoro-4-bora-3a,4a-diaza-*s*-indacene (hereafter referred to as BODIPY) dyes. This chapter discusses some of the underlying theory behind luminescence (i.e. fluorescence, section 1.1.1), circularly polarised light and solution phase circularly polarised luminescence (section 1.1.2) and finally the synthesis and modification of BODIPY architectures, with a focus on the synthesis of chiral BODIPYs including those known to exhibit CPL (sections 1.2 and 1.3).

1.1 Fluorescence and Circularly Polarised Light

1.1.1 Fluorescence

The photophysics of organic molecules is often visualised using a molecular energy level (or Jablonski) diagram (figure 1.1). Here the singlet excited states (S_0, S_1, etc.) and vibrational energy levels (v_1, v_2, etc.) are visually represented, as well as the changes in energy levels resulting from or in a photon (solid lines) and those resulting from changes in vibrational energy (wavy lines). In the absence of external stimuli, molecules exist in the S_0 or ground state. Upon the absorption of a photon (1) the molecule transitions from the ground state to the singlet excited states. Then through vibrational relaxation and internal conversion (2) the molecule relaxes to the lowest energy level of the S_1 excited state. From here, there are two main pathways which can be taken: internal conversion (2), whereby the molecule undergoes non-radiative relaxation to return to the ground state, and fluorescence (3), whereby the molecule emits a photon and returns to the ground state.[9]
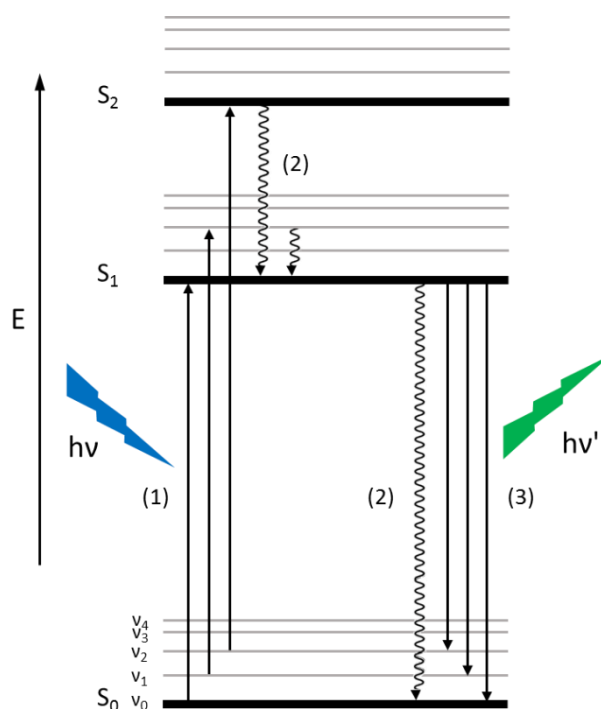
Figure 1.1: A Jablonski diagram showing the light-induced transitions between the electronic (black) and vibrational (grey) energy levels of an organic molecule: (1) absorption of a photon, (2) internal conversion, (3) fluorescence.

It should be noted that although emission typically occurs from the lowest energy level of the S_1 excited state, it can result in the population of any of the vibrational energy levels of the S_0 state. Similarly the excitation of an organic molecule can result in the population of any vibrational energy level of the singlet excited states.

The population of these vibrational energy levels is dictated by the Franck-Codon principle, and is visually represented in figure 1.2. The Franck-Codon principle states that because nuclei are much larger than electrons, electronic transitions occur much faster than the motion of the nuclei. Thus upon absorption or emission of a photon from a molecule, the nuclear separation (Q) of the molecule does not change considerably. In terms of absorption, this results in the highest population of the excited state vibrational energy level which has the largest overlap with the lowest vibrational energy level of the ground state. In terms of emission, the same is true: the most populated ground state energy level is that which has the largest overlap with the lowest vibrational energy level of the excited state. Other transitions between vibrational energy levels of the ground and excited states are still possible, but will be less intense.
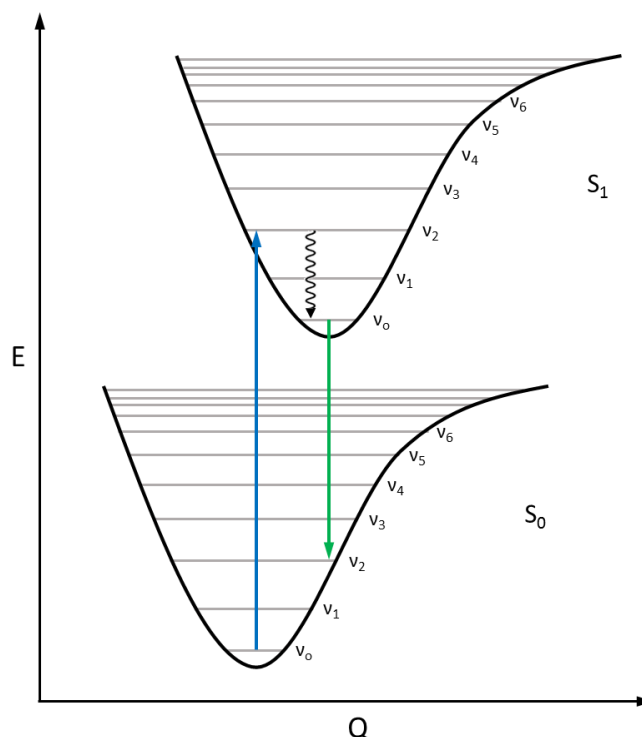
Figure 1.2: Franck-Codon energy principle diagram showing the highest probability absorptive transition (blue arrow), highest probability emissive transition (green arrow) and internal conversion (wavy arrow).

1.1.2 Circularly Polarised Light

We will discuss in this section two polarisation states of an electromagnetic wave: linear and circular. Our interest is in the circular polarisation of light, which occurs when the electric field of light has a constant magnitude but the direction rotates at a steady rate in a plane which is perpendicular to the direction of the light wave.[10] Both a 'packet' of photons and an individual photon can be circularly polarised. Circular polarisation of individual photons arises because the spin of an individual photon can be either +1 or -1. The spin angular momentum of a photon is the coefficient of h, therefore the spin angular momentum of a photon is $\pm 1h$ (where h is Planck's constant).[11] Linear polarisation is the result of a superposition of equal amounts of left-handed ($-1h$) and right-handed ($+1h$) photons. Conversely circular polarisation is the result of a superposition of an unequal amount of left-handed and right-handed photons.

The circular polarisation of an individual photon can be visualised by representing the electrical field of a photon as two perpendicular sine waves. If these sine waves are in phase (i.e. the maxima and minima occur at the same point along the axis of time) then the resultant wave is described as linearly polarised (figure 1.3a). However if these sine waves are out of phase by $\pi/2$ (or a quarter-wave) then the resulting wave is described as circularly polarised (figure 1.3b). Right-handed circularly polarised

light forms a clockwise helix, and left-handed circularly polarised light forms an anti-clockwise helix. Thus circular polarisation infers chirality to a beam of light, which is the basis of chiral photonics or chiroptics.[1,2,11]
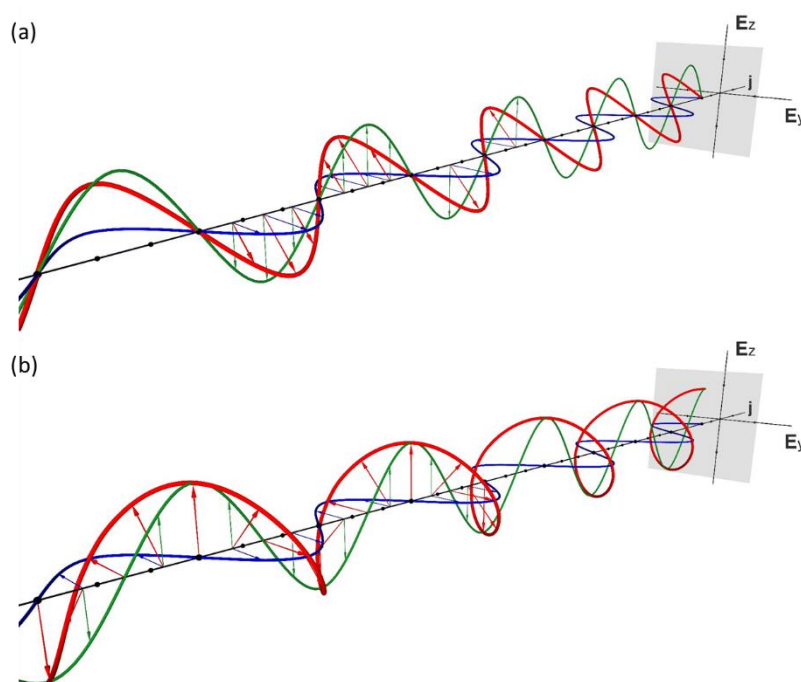
Figure 1.3: (a) two sine waves which represent the z and y components of the electrical field of a photon (green and blue respectively) and the resultant linearly polarised wave (red); (b) two sine waves representing the z and y components of the electrical field of a photon which are a quarter wave out of phase (green and blue respectively) and the resultant circularly polarised wave (red, left-handed CPL shown).

1.1.2.1 Circularly Polarised Luminescence

The differential emission of right- or left-handed circularly polarised light from chiral, non-racemic luminescent systems is known as circularly polarised luminescence (hereafter referred to as CPL).[1,2] The study of CPL provides valuable information about the structures of the involved excited states. Interest in CPL-active luminescent systems has grown significantly in recent years due to the promising applications of CPL in the improvement and development of chiroptical technologies. Some applications of CPL include: 3D optical displays,[12] enantioselective CPL sensors,[13] biological probes[3,5,14,15] and CPL lasers.[16] Moreover the overwhelming presence of chirality in the natural world makes CPL an indispensable tool in the study of biological systems, such as in the development of CPL microscopes.[3,4]

For example Zhu, Cheng *et al.* have disclosed a Eu(III)-containing polymer which, in the presence of either D- or L-proline, displayed induced CPL emission of opposite signs (dependant on the enantiomer

of proline used) upon irradiation in solution, thus providing an example of an enantioselective CPL sensor.[13] The use of CPL as a tool to probe biological systems has been explored by Kawai *et al.* through their synthesis and chiroptical characterisation of proteins (namely *Staphylococcus aureus* nuclease, bovine serum albumin and insulin) covalently bonded to Eu(III) chelates.[15]

In order to make these technologies workable, the efficiency of CPL emission must be high. The extent of asymmetry in fluorescence is quantified using the luminescence dissymmetry factor (g_{lum}). Experimentally g_{lum} is defined by the following equation:

$$g_{lum} = \frac{I_L - I_R}{\frac{1}{2}(I_L + I_R)}$$

Where I_L is the intensity of left-handed circularly polarised light and I_R is the intensity of right-handed circularly polarised light. Thus CPL spectroscopy is the measurement of the differential emission of circularly polarised light. The theoretical equation which defines g_{lum} is as follows:

$$g_{lum} = \frac{4(\boldsymbol{\mu} \cdot \boldsymbol{m} \cdot cos\tau)}{(\boldsymbol{\mu}^2 + \boldsymbol{m}^2)}$$

Where $\boldsymbol{m}$ and $\boldsymbol{\mu}$ are the magnetic and electric transition dipole moment vectors and τ is the angle between them. It should be noted here that CPL spectroscopy is the emission analogue of electronic circular dichroism (ECD) spectroscopy. Whereas CPL reflects the structure of the excited state of the involved fluorophore, ECD reflects the structure of the ground state. In ECD spectroscopy the absorptive dissymmetry factor (g_{abs}) is defined by the following equation:

$$g_{abs} = \frac{\varepsilon_L(\lambda) - \varepsilon_R(\lambda)}{\frac{1}{2}(\varepsilon_L(\lambda) + \varepsilon_R(\lambda))}$$

Where $\varepsilon_L(\lambda)$ and $\varepsilon_R(\lambda)$ are the molar extinction coefficients of left- and right-handed circularly polarised light at a particular wavelength (λ).

Commonly chiral lanthanide complexes are employed in studies of CPL emission. This is due to their high luminescence dissymmetry factors, which stem from their electric dipole forbidden, magnetic dipole allowed $f \rightarrow f$ transitions. Typical g_{lum} values from chiral lanthanides are in the range 0.1-0.5, and the largest g_{lum} value measured from a chiral lanthanide complex has been reported by the group of Kaizaki and Muller ($|g_{lum}|$ = 1.38).[7] However the overall brightness of chiral lanthanide complexes is sub-optimal, due to the typically low fluorescence quantum yields (ϕ_F) of these systems.

Thus there is considerable interest in the development of small organic molecules as CPL-emitters (CPL-SOMs).[17,18] The photonic properties of organic molecules make CPL-SOMs one of the most promising alternatives to chiral lanthanide complexes. These desirable properties include:

- ability to display high fluorescence quantum yields,
- facile modulation of the photonic properties through simple structural modifications, and
- low toxicity, allowing for potential live cell imaging.

The first example of CPL emission from a small organic molecule was described by Emeis and Oosterhoff, where they showed that chiral cyclic ketone **1.1** was capable of CPL emission upon irradiation in solution (g_{lum} = 3.5×10^{-3}). Later other systems have been examined as CPL-SOMs, including other chiral cyclic ketones,[19–21] helicenes,[22–25] cyclophanes[26–28] and biaryls[29–31] (figure 1.4). For example the two binapthyl systems **1.9** and **1.10** were described by Imai, Fujiki *et al.*, wherein they found that the sign of CPL could be controlled by the choice of either 'open' ((*S*)-**1.9**, positive CPL) or 'closed' ((*S*)-**1.10**, negative CPL) type binapthyls exhibiting the same axial chirality.

Chiral cyclic ketones

1.1   1.2   1.3

Helicenes

1.4   1.5   1.6

Cyclophanes

1.7   1.8

Biaryls

1.9   1.10   1.11
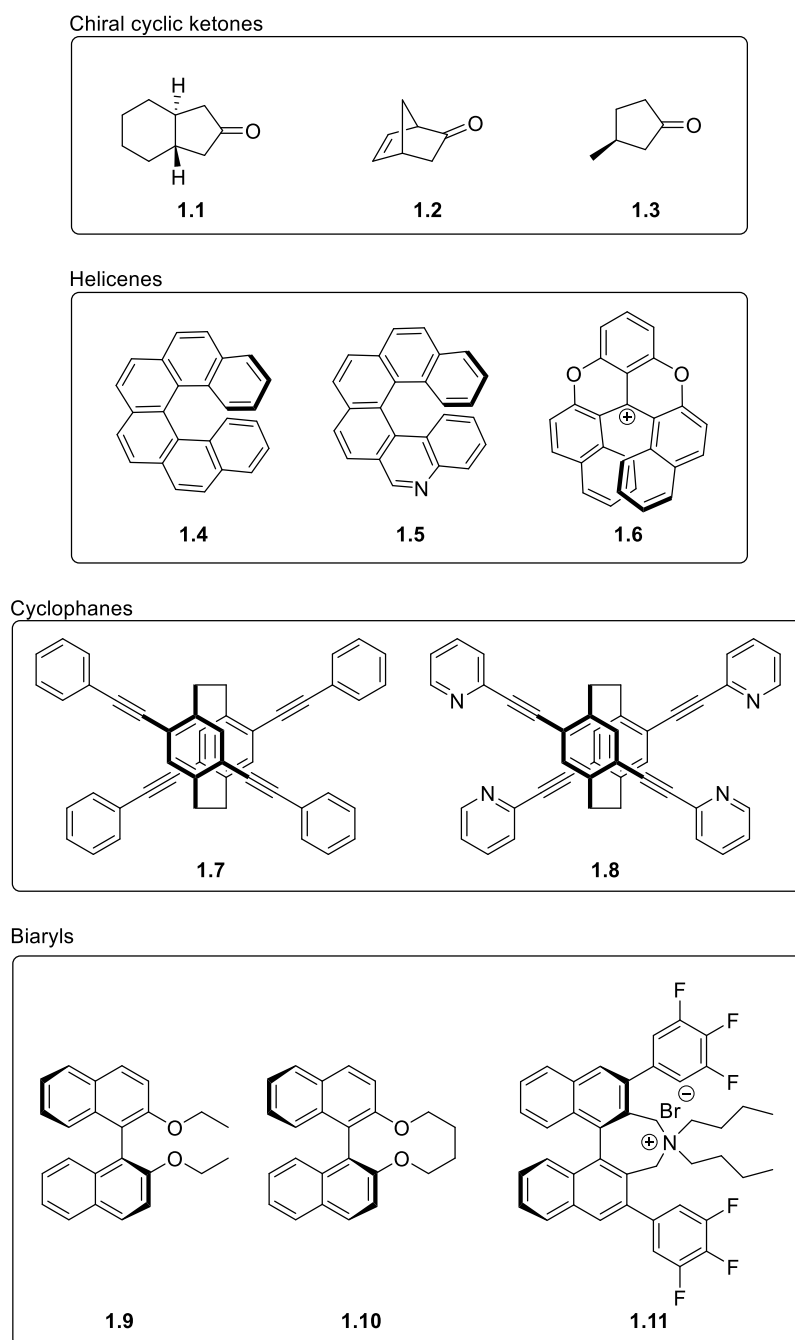
Figure 1.4: A selection of CPL-SOMs: chiral cyclic ketones (**1.1**-**1.3**), helicenes (**1.4**-**1.6**), cyclophanes (**1.7** and **1.8**) and biaryls (**1.9**-**1.11**).

1.2 General Introduction to BODIPYs

In this work, we have focused on the development of chiral 4,4'-difluoro-4-bora-3a,4a-diaza-*s*-indacene (BODIPY) fluorophores as CPL-SOMs.

The BODIPY dyes are a class of fluorophores whose core structure consists of two methylene-bridged pyrrole moieties chelated by a central boron atom (figure 1.5). In recent years BODIPY dyes have become a ubiquitous class of fluorophores, finding use in a wide range of applications including live

cell bioimaging,[32] fluorescent sensing,[33] photodynamic therapy,[34] and dye sensitised solar cells.[35] The success of BODIPY dyes for use in a wide range of applications can be attributed to both their desirable photophysical properties (high fluorescence quantum yields, high molar extinction coefficients and sharp absorption and emission bands), and their relative insensitivity to their chemical environments (such as pH and polarity). Furthermore, simple synthetic modifications to the BODIPY core (section 1.2.2) can be performed in order to fine-tune the photophysical properties of the BODIPY.
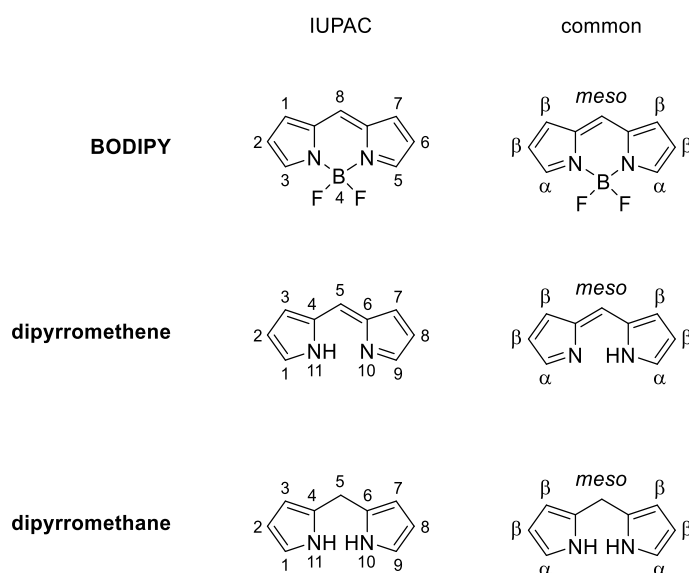
Figure 1.5: The core structure of a BODIPY dye, and of two key synthetic precursors dipyrromethene and dipyrromethane. Two numbering systems are shown, the IUPAC numbering (left) and common numbering system (right).

1.2.1 General Synthetic Strategies towards BODIPYs

We will now discuss general methods to synthesise BODIPYs (section 1.2.1), and common synthetic modifications which can be used to introduce functionality to the BODIPY system (section 1.2.2). These sections are adapted from a recent book chapter entitled 'Recent developments in the synthesis of BODIPYs' written by R. G. Clarke and M. J. Hall and published in Advances in Heterocyclic Chemistry, Volume 128.[36]

1.2.1.1 Synthesis of Symmetrical BODIPYs

The first BODIPY dye was disclosed by Triebs and Kreuzer in 1968.[37] Their synthetic approach involved a one-pot procedure, in which two equivalents of 2,4-dimethylpyrrole **1.12** undergo a Lewis acid catalysed condensation with one equivalent of acetic anhydride. Subsequent chelation of the nitrogen atoms by boron was achieved through treatment with boron trifluoride diethyl etherate to form the BODIPY core. The presence of an excess of acetic anhydride resulted in a subsequent *in situ* electrophilic aromatic (S$_E$Ar) acetylation of the 2- or 2,6-positions, leading to the formation of BODIPYs

1.13 and **1.14**. This approach (i.e. the condensation of pyrrole with acid anhydride) is commonly employed in the synthesis of C_2-symmetric BODIPYs.[38,39]
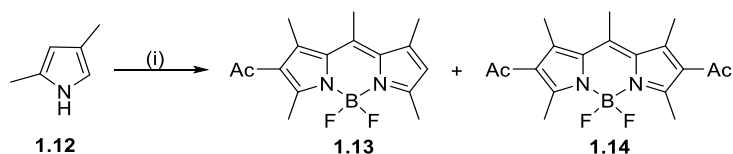
Scheme 1.1: Reagents and conditions: (i) Ac_2O, $BF_3.Et_2O$.

Another frequently utilised approach is the condensation of two equivalents of pyrrole with one equivalent of an activated ester (or equivalent). The resulting dipyrromethenes are chemically unstable, and so are typically not isolated. In this case chelation with boron trifluoride diethyletherate in the presence of a suitable amine base is performed *in situ* to give the desired BODIPY. For example Tour *et al*. have employed this approach, wherein reaction between 2,4-dimethyl pyrrole **1.12** and acid chloride **1.15** is used to form BODIPY **1.16**.[40] BODIPY **1.16** was then used in the synthesis of a light driven nanocar **1.17**, which features two BODIPY axles.
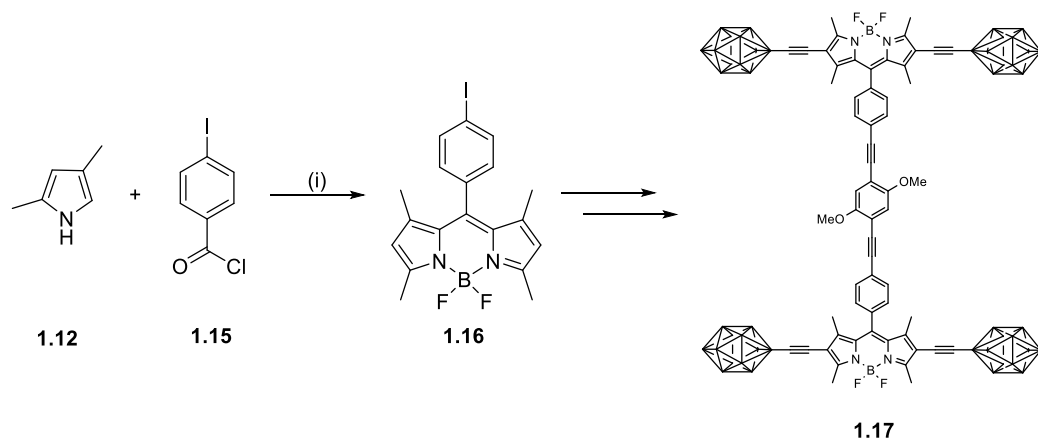
Scheme 1.2: Reagents and conditions: (i) 1,2-dichloroethane, reflux, 13 h then $BF_3 \cdot OEt_2$, Et_3N, reflux, 2 h (24%).

A further strategy used to synthesise C_2-symmetric BODIPYs involves the use of an orthoester as the electrophilic component of the initial condensation reaction, rather than an acyl chloride or acetic anhydride. This is followed by boron chelation under standard conditions to form the BODIPY core structure. Whilst allowing access to BODIPYs with *meso*-alkyl substituents and *meso*-unsubstituted BODIPYs (through the use of an orthoformate), one drawback of this approach is that it is limited by the availability of commercial orthoesters. The condensation of pyrroles with orthoesters was first reported by Reese and Yan, in their synthesis of tri-(pyrrol-2-yl)alkanes.[41] This condensation reaction was first applied to the synthesis of BODIPYs by Suzuki *et al*. in their synthesis of BODIPY **1.18**, which

was synthesised *via* an acid catalysed condensation between 2,4-dimethylpyrrole **1.12** and triethylorthoformate. Boron chelation under standard conditions then lead to the synthesis of BODIPY **1.18**, which is a key intermediate in the synthesis of a BODIPY-based chemiluminescent probe **1.19**.[42]
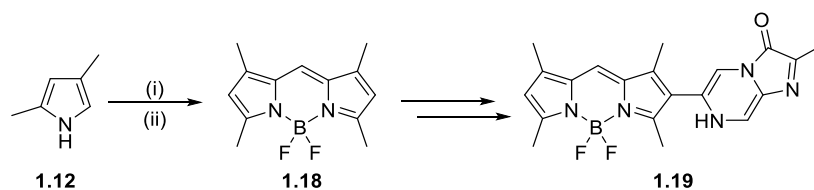
Scheme 1.3: Reagents and conditions: (i) CH(OEt)$_3$, TFA, CH$_2$Cl$_2$, R.T., 2 h; (ii) BF$_3$·OEt$_2$, Et$_3$N, toluene, R.T. 30 min (57%).

One of the most popular methods to synthesise BODIPYs was developed by Lindsey *et al*., wherein an aldehyde (typically an arylaldehyde, such as **1.20**) undergoes acid catalysed condensation with two equivalents of α-substituted pyrrole (such as 2-methylpyrrole **1.21**). The resultant symmetrical dipyrromethane **1.22** is then oxidised using DDQ or *p*-chloranil to form the corresponding dipyrromethene **1.23**. A final boron chelation step under standard conditions affords the desired 3,5-methyl-8-aryl substituted BODIPY (for example, BODIPY **1.24**, scheme 1.4). The use of α-substituted pyrrole is key to this method, as the substituent at the α-position prevents further condensation reactions and thus the formation of porphyrins.
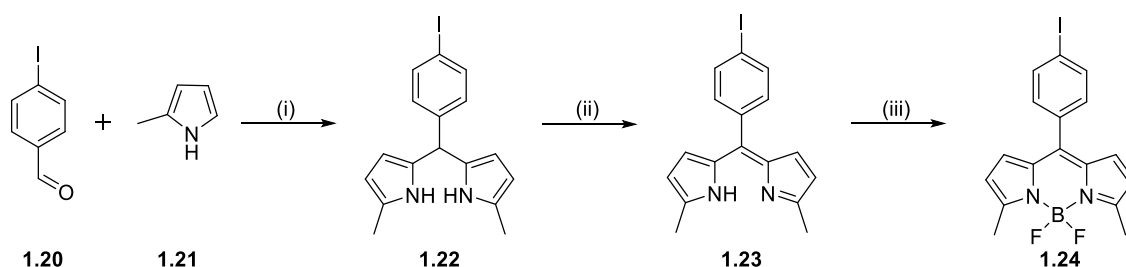
Scheme 1.4: Reagents and conditions: (i) CH$_2$Cl$_2$, TFA$_{(cat.)}$, R.T., 1.5 h (95%); (ii) *p*-chloranil, toluene, R.T., 5 min, then Et$_3$N, BF$_3$·OEt$_2$, R.T., 1 h (15%).

However this method may only be used to synthesise α-substituted BODIPYs. If instead α-unsubstituted BODIPYs are required, an alternative strategy must be used. Lindsey *et al*. have developed a 'solventless' approach in which pyrrole is used in a large excess as both reagent and solvent.[43] Here the use of a large excess of pyrrole prevents the occurrence of over condensation, and thus the formation of porphyrins and other higher order condensates is suppressed. The acid catalysed condensation between 1*H*-pyrrole and an aryl aldehyde thus gives the corresponding dipyrromethane. Following oxidation and chelation under standard conditions, the desired BODIPY can be isolated.

An alternative method towards the synthesis of α-unsubstituted BODIPYs was described by Dehaen *et al.*, in which near stoichiometric amounts of α-unsubstituted pyrroles are condensed with arylaldehydes under aqueous acidic conditions.[44] The success of this approach stems from the comparative solubility of the reagent arylaldehyde and the product dipyrromethane, the latter of which precipitates from solution during the course of the reaction. Not only does this prevent porphyrin formation (as there is little dipyrromethane available in solution to undergo further condensation processes) but also allows for purification by simple filtration.

1.2.1.2 Synthesis of Unsymmetrical BODIPYs

The synthetic strategies we have so far discussed involve the condensation of two equivalents of pyrrole with an electrophilic centre, resulting in the synthesis of C_2-symmetric BODIPYs. In order to break this symmetry and produce unsymmetrical dyes, an alternative approach must be used. Mély, Bonnet *et al.* described the step-wise formation of BODIPY dyes *via* keto-pyrrole intermediates.[45] The 2-ketopyrrole **1.25** was synthesised through the Grignard addition of 2,4-dimethyl pyrrole **1.12** to 4-iodobenzoyl chloride. This was followed by the addition of a second equivalent of 2,4-dimethyl pyrrole to 2-ketopyrrole **1.25** in the presence of phosphorous oxychloride to form dipyrromethene **1.26**. Subsequent oxidation and boron chelation under standard conditions afforded BODIPY **1.16**. Although in this work this approach was used to synthesise symmetrical BODIPY **1.16**, it can be imagined that this approach could be employed to form unsymmetrical BODIPYs.
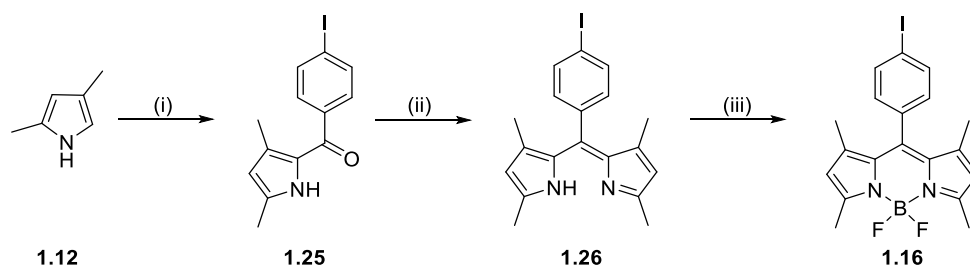
Scheme 1.5: Reagents and conditions: (i) CH_3MgBr, Et_2O, reflux, 30 min then IC_6H_4COCl, R.T., 12 h (81%); (ii) 2,4-dimethylpyrrole, $POCl_3$, CH_2Cl_2, pentane, 0 °C then R.T., 24 h (46%); (iii) $BF_3 \cdot Et_2O$, NEt_3, toluene 80 °C, 30 min (80%).

This approach was used by Hall *et al.* in the synthesis of an unsymmetrical BODIPY displaying axial chirality.[46] Bromination of 2-ketopyrrole **1.27** was followed by condensation with 2,4-dimethyl-3-ethyl pyrrole to give dipyrromethene **1.28**. Chelation by boron under standard conditions was followed by a Mizoroki-Heck coupling with ethyl acrylate to give BODIPY **1.29**. The restricted rotation around the *meso*-aryl bond of BODIPY **1.29** (due to the steric clash between the *ortho*-methyl group of the *meso*-aryl ring and the 1,7-methyl substituents of the BODIPY core) combined with the unsymmetrical BODIPY core result in axial chirality (sections 1.3.1.3 and 1.3.2.2).
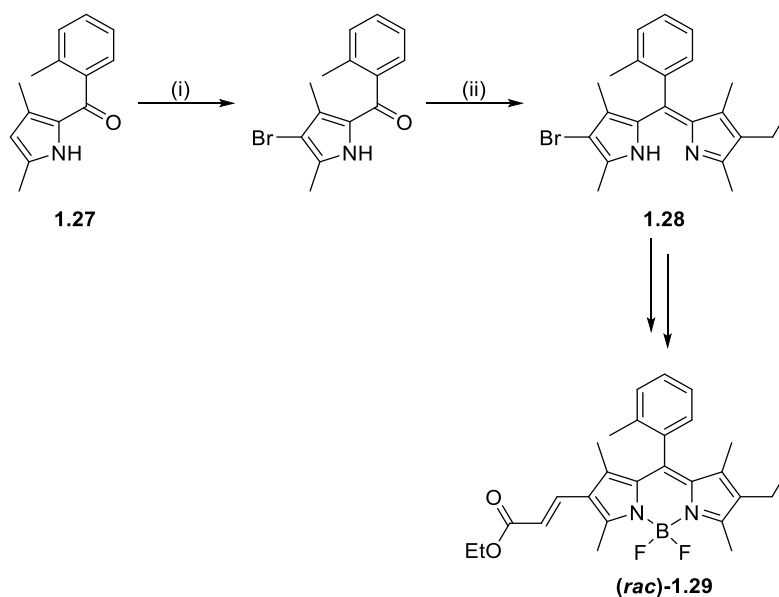
Scheme 1.6: Reagents and conditions: (i) Br_2, CH_2Cl_2, R.T., 24 h (100%); (ii) (a) 2,4-dimethyl-3-ethylpyrrole, TFA, CH_2Cl_2, R.T., 18 h (47%).

1.2.2 Modifications to the BODIPY core

Modifications to the BODIPY core are commonly used to fine tune the photophysical properties of the dye. For example the extension of the π-system of the BODIPY core results in a bathochromic shift of the absorption and emission bands of the BODIPY. Additionally modifications to the BODIPY core can be used to introduce functionality to the BODIPY system. There are many synthetic methodologies to introduce functionality to the BODIPY core, which are summarised in figure 1.6. In this section we will discuss only the modifications which are highlighted in red.

1a.S_NAr
2a.LCC coupling
3b. Halogenation
   - S_NAr
   - Metal catalysed cross-coupling
4b. Lithiation-functionalisation
5b. Cyanation

1. Halogenation
   - S_NAr
   - Metal catalysed cross-coupling

a   b
MeS/H

1. Halogenation
     - Metal catalysed cross-coupling
2. Metal catalysed C-H functionalisation
3. Sulfonation
4. Nitration

Me/H   R' R

1. S_N with C nucleophile
2. S_N with O nucleophile
3. S_N with X
   - S_N with N nucleophile

1a. Knoevenagel Condensation
2b. Halogenation
   - S_NAr
   - Metal catalysed cross-coupling
3b. Oxidative nucleophilic substitution
4b. Vicarious nucleophilic substitution
5b. Metal catalysed C-H functionalisation
6b. Radical reactions
   - Diazonium salts
   - Boronic acids / trifluoroborates
   - Diaryliodonium salts

Figure 1.6: Reported modifications which can be made to the BODIPY core, with those discussed in this section highlighted in red.

1.2.2.1 Electrophilic Aromatic Substitutions (S_EAr)

BODIPY dyes are intrinsically electron rich heteroaromatics. As such they are susceptible to electrophilic aromatic substitution (S_EAr) chemistry. The electrophilic aromatic substitution of BODIPYs is highly regioselective for the 2- and 6-positions, as these are the positions which bear the largest negative charge. Examples of S_EAr nitration,[47] sulfonation[48–50] and halogenation[49,51] are commonly found throughout BODIPY literature.

Halogenation of the 2,6-positions BODIPYs using reagents such as liquid bromine[49] or iodic acid[51] can result in over-halogenation. Once reaction at the 2,6-positions is complete, further unwanted halogenation can then occur at any unsubstituted positions of the BODIPY. Milder halogenation methodologies are therefore attractive, since they provide greater regioselectivity and reduce the occurrence of over-halogenation by-products. The relatively mild *N*-halosuccinimide (NXS) reagents (NCS, NBS and NIS) are therefore commonly employed to halogenate BODIPYs.

Ortiz, García-Moreno, Chiara *et al*. have examined the stepwise chlorination of BODIPY **1.30**, allowing

the selective synthesis of a series of chlorinated BODIPYs **1.31**-**1.34**.[52] Reaction between BODIPY **1.30**

and two equivalents of NCS gave 2-chloro-BODIPY **1.31**. By increasing the equivalents of NCS used 2,6-

chloro-BODIPY **1.32** (3 eq.), 2,3,5-chloro-BODIPY **1.33** (4 eq.) and 2,3,5,6-chloro-BODIPY **1.34** (10 eq.)

were selectively synthesised.
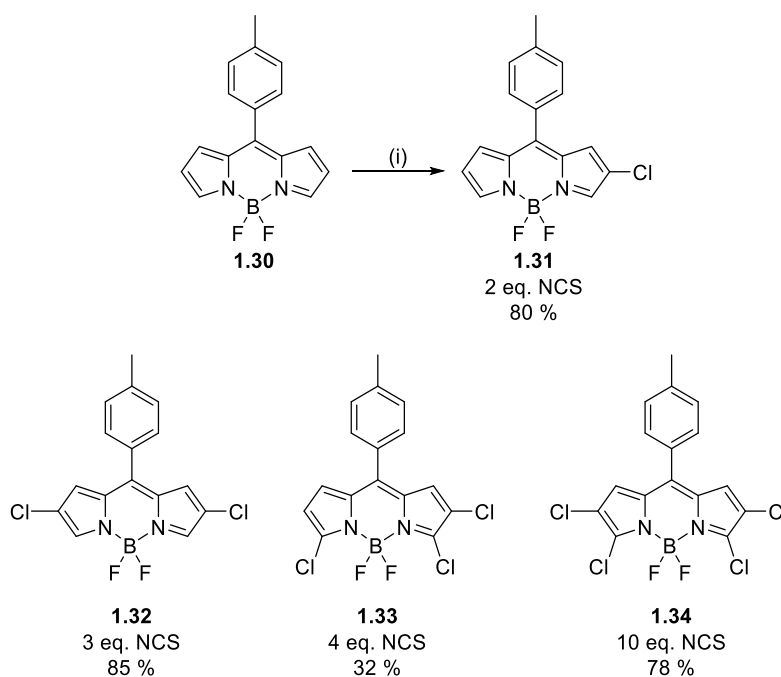
Scheme 1.7: Reagents and conditions: (i) NCS, THF, R.T., 12-72 h.

One limitation which is implied by the high regioselectivity of the S_EAr chemistry of BODIPYs is that

the substitution of the 3,5-positions is not possible unless the 2,6-positions are sterically blocked.

However the 3,5-positions are the most spectroscopically interesting positions to decorate,[53,54] and so

there is interest in methodologies to substitute the 3,5-positions.

Dipyrromethanes, commonly used BODIPY precursors, display complimentary regioselectivity to the

corresponding BODIPYs. Dipyrromethanes are more pyrrole-like in their chemistry, and so S_EAr

substitution occurs preferentially at the α- or 1,9-positions (corresponding to the 3,5-positions of the

subsequently formed BODIPY). Thus the S_EAr α-functionalisation of dipyrromethenes serves as a route

to 3- or 3,5-substituted BODIPYs.

For example Dehaen *et al.* have described the highly regioselective S_EAr reaction between

dipyrromethane **1.35** and NCS to give 3,5-dichlorinated dipyrromethane **1.36**. Following oxidation and

boron chelation under standard conditions, 3,5-dichloro-BODIPY **1.37** was synthesised.[55,56] A similar

methodology can be used to synthesise 3,5-dibromo-BODIPYs, through the reaction of

dipyrromethanes with NBS at low temperatures to form α,α-dibrominated dipyrromethanes. After oxidation and boron chelation under standard conditions, 3,5-dibromo-BODIPYs may be isolated.[57,58]
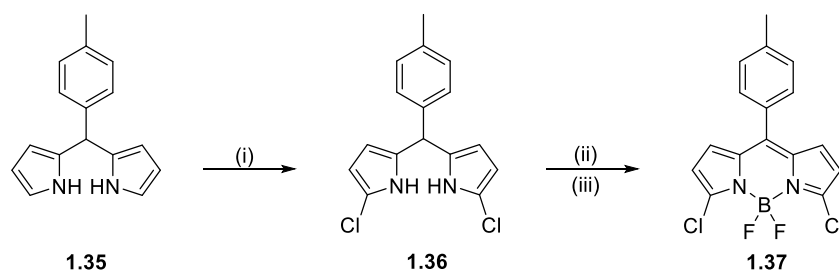
Scheme 1.8: Reagents and conditions: (i) NCS, THF, -78 °C for 2h, then -20 °C overnight; (ii) *p*-chloranil, CH$_2$Cl$_2$, 1 h; (iii) BF$_3$·Et$_2$O, NEt$_3$, toluene, reflux, 2.5 h (47%).

1.2.2.2 Nucleophilic Aromatic Substitutions (S$_N$Ar)

BODIPYs which contain leaving groups in the 3- or 3,5-positions are susceptible to nucleophilic aromatic substitution (S$_N$Ar) chemistry. Commonly S$_N$Ar chemistry is performed on 3,5-dichloro-BODIPYs, since the electron withdrawing nature and good leaving group ability of the chloride substituents result in typically facile, high yielding substitutions.

Dehaen *et al.* first reported the application of S$_N$Ar chemistry to BODIPYs,[55,59] wherein oxygen, nitrogen and sulfur centred nucleophiles were shown to react with 3,5-dichloro-BODIPY **1.37** to produce 3- and 3,5-substituted BODIPYs. Control over mono- versus di-substitution was easily achieved through control of the reaction temperature.

1.38 Nu = piperidine
1.39 Nu = aniline
1.40 Nu = EtOOCCH$_2$SH
1.41 Nu = diethyl malonate

1.42 Nu = piperidine
1.43 Nu = aniline
1.44 Nu = EtOOCCH$_2$SH
1.45 Nu = diethyl malonate
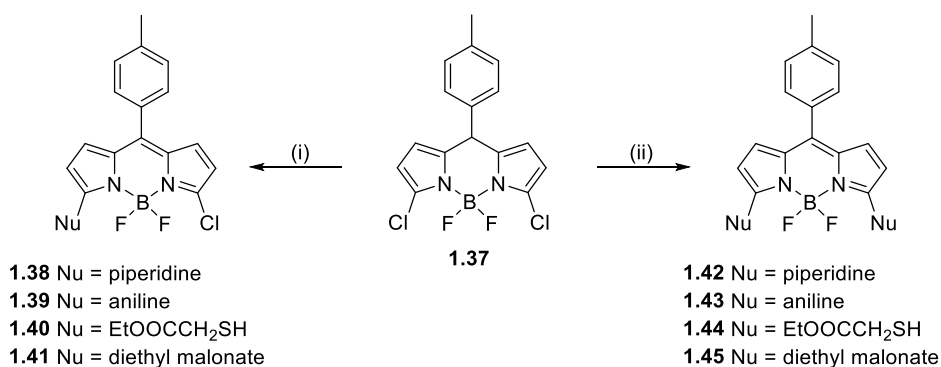
Scheme 1.9: Reagents and conditions: (i) Nucleophile (2 eq.), MeCN, R.T. (**1.38** 74%; **1.39** 69%; **1.40** 65%; **1.41** 67%); (ii) Nucleophile (4 eq.), MeCN, reflux (**1.42** 78%; **1.43** 64%; **1.44** 70%; **1.45** 71%).

This chemistry was further expanded by Dehaen *et al.*, wherein the substitution of 3,5-dichloro-BODIPY **1.37** with 2-bromophenol was described.[60] It was then shown that the resulting BODIPY **1.46** was susceptible to a palladium catalysed, intramolecular benzofuran formation to produce ring-fused, bathochromically shifted BODIPY **1.47**.
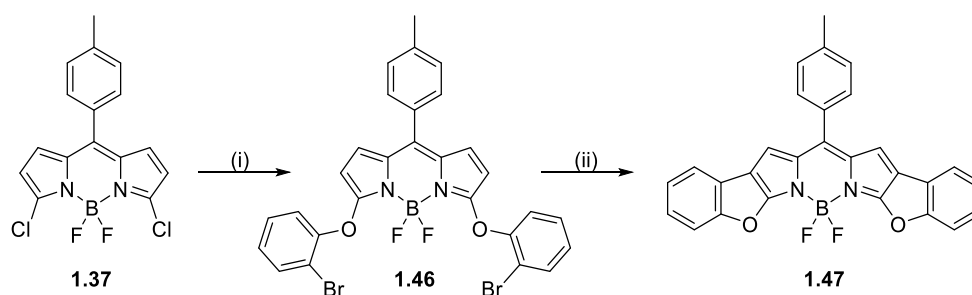
Scheme 1.10: Reagents and conditions: (i) 2-bromophenol (2 eq.), Na$_2$CO$_3$ (2 eq.), MeCN, reflux, 1 h (94%); (ii) Pd(OAc)$_2$, PPh$_3$ (10 mol%), K$_2$CO$_3$ (3 eq.), toluene, reflux, 48 h (69%).

Nitrogen-centred nucleophiles undergo S$_N$Ar chemistry with 3,5-dichloro-BODIPYs at relatively fast rates, even at room temperature. For example, Zhao *et al.* have reported the S$_N$Ar reaction of 3,5-dichloro-BODIPYs with a range of *N*-heteroaromatic molecules.[61] Matano *et al.* later described a further improvement to the substitution of 3,5-dichloro-BODIPYs with *N*-heteroaromatics.[62] Initial experiments by Matano *et al*. showed that the S$_N$Ar addition of pyrazole to 3,5-dichloro-BODIPY **1.48** was slow and selective for mono-addition, even after extended reaction times. However the addition of two equivalents of sodium hydride to the reaction conditions resulted in the formation of 3,5-disubstituted BODIPY **1.49** after a dramatically shortened reaction time.
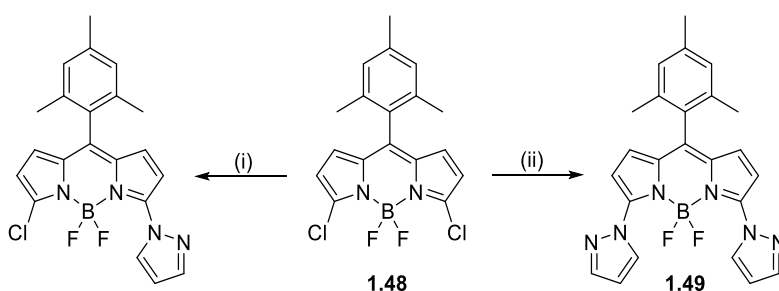
Scheme 1.11: Reagents and conditions: (i) pyrazole (10 eq.), THF, reflux, 22 h (61%); (ii) pyrazole (2 eq.), NaH (2 eq.), THF, R.T., 1 h (87%).

The use of sodium hydride as a base to activate the *N*-heteroaromatic nucleophile allowed for the addition of a wide range of *N*-heteroaromatics to 3,5-dichloro-BODIPY **1.48** (scheme 1.12).
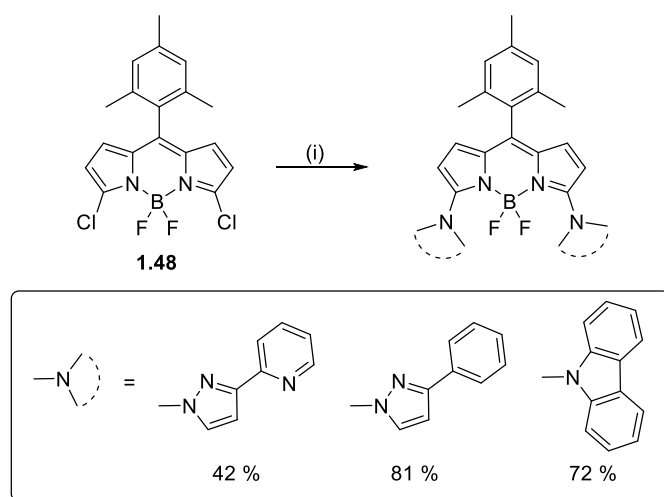
Scheme 1.12: Reagents and conditions: (i) *N*-heteroaromatic, NaH, THF, R.T.

As previously discussed, Dehaen *et al.* showed that carbon centred nucleophiles undergo S_NAr chemistry with 3,5-dichloro-BODIPY **1.48** to produce 3- and 3,5-substituted BODIPYs.[55] An expansion of this work was reported by Hao *et al.*, in which electron rich heteroaromatics are used as carbon-centred nucleophiles in the S_NAr reaction of BODIPYs. Thus 2,3,4,6-tetrachloro-BODIPY **1.50** was reacted with pyrrole to produce either mono- or di-pyrrolyl-BODIPYs **1.51** or **1.52**, dependant on the reaction time and temperature.
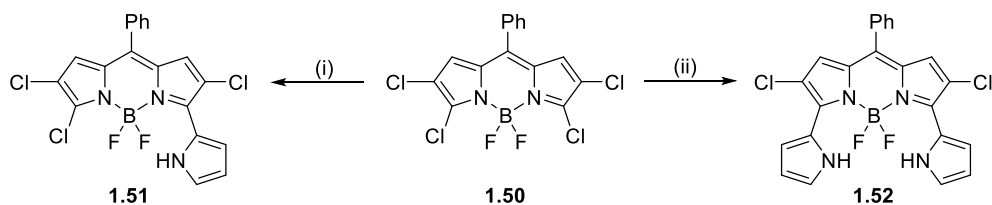
Scheme 1.13: Reagents and conditions: (i) pyrrole (neat), 60 °C, 24 h (78%); (ii) pyrrole (neat), 120 °C, 72 h (52%).

The drawback of this approach is that relatively forcing conditions are used, for example the use of pyrrole as the reaction solvent and high temperatures are required. If a more electron rich pyrrole, such as 2,4-dimethylpyrrole, is used then lower reaction temperatures can be employed to synthesise 3- and 3,5-dipyrrolyl-BODIPYs **1.53** and **1.54**. Furthermore the use of electron rich pyrroles allows for the use of a reaction solvent instead of an excess of pyrrole (in this case, toluene).
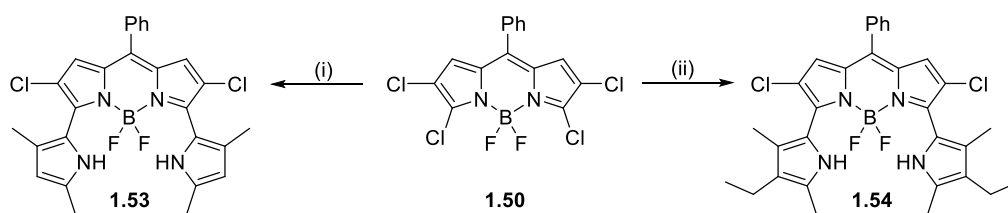
Scheme 1.14: Reagents and conditions: (i) 2,4-dimethylpyrrole (19 eq.), toluene, 60 °C, 24 h (44%); (ii) 2,4-dimethyl-3-ethylpyrrole (19 eq.), toluene, 60 °C, 24 h (67%).

Aryl and alkyl chalcogens are good nucleophiles, and as such we would expect that they would undergo S_NAr chemistry with suitably functionalised BODIPYs. The synthesis of a series of 3,5-dichalcogen substituted BODIPYs was described by Vosch *et al.*, synthesised through the S_NAr addition of a range of aryl chalcogens to 3,5-dichloro-BODIPY **1.37**. Thus 3,5-dithiophenol-BODIPY **1.55** was formed through reaction of 3,5-dichloro-BODIPY **1.37** and thiophenol, in the presence of sodium carbonate. In the case of the more easily oxidisable fourth and fifth row chalcogens, selenium and tellurium, the corresponding nucleophile was first formed through reductive cleavage of 1,2-diphenyldiselane or 1,2-diphenylditellane using sodium borohydride. The resulting aryl chalcogen then underwent S_NAr chemistry with 3,5-dichloro-BODIPY **1.37** to give 3,5-diselenophenolyl-BODIPY **1.56a** and 3,5-ditellurphenolyl-BODIPY **1.56b**.
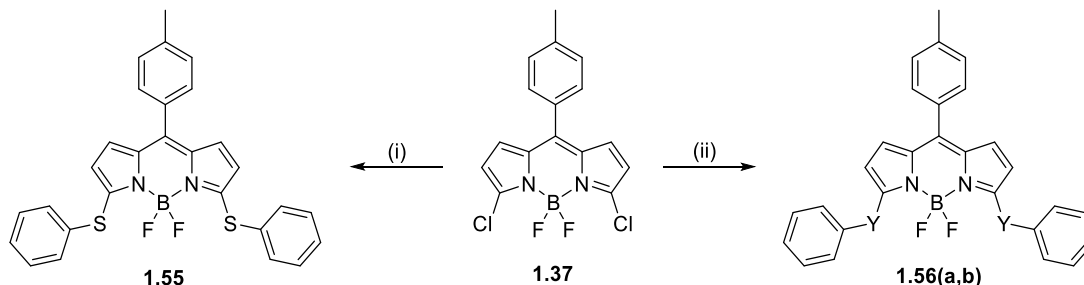
Scheme 1.15: Reagents and conditions: (i) thiophenol (10 eq.), K_2CO_3 (10 eq.), DMF, 50 °C, 12 h (87%); (ii) $NaBH_4$ (2.4 eq.), Ph_2Y_2 (2.1 eq.), EtOH, THF, R.T., 12 h (**1.56a**: Y = Se (96%), **1.56b**: Y = Te (91%)).

It should be noted here that S_NAr chemistry is also possible from 1,7-dichloro-BODIPYs[63] and 8-halo-BODIPYs,[64–67] provided there is not significant steric bulk in either the 8- (for 1,7-substitutions) or 1,7-positions (for 8-substitutions) to block the incoming nucleophile.

1.2.2.3 Substitutions at Boron

The 4-position (i.e. the boron atom) of the BODIPY framework can also be functionalised, where the BF_2 chelating group is replaced by a BX_2 group.[68] Stable chelates can be formed when X is C, O or N, and useful synthetic intermediates can be formed when X is Cl. Typically exchange of the fluorine

atoms (to form a BX$_2$ BODIPY complex) is achieved using a nucleophilic aromatic substitution approach, usually (but not always) in the presence of a suitable Lewis acid catalyst. Another route to BX$_2$ complexed BODIPYs is the chelation of the precursor dipyrromethene with a boron reagent already bearing the desired X groups.

The replacement of the fluorine atoms with carbon based ligands through reaction with a suitable organometallic reagent is one of the most commonly used approaches to BX$_2$-BODIPYs.[69–72] The first report of this type of transformation was described by Ziessel *et al.*, in which ethynylpyrene and ethynyltoluene functionalised BODIPYs **1.58** and **1.59** were formed through reaction between BODIPY **1.57** and the corresponding lithium acteylides.[73] This approach can also be applied to aryl or alkyl lithium reagents, to produce 4-arylated- or 4-alkylated-BODIPYs, respectively.
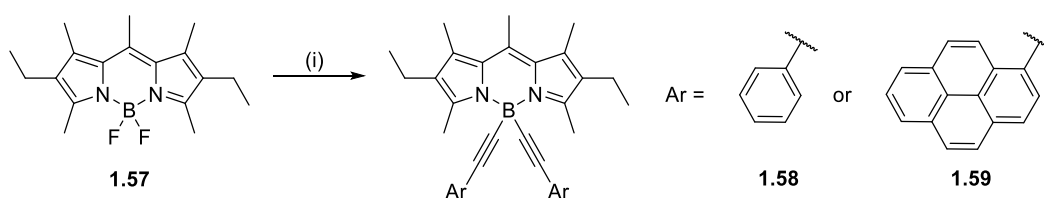
Scheme 1.16: Reagents and conditions: (i) 1-ethynylpyrene or 1-ethynyltoluene (2 eq.), *n*-butyllithium (2.5 eq.), THF, -78 °C for 1 h, then R.T. for 30 min (**1.58** 62%, **1.59** 30%).

Alternatively other organometallic reagents can be employed, such as Grignard reagents, in place of organolithiums. This strategy was first described by Ziessel *et al.*, wherein BODIPY **1.57** was diarylated at boron through reaction with arylmagnesium bromides to produce BODIPYs **1.60** and **1.61**.[74] Substitutions with alkynyl and alkyl Grignard reagents have been shown to produce the corresponding 4-alkynyl- and 4-alkyl-BODIPYs.[75–78]
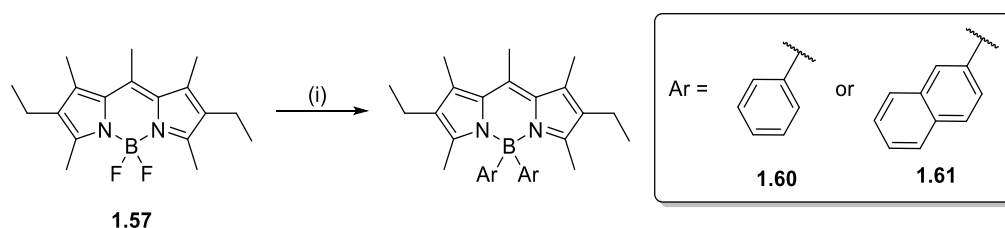
Scheme 1.17: Reagents and conditions: (i) phenylmagnesium bromide or 2-napthylmagnesium bromide (2 eq.), diethyl ether, R.T., 1 h (**1.60** 25%, **1.61** 35%).

The replacement of the fluorine atoms of a BODIPY with oxygen atoms has been achieved through both intramolecular and intermolecular substitutions with appropriate oxygen centred nucleophiles. Burgess *et al.* reported the first example of a tetradentate dipyrromethene ligand, *N,N,O,O*-BODIPY **1.64**, which contains a central boron atom directly bonded to the oxygen atoms of the 3,5-phenolic

substituents.[79] The synthesis of *N,N,O,O*-BODIPY **1.64** involved the formation of dipyrromethene **1.62**, followed by chelation under standard conditions to form BODIPY **1.63**. A subsequent double demethylation of the phenolic oxygens using boron tribromide was followed by an *in situ* double B-O bond formation to form *N,N,O,O*-BODIPY **1.64**. The tetradentate *N,N,O,O*-chelation motif of **1.64** was shown to induce bathochromically shifted absorption and emission bands, as a result of the highly conjugated and constrained ring system.
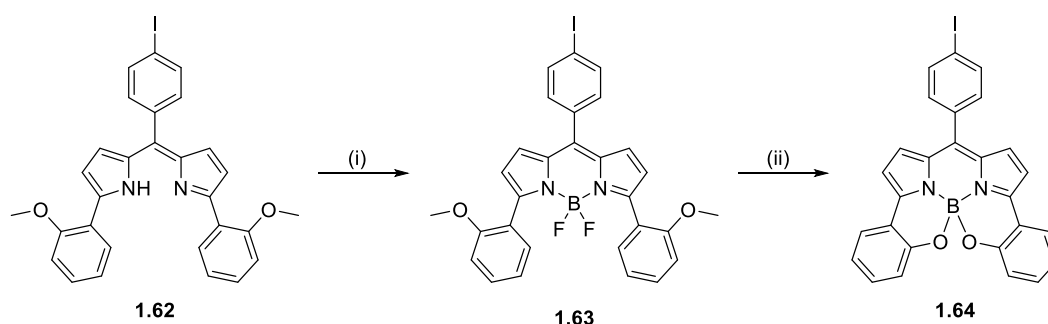
Scheme 1.18: Reagents and conditions: (i) Et$_3$N, BF$_3$·Et$_2$O, toluene, 80 °C, 20 min; (ii) BBr$_3$, 0 to 25 °C, 5 h (93%).

Since this initial report, there have been further examples of using this demethylation, *in situ* boron chelation approach to produce highly constrained, bathochromically shifted BODIPYs.[80–84] These reactions are driven in part by the entropically favourable formation of a tetra- or tri-dentate coordination geometries around the central boron atom.

Intermolecular substitutions at boron are also possible for oxygen centred nucleophiles, if a suitable base or Lewis acid is used to mediate the process. The first instance of this type of substitution at boron was described by Nagano *et al.*, in which BODIPY **1.65** was reacted with sodium methoxide (methanol, reflux) to form the mono- and di-methoxy BODIPYs **1.66** and **1.67**.[85]
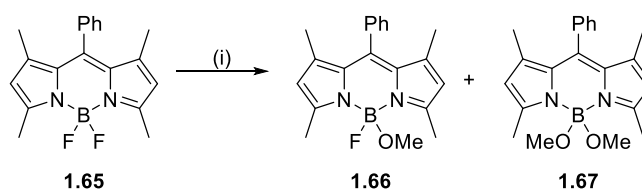
Scheme 1.19: Reagents and conditions: (i) MeONa, MeOH, reflux, 14 h (**1.66** 37%, **1.67** 52%).

Another strategy reported by Mély, Bonnet *et al.* described the nucleophilic substitution of the fluorine atoms of boron with alcohols under Lewis acidic conditions.[45] Activation of BODIPY **1.65** by treatment with aluminium trichloride was followed by the addition of methanol, to give dimethoxy-BODIPY **1.67** in a quantitative yield. This methodology was subsequently extended to include a wider

range of alcohols, including pyrocatechol and 1,1'-bi-2-napthol (BINOL). This approach has since been widely used to access *N,N,O,O*-BODIPYs.[86–91]
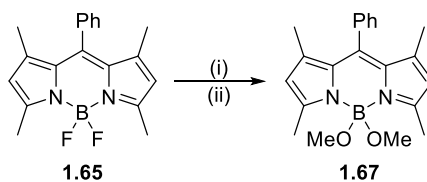
Scheme 1.20: Reagents and conditions: (i) AlCl$_3$, CH$_2$Cl$_2$, reflux, 5 min; (ii) MeOH, R.T., 5 min (quantitative).

A similar approach involves the activation of the fluorine atoms of the BODIPY through treatment with trimethylsilyl trifluoromethanesulfonate (TMSOTf). Mazitschek *et al.* have examined the substitution of one fluorine atom of the BODIPY boron with alkoxy groups.[92] BODIPY **1.68** was reacted with TMSOTf (10 equivalents) before the rapid addition of methanol (100 equivalents) gave the *N,N,O,F*-BODIPY **1.69**. This approach was shown by Mazitschek *et al.* to be a general route to 4-monoalkoxy-BODIPYs through the introduction of a wide range of alcohols. This approach has since been applied to the synthesis of 4,4-dialkoxy-BODIPYs.[93] Furthermore the generation of TMSOR from TMSCl and the appropriate carboxylic acid ROOH has allowed for the incorporation of more complex alkoxy substituents.[94,95]
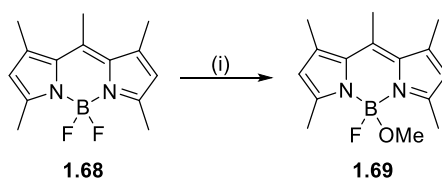
Scheme 1.21: Reagents and conditions: (i) 5 eq. TMSOTf, CH$_2$Cl$_2$, 0 °C, 2.5 min, then 100 eq. MeOH, ^{i}Pr$_2$NEt (46%).

The replacement of the fluorine atoms of BODIPYs with chlorine atoms results in the formation of more easily substitutable boron centres. This is because B-Cl bonds are significantly weaker than B-F bonds, resulting in facile substitutions from BCl$_2$-BODIPYs. Lundrigan and Thompson have reported the conversion of BF$_2$-BODIPY **1.70** to BCl$_2$-BODIPY **1.71** through treatment of **1.70** with boron trichloride.[96] The BCl$_2$-BODIPY **1.71** can be isolated, or alternatively can be reacted directly with, for example, sodium methoxide or ethylmagnesium bromide to give *N,N,O,O*-BODIPY **1.72** or *N,N,C,C*-BODIPY **1.73**.
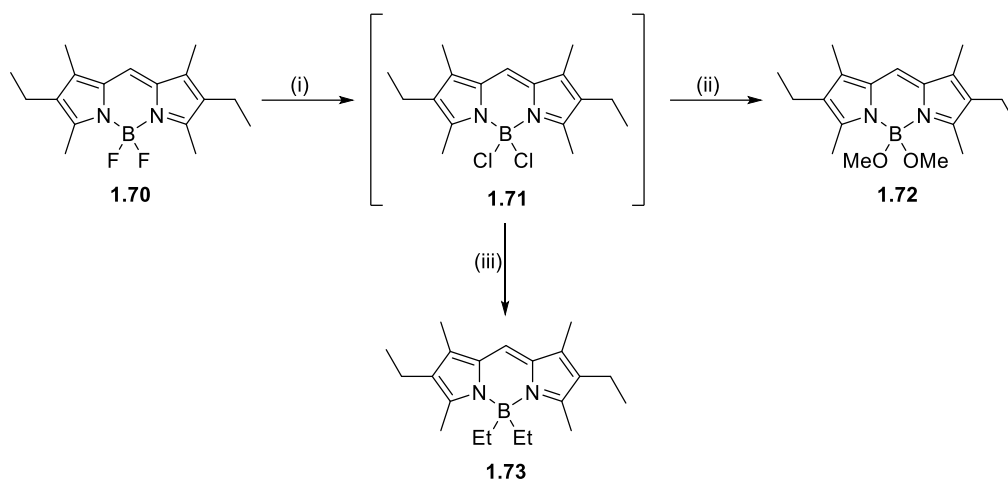
Scheme 1.22: Reagents and conditions: (i) BCl$_3$ (1 eq.), CH$_2$Cl$_2$, 22 °C, 1 h; (ii) NaOMe, CH$_2$Cl$_2$, 22 °C, 1 h (98%); (iii) EtMgBr, CH$_2$Cl$_2$, 22 °C, 1 h (98%).

Thompson *et al*. have also reported the formation of BBr$_2$-BODIPY **1.74**, which was formed through reaction of BODIPY **1.70** with boron tribromide.[97] BBr$_2$-BODIPY **1.74** was isolated by removal of the reaction solvent, however the reaction chemistry of BBr$_2$-BODIPY **1.74** has yet to be reported.
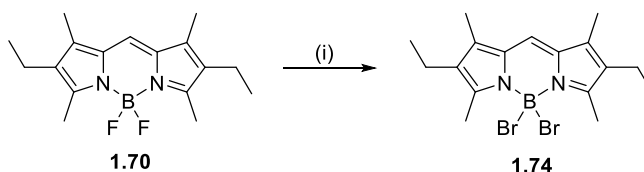
Scheme 1.23: Reagents and conditions: (i) BBr$_3$ (1 eq.), CCl$_4$, R.T. (quantitative).

Another strategy towards the synthesis of BODIPYs with functionality at the boron atom (or 4-position) is the chelation of dipyrromethenes with boron species containing the desired functionality. For example Ikeda and Nabeshima have reported the synthesis of a series of head-to-tail cyclic BODIPY oligomers **1.76a**-**1.76c**. These were formed through reaction of dipyrromethene **1.75** with boron trichloride to form a more reactive BCl$_2$-BODIPY intermediate, followed by self-condensation to form the supramolecular *N,N,O,O*-BODIPYs **1.76a**-**1.76c**.[98]
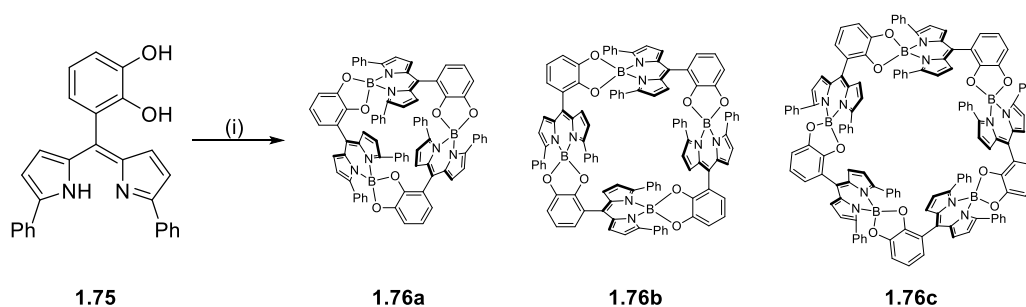
Scheme 1.24: Reagents and conditions: (i) BCl$_3$, ^{i}Pr$_2$NEt, toluene, reflux, 16 h (**1.76a** 2%, **1.76b** 5%, **1.76c** 0.3%).

A further example of this methodology was described by Holten *et al.*,[99] wherein chelation of a dipyrromethene with three dialkylboranes resulted in the synthesis of a series of 4-functionalised BODIPYs. The scope of this methodology was subsequently extended by Thompson *et al.*,[100] in which monofluoroaryl *N,N,F,C*-BODIPY **1.78a** and *N,N,C,C*-BODIPYs **1.78b** and **1.78c** were produced through treatment of the HBr salt of dipyrromethene **1.77** with C$_6$F$_5$BF$_2$ (**1.78a**), (C$_6$F$_5$)$_2$BCl (**1.78b**) or perfluorinated 9-bromoborafluorene (**1.78c**).
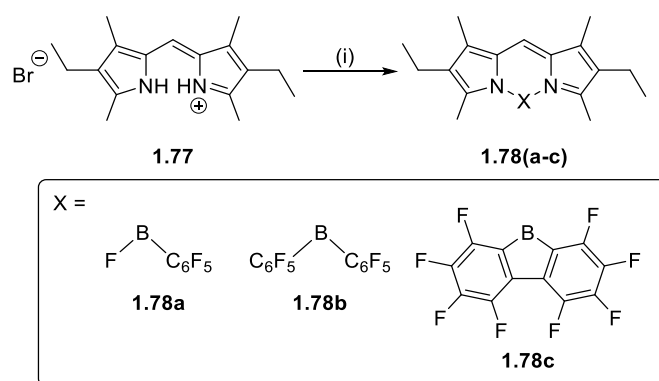
Scheme 1.25: Reagents and conditions: (i) NEt$_3$, CH$_2$Cl$_2$, 15 min, then C$_6$F$_5$BF$_2$, (C$_6$F$_5$)$_2$BCl or perfluorinated 9-bromoborafluorene, 15 min (**1.78a** 48%, **1.78b** 89%, **1.78c** 62%).

Nabeshima *et al.* have described an alternative strategy which does not involve the use of reactive boranes as chelating reagents. Instead dipyrromethenes have been shown to chelate a range of boronic acids. For example reaction between dipyrromethene **1.79** and phenylboronic acid gave *N,N,O,C*-BODIPY **1.80** following chelation and intramolecular B-O bond formation.[101]

23
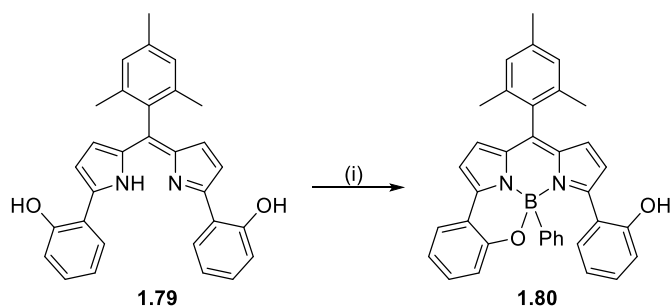
Scheme 1.26: Reagents and conditions: (i) phenyl boronic acid, CHCl₃, reflux, 3 h (quant.).

This approach has been employed by Nabeshima *et al*. to synthesise a number of *N,N,O,C*-BODIPY systems.[102,103] A further development was described by Jiao *et al.* through their 'one-pot' synthesis of *N,N,O,C*-BODIPYs through reaction between pyrrole and a 2-ketopyrrole, followed by an *in situ* chelation of the dipyrromethene formed with a boronic acid.[104]

1.2.2.4 Cross-Coupling Reactions of BODIPYs

Palladium catalysed cross-coupling reactions to make carbon-carbon bonds are widely used in organic chemistry, and have unsurprisingly found significant use in the synthesis of BODIPYs. Suitably halogenated BODIPYs have been shown to undergo Suzuki-Miyaura, Migita-Kosugi-Stille, Mizoroki-Heck and Sonogashira cross-coupling reactions, with many of these examples coming from Dehaen and coworkers.[105] Palladium cross-couplings in all positions (3,5-positions,[84,105–108] 2,6-positions,[103,106,107,109–111] 1,7-positions[63,112–114] and 8-position[64,113,115–119]) of the BODIPY framework have been reported.

Jiao, Hao *et al.* have examined the regioselectivity of palladium cross-couplings, including Suzuki-Miyaura, Migita-Kosugi-Stille, Mizoroki-Heck and Sonogashira cross-couplings. It was found that when 2,3,5,6-tetrabromo-BODIPY **1.81** was reacted under a variety of palladium cross-coupling conditions, there was always a strong preference for 3,5-addition. The tetra-substituted BODIPYs were accessible when an excess of the coupling reagent was used, along with more forcing reaction conditions.
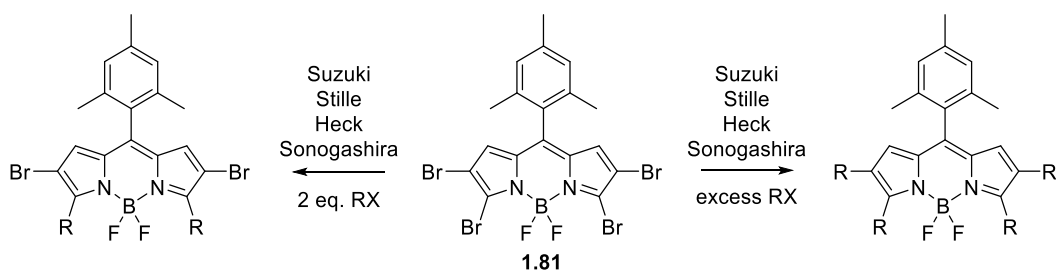
Scheme 1.27: Regiochemistry of palladium cross-coupling reactions with 2,3,5,6-tetrabromo-BODIPY **1.81**.

In their seminal work, Ortiz *et al*. have shown that Negishi cross-coupling reactions can be performed on 3,5-dihalo-BODIPYs. Reaction of 3,5-dichloro-BODIPY **1.37** or 3,5-dibromo-BODIPY **1.82** under Negishi cross-coupling conditions resulted in the formation of 3- and 3,5-substituted BODIPYs containing alkyl, aryl and alkynyl substituents.[120] The Negishi cross-coupling of 1,7- and 8-halo-BODIPYs has subsequently been described.[121]

1.37 X = Cl
1.82 X = Br
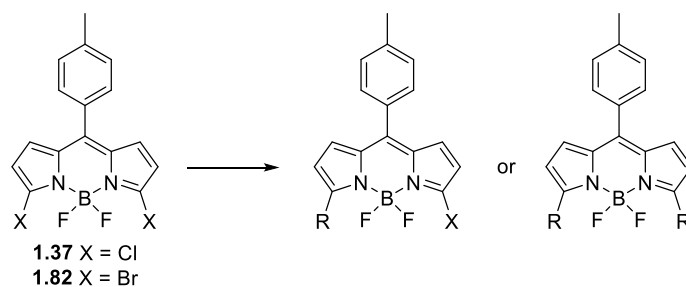
Entry	X	R$_2$Zn or RZnBr	R	Product	Yield/%
1	Br	ZnEt$_2$	Et	di	86
2	Br	ZnEt$_2$	Et	mono	61
3	Cl	ZnEt$_2$	Et	di	73
4	Cl	ZnEt$_2$	Et	mono	75
5	Cl	ZnMe$_2$	Me	di	80
6	Cl	ZnMe$_2$	Me	mono	77
7	Cl	BuZnBr	Bu	di	52
8	Cl	BuZnBr	Bu	mono	62
9	Cl	BnZnBr	Bn	di	20
10	Cl	BnZnBr	Bn	mono	18
11	Cl	PhZnBr	Ph	di	56
12	Cl	PhZnBr	Ph	mono	70
13	Cl	PhC≡CZnBr	PhC≡C	di	54
14	Cl	PhC≡CZnBr	PhC≡C	mono	56
15	Cl	TMSC≡CZnBr	TMSC≡C	di	65

Table 1.1: Negishi cross-couplings of 3,5-dihalo BODIPYs **1.37** and **1.82**. Reagents and conditions: Pd(PPh$_3$)$_2$Cl$_2$ (10 mol %), R$_2$Zn or RZnBr, toluene.

1.3 Chirality in BODIPYs

One of the main considerations in the investigation of BODIPYs as CPL-SOMs is the induction of chirality to these planar fluorophores. There have been a number of reports of chiral BODIPY systems

before the exploration of BODIPYs as CPL-SOMs. We will now discuss some of the methodologies which have been used to induce chirality in mono-BODIPY systems.

1.3.1 Strategies to induce chirality in BODIPYs

1.3.1.1 BODIPYs with chiral substituents

The most obvious method to induce chirality in BODIPYs is the covalent attachment of chiral substituents to the BODIPY core. One example of the application of this methodology was described by Grimme, Daub *et al.* in their synthesis of the 1,1'-binapthyl (BINOL) derived BODIPY **1.84**.[122] BODIPY **1.84** was synthesised through condensation between an enantiomerically pure BINOL carbaldehyde precursor **1.83** and 2,4-dimethyl pyrrole **1.12**. Subsequent oxidation and chelation afforded an enantiomerically pure sample of BODIPY **1.82**.
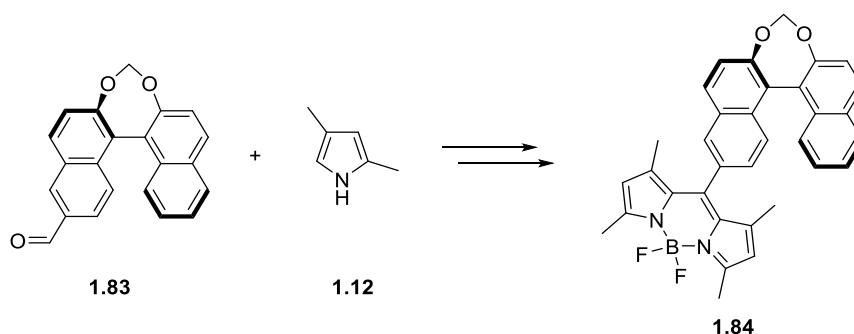
Scheme 1.28: Synthesis of 1,1'-binapthyl (BINOL) derived BODIPY **1.84**.

The chiroptical properties of enantiomerically pure BODIPY **1.84** were then investigated. The electronic circular dichrosim (ECD) spectrum showed a number of short wavelength transitions corresponding to the BINOL moiety, as well as a longer wavelength absorption corresponding to the BODIPY S_0-S_1 transition (λ = 495 nm). In the ECD spectrum, a moderate positive Cotton effect was observed ($\Delta\varepsilon_{max}$ = +10 L mol^{-1}cm^{-1}) in the S_0-S_1 absorption band of the BODIPY core. This result supports the notion that the inclusion of chiral substituents successfully induces chirality in BODIPY systems.

1.3.1.2 BODIPYs with a chiral boron centre

A further methodology to induce chirality in BODIPY systems is the assembly of a BODIPY with a chiral boron centre. Ulrich, Ziessel *et al*. disclosed the first example of a BODIPY containing a chiral boron centre (named *B**-BODIPY).[123] The design requirements of *B**-BODIPYs outlined by Ziessel, Ulrich *et al*. included:

- an asymmetrical BODIPY core,
- a polar group in the 3- or 5-position of the BODIPY capable of interacting with the boron centre and

- a polyaromatic moiety to induce steric hindrance around the boron centre.

Thus racemic *B**-BODIPY **1.86** was synthesised in a multi-step procedure from the corresponding parent BODIPY **1.85**. The first step was to displace one of the fluorine atoms through reaction of BODIPY **1.85** with napthylmagnesium bromide at low temperature. This was then followed by selective oxidation of the 5-methyl group with DDQ to desymmetrise the BODIPY core. The resulting 5-formyl moiety formed an intramolecular CH···F hydrogen bond, which was confirmed by the observation in the ^{1}H NMR spectrum of long-range coupling between the proton of the formyl moiety and the fluorine atom of the BF$_2$ moiety.
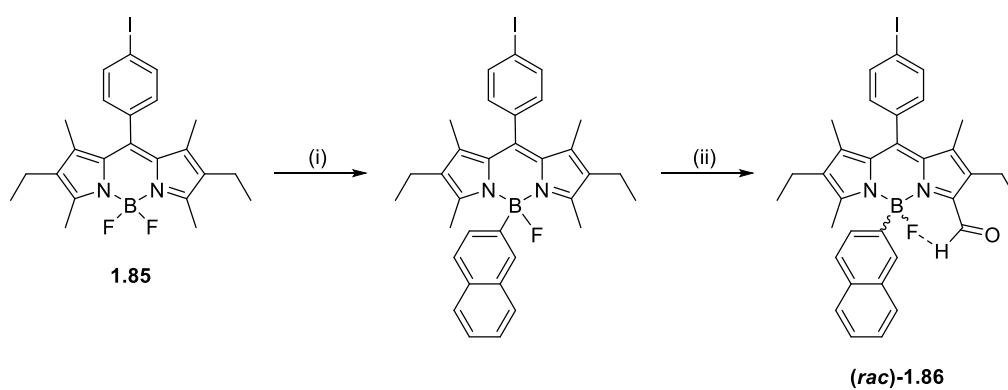
Scheme 1.29: Reagents and conditions: (i) napthylmagnesium bromide, THF, 20 °C (25%); (ii) DDQ, THF/H$_2$O, 0 °C (61%).

Following resolution by chiral HPLC (Chiralcel-OD, hexane/2-propanol), the ECD spectra of the corresponding enantiomers were obtained. A strong Cotton effect was observed in the short wavelength transitions, which are associated with the carbonyl group. However the S$_0$-S$_1$ transition band of the BODIPY chromophore only gave a weak signal in the ECD spectrum.

1.3.1.3 Axially chiral BODIPYs

The highly aromatic, planar structure of the BODIPY core lends itself well to the induction of axial chirality. The formation of atropisomers based on the BODIPY architecture can be achieved through both the desymmetrisation of the BODIPY core and the inclusion of a rotationally restricted BODIPY-aryl bond. For example Hall *et al*. have described the synthesis of axially chiral BODIPY **1.29** (section 1.2.1.2). The axial chirality in this system arises from the lateral differentiation of the BODIPY core (due to the 2-ethyl acrylate moiety) and the restricted rotation of the 8-aryl substituent (due to a methyl-methyl clash).
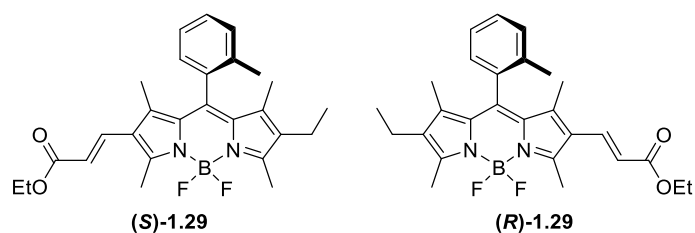
Figure 1.7: (*R*)- and (*S*)- enantiomers of the axially chiral BODIPY **1.29**.

Resolution of the (*R*)- and (*S*)- enantiomers of BODIPY **1.29** was achieved through semi-preparative chiral HPLC (Chiralpak, AD-H, heptane/2-propanol). Subsequently the ECD spectra of the resolved enantiomers was measured, however there was no significant Cotton effect observed in the absorption band corresponding to the S_0-S_1 transition of the BODIPY. Instead the only significant Cotton effect was observed in the short wavelength transitions corresponding to the 8-aryl substituent.

1.3.1.4 Helically chiral BODIPYs

The group of Burgess *et al.* have described the synthesis of *N,N,O,O*-BODIPY **1.64** (section 1.2.2.3).[79] In this system helical chirality arises from the tetrahedral geometry at boron, which ensures that the aryl rings are twisted to direct the B-O bonds to opposite faces of the planar BODIPY core. The racemic mixture of (*P*)- and (*M*)-**1.64** was shown to be separable by chiral HPLC (Pirkle covalent (*S,S*) whelk-01, hexane/2-propanol), however isolation of the single enantiomers was not achieved and thus no chiroptical measurements were made.
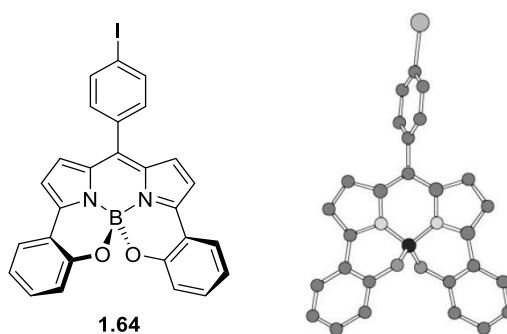
Figure 1.8: Helically chiral *N,N,O,O*- BODIPY **1.64** ((*P*)-enantiomer shown).

Following this work, several other helically chiral *N,N,O,O*-BODIPY systems have been disclosed.[80,81,124] However in these instances the bathochromic shift induced by the highly constrained and conjugated ring system was the focus of the discussion, rather than the chiroptical properties of this BODIPY architecture.

Subsequently similar helically chiral BODIPY systems were disclosed wherein only one of the *ortho*-phenolic moieties is chelated to the central boron atom. For example, Nabeshima *et al.* reported the

synthesis of the *N,N,O,C*-BODIPY **1.80** through the chelation of the corresponding dipyrromethene by an aryl boronic acid (section 1.2.2.3).[125]
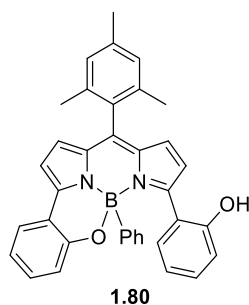
Figure 1.9: Helically chiral *N,N,O,C*-BODIPY **1.80**.

More recently, Nabeshima *et al.* have reported the synthesis of a similar helically chiral *N,N,O,C*-BODIPY system.[103] An initial Suzuki-Miyaura cross-coupling between 2-bromo-BODIPY **1.87** and the biaryl boronic acid **1.88** gave BODIPY **1.89**. The following steps included: an oxidative annulation of BODIPY **1.89** and removal of the BF$_2$ moiety using anhydrous FeCl$_3$, demethylation of the methoxy substituents with boron tribromide and finally rechelation by phenylboronic acid to form *N,N,O,C*-BODIPY **1.90**.
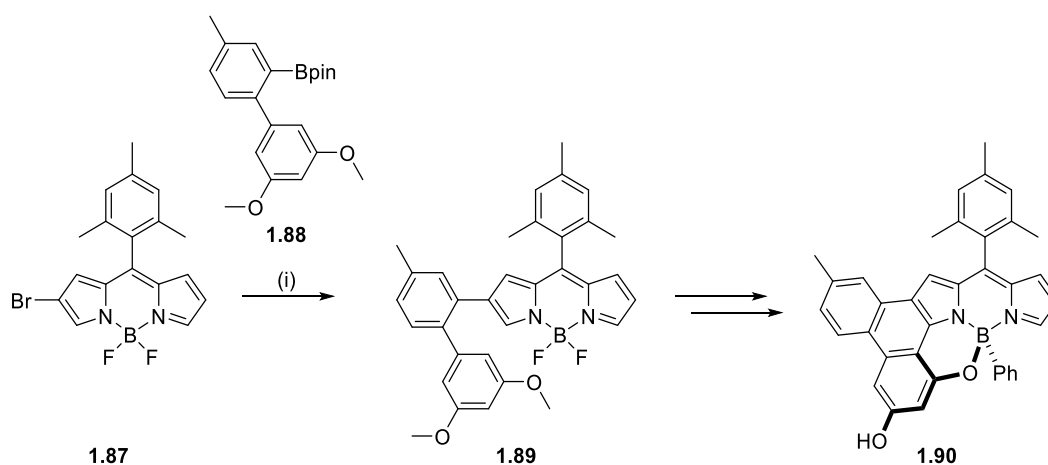
Scheme 1.30: Reagents and conditions: (i) **1.88**, Pd$_2$(dba)$_3$, ᵗBu$_3$PH.BF$_4$, Cs$_2$CO$_3$, THF, H$_2$O, R.T., 16 h (quant.).

Following resolution of the enantiomers of *N,N,O,C*-BODIPY **1.90** by chiral HPLC (Daicel Chiralpak IA, hexane/CHCl$_3$), mirror image ECD spectra were obtained. A moderate Cotton effect ($\Delta\varepsilon_{max} = \pm 20$ L mol^{-1}cm^{-1}) was observed in the S$_0$-S$_1$ transition of the BODIPY chromophore (λ = 655 nm), however no CPL studies were reported on this system.

1.3.2 CPL-active BODIPYs

As we have seen, the induction of chirality to BODIPYs can be achieved through a number of different strategies. However in order for a BODIPY system to be applicable as a CPL-SOM, a CPL signal must be observable upon irradiation. We will now discuss some chiral BODIPY systems which are CPL-emissive.

1.3.2.1 BODIPYs with chiral substituents

The first report of CPL emission from a BODIPY fluorophore was described by Gossauer *et al*., in studies into the urobilin derivative BODIPY **1.91**.[126] The ECD spectrum of the non-racemisable BODIPY **1.91** showed a Cotton effect in the long-wavelength absorbance band corresponding to the S_0-S_1 transition of the BODIPY fluorophore ($\lambda \approx 535$ nm), suggesting that the peripheral chiral carbon centres are sufficient to induce chirality to the BODIPY chromophore. Interestingly it was found that upon changing the solvent from CHCl$_3$ to DMF, inversion of the Cotton effect was observed in the long wavelength transition at approximately 535 nm. This indicates that there is a conformational change in BODIPY **1.91** upon solvation in a polar solvent, due to the competition between intramolecular NH···F hydrogen bond in CHCl$_3$ and intermolecular NH···F hydrogen bond in DMF. Furthermore CPL emission was recorded from urobilin-derived BODIPY **1.91** in CHCl$_3$, and a g_{lum} value of +0.94×10^{-3} was measured. Thus BODIPY **1.91** represents the first chiral BODIPY system from which CPL emission was reported.

1.91 in CH$_2$Cl$_2$ **1.91** in DMF
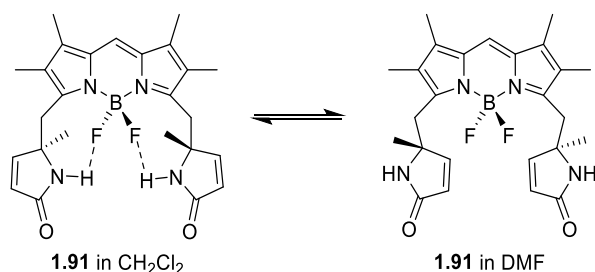
Figure 1.10: Molecular structure of urobilin-derived BODIPY **1.91**, showing the suggested conformational change upon solvation in non-polar (left, CHCl$_3$) and polar (right, DMF) solvents.

1.3.2.2 Axially chiral BODIPYs.

The group of de la Moya reported the enantioselective synthesis of the axially chiral, BINOL-derived BODIPY **1.92**.[127] Substitution of the fluorine atoms of BODIPY **1.57** by (*R*)- or (*S*)- BINOL through the use of aluminium trichloride (section 1.2.2.3) afforded enantiopure samples of (*R*)- and (*S*)-BODIPY **1.92** in high yields. The commercial availability of the precursors (i.e. achiral *F*-BODIPYs and enantiopure 1,1'-biphen-2-ols) make this an accessible route to enantiopure, chiral BODIPYs.
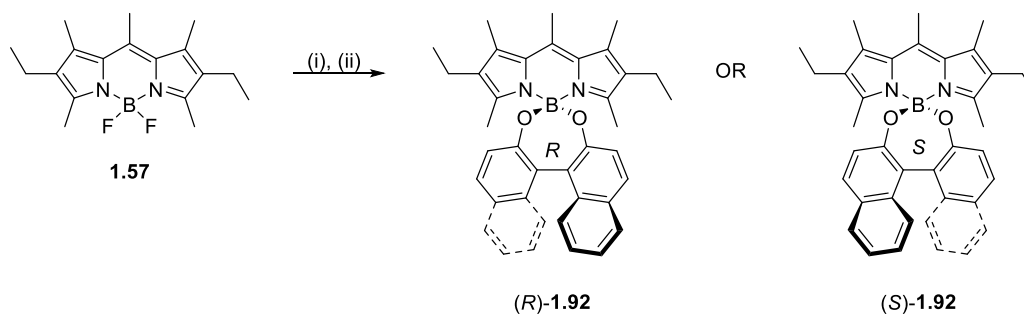
Scheme 1.31: Reagents and conditions: (i) AlCl$_3$, DCM, reflux; (ii) either (*R*)- or (*S*)-1,1'-bi(2-napthol), R.T., 6 h ((*R*)-**1.92** 60%, (*S*)-**1.92** 58%).

A study of the chiroptical properties of (*R*)- and (*S*)-BODIPY **1.92** was conducted. In the ECD spectra, a strong Cotton effect was observed in the BODIPY S$_0$-S$_1$ transition ($\lambda \approx 525$ nm), which was opposite for each enantiomer. This suggests that the BINOL moiety is successfully inducing chirality to the achiral BODIPY fluorophore. Further evidence to support this is the successful measurement of CPL emission from the enantiomers of BODIPY **1.92** ($|g_{lum}| \approx 10^{-3}$). The CPL maxima ($\lambda \approx 570$ nm) were consistent with the emission maxima recorded for the BODIPY fluorophore, indicating that the CPL emission arises from the BODIPY moiety, and not the BINOL moiety.

1.3.2.3 Helically chiral BODIPYs

Inspired by the work of Burgess *et al.*,[79] the group of Hall, Knight *et al.* synthesised a series of *N,N,O,O*-BODIPYs **1.93**-**1.96** to evaluate the potential use of these systems as CPL-SOMs.[84] The *meso*-aryl substituents are electronically separated from the BODIPY chromophore, however subtle changes to the photophysical properties are evident due to the steric influence of these groups on the conformational flexibility of the BODIPY core.

1.93	**1.94**	**1.95**	**1.96**
$|g_{lum}| = 4.7 \times 10^{-3}$	$|g_{lum}| = 3.3 \times 10^{-3}$	$|g_{lum}| = 4.3 \times 10^{-3}$	$|g_{lum}| = 4.2 \times 10^{-3}$
$\phi = 0.65$	$\phi = 0.73$	$\phi = 0.52$	$\phi = 0.28$
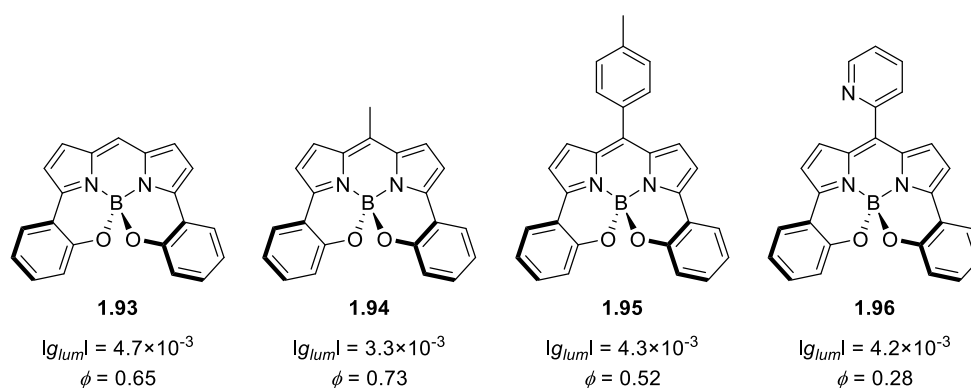
Figure 1.11: Helically-chiral *N,N,O,O*-BODIPYs **1.93**-**1.96** ((*M*)-enantiomer shown in each case) and the associated g_{lum} values and fluorescence quantum yields.

The *N,N,O,O*-BODIPYs **1.93**-**1.96** were formed as racemic mixtures, and so following resolution of the enantiomers by chiral HPLC (Daicel Chiralpak OB, toluene/*n*-hexane (**1.93**); Daicel Chiralpak OD-H, *i*-

PrOH/*n*-hexane (**1.94**-**1.96**) chiroptical measurements were performed. ECD spectra of the resolved enantiomers showed strong Cotton effects in the transitions corresponding to the S_0-S_1 transition of the BODIPY chromophore. Moreover red-shifted CPL emission was observed from all four related systems (($|g_{lum}|$ = 4.7×10^{-3}, 3.3×10^{-3}, 4.3×10^{-3} and 4.2×10^{-3} for **1.93-1.96** respectively), with the emission maxima corresponding to the S_1-S_0 transition of each BODIPY chromophore. In the case of *N,N,O,O*-BODIPY **1.93**, the relatively large $|g_{lum}|$ combined with the high fluorescence quantum yield gave an overall quantum efficiency ($|g_{lum}| \cdot \phi_F$) of 3×10^{-3}. Thus at the time of publishing, *N,N,O,O*-BODIPY **1.93** represented the most efficient single-fluorophore, red-emitting CPL-SOM described.[18,128]

1.4 Project Aims

The aim for this thesis was to synthesise novel chiral BODIPYs, to explore their chiroptical properties (with a focus on CPL) *en route* to the development of new small organic fluorophores capable of solution phase CPL (CPL-SOMs).

In chapter 2 we will report the results of our initial investigations into the synthesis of the *N,N,O,O*-BODIPYs described by Hall *et al.* (figure 1.11), with a focus on both the improvement of synthetic yields and the synthesis of further analogues. We hoped to thus identify new chiral BODIPYs which would be CPL-emissive and through the study of their chiroptical properties, including g_{lum}, gain insight into CPL-SOM BODIPY design. Furthermore in chapter 2 we will seek to employ computational techniques to support our experimental findings, and thus hope to validate the computational method for predicting the g_{lum} of helically chiral BODIPYs.

In chapter 3 we will discuss our attempts to produce helically chiral BODIPYs with enhanced g_{lum} values. Our hypothesis was that an increase the orbital angular momentum of helically chiral BODIPYs would lead to an increase in the magnetic (**m**) transition dipole moment, in turn leading to an increase in g_{lum}. We planned to achieve this increase in orbital angular momentum by the induction of sulfur atoms to the helically chiral BODIPY architecture. Therefore in chapter 3 we will discuss the synthetic methodologies we have examined to introduce sulfur atoms into helically chiral BODIPYs.

Finally in chapter 4 we will report our investigations into the effect that modulation of the helical pitch of helically chiral *N,N,O,O*-BODIPYs has on the angle (τ) between the magnetic (**m**) and electronic (**μ**) transition dipole moments. We thought that through the extension of the BODIPY π-system we would be able to exhibit control over the helical pitch, and thus over the angle τ, potentially leading to the development of helically chiral *N,N,O,O*-BODIPYs with enhanced g_{lum} values. Thus in chapter 4 we will discuss the synthesis and chiroptical characterisation of an *N,N,O,O*-BODIPY with an extended π-system.

Chapter 2. Synthesis and Chiroptical Characterisation of *N,N,O,C*-BODIPYs

2.1 Introduction

2.1.1 Aims and molecular design principles

In this chapter we will discuss our progress towards investigating new chiral BODIPYs as CPL-SOMs. A significant challenge in the design of new CPL-SOMs is that they often exhibit low CPL quantum efficiencies ($|g_{lum}| \cdot \phi_F$) due to low luminescence dissymmetry factors (g_{lum}). In order to produce BODIPY-based CPL-SOMs with improved g_{lum} values, there are some fundamental design principles which must be considered.

2.1.1.1 Twisting deformations/chiral perturbations of the inherently planar BODIPY core

The first of these design principles was highlighted by Gossauer *et al.*, in their comparison of three chiral BODIPY derivatives. Gossauer *et al*. reported the first example of CPL emission from a chiral BODIPY **1.91**, derived from urobilin (g_{lum} = +0.94(±0.1)×10^{-3}).[126] In a later report from the same group, two further homochiral dyes were described, containing asymmetric phenyl substituents at either the 8- (**2.2**) or 3,5-positions (**2.1**)[129]. However neither of these two dyes displayed an appreciable CPL signal. Comparison of the crystal structures of these three chiral BODIPY revealed that only the urobilin derivative **1.91** contained a twisting deformation of the planar BODIPY core. This led Gossauer to speculate that "both a "chiral perturbation" of an inherently planar dipyrrin chromophore and a twisting deformation of the latter may (be required to) give rise to high optical activity".
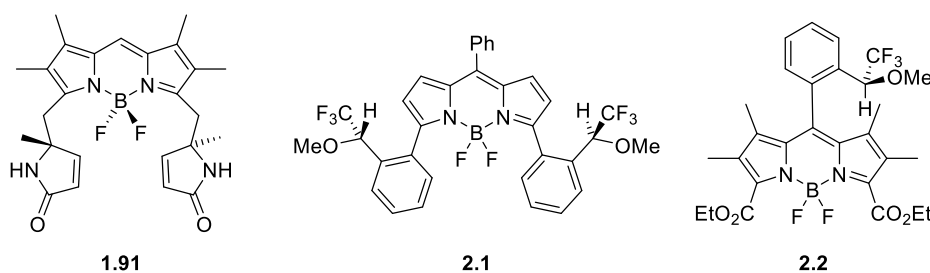
Figure 2.1: Early chiral BODIPYs: urobilin based BODIPY **1.91** and homochiral BODIPYs **2.1** and **2.2**.

Thus in our planned work towards new CPL-SOM BODIPYs, we aim to design and synthesise BODIPY dyes which are both chiral and possess a twisting deformation of the planar BODIPY core.

2.1.1.2 Controlling the magnetic and electric transition dipole moments in CPL-SOMs

In the design of new BODIPY based CPL-SOMs we must also consider the underlying physical chemistry principles which determine the g_{lum} value for a compound. The luminescence dissymmetry factor is theoretically defined by the equation:

$$g_{lum} = \frac{4(\boldsymbol{\mu} \cdot \boldsymbol{m} \cdot cos\tau)}{(\boldsymbol{\mu}^2 + \boldsymbol{m}^2)}$$

Where **m** and **μ** are the magnetic and electric transition dipole moment vectors and τ is the angle between them. The maximum value of g_{lum} is 2, and can only be obtained when **m** is equal in magnitude to **μ**, and when τ = 0° or 180°. In chiral lanthanide complexes, g_{lum} values are typically large. This is a consequence of the magnetic-dipole-allowed, electric-dipole-forbidden $f{\rightarrow}f$ transitions[130–133] common to these complexes, which result in magnetic (**m**) and the electronic (**μ**) transition dipole moments of similar magnitudes. Small g_{lum} values are common for typical CPL-SOMs as **m** is usually several orders of magnitude smaller than **μ** for the π-π* transition of most simple organic fluorophores. Therefore to increase $|g_{lum}|$ for a typical CPL-SOM, the magnitude of the magnetic transition dipole moment ($|\boldsymbol{m}|$) must be increased, and the magnitude of the electric transition dipole moment ($|\boldsymbol{\mu}|$) must be decreased, so that these vectors are of a similar magnitude. Additionally τ should be as close to either 0° or 180° as possible.

Thus in our planned work towards new CPL-SOM BODIPYs, we aim to control these fundamental molecular properties, decreasing $|\boldsymbol{\mu}|$ whilst simultaneously increasing $|\boldsymbol{m}|$ and controlling the angle between these vectors (τ).

2.1.1.3 Rapid evaluation of g_{lum} by CD spectroscopy

In a recent review article from Mori *et al.*[134], the relationship between g_{abs} and g_{lum} was examined. These values were correlated for a range of CPL-SOMs, including cyclophanes, helicenes and biaryls. Most importantly for our work, the relationship between g_{abs} and g_{lum} were also examined for a range CPL-SOM BODIPYs (figure 2.2).
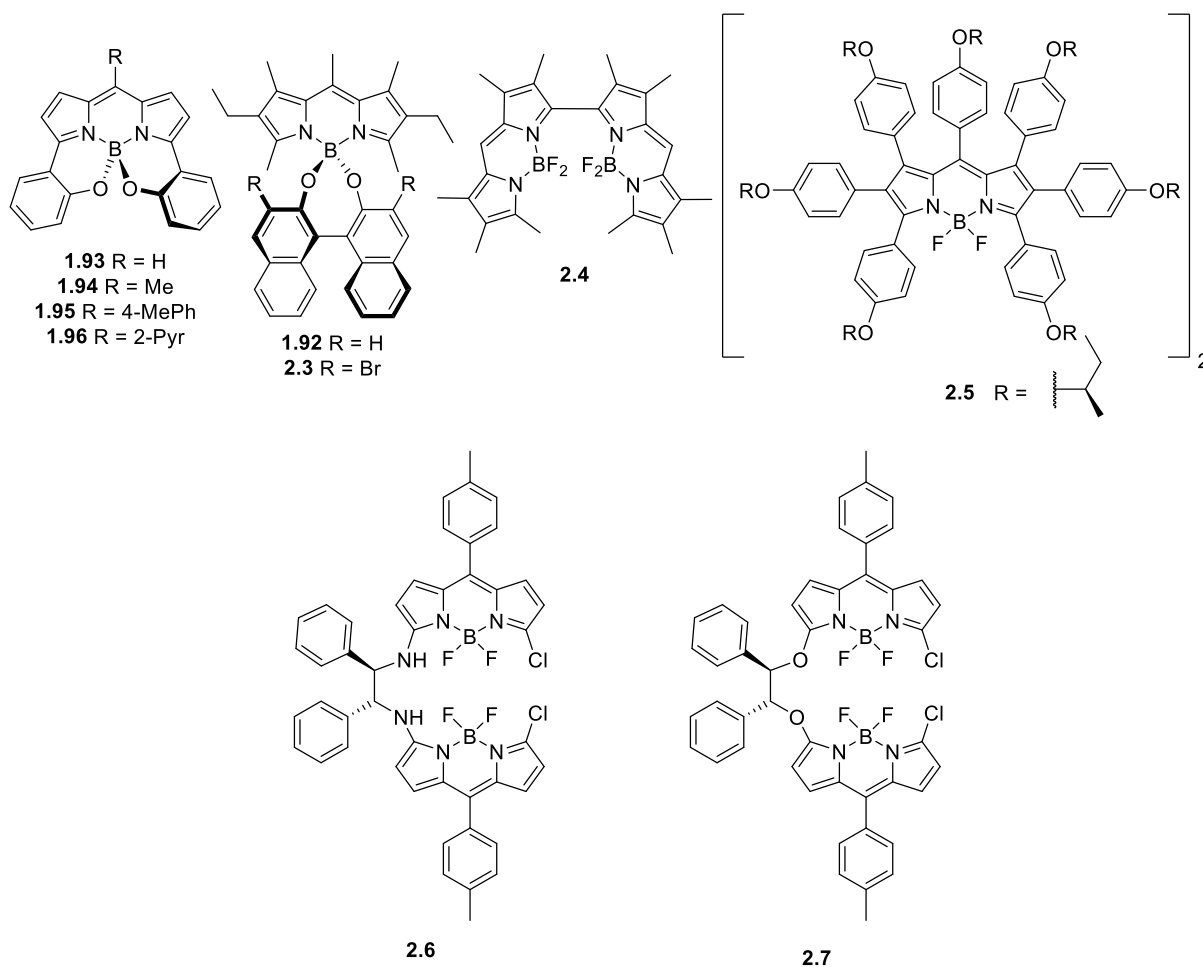
Figure 2.2: CPL-active BODIPYs for which g_{abs} and g_{lum} are correlated.[134]

Mori and co-workers found that for rigid homochiral mono(BODIPY)s (**1.93-1.96**, **1.92** and **2.3-2.5**) g_{abs} and g_{lum} exhibit a good linear correlation (ie. $|g_{lum}| = 1.02 \times |g_{abs}|$ ($r^2=0.90$)). However flexible homochiral di(BODIPY)s (**2.6** and **2.7**) deviate from this correlation, and the inclusion of these data points results in a worse linear correlation ($|g_{lum}| = 0.77 \times |g_{abs}|$ ($r^2=0.49$)). It is postulated that the linear correlation between g_{abs} and g_{lum} factors is much improved for rigid chiral BODIPYs, due to significant structural similarity between the S_0 ground states and the excited S_1 states of these molecules. This similarity is a result of minimal vibrational relaxation of the excited S_1 state.

Therefore in our planned work towards new CPL-SOM BODIPYs we will attempt to use the measurement of g_{abs} as a preliminary assessment of the potential for high g_{lum}. Since we are planning to synthesise rigid, homochiral mono(BODIPY)s we will attempt to corroborate the good linear correlation between g_{abs} and g_{lum} for these systems, as observed by Mori.

2.1.1.4 Chapter Aims

Our aim for this chapter is to examine the design of new CPL-SOM BODIPYs, which include induced twists in the planar BODIPY core. We will also attempt to control the magnitudes of the electric (μ)

and magnetic (**m**) dipole moments and the angle between them (τ) to maximise possible g_{lum} for these systems.

As a starting point for our work we first decided to re-examine helically chiral *N,N,O,O*-BODIPY **1.93** (figure 2.3). The *N,N,O,O*-BODIPY architecture was first reported by Burgess *et al.*[79], and subsequently the *N,N,O,O*-BODIPYs **1.93** and **1.95** were reported by Hall and co-workers. In particular *N,N,O,O*-BODIPY **1.93** was shown to be an efficient emitter of CPL ($|g_{lum}| = 4.7×10^{-3}$)[84]. In keeping with the design principles outlined above, *N,N,O,O*-BODIPY **1.93** has a chirally perturbed BODIPY core, with a twist angle of 11.2° between the planes of two pyrrolic rings. We therefore thought that the *N,N,O,O*-BODIPY architecture would be an appropriate starting point to validate the design principles outlined in section 2.1.1.
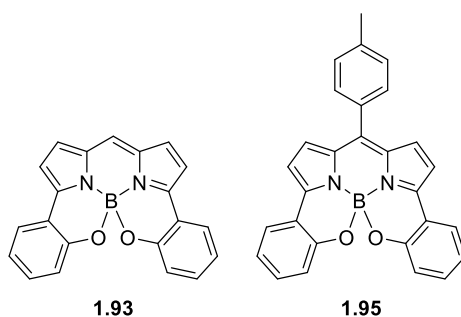
Figure 2.3: Helically chiral *N,N,O,O*-BODIPY **1.93** and *N,N,O,O*-BODIPY **1.95**.

In the original work by Hall *et al.*, the synthetic routes towards the helically chiral *N,N,O,O*-BODIPYs were un-optimised and as such had poor overall yields. Therefore our initial plan was to re-examine the synthesis of *N,N,O,O*-BODIPY **1.95** in order to improve yields over some of the more problematic synthetic steps. We reasoned that this would allow us to efficiently synthesise further analogues of the *N,N,O,O*-BODIPYs, detailed study of which would allow us an improved understanding of the key molecular properties (**m**, **μ** and τ), and thus the required design constraints for the production of homochiral mono(BODIPY) CPL-SOMs with improved $|g_{lum}|$.

2.1.2 Synthetic strategy towards an *N,N,O,O*-BODIPY

2.1.2.1 Planned synthesis of *N,N,O,O*-BODIPY **2.13**

Aryl substituents at the 8-position of BODIPYs are electronically separated from the chromophore, and as such do not have a considerable impact on the photophysical properties. Since our ultimate aim is to use CPL-SOMs in CPL bioimaging, we wished to include a handle for possible late-stage functionalisation. We therefore elected to incorporate an aromatic ring at the 8-position, containing a methyl ester functional group, which can be used as a functionalisation handle.

In order to synthesise *N,N,O,O*-BODIPY **2.13**, we planned to first synthesise the intermediate 3,5-dibromo-BODIPY **2.11** (scheme 2.1). In Hall's reported synthesis of *N,N,O,O*-BODIPY **1.95**, the total overall yield over the three steps (condensation, bromination, oxidation and chelation) was 47%.[84] We aimed to improve the overall yield of this approach to 3,5-dibromo-BODIPY **2.11**. In particular the condensation reaction had a poor yield (69%) and we looked to improve this step.
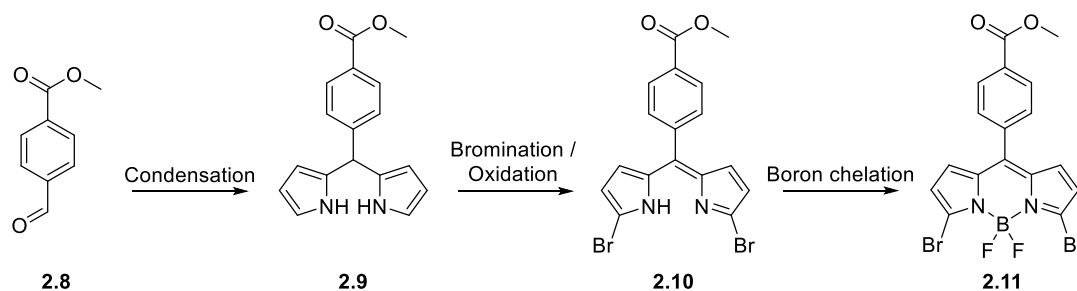
Scheme 2.1: Planned synthetic route to 3,5-dibromo-BODIPY **2.11**.

Following Hall's reported synthesis,[84] we planned to use a Suzuki-Miyaura cross-coupling between 3,5-dibromo-BODIPY **2.11** and 2-methoxyphenyl boronic acid to give 3,5-diaryl-BODIPY **2.12**. This would be followed by a double demethylation reaction and *in situ* double B-O bond formation to give *N,N,O,O*-BODIPY **2.13** (route A, scheme 2.2). We also considered an alternative approach involving the use of 2-hydroxyphenylboronic acid **2.13** (route B, scheme 2.2). We reasoned that this alternative approach should eliminate the need for a double demethylation step, since the double B-O bond formation event would occur *in situ* after the Suzuki-Miyaura cross-coupling was complete. We planned to test both route A and route B, and compare the overall obtained yields of *N,N,O,O*-BODIPY **2.13**.
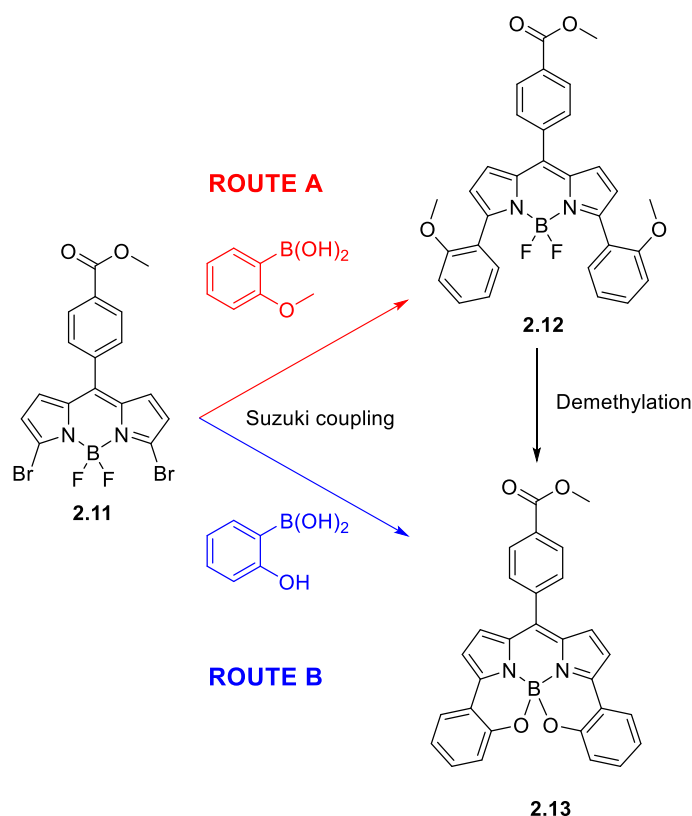
Scheme 2.2: Planned synthetic routes A and B to *N,N,O,O*-BODIPY **2.13**.

2.1.2.2 Synthesis of *N,N,O,O*-BODIPY **2.13**

In the previously reported synthesis of *N,N,O,O*-BODIPY **1.95**,[84] Lindsey's method[43] was used to perform the condensation between 4-methylbenzaldehyde and 1*H*-pyrrole (i.e. the use of a large excess of 1*H*-pyrrole). However this approach has a number of practical limitations, for example the removal of the residual excess pyrrole from the reaction mixture. Therefore we decided to evaluate alternative approaches to this key condensation step involving the use of stoichiometric amounts of the pyrrole condensation partner.

Therefore our first step was to examine the feasibility of an alternative condensation route, following a procedure optimised by Dehaen (section 1.2.1.2).[44] Dehaen's procedure involves an acid catalysed condensation reaction between a benzaldehyde and a pyrrole under aqueous conditions. The use of water as a solvent is key to success in this reaction, allowing precipitation of the product dipyrromethane during the course of the reaction. The precipitation of dipyrromethane from the reaction prevents the formation of higher oligomers, and therefore allows the use of close to stoichiometric amounts of the pyrrole condensation partner.

The first reaction we attempted was the condensation between benzaldehyde **2.8** and 1*H*-pyrrole (scheme 2.3) on a 1 mmol (280 mg) scale of benzaldehyde **2.8**. Immediately after the addition of 1*H*-

pyrrole to the reaction mixture, precipitation of dipyrromethane **2.9** began to occur. After four hours at room temperature no further precipitation was observed, indicating that the reaction was complete. In order to obtain an analytically pure sample of dipyrromethane **2.9**, we elected to perform purification by silica gel chromatography. Purification by silica gel chromatography, with dichloromethane as eluent, gave dipyrromethane **2.9** in an 88% yield. The structure of dipyrromethane **2.9** was confirmed by the observation of a set of signals in the ^{1}H NMR spectrum corresponding to the pyrrolic hydrogens typical of a C-2 substituted pyrrole (δ_H 6.75 ppm, m, 2H; 6.19 ppm, dd, 2H, J = 3.7, 3.2 Hz; 5.92 ppm, m, 2H) and a signal corresponding to the methyl group of the aryl ester (δ_H 3.93 ppm, s, 3H).

The condensation reaction between benzaldehyde **2.8** and 1*H*-pyrrole was repeated a number of times, at scales of up to 9 mmol of benzaldehyde **2.9** (2.5 g). Dipyrromethane **2.9** could be obtained in isolated yields of up to 90 %. In the case of the larger scale reactions, analysis of the crude ^{1}H NMR spectrum showed that dipyrromethane **2.9** could be isolated in high purity following a simple filtration step, thus we elected to forgo silica gel chromatography to improve experimental efficiency. Therefore dipyrromethane **2.9** was typically used in the next synthetic steps following purification by filtration.
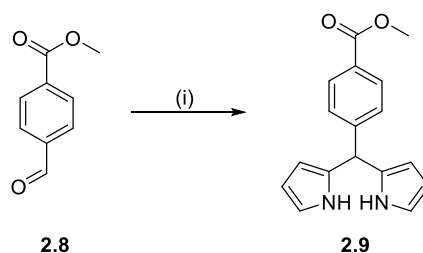
Scheme 2.3: Reagents and conditions: (i) 1*H*-pyrrole (3 eq.), HCl$_{(aq)}$ (0.05 M), R.T., 4 h (>90%).

The next synthetic step we wished to investigate was the one-pot bromination/oxidation of dipyrromethane **2.9**. We wished to dibrominate the 1,9-positions of dipyrromethane **2.9**, corresponding to the 3,5-positions of the target 3,5-dibromo-BODIPY **2.11**. The resulting bromo-groups of 3,5-dibromo-BODIPY **2.11** will be used in subsequent steps to introduce the required 3,5-aryl groups using Suzuki-Miyaura cross-coupling chemistry. To ensure selective 1,9-dibromination of dipyrromethane **2.9**, we planned to use the brominating agent NBS at low temperatures.[57,58]

Our initial attempts at this reaction resulted in complex mixtures of bromination products, from which we were unable to isolate the desired 1,9-dibrominated dipyrromethene **2.10**. Analysis of the ^{1}H NMR spectrum of a typical crude reaction mixture revealed that there were at least three different brominated dipyrromethenes formed as major products, shown by the presence of three overlapping peaks pertaining to the methyl groups of at least three different aryl methyl esters (δ_H 3.99-3.95 ppm,

figure 2.4). Further analysis of the ^{1}H NMR spectrum of the crude reaction mixture confirmed the presence of at least three different dipyrromethenes, through the observation of sets of signals corresponding to C-2,5 disubstituted and C-2,3,5 trisubstituted pyrrolic moieties, which we have attributed to the presence of a mixture of 1,9-dibrominated dipyrromethene **2.10**, 1,2,9-tribrominated dipyrromethene **2.14** and 1,2,8,9-tetrabrominated dipyrromethene **2.15** (figure 2.5).
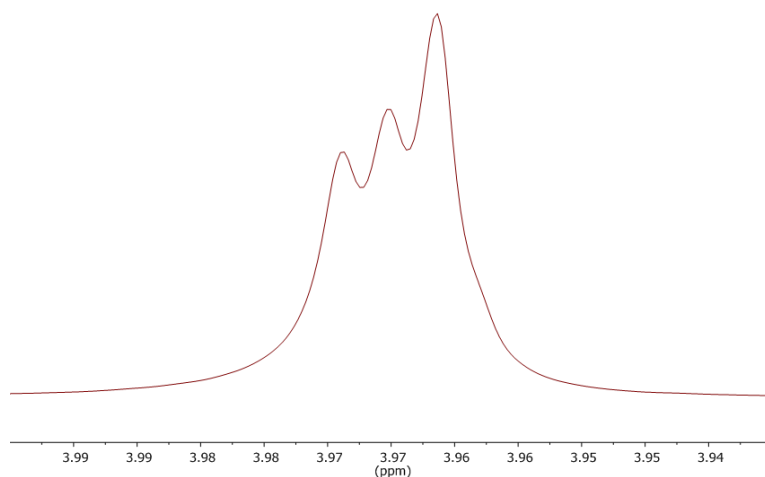
Figure 2.4: ^{1}H NMR spectrum of a crude reaction mixture of the bromination/oxidation of dipyrromethane **2.9**, showing three overlapping peaks pertaining to the methyl groups of at least three different aryl methyl esters.

(a)

(b)

2.10   2.14   2.15
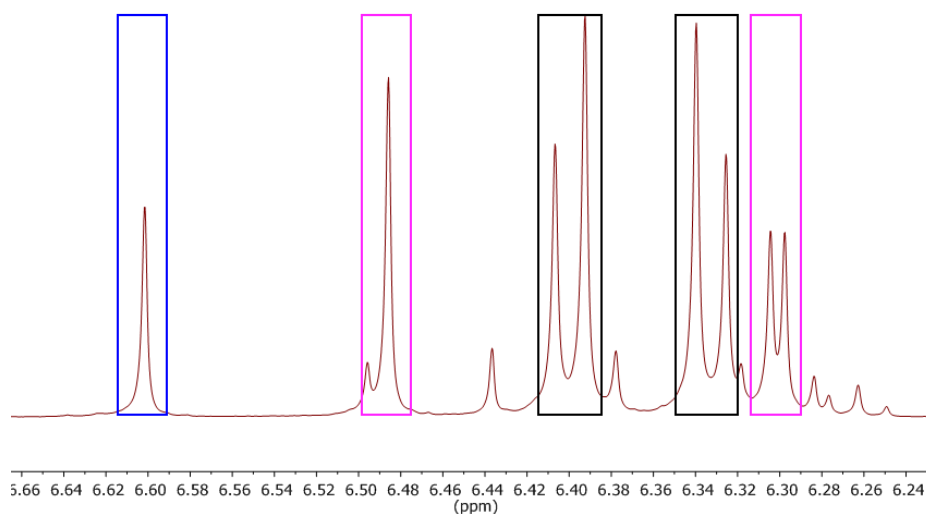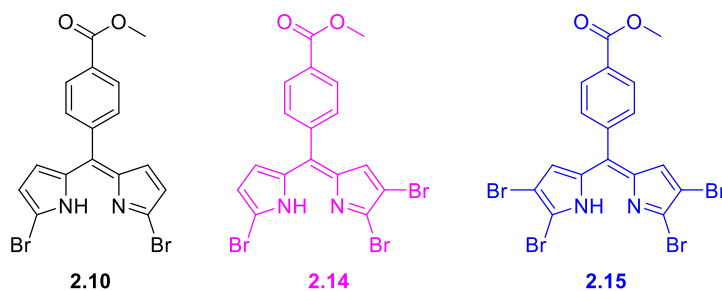
Figure 2.5: (a) ^{1}H NMR spectrum of a crude reaction mixture of the bromination/oxidation of dipyrromethane **2.9**, showing sets of signals corresponding to C-2,5 disubstituted and C-2,3,5 trisubstituted pyrrolic moieties; (b) brominated dipyrromethenes **2.10**, **2.14** and **2.15** proposed to be the products of the bromination/oxidation of dipyrromethane **2.9**.

Further analysis of the proposed brominated dipyrromethenes **2.10**, **2.14** and **2.15** was hindered due to their poor solubility in organic solvents, making separation by silica gel chromatography challenging. To confirm the formation of multiple brominated dipyrromethenes in the bromination/oxidation of dipyrromethane **2.9**, we elected to transform them into the corresponding brominated BODIPYs to facilitate isolation and further analysis. Thus we reacted the mixture of brominated dipyrromethenes **2.10**, **2.14** and **2.15** with boron trifluoride diethyl etherate in the presence of Hunig's base. Once boron chelation was complete, the resulting mixture of brominated BODIPYs (**2.11**, **2.16** and **2.17**) was then separated by silica gel chromatography.

Analysis of the ^{1}H NMR spectra of the three isolated brominated BODIPYs (**2.11**, **2.16** and **2.17**) allowed us to confirm their structures (figure 2.6). The ^{1}H NMR spectrum of BODIPY **2.11** showed the presence of an AB system consisting of a pair of roofed doublets pertaining to a C-2,5 disubstituted pyrrolic

moiety (δ_H 6.73 ppm, d, 2H, *J* = 4.2 Hz and 6.55 ppm, d, 2H, *J* = 4.2 Hz), suggesting a BODIPY with a 3,5-dibromination pattern. The ^{1}H NMR spectrum of BODIPY **2.17** showed the presence of a singlet peak (δ_H 6.85 ppm, s, 2H) corresponding to a C-2,3,5 trisubstituted pyrrolic moiety, consistent of a BODIPY with a 2,3,5,6-tetrabromination pattern. Finally analysis of the ^{1}H NMR spectrum of BODIPY **2.16** showed the presence of an AB system consisting of a pair of roofed doublets corresponding to a C-2,5 disubstituted pyrrolic moiety (6.60 ppm, d, 1H, *J* = 4.5 Hz). The appearance of a singlet peak (6.80 ppm) corresponding to a C-2,3,5 trisubstituted pyrrolic moiety allowed us to conclude that BODIPY **2.16** has a 2,3,5-tribromination pattern.
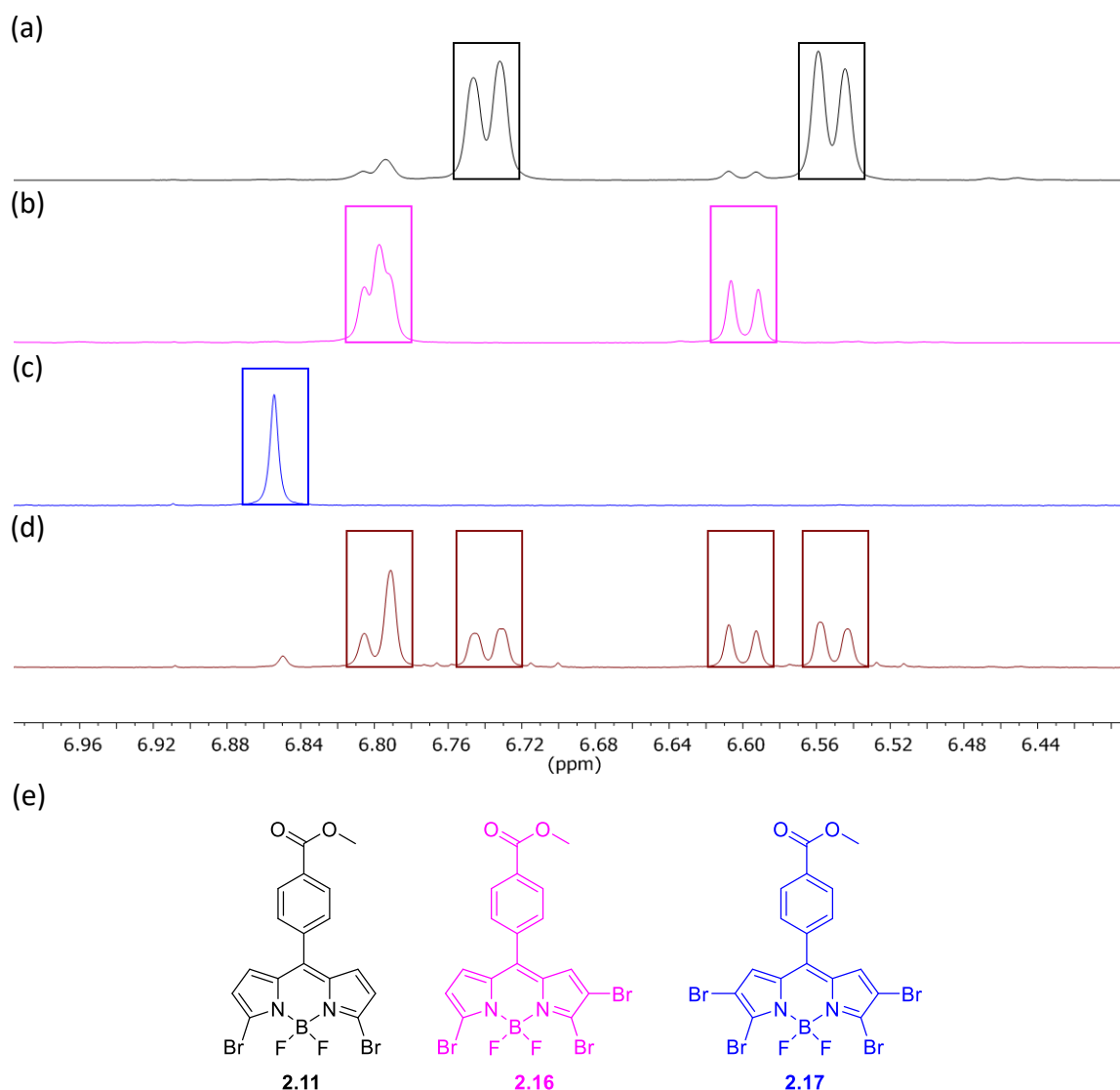
Figure 2.6: (a) ^{1}H NMR spectrum of 3,5-dibromo-BODIPY **2.11**; (b) ^{1}H NMR spectrum of 2,3,5-tribromo-BODIPY **2.16**; (c) ^{1}H NMR spectrum of 2,3,5,6-tetrabromo-BODIPY **2.17**; (d) ^{1}H NMR spectrum of the crude reaction mixture arising from the boron chelation of the mixture of brominated BODIPYs **2.11**, **2.16** and **2.17**; (e) structures of brominated BODIPYs **2.11**, **2.16** and **2.17**.

Following the structural assignment of brominated BODIPYs **2.11**, **2.16** and **2.17**, re-analysis of the ^{1}H NMR spectrum of the crude reaction mixture (arising from the boron chelation of the mixture of brominated dipyrromethenes **2.10**, **2.14** and **2.15**) showed that brominated BODIPYs **2.11**, **2.16** and **2.17** had been formed in a 8:3:1 ratio. This implies a significant degree of over-bromination in the original bromination/oxidation reaction, thus further optimisation of this step focused on minimising over-bromination products.

After further reaction optimisation, we found that over-bromination in the bromination/oxidation reaction of dipyrromethane **2.9** could be avoided by using lower reaction temperatures, and through the controlled addition of NBS (portion-wise addition of solid NBS to the reaction at -78 °C, scheme 2.4). This allowed us isolate 1,9-dibrominated dipyrromethene **2.10** in a much improved yield of 86%.
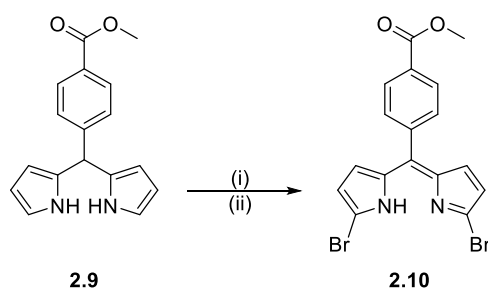
Scheme 2.4: Reagents and conditions: (i) NBS (2 eq.), THF, -78 °C, 1 h; (ii) DDQ, -78 °C to R.T., 10 min (86%).

Our next step was to perform the boron chelation of 1,9-dibrominated dipyrromethene **2.10** to access 3,5-dibromo-BODIPY **2.11**. Therefore we reacted 1,9-dibrominated dipyrromethane **2.10** under standard conditions (boron trifluoride diethyletherate, Hunig's base, DCM) which afforded 3,5-dibromo-BODIPY **2.11** in an excellent isolated yield of 85% (scheme 2.5).
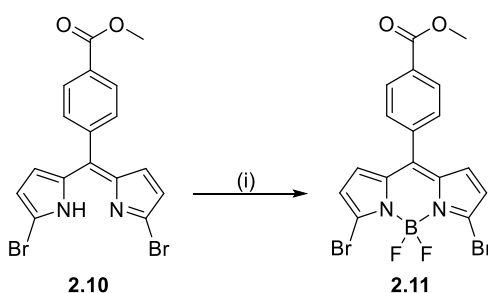
Scheme 2.5: Reagents and conditions: (i) BF$_3$.OEt$_2$, ^{i}Pr$_2$NEt, DCM, R.T., 1 h (85%).

From 3,5-dibromo-BODIPY **2.11** we next examined two pathways to produce our target *N,N,O,O*-BODIPY **2.13**. The first involves a Suzuki-Miyaura cross-coupling with 2-methoxyphenyl boronic acid, followed by a boron tribromide mediated double demethylation and *in situ* double B-O bond

formation to form *N,N,O,O*-BODIPY **2.13**, following the original procedures.[79,84] In the second approach we will attempt the Suzuki-Miyaura cross-coupling of 3,5-dibromo-BODIPY **2.11** with 2-hydroxyphenylboronic acid, with the aim that the desired B-O bond formation event would occur *in situ* to allow direct access to *N,N,O,O*-BODIPY **2.13**.

Therefore in our first approach, we attempted a Suzuki-Miyaura cross-coupling between 3,5-dibromo-BODIPY **2.11** and 2-methoxyphenyl boronic acid, using catalytic Pd(PPh$_3$)$_4$ (5 mol %). After 80 minutes we observed the disappearance of the 3,5-dibromo-BODIPY **2.11** and the appearance of a new major compound by TLC analysis. After purification by silica gel chromatography, 3,5-diaryl BODIPY **2.12** was isolated in a moderate yield of 58%. The structure of 3,5-diaryl BODIPY **2.12** was confirmed by the presence of peaks in the ^{1}H NMR spectrum corresponding to both the methyl group of the aryl ester (δ_H 4.00 ppm, s, 3H) and the two methoxy groups of the 3,5-diaryl substituents (δ_H 3.78 ppm, s, 6H).
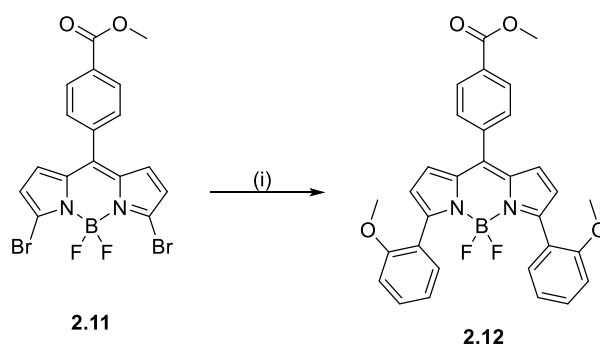
Scheme 2.6: Reagents and conditions: (i) 2-methoxyphenyl boronic acid (4 eq.), Pd(PPh$_3$)$_4$ (5 mol %), K$_3$PO$_4$, toluene, 1,4-dioxane, 90 °C, 1 h 20 min (58%).

The next step in our planned synthetic pathway was the double demethylation reaction of 3,5-diaryl-BODIPY **2.12**, followed by *in situ* double B-O bond formation between the two *ortho*-phenolic hydroxyl groups and the central boron atom. Our first attempt at this reaction was performed at 0 °C using boron tribromide in DCM. The formation of target *N,N,O,O*-BODIPY **2.13** could be observed in the ^{1}H NMR spectrum of the reaction mixture, due to the presence of signals corresponding to the pyrrolic hydrogens (δ_H 7.05 ppm, d, 2H, *J* = 4.4 Hz and 6.93 ppm, d, 2H, *J* = 4.4 Hz), the hydrogens of the 3,5-phenolic rings (δ_H 7.35 ppm, ddd, 2H, *J* = 8.3, 7.4, 1.5 Hz; 7.08 ppm, dd, 2H, *J* = 7.4, 1.5 Hz; 6.97 ppm, dd, 2H, *J* = 8.3, 1.2 Hz) and the loss of the signals corresponding to the two methoxy groups. However following silica gel column chromatography the isolated yield of *N,N,O,O*-BODIPY **2.13** was low, (<10%) with no starting material recovered. We therefore looked to test an alternative Suzuki-Miyaura cross-coupling partner to synthesise *N,N,O,O*-BODIPY **2.13**.

2.12 → **(rac)-2.13**
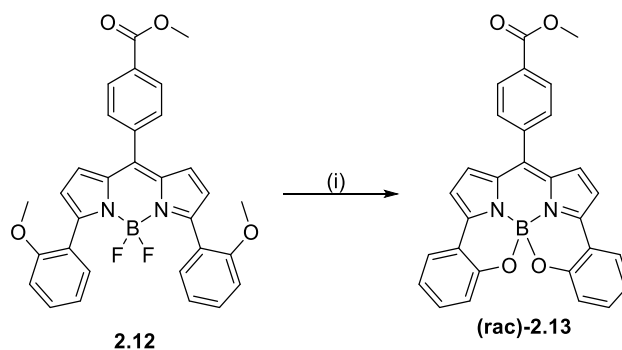
Scheme 2.7: Reagents and conditions: (i) BBr$_3$ (10 eq.), DCM, 0 °C (<10%).

Thus we turned our attention to the second approach towards *N,N,O,O*-BODIPY **2.13**, using a Suzuki-Miyaura cross-coupling between 3,5-dibromo-BODIPY **2.11** and 2-hydroxyphenylboronic acid. Under these conditions we anticipated the desired B-O bond formation would occur *in situ* following the Suzuki-Miyaura cross-coupling, allowing direct access to *N,N,O,O*-BODIPY **2.13**.

We therefore performed a Suzuki-Miyaura cross-coupling between 3,5-dibromo-BODIPY **2.11** and 2-hydroxyphenyl boronic acid, catalysed by Pd(PPh$_3$)$_4$ (5 mol%). Gratifyingly this reaction gave a 43% isolated yield of *N,N,O,O*-BODIPY **2.13**, resulting from a successful double Suzuki-Miyaura cross-coupling and *in situ* double intramolecular B-O bond formation. The formation of the B-O bonds within *N,N,O,O*-BODIPY **2.13** was confirmed by comparison of the ^{11}B NMR spectra of 3,5-dibromo-BODIPY **2.11** and of *N,N,O,O*-BODIPY **2.13**. The ^{11}B NMR spectrum of 3,5-dibromo-BODIPY **2.11** showed a triplet at δ_B 0.33 ppm (t, J_{B-F} = 28 Hz) corresponding to a BF$_2$ moiety in which the boron signal is split by coupling to two equivalent fluorine atoms. Conversely the ^{11}B NMR spectra of *N,N,O,O*-BODIPY **2.13** showed only a singlet at δ_B -0.90 ppm. Typical ^{11}B NMR shifts for unconstrained *N,N,O,O*-BODIPYs are typically in the range of δ_B 1.8 – 2.6 ppm[93,135,136], and typical ^{11}B NMR shifts of a constrained *N,N,O,O*-BODIPY are in the range of δ_B -0.3 – -1.8 ppm.[84,137,138] Based on this information, we concluded that that the fluorines of the central boron atom had been successfully replaced by oxygens.

2.11 → **(rac)-2.13**
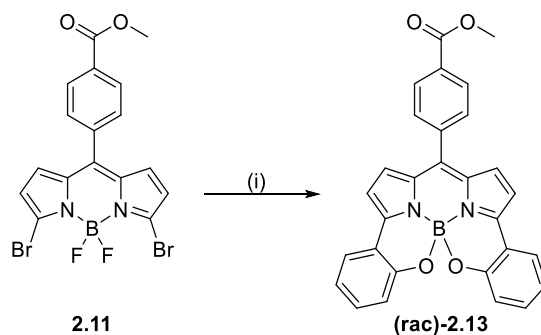
Scheme 2.8: Reagents and conditions: (i) 2-hydroxyphenyl boronic acid (4 eq.), Pd(PPh$_3$)$_4$ (5 mol %), Na$_2$CO$_3$, toluene, 1,4-dioxane, 90 °C, 1 h 20 min (43%).

We have successfully developed a new route to *N,N,O,O*-BODIPY **2.13** (four steps, 28% overall yield) through the use of a Suzuki-Miyaura cross-coupling/B-O bond formation reaction between 2-hydroxyphenylboronic acid and 3,5-dibromo-BODIPY **2.11**, eliminating the need for a late stage demethylation. However the overall yield of this synthetic approach is limited by the low yielding (43%) final Suzuki-Miyaura cross-coupling/B-O bond formation, thus we decided that further investigation of this key reaction was warranted.

Interestingly we observed that another highly coloured compound (which we will designate **2.18**) was formed during the Suzuki-Miyaura cross-coupling/B-O bond formation reaction between 3,5-dibromo-BODIPY **2.11** and 2-hydroxyphenyl boronic acid, and could be isolated following silica gel chromatography (scheme 2.9).
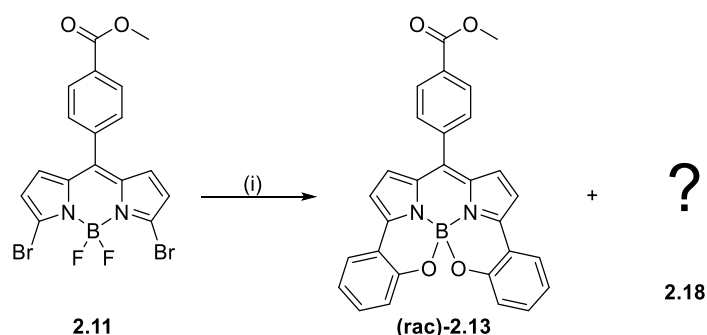
Scheme 2.9: Reagents and conditions: (i) 2-hydroxyphenyl boronic acid (4 eq.), Pd(PPh$_3$)$_4$ (5 mol %), Na$_2$CO$_3$, toluene, 1,4-dioxane, 90 °C, 1 h 20 min (**2.13** 43%).

We therefore endeavoured to elucidate the structure of **2.18** in order to better understand how this by-product was formed under the reaction conditions. In this way, we hoped to be able to improve the Suzuki-Miyaura cross-coupling/B-O bond formation and thus the overall yield to *N,N,O,O*-BODIPY **2.13**.

2.1.3 Isolation and structural determination of unknown compound **2.18**

Postulating that compound **2.18** may be a BODIPY, we first obtained absorption and emission spectra for the isolated molecule (figure 2.7a). The absorption and emission spectra of **2.18** were indeed characteristic of a BODIPY dye, showing an intense absorption band (ε = 30 000 M^{-1}cm^{-1} with a half-height band width of 46 nm) at λ_{max} = 587 nm, and a fluorescence emission band at λ_{max} = 613 nm with a small Stoke's shift (3.85×10^5 cm^{-1}).
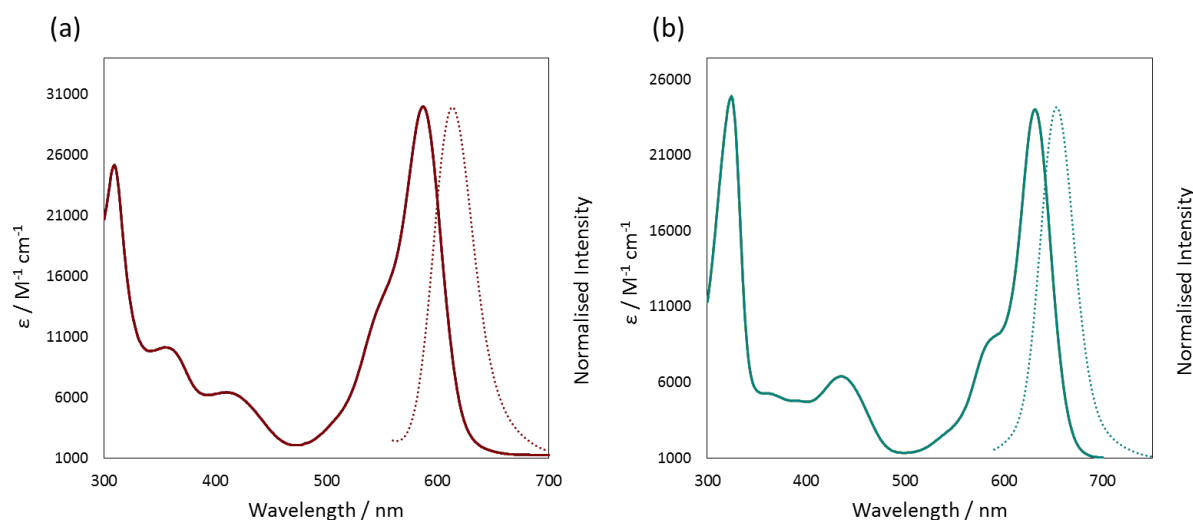
Figure 2.7: (a) Absorption (solid line) and emission (dotted line) spectra of **2.18** in DCM; (b) Absorption (solid line) and emission (dotted line) spectra of **2.13** in DCM.

We next obtained high resolution mass spectrometry (HRMS) spectra of both *N,N,O,O*-BODIPY **2.13** and unknown BODIPY **2.18** (provided by the EPSRC National Mass Spectrometry Service at Swansea University). *N,N,O,O*-BODIPY **2.13** was analysed on a Xevo G2-S mass spectrometer by ASAP-ToF (Atmospheric Solids Analysis Probe-Time of Flight) HRMS in positive mode. We observed a peak at 471.1519 m/z assigned as [M+H]$^+$ in the mass spectrum of *N,N,O,O*-BODIPY **2.13**, suggesting a molecular formula of $C_{29}H_{19}BN_2O_4$. Unknown BODIPY **2.18** was analysed on a LTQ Orbitrap XL mass spectrometer using nanospray ionisation in positive mode. We observed a peak at 471.1508 m/z assigned as [M+H]$^+$ in the mass spectrum, suggesting that molecular formula of unknown BODIPY **2.18** was also $C_{29}H_{19}BN_2O_4$. Therefore both *N,N,O,O*-BODIPY **2.13** and unknown BODIPY **2.18** have molecular formulae of $C_{29}H_{19}BN_2O_4$, and as such are structural isomers.

We then compared the ^{1}H NMR spectra of *N,N,O,O*-BODIPY **2.13** and unknown BODIPY **2.18** (figure 2.8). We found that in the ^{1}H NMR spectrum of *N,N,O,O*-BODIPY **2.13**, we could observe an AB system consisting of two roofed doublets pertaining to the pyrrolic hydrogens H_1 and H_2 (δ_H 7.05 ppm, d, 2H, *J* = 4.4 Hz and δ_H 6.93 ppm, d, 2H, *J* = 4.4 Hz). In the ^{1}H NMR spectrum of unknown BODIPY **2.18**, we observed that there were four doublets pertaining to pyrrolic hydrogens. Furthermore, analysis of the ^{13}C NMR spectra of *N,N,O,O*-BODIPY and unknown BODIPY **2.18** revealed that there were ten additional peaks in the spectra of **2.18**, indicating that there had been a loss of C_2 symmetry.
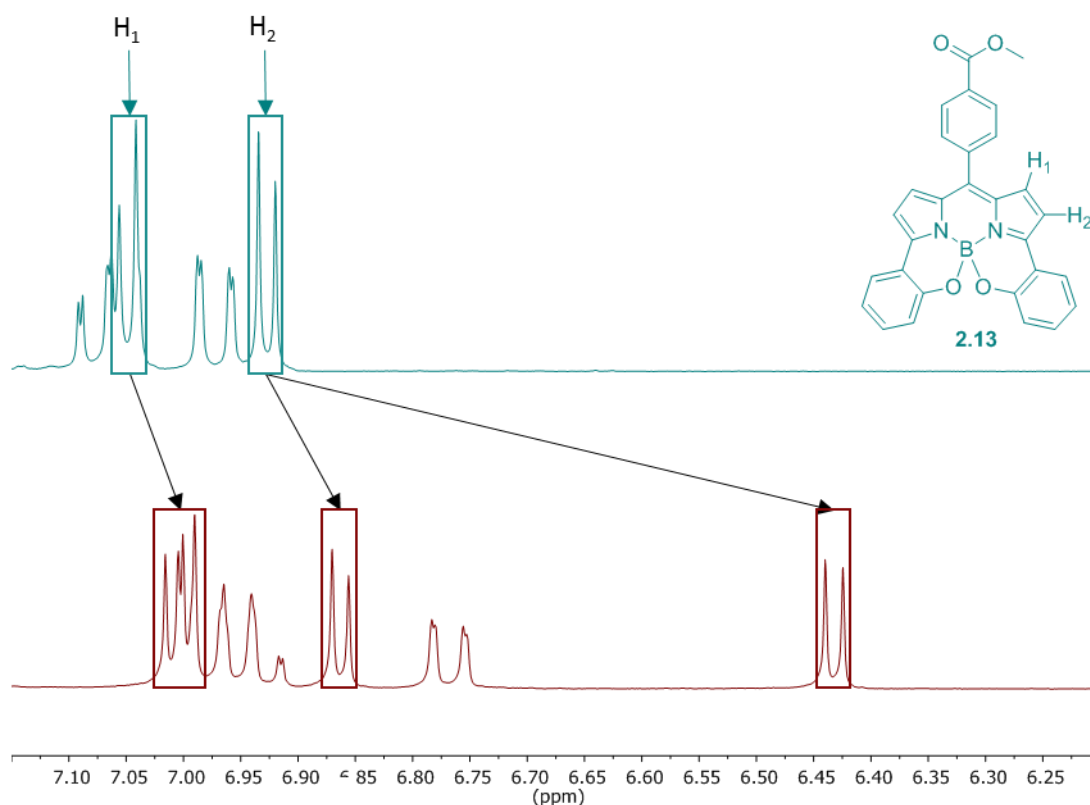
Figure 2.8: ^{1}H NMR spectra of *N,N,O,O*-BODIPY **2.13** (green, top) and unknown BODIPY **2.18** (red, bottom) showing the signals corresponding to the pyrrolic hydrogens of **2.13** and **2.18**.

In order to unambiguously determine the structure of BODIPY **2.18**, we grew crystals by slow evaporation from a chloroform solution, suitable for single crystal X-ray diffraction analysis. Analysis of the crystal structure enabled us to determine the structure of *N,N,O,C*-BODIPY **2.18** (figure 2.9) as containing an unusual *N,N,O,C*-boron chelated motif. The structure of *N,N,O,C*-BODIPY **2.18** obtained from X-ray diffraction analysis was consistent with the ^{1}H and ^{13}C NMR spectra obtained previously, containing an inverted phenolic ring (i.e. connected to the BODIPY core through the phenolic oxygen instead of *via* an aryl-aryl C-C bond), thereby breaking the C_2 symmetry.

It can be observed from the X-ray crystal structure of *N,N,O,C*-BODIPY **2.18** that the 3,5-*ortho*-phenolic substituents are held in a 'propeller-like' arrangement, which gives rise to helical chirality. Thus *N,N,O,C*-BODIPY **2.18** represents a new structural class of helically chiral BODIPYs.

As discussed previously (section 2.1.1.1), Gossauer has suggested that in order for a BODIPY to be CPL-emissive, it must contain a perturbed or 'twisted' core.[126,129] Examination of the X-ray crystal structure of **2.18** revealed that there is a twist in the core of *N,N,O,C*-BODIPY **2.18**, with a twist angle of approximately 7.7° between the planes of the two pyrrolic rings. As such isolated enantiomers of

N,N,O,C-BODIPY **2.18** might be expected to be CPL active, since **2.18** contains both a intrinsically chiral structure and a chiral perturbation of the BODIPY core.

(a)

(b)
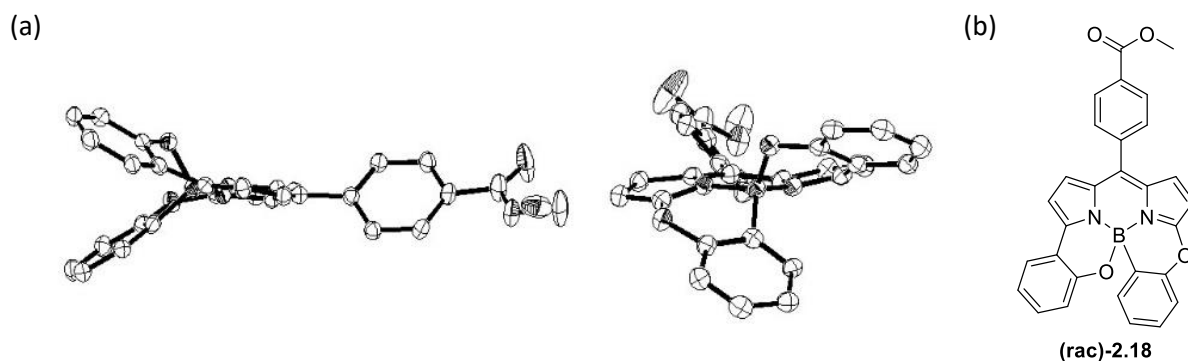
(rac)-2.18

Figure 2.9: (a) Two views of a molecule in the crystal structure of (*rac*)-**2.18** illustrating the asymmetry in the fluorophore core and the helical arrangement of the phenolic substituents (H atoms are omitted for clarity, *M*-isomer is shown); (b) Molecular structure of (*rac*)-**2.18**.

This *N,N,O,C*-boron chelation motif is highly unusual in BODIPY dyes. When we elucidated the structure of *N,N,O,C*-BODIPY **2.18** there were only 14 *N,N,O,C*-boron chelated BODIPYs known across 3 articles.[101,102,139] These included examples from the group of Vicente, wherein chelation of a dipyrromethane (**2.19** or **2.20**) with dichlorophenylborane is followed by substitution of the chloride with oxygen-centered nucleophiles to produce *N,N,O,C*-BODIPYs (**2.21-2.22**).[139] *N,N,O,C*-BODIPYs (**2.21-2.22**) are examples of bidentate *N,N*-dipyrromethene ligands.

2.19 R = H
2.20 R = Et

2.21a-d
2.22a-d
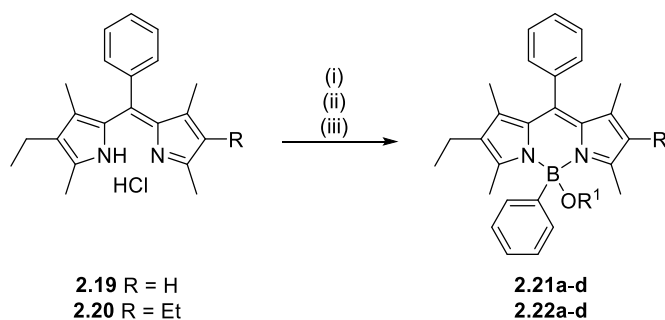
Scheme 2.10: Reagents and conditions: (i) Et$_3$N, DCM; (ii) PhBCl$_2$, R.T., 1 h; (iii) Nucleophile, 1-2 h (R = Et or H, R^1 = COMe, OCH$_2$CCH, O(CH$_2$CH$_2$O)$_3$Me, OCH$_2$Ch$_2$NHCOO^{t}Bu).

Further examples of *N,N,O,C*-BODIPYs were synthesised by Nabeshima *et al.* through the chelation of a dipyrromethene (**1.79** or **2.23**) by an arylboronic acid to produce *N,N,O,C*-BODIPYs (**1.80**, **2.24b-f** and **2.25a-f**, scheme 2.11).[101,102] These examples from the group of Nabeshima are tridentate *N,N*-dipyrromethene ligands.

1.79 R = H
2.23 R = Me

1.80, 2.24b-f
2.25a-f
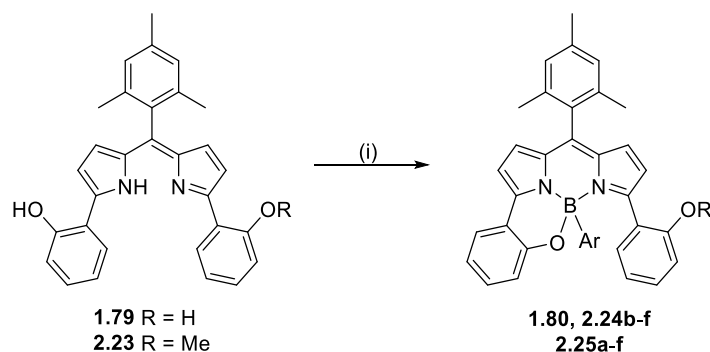
Scheme 2.11: Reagents and conditions: (i) Ar-B(OH)$_2$, toluene or chloroform (Ar = Ph, naphth-1-yl, 4-methoxyphenyl, pyrid-4-yl, pyrid-3-yl, pyren-1-yl).

It should be noted that since the discovery of *N,N,O,C*-BODIPY **2.18**, a number of other bi-[140–142] and tridentate[102,103] *N,N,O,C*-BODIPYs have been reported.

N,N,O,C-BODIPY **2.18** is, to the best of our knowledge, the only *N,N,O,C*-BODIPY which is a tetradentate *N,N*-dipyrromethene ligand, thus imparting a high degree of rigidity to the structure. This rigid structure should result in a high fluorescence quantum yield (φ$_F$), because less energy is lost from the S$_1$ excited state through vibrational relaxation. We hoped that a high φ$_F$ would result in an improvement in our overall CPL quantum efficiency ($|g_{lum}|\cdot$φ$_F$).

Preliminary computational modelling of *N,N,O,C*-BODIPY **2.18** (performed by Dr Thomas Penfold) indicated that there was an increase in excited-state charge-transfer character in *N,N,O,C*-BODIPY **2.18** (as compared to *N,N,O,O*-BODIPY **2.13**). We would predict that an increase in excited-state charge-transfer character would result in a decrease in the magnitude of the electric dipole moment, which in turn would lead to an increased $|g_{lum}|$ (section 2.1.1.2). We were therefore eager to study the CPL capability of *N,N,O,C*-BODIPY **2.18**, and thus examine the effect this charge-transfer character has on $|g_{lum}|$.

2.2 Investigation of a new chiral BODIPY architecture

2.2.1 Resolution of *N,N,O,C*-BODIPY **2.18** by chiral HPLC

In order to investigate the chiroptical properties of *N,N,O,C*-BODIPY **2.18**, it was first necessary to resolve our racemic mixture of **2.18** into its respective enantiomers. We therefore performed semi-preparative chiral HPLC separation on a racemic mixture of **2.18** using a Daicel Chiralpak® IB column (1 mL/ minute, 85:15 hexane:ethyl acetate) to give approximately 10 µg of each enantiomer after combining multiple runs. We assigned the two isolated enantiomers as (+)-**2.18** and (-)-**2.18** respectively by retention time and by measuring the specific optical rotation ($[\alpha]_D$).
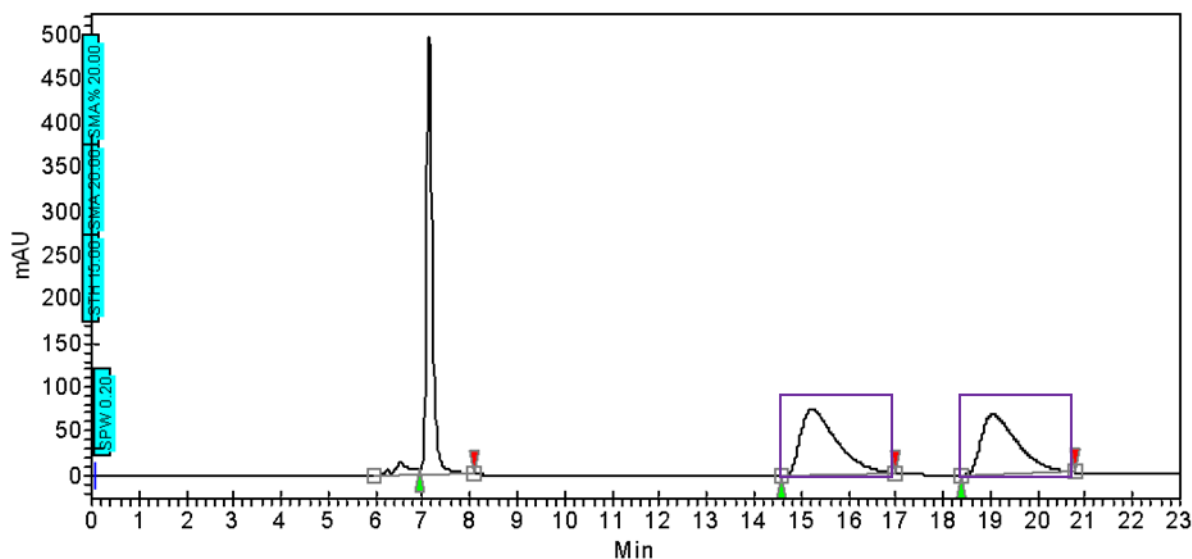
Figure 2.10: A typical chiral HPLC trace of a racemic sample of **2.18**. Daicel Chiralpak® IB column, 4.6 x 250 mm, 5µm particle size, hexane : ethyl acetate (85:15), 1 mL/min.

After separation of the enantiomers of *N,N,O,C*-BODIPY **2.18**, the enantiomeric excess (*ee*) of each enantiomer was measured by resubmitting them to the chiral HPLC conditions ((+)-**2.18** %*ee* = >95%, (-)-**2.18** %*ee* = >95%). Once we were satisfied that we had isolated enantiopure samples of each enantiomer of *N,N,O,C*-BODIPY **2.18**, we turned our attention to the measurement of the chiroptical properties.

2.2.2 Electronic Circular Dichroism of *N,N,O,C*-BODIPY **2.18**

With our single enantiomers in hand, our next step was to measure electronic circular dichroism spectra (ECD, performed by Jonathan Bogaerts). Electronic circular dichroism spectroscopy involves the differential absorption of left- and right-handed light by an intrinsically chiral chromophore or a chromophore in a chiral environment. We expect that for a pair of enantiomers, we should observe equal and opposite (or 'mirror image') ECD spectra.

As we had expected, we obtained mirror image ECD spectra from the (+)-and (-)-enantiomers of *N,N,O,C*-BODIPY **2.18** (figure 2.11a). The ECD spectra of the enantiomers showed strong Cotton effects corresponding to the S_0-S_1 transition of *N,N,O,C*-BODIPY **2.18** (λ_{max} = 593 nm, $\Delta\varepsilon_{max}$ = ±92 L mol^{-1}cm^{-1} in hexane), which confirmed that the chiral species in the sample is indeed *N,N,O,C*-BODIPY **2.18**. We were then able to measure a g_{abs} value of 3.1×10^{-3} at 593 nm in hexane.

Boltzmann-weighted ECD spectra for the postulated enantiomer were then obtained from TD-DFT calculations at the cam-B3LYP/6-311++G(93df,2pd) level for the *M* enantiomer of **2.18** (figure 2.11b, calculations performed by Professor Wouter Herrebout). By comparing the theoretical ECD spectra

with our experimental ECD spectra, we were able to assign the enantiomers as (*P*)-(-)-**2.18** (blue) and (*M*)-(+)-**2.18** (red).
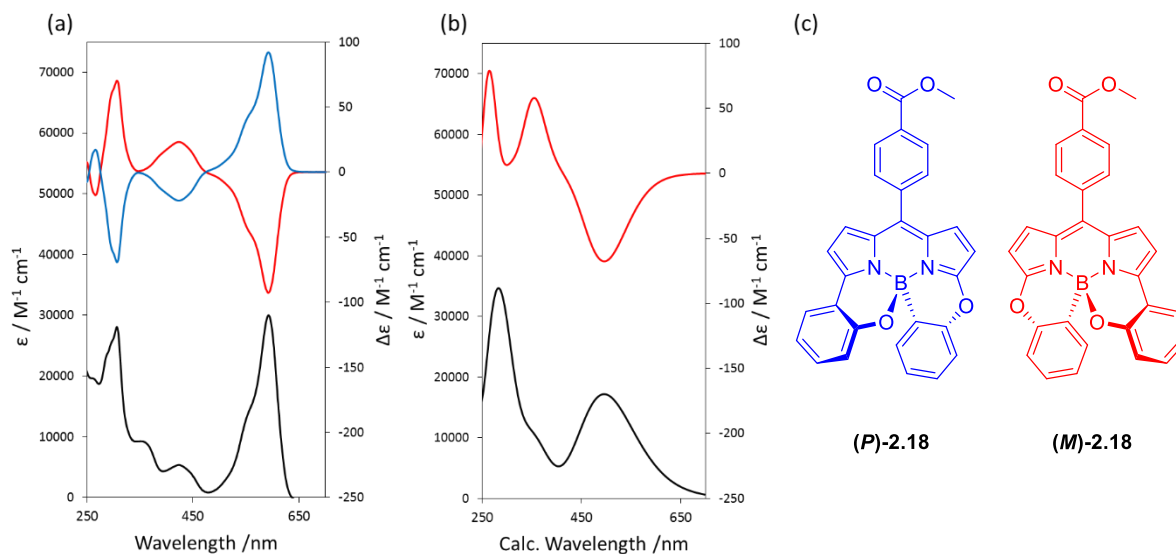
Figure 2.11: (a) Experimental ECD spectra (red – (*M*)-**2.18**, blue – (*P*)-**2.18**) and UV/Vis absorption spectrum (black) measured in hexane; (b) Calculated Boltzmann-weighted spectra, ECD (red – postulated (*M*)-**2.18** (wavelength uncorrected) and UV/Vis absorption spectra (black – postulated (*M*)-**2.18** (wavelength uncorrected); (c) (*P*)-**2.18** and (*M*)-**2.18**.

	Solvent	λ_{abs} /nm	ε /mol^{-1} cm^{-1}	λ_{em} /nm	ϕ_F	$|g_{abs}|$	$\Delta\varepsilon_{max}$ / L mol^{-1}cm^{-1}
2.18	hexane	593	30 000	622	0.49	3.1×10^{-3}	$\pm$92

Table 2.1: Experimental photophysical and chiroptical properties of *N,N,O,C*-BODIPY **2.18**.

2.2.3 Evidence to support increased charge-transfer character in *N,N,O,C*-BODIPY **2.18**

Since preliminary computational modelling of *N,N,O,C*-BODIPY **2.18** had suggested that there was increased charge-transfer character in the excited state of *N,N,O,C*-BODIPY **2.18** (as compared to *N,N,O,O*-BODIPY **2.13**), we decided to seek evidence to support this notion. We elected to perform cyclic voltammetry of (*rac*)-**2.18** (performed by Dr Owen Woodford).

Cyclic voltammetry of *N,N,O,C*-BODIPY **2.18** was performed in deoxygenated, freshly distilled dichloromethane containing 0.2 M tetra-*N*-butyl ammonium hexafluorophosphate as the background electrolyte. The working electrode was a highly polished glassy carbon disk, and the counter electrode was a Pt wire. An Ag/Ag$^+$ reference electrode was used, and was calibrated against ferrocene.

On reductive scans of *N,N,O,C*-BODIPY **2.18**, a reversible one-electron wave was observed with a half wave potential of -1.17 V vs Ag/Ag$^+$ with a peak separation of 100 mV at a scan rate of 0.1 V per second (figure 2.12). On oxidative scans, an irreversible one-electron wave was found, with a peak potential

of 0.84 V vs Ag/Ag⁺. A second oxidation wave could be observed at higher potentials (approximately 1.01 V, as estimated using simulation techniques), and was electrochemically irreversible at all scan rates.
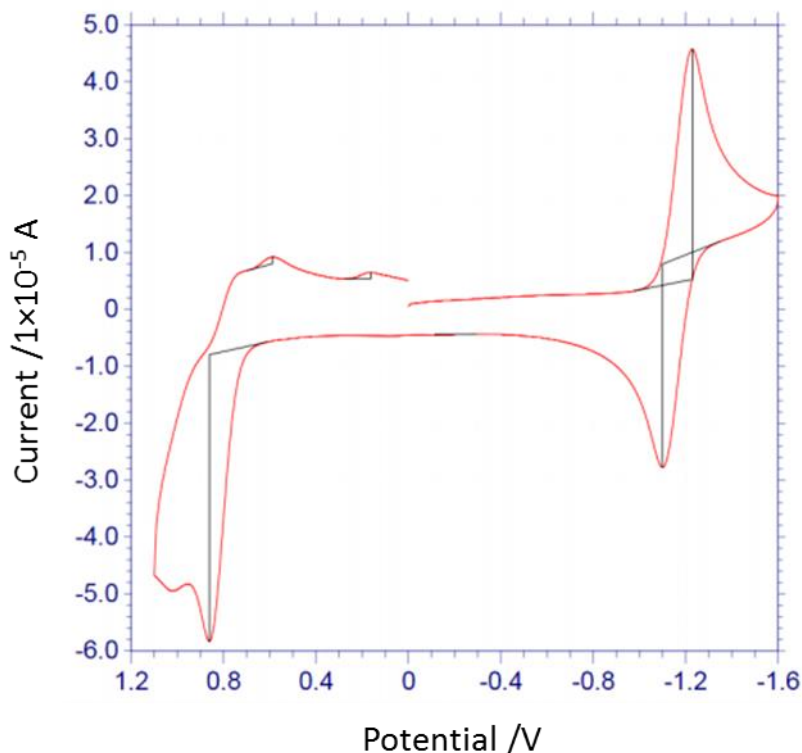
Figure 2.12: Cyclic voltammogram recorded for *N,N,O,C*-BODIPY **2.18** in deoxygenated dichloromethane. The x-axis is referenced to the Ag/Ag⁺ electrode.

A series of DFT calculations were made (performed by Dr Owen Woodfood, see Appendix) to calculate the energies and electronic distribution of the HOMO, HOMO(-1) and LUMO of *N,N,O,C*-BODIPY **2.18**, and thus assign the oxidation and reduction peaks observed in the CV of (*rac*)-**2.18**.

The reduction wave at -1.17 V was thereby assigned as the preferential addition of a single electron to the dipyrrin unit (i.e. a single electron reduction of the dipyrrin unit). The first oxidation wave at 0.84 V was assigned to the removal of a single electron from the dipyrrin unit (i.e. a single electron oxidation of the dipyrrin unit). The second oxidation wave (1.01 V) can be assigned to the removal of a single electron from the boron-chelated phenolic rings. Based on these findings, we should expect to find a charge-transfer state located slightly above the lowest energy π-π* excited-singlet state.

2.2.4 Circularly polarised luminescence of *N,N,O,C*-BODIPY **2.18**

We next measured the CPL spectra of the enantiomers (*P*)-(-)-**2.18** and (*M*)-(+)-**2.18** of *N,N,O,C*-BODIPY **2.18** (performed by Dr Robert Pal). Gratifyingly, we obtained mirror image CPL spectra for (*M*)-(+)-**2.18**

and (*P*)-(-)-**2.18**, which confirmed that *N,N,O,C*-BODIPY **2.18** is a CPL-active BODIPY dye. As we would expect for a pair of enantiomers, the signals were opposite at the emission maxima (624 nm in hexane), corresponding to the S_1-S_0 transition of *N,N,O,C*-BODIPY **2.18**.

We measured the $|g_{lum}|$ of *N,N,O,C*-BODIPY **2.18**, and it was found to be 3.7×10^{-3} at 624 nm in hexane (figure 2.13). In order to compare the brightness of CPL with other CPL-SOM systems, we can calculate the overall quantum efficiency ($|g_{lum}|\cdot\phi_F$), which for **2.18** is 1.8×10^{-3}.
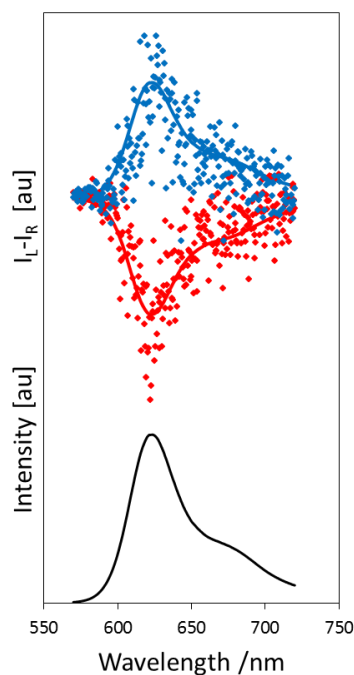
Figure 2.13: Normalised CPL (I_L-I_R) (red – (*M*)-(+)-**2.18**, blue – (*P*)-(-)-**2.18**) and fluorescence spectra (black – (*rac*)-**2.18**) measured in hexane.

	Solvent	λ_{abs} /nm	ϵ /mol^{-1} cm^{-1}	λ_{em} /nm	ϕ_F	$|g_{abs}|$	$\Delta\epsilon_{max}$ / L mol^{-1}cm^{-1}	$|g_{lum}|$	($|g_{lum}|\cdot$ ϕ_F)
2.18	hexane	593	30 000	622	0.49	3.1×10^{-3}	±92	3.7×10^{-3}	1.8×10^{-3}

Table 2.2: Experimental photophysical and chiroptical properties of *N,N,O,C*-BODIPY **2.18**.

Thus we have reported the isolation, structural determination and full chiroptical characterisation of *N,N,O,C*-BODIPY **2.18**. The observation of CPL emission from (*P*)-(-)-**2.18** and (*M*)-(+)-**2.18** validates Gossauer's theory (section 2.1.1.1), since *N,N,O,C*-BODIPY **2.18** contains both an intrinsically chiral structure, and a chirally perturbed planar core.

2.2.4.1 Rationalising the *g_{lum}* value observed for *N,N,O,C*-BODIPY **2.18**

As a consequence of the increased charge-transfer character in the excited state of *N,N,O,C*-BODIPY **2.18**, we had hoped to observe a higher *g_{lum}* value for *N,N,O,C*-BODIPY **2.18** than that which had been

previously reported for *N,N,O,O*-BODIPY **2.18**. However the $|g_{lum}|$ measured for *N,N,O,C*-BODIPY **2.18** (3.7×10^{-3}) was marginally lower than that of *N,N,O,O*-BODIPY **1.93** (4.7×10^{-3}). We therefore sought to investigate why the presence of the increased charge-transfer character in the excited state of *N,N,O,C*-BODIPY **2.18** did not improve the g_{lum}.

The electronic (**μ**) and magnetic (**m**) transition dipole moments and the angle between these vectors (τ) are related to g_{lum} by the following equation:

$$g_{lum} = \frac{4(\boldsymbol{\mu} \cdot \boldsymbol{m} \cdot cos\tau)}{(\boldsymbol{\mu}^2 + \boldsymbol{m}^2)}$$

We wished to calculate the magnitude of **m**, **μ** and the angle τ, in order to investigate the effect the charge-transfer character in the excited state of **2.18** had on these molecular properties. Furthermore by comparing our theoretically determined g_{lum} values with our experimentally determined g_{lum} values, we can assess the accuracy of the computational method. If theoretically derived g_{lum} values are proven to be accurate, this would open up the possibility of designing new BODIPY CPL-SOMs based upon theoretical predictions.

Thus the excited states of both *N,N,O,C*-BODIPY (*P*)-**2.18** and *N,N,O,O*-BODIPY (*P*)-**1.93** were calculated using DFT(PBE0) with a def2-TZVP basis set (table 2.3, performed by Dr Thomas Penfold) as implemented within the ORCA quantum chemistry package.[143]

Compound	**μ** [au]	**m** [au]	τ [°]	$|g_{lum}|_{calc}$	$|g_{lum}|_{exp}$[a]
2.18	6.0×10^{-1}	7.3×10^{-4}	70	1.7×10^{-3}	3.7×10^{-3}
1.93	7.6×10^{-1}	1.4×10^{-3}	65	3.1×10^{-3}	4.7×10^{-3}

Table 2.3: Calculated magnitudes of the electric (**μ**) and magnetic (**m**) transition dipole moments, the angle between them (τ) and $|g_{lum}|_{calc}$ compared to $|g_{lum}|_{exp}$ for (*P*)-**2.18** and (*P*)-**1.93**. [a] $|g_{lum}|_{exp}$ given at the respective λ_{max} value in hexane.

We were pleased to discover that the trend observed in the calculated g_{lum} values for *N,N,O,O*-BODIPY **1.93** and *N,N,O,C*-BODIPY **2.18** matched the trend observed in our experimental measurement of the g_{lum} values of **2.18** and **1.93**. This validates the accuracy of the computational method, and thus we continued with our analysis of the theoretically derived values of **m**, **μ** and τ.

Comparison of the calculated electric (**μ**) transition dipole moments for *N,N,O,C*-BODIPY **2.18** and *N,N,O,O*-BODIPY **1.93** confirmed the presence of increased charge-transfer in the excited state of *N,N,O,C*-BODIPY **2.18**, since a smaller value for **μ** was calculated. This indicates that the introduction of charge-transfer character would increase $|g_{lum}|$. However any potential increase in g_{lum}, which might have arisen from the reduced $|\boldsymbol{\mu}|$, was offset by a reduced $|\boldsymbol{m}|$ and an unfavourable change in

the angle (τ) between these two vectors (from 65° in *N,N,O,O*-BODIPY **1.93** to 70° in *N,N,O,C*-BODIPY **2.18**).

Interestingly we observed from these calculations that **m** aligns with the helical axis, whilst **μ** aligns with the π system in both *N,N,O,C*-BODIPY **2.18** and *N,N,O,O*-BODIPY **1.93** (figure 2.14). This is also the observed orientation of **m** and **μ** in the carbo[*n*]helicenes series.[144] This observation leads us to believe that it may be possible to control the relative directions of **m** and **μ** by controlling the helical pitch and the extent of the π-conjugation of the BODIPY.
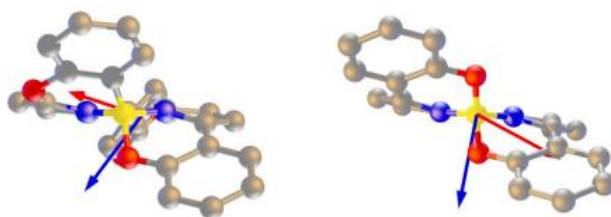
Figure 2.14: Electronic (red) and magnetic (blue) transition dipole moments for *N,N,O,C*-BODIPY **2.18** (left) and *N,N,O,O*-BODIPY **1.93** (right).

We have concluded that the introduction of charge-transfer character does decrease |**μ**|, however we must also attempt to control |**m**| and the angle τ. We have also validated the use of computational modelling to predict g_{lum} values. Based on predictive models (given by Dr Thomas Penfold), we identified some new strategies to increase g_{lum}:

- Inclusion of sulfur, in order to increase |**m**| (chapter 3)
- Inclusion of 3,5-dinapthyl rings, in order to increase the helical pitch (resulting in a favourable angle between **m** and **μ**, i.e. $\tau \approx 0°$ or 180°, chapter 4).

2.2.5 Mechanistic investigation and new synthetic strategy

N,N,O,C-BODIPY **2.18** is the first reported CPL-active 'tetradentate' *N,N,O,C*-BODIPY system (section 2.1.3), and as such represents a new structural class of CPL-active BODIPYs. We were therefore interested in studying analogues of *N,N,O,C*-BODIPY **2.18** to further understand both their synthetic chemistry and their chiroptical properties. *N,N,O,C*-BODIPY **2.18** was initially formed as a minor product of the Suzuki-Miyaura cross-coupling between 3,5-dibromo-BODIPY **2.11** and 2-hydroxyphenyl boronic acid (scheme 2.12). Our highest isolated yield of *N,N,O,C*-BODIPY **2.18** was 36%, but this does not reflect the typical obtained yields of **2.18**. Attempts to repeat the synthesis of *N,N,O,C*-BODIPY **2.18** resulted in much lower obtained yields, ranging from 2%-9% over 7 experiments with a mean of 6% (±3%).
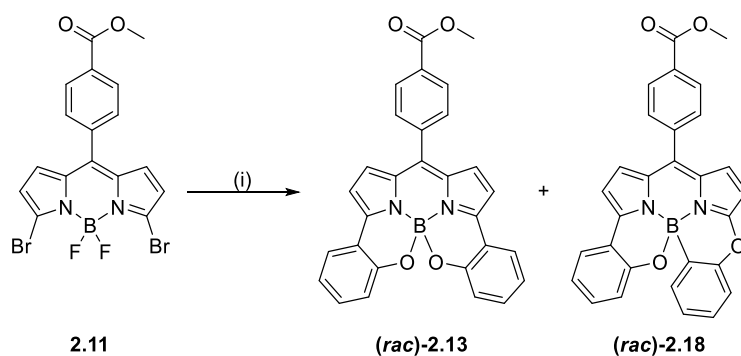
Scheme 2.12: Reagents and conditions: (i) 2-hydroxyphenyl boronic acid (4 eq.), Pd(PPh$_3$)$_4$ (5 mol %), Na$_2$CO$_3$, toluene, 1,4-dioxane, 90 °C, 1 h 20 min (43% **2.13**, average of 7% **2.18**).

This capricious synthesis limited our investigations into this new class of CPL-active BODIPYs. We therefore sought to better understand how *N,N,O,C*-BODIPY **2.18** was formed under the reaction conditions, in order to improve the isolated yield of **2.18** and the accessibility of this class of BODIPYs.

Our first challenge was to carry out some initial mechanistic investigation, which was performed in collaboration with Jake Weatherston. We proposed that there were two possible reaction pathways to *N,N,O,C*-BODIPY **2.18** (route A and route B, scheme 2.13).

Route A involves the boron metathesis of the BF$_2$ group with the boron of the 2-hydroxyphenylboronic acid (step A1), followed by an intramolecular S$_N$Ar between the phenolic hydroxyl and the 3-bromo substituent (step A2). Then a Suzuki-Miyaura cross-coupling with 2-hydroxyphenyl boronic acid would install the 3-phenolic ring (step A3), and finally B-O bond formation between the free phenolic hydroxyl group and the chelating boron atom (step A4) would produce *N,N,O,C*-BODIPY **2.18**.

Route B first involves a Suzuki-Miyaura cross-coupling with 2-hydroxyphenyl boronic acid (step B1), followed by B-O bond formation between the phenolic hydroxyl group and the boron atom (step B2). This is followed by boron metathesis of the BF$_2$ moiety with the 2-hydroxyphenyl boronic acid (step B3) and finally an intramolecular S$_N$Ar between the free phenolic hydroxyl and the 3-bromo substituent (step B4) to form *N,N,O,C*-BODIPY **2.18**.
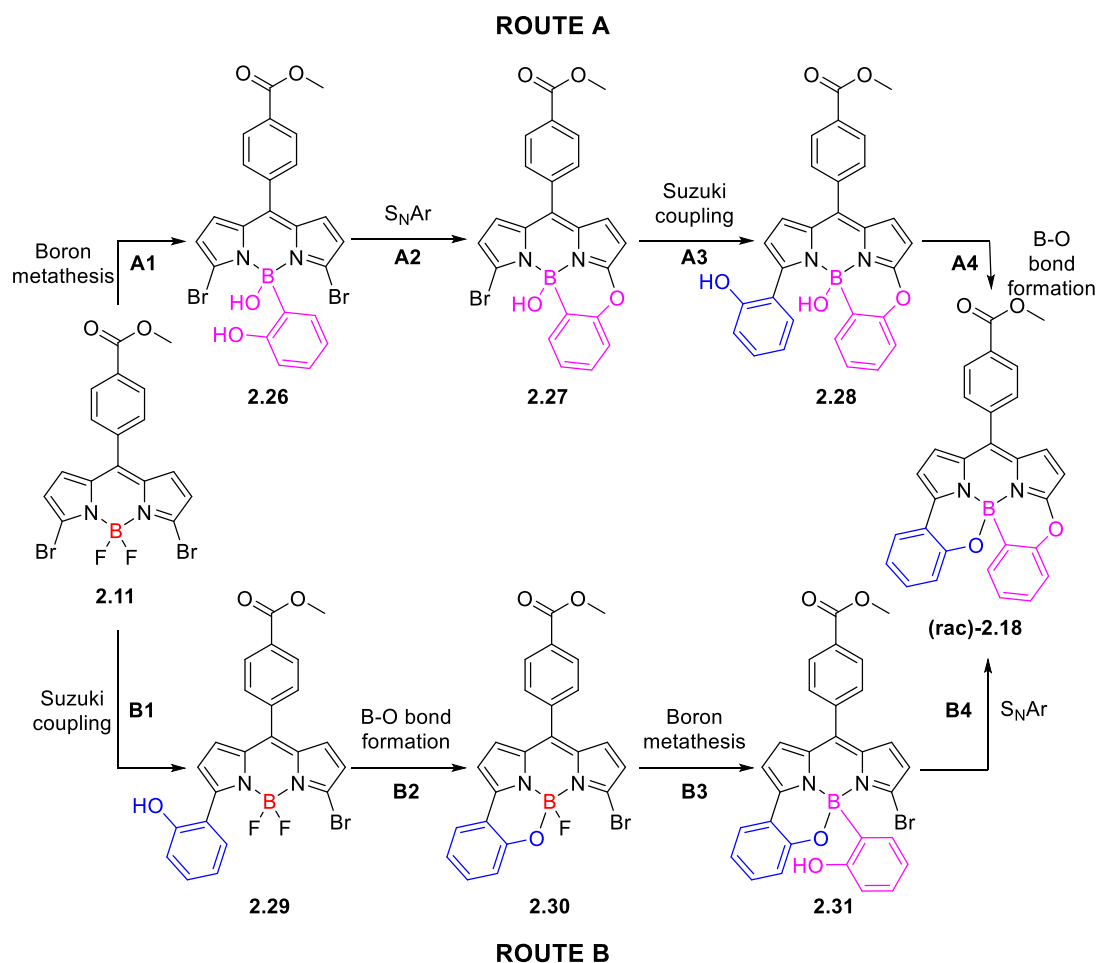
ROUTE A

ROUTE B

Scheme 2.13: Two proposed routes A and B to *N,N,O,C*-BODIPY **2.18**, showing the different step order possibilities.

We first wanted to investigate the synthetic pathway taken to form *N,N,O,C*-BODIPY **2.18** (ie. route A or route B). We reasoned that if *N,N,O,C*-BODIPY **2.18** is formed via route A, excluding palladium from the reaction might result in the formation of the intermediate BODIPY **2.27**. However experiments carried out in the absence of a palladium catalyst (entry 2, table 2.4) did not form either *N,N,O,O*-BODIPY **2.13**, *N,N,O,C*-BODIPY **2.18** or any intermediate compounds **2.26**-**2.31**. This suggested to us that *N,N,O,C*-BODIPY **2.18** is formed via a palladium catalysed pathway.

We therefore wished to investigate the role of palladium(0)/palladium(II) in a possible boron metathesis (step A1 or B3, scheme 2.13), involving the exchange of the BF_2 moiety with the boron on the incoming arylboronic acid. Examples in the literature of the spontaneous chelation of dipyrromethenes by boronic acids[101,102,104,145] led us to examine instead precedent for the loss of BF_2 from BODIPY dyes.

There are examples in the literature of BF_2 removal from BODIPYs using Brønsted acids (for example, trifluoroacetic acid[146,147] and methanolic hydrogen chloride[147]), and ligand exchange at boron is known

to be mediated by Lewis acids (for example, aluminium trichloride,[17,148,149] trimethylsilyl trifluoromethanesulfonate,[150] trimethylsilylchloride,[95,151] tin tetrachloride,[152] and boron tribromide[146]). We concluded that trace amounts of Lewis acidic palladium(II) could be formed by air oxidation, and subsequently mediate the loss of BF_2 from 3,5-dibromo-BODIPY **2.11**.

We therefore reacted together 3,5-dibromo-BODIPY **2.11**, 2-hydroxyphenyl boronic acid and $Pd(PPh_3)_4$ (5 mol%) in the presence of air, to allow for oxidation by air of palladium(0) to palladium(II) (entry 3, table 2.4). We also tested the use of a palladium(II) catalyst, $Pd(OAc)_2$ (entry 4, table 2.4). These experiments resulted in a lower isolated yield of both BODIPYs, but gratifyingly, we observed a change in selectivity from *N,N,O,O*-BODIPY **2.13** to *N,N,O,C*-BODIPY **2.18**.

2.11   (rac)-**2.13**   (rac)-**2.18**
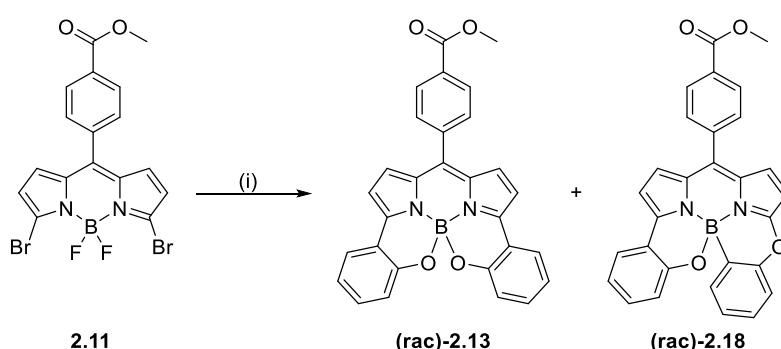
Scheme 2.14: Reagents and conditions: (i) 2-hydroxyphenyl boronic acid (4 eq.), Pd catalyst (5 mol %), Na_2CO_3, toluene, 1,4-dioxane, 90 °C.

	Catalyst	Yield of **2.13** /%	Yield of **2.18** /%	Ratio **2.13**:**2.18**
1	$Pd(PPh_3)_4$	34	14	2.4 : 1
2[a]	-	0	0	-
3[b]	$Pd(PPh_3)_4$	9	16	1 : 1.7
4	$Pd(OAc)_2$	3	39	1 :13

Table 2.4: Isolated yields of **2.13** and **2.18** from test reactions intended to probe the mechanism of the formation of **2.18**. [a]Reaction performed without palladium catalyst. [b]Reaction performed in the presence of air.

The change in selectivity from *N,N,O,O*-BODIPY **2.13** to *N,N,O,C*-BODIPY **2.18** upon using a palladium(II) catalyst suggested that Lewis acidic palladium(II) is aiding in the removal of the BF_2 moiety, improving the rate of the boron metathesis step (step A1 or B3, scheme 2.13). We reasoned

that by starting from dipyrromethene **2.10**, which does not contain a BF_2 moiety, we should further improve the synthesis of *N,N,O,C*-BODIPY **2.18**.

Indeed when we reacted dipyrromethene **2.10** together with 2-hydroxyphenyl boronic acid in the presence of $Pd(OAc)_2$ (5 mol%), we observed the selective formation of *N,N,O,C*-BODIPY **2.18**. However the yield was sub-optimal, owing to the poorer activity of palladium(II) catalysts in Suzuki-Miyaura cross-couplings. By reverting to the palladium(0) catalyst $Pd(PPh_3)_4$ (5 mol%), we were able to selectively synthesise *N,N,O,C*-BODIPY **2.18** in a high yield of 85%.

2.10   **(rac)-2.18**
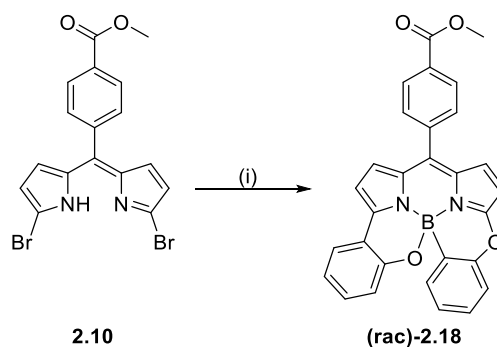
Scheme 2.15: Reagents and conditions: (i) 2-hydroxyphenyl boronic acid (4 eq.), Pd catalyst (5 mol %), Na_2CO_3, toluene, 1,4-dioxane, 90 °C.

	Catalyst	Yield of **2.18** /%
1	$Pd(OAc)_2$	22
2	$Pd(PPh_3)_4$	85

Table 2.5: Isolated yields of **2.18** from our optimised synthetic pathway.

This new synthetic strategy offers high yields and selectivity for *N,N,O,C*-BODIPY **2.18**, which was previously isolated as a minor product in capricious yields. Furthermore we have also reduced the number of synthetic steps taken to *N,N,O,C*-BODIPY **2.18** by one step. This work represents the first key step in investigating this class of CPL-active BODIPY dyes.

2.3. Expansion of the *N,N,O,C*-BODIPY series

2.3.1 Testing the substrate scope

If improving the synthesis of *N,N,O,C*-BODIPY **2.18** was the first step in investigating the *N,N,O,C*-BODIPYs, the second step is the expansion of the *N,N,O,C*-BODIPY series. We planned to do this by applying our new synthetic strategy to a range of substrates. We therefore selected a range of commercially available aryl boronic acids which contained a 2-hydroxy functional group.

We chose an electron poor (entry 5, table 2.6) and an electron rich (entry 3, table 2.6) boronic acid, to examine the effect electronics might have on the reaction. We also chose an example which we anticipated would be sterically challenging, due to a 3-methyl substituent close to the 2-hydroxy functional group (entry 2, table 2.6). Finally we selected 5-chloro-2-hydroxyphenyl boronic acid, as the chloride functional group could be used as a handle for further functionalisation.
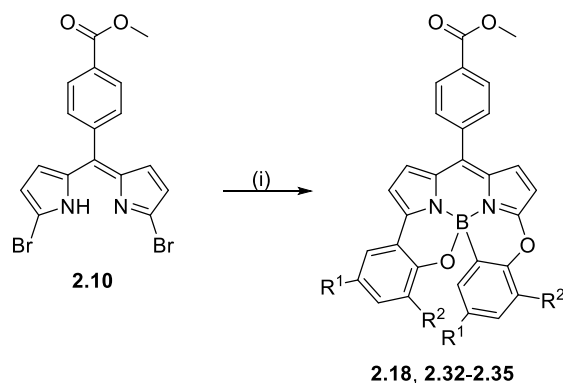
Scheme 2.16: Reagents and conditions: (i) Pd(PPh$_3$)$_4$ (5 mol %), boronic acid (4 eq.), Na$_2$CO$_3$, toluene:1,4-dioxane 1:1, 90 °C.

	R^1	R^2	Product	Reaction time (h)	Yield (%)
1	H	H	**2.18**	1	85
2	H	Me	**2.32**	18	38
3	Me	H	**2.33**	1	55
4	Cl	H	**2.34**	1	71
5	F	H	**2.35**	1	73

Table 2.6: Results of testing the substrate scope.

We found that all of the boronic acids tested successfully formed the corresponding *N,N,O,C*-BODIPYs **2.32**-**2.35** under our reaction conditions. After some reaction optimisation, we found that for all but the most sterically hindered system (entry 2, table 2.6), the best yield was obtained after 1 hour. For *N,N,O,C*-BODIPY **2.32** however, we found that an extended reaction time of 18 hours produced the highest yield.

2.3.1.1 X-ray crystallography of *N,N,O,C*-BODIPY **2.33**

In order to unambiguously determine the structure of *N,N,O,C*-BODIPY **2.33**, we performed crystallisation of (*rac*)-**2.33** by slow diffusion from a chloroform solution. This afforded single crystals suitable for single-crystal X-ray analysis. Analysis of the crystal structure (figure 2.15) allowed us first to confirm the structure of *N,N,O,C*-BODIPY **2.33**. Furthermore we measured a twist angle of 8.2° between the two pyrrolic rings of *N,N,O,C*-BODIPY **2.33**. Comparison of the twist angle observed in the crystal structure of *N,N,O,C*-BODIPY **2.33** (8.2°) with that observed in *N,N,O,C*-BODIPY **2.18** (7.7°) revealed that the aryl methyl groups impart a higher degree of chiral perturbation to the planar BODIPY core. We look to grow single crystals suitable for X-ray analysis of the remaining *N,N,O,C*-BODIPYs **2.32**, **2.34** and **2.35** in the future, in order to assess the effect of the twist angle has on the g_{lum} of *N,N,O,C*-BODIPYs.

(a) (b)
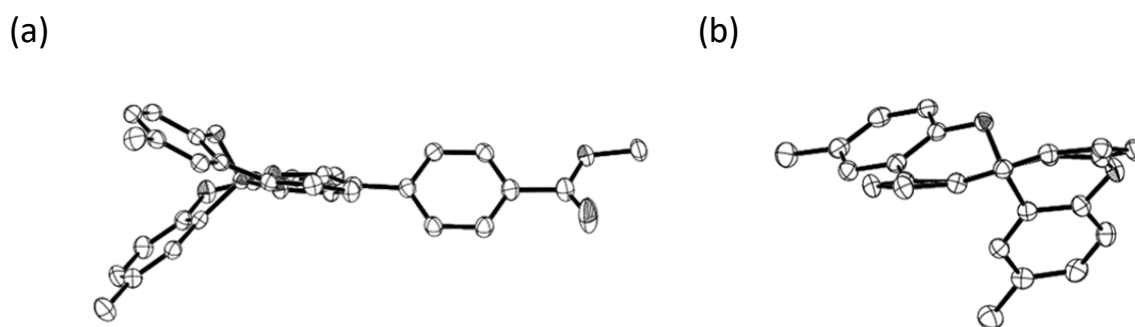
Figure 2.15: Two views of a molecule in the crystal structure of (*rac*)-**2.33**: (a) illustrating the asymmetry in the fluorophore core (H atoms are omitted for clarity, *M*-isomer is shown); (b) the twist in the planar BODIPY core (H atoms and *meso*-aryl ring are omitted for clarity, *M*-isomer is shown).

2.3.2 Synthesis of 'mixed' *N,N,O,C*-BODIPYs **2.38** and **2.39**

It occurred to us that it would be interesting to examine the chiroptical properties of 'mixed' *N,N,O,C*-BODIPYs (ie. containing two rings derived from different boronic acids). We considered that an electron deficient arylboronic acid may undergo chelation with dipyrromethene **2.10** faster than an electron rich arylboronic acid. We therefore selected the most electron rich (**2.37**) and the most electron deficient (**2.36**) arylboronic acids from our series to examine any selectivity present in the step involving the chelation of dipyrromethene **2.10** by the boronic acid.

Initial experiments using two equivalents of 2-hydroxy-5-fluorophenyl boronic acid (**2.36**) and two equivalents of 2-hydroxy-5-methylphenyl boronic acid (**2.37**) revealed that there were four products formed under the reaction conditions. Separation of these four products was challenging using silica

gel column chromatography, due to mixed column fractions. However we were able to isolate a small, impure sample of each product.

Two of the products were shown to be *N,N,O,C*-BODIPYs **2.33** and **2.35** by comparison of the ^{1}H and ^{19}F NMR spectra of the impure samples (obtained from the reaction between 2-hydroxy-5-fluorophenyl boronic acid, 2-hydroxy-5-methylphenyl boronic acid and dipyrromethene **2.10**) with the previously obtained NMR data for *N,N,O,C*-BODIPYs **2.33** and **2.35**.

We assigned the remaining two products as 'mixed' *N,N,O,C*-BODIPYs **2.38** and **2.39**. We confirmed the synthesis of 'mixed' *N,N,O,C*-BODIPYs **2.38** and **2.39** through analysis of the ^{1}H NMR and ^{19}F NMR spectra of the remaining impure samples obtained from the reaction between 2-hydroxy-5-fluorophenyl boronic acid, 2-hydroxy-5-methylphenyl boronic acid and dipyrromethene **2.10**. In each set of spectra (^{1}H NMR and ^{19}F NMR) for 'mixed' *N,N,O,C*-BODIPYs **2.38** and **2.39** we observed one singlet peak in the ^{19}F NMR spectra and one singlet peak corresponding to the methyl group of the 3- or 5- aryl ring in the ^{1}H NMR spectra.
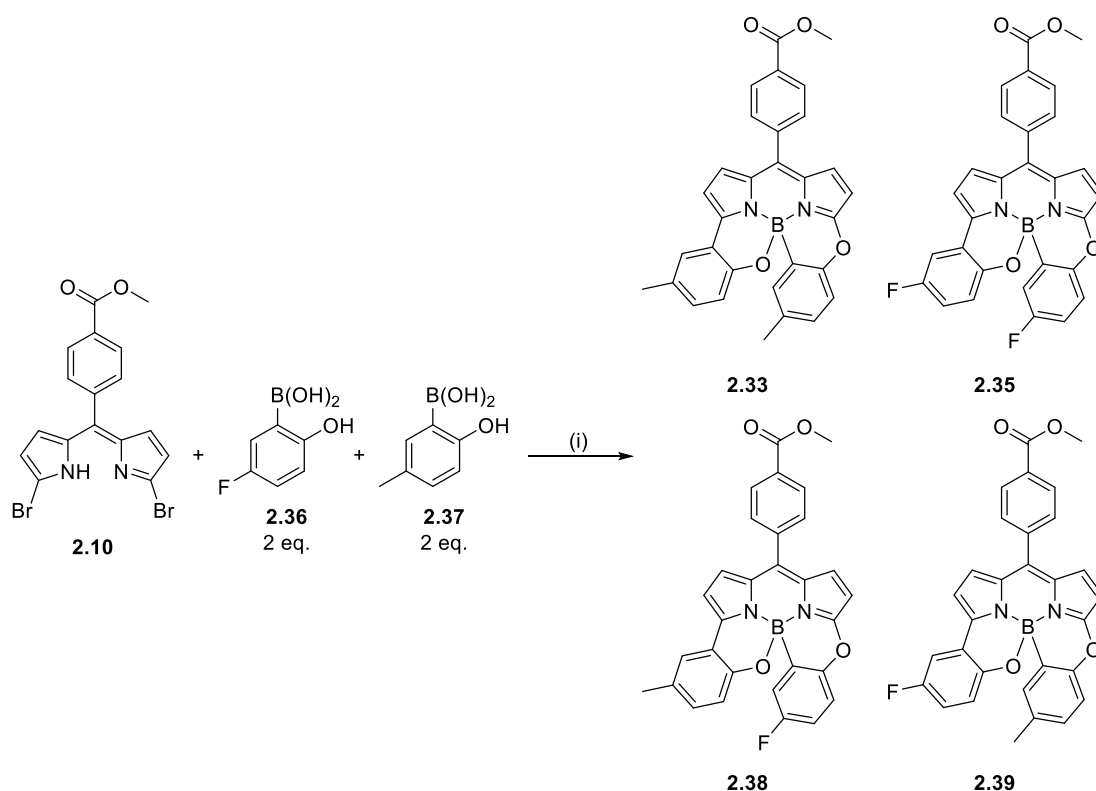
Scheme 2.17: Reagents and conditions: (i) Pd(PPh$_3$)$_4$ (5 mol %), Na$_2$CO$_3$, toluene:1,4-dioxane (1:1), 90 °C, 1 h.

2.3.2.1 Structural assignment of *N,N,O,C*-BODIPY **2.35**

Due to the structural similarity between 'mixed' *N,N,O,C*-BODIPYs **2.38** and **2.39**, we could not confidently assign the impure samples obtained from the reaction between boronic acids **2.36** and **2.37** and dipyrromethene **2.10** as either **2.38** or **2.39**. We therefore elected to perform HMQC (^{13}C-^{19}F) HMBC (^{1}H-^{13}C, multiple bond correlation), and ROESY NMR experiments on *N,N,O,C*-BODIPY **2.35**, in order to assign the ^{19}F NMR signals corresponding to the fluorine substituents (performed by Professor William McFarlane, see Appendix). We then planned to assign the structures of *N,N,O,C*-BODIPYs **2.38** and **2.39** through comparison of the ^{19}F NMR spectra of *N,N,O,C*-BODIPY **2.35** and the ^{19}F NMR spectra of the impure samples of *N,N,O,C*-BODIPYs **2.38** and **2.39**.

Through our analysis of the ROESY NMR spectra of *N,N,O,C*-BODIPY **2.35**, we observed a correlation from a doublet signal at 6.84 ppm to a double doublet signal at 7.42 ppm. No correlation was observed from the doublet signal at 6.44 ppm to any aryl protons. We therefore assigned these protons as H^{20} (6.84 ppm), H^{23} (7.42 ppm) and H^{10} (6.44 ppm) (figure 2.16). Analysis of the ^{13}C-^{19}F HMQC showed a correlation from the fluorine singlet at -117.0 ppm to a carbon signal at 156.8 ppm, and a second correlation from the fluorine singlet at -123.1 ppm to a carbon signal at 159.3 ppm. Finally analysis of the ^{1}H-^{13}C HMBC spectrum showed a correlation between the carbon signal at 156.8 ppm to the proton H^{23} (7.42 ppm). We therefore concluded that the signal in the ^{19}F NMR spectrum at -123.1 ppm corresponded to F^{28}, and that H^{23} and F^{28} resided within the directly C-C linked aryl ring. We can conclude that F^{29} resides within the indirectly C-O-C linked aryl ring.

H	δ_H
4	8.19
5	7.74
9	7.03
10	6.44
19	7.00
20	6.84
23	7.42
F	δ_F
28	-123.1
29	-117.0
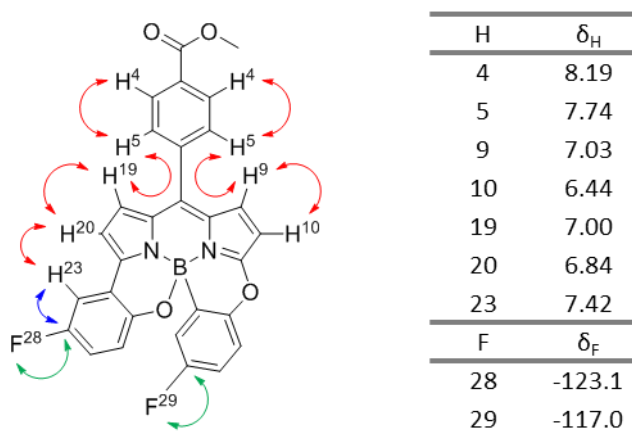
Figure 2.16: ^{1}H and ^{19}F assignment of key atoms of *N,N,O,C*-BODIPY **2.35**, showing key ROESY (red), ^{13}C-^{19}F HMQC (green) and HMBC (blue) correlations.

Further confirmation of this assignment was found by performing ^{1}H-{^{19}F} NMR spectra of *N,N,O,C*-BODIPY **2.35** (performed by Professor William McFarlane). We observed that when the spectra was irradiated at -123.005 ppm the signal at 7.42 ppm corresponding to H^{23} was now a doublet, instead of

a double doublet (figure 2.17). Furthermore, when the spectra was irradiated at -117.935 ppm the signal at 7.42 ppm remained a double doublet. We were therefore confident in our assignment of the fluorine signals of *N,N,O,C*-BODIPY **2.35**.
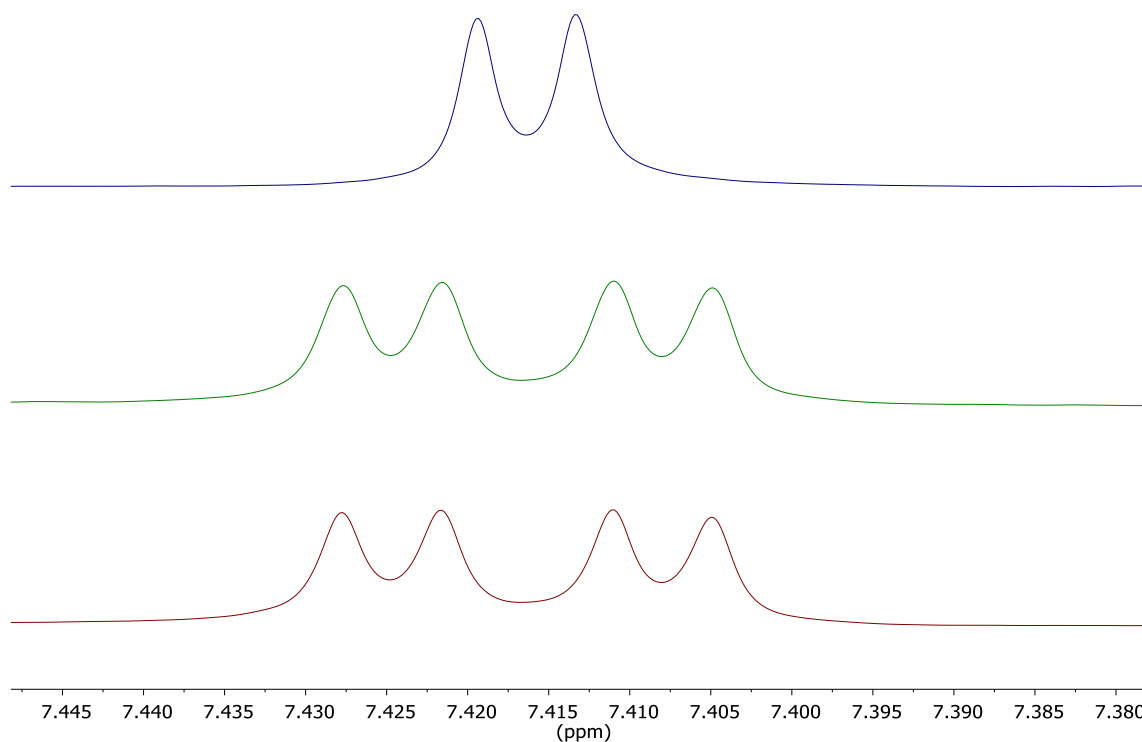
Figure 2.17: ^{1}H-{^{19}F} NMR spectra of *N,N,O,C*-BODIPY **2.35** showing the signal corresponding to H^{23} decoupled at -123.005 ppm (top, blue), -117.935 ppm (middle, green) and the ^{1}H NMR spectrum of *N,N,O,C*-BODIPY **2.35** (bottom, red).

Once we had confidently assigned the ^{19}F NMR spectrum of *N,N,O,C*-BODIPY **2.35**, we were able to assign the impure samples obtained from the reaction between boronic acids **2.36** and **2.37** and dipyrromethene **2.10** as *N,N,O,C*-BODIPYs **2.39** and **2.38** respectively by retention time on silica gel. Once we had completed the assignment of *N,N,O,C*-BODIPYs **2.38** and **2.39**, we decided to examine the reaction conditions used to synthesise *N,N,O,C*-BODIPYs **2.38** and **2.39** to see if we could improve the selectivity for either *N,N,O,C*-BODIPY.

2.3.2.2 Examination of the reaction conditions to synthesise 'mixed' *N,N,O,C*-BODIPYs

We tested how changing the ratio of boronic acids **2.36**, **2.37** and dipyrromethane **2.10** affected which *N,N,O,C*-BODIPYs were formed under the reaction conditions. Since the 'mixed' *N,N,O,C*-BODIPYs **2.38** and **2.39** have both an aryl methyl group and a fluorine in their structure, we were able to estimate the yields of each product *N,N,O,C*-BODIPY by analysis of the crude ^{19}F and ^{1}H NMR spectra (table 2.7).
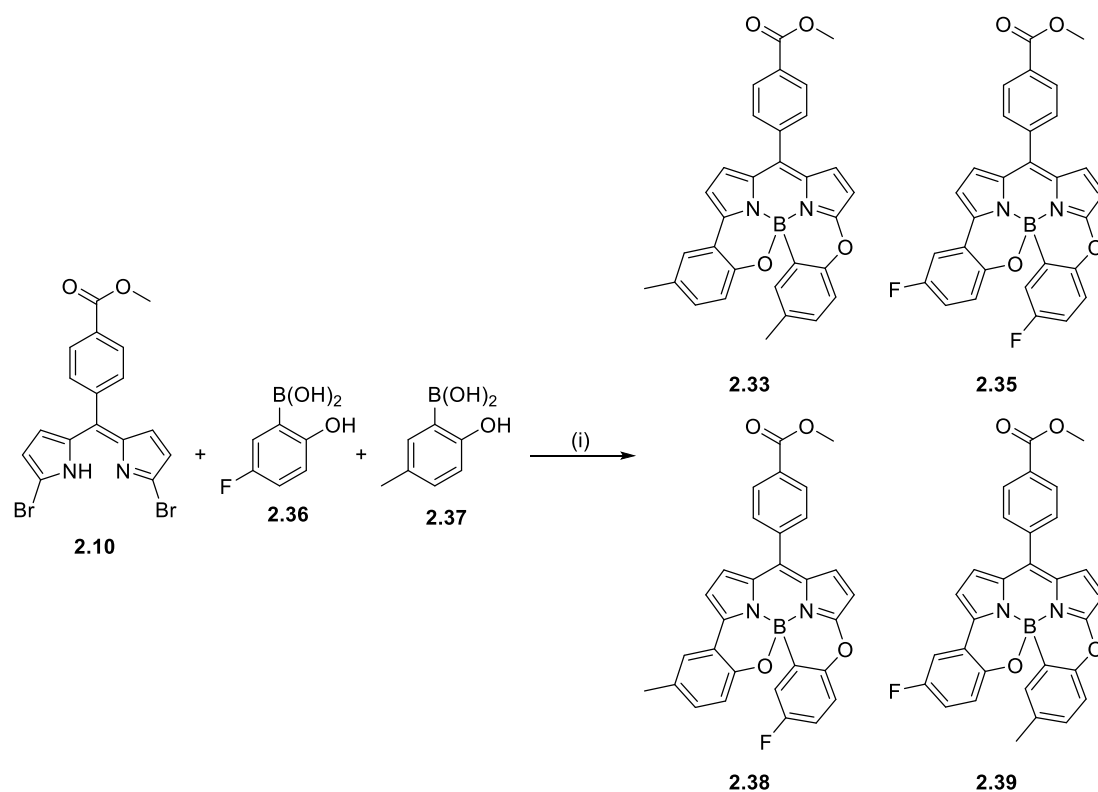
Scheme 2.18: Reagents and conditions: (i) Pd(PPh₃)₄ (5 mol %), Na₂CO₃, toluene:1,4-dioxane (1:1), 90 °C, 1 h.

Ratio of		Product			
2.36:2.37:2.10		**2.33**	**2.38**	**2.39**	**2.35**
1:1:1	Product ratio[a]	1	1.6	1.2	1.5
	Yield /%	15	25	18	23
2:2:1	Product ratio[a]	1	1.5	1.1	1.2
	Yield /%	14	22	16	18
1.5:1.5:1	Product ratio[a]	1	1.2	1.2	1.2
	Yield /%	15	17	17	17
2:1:1	Product ratio[a]	1	0.8	0.5	0.26
	Yield /%	20	16	10	5
1:2:1	Product ratio[a]	1	3.8	2.2	4.6
	Yield /%	4	14	8	17

Table 2.7: Results from the mixed experiments, including ratios of boronic acids **2.36**, **2.37** and starting material **2.10** used. [a]Ratio of products determined by ¹⁹F and ¹H NMR.

The outcomes of these experiments suggest that the selective synthesis of *N,N,O,C*-BODIPY **2.38** or **2.39** is not possible using our synthetic strategy. However we did observe that when the molar ratio

of boronic acids **2.36**:**2.37** is equal, *N,N,O,C*-BODIPY **2.38** is formed in the highest proportion. This indicates that the boron chelation step occurs faster with an electron deficient boronic acid. In order to achieve the selective synthesis of a 'mixed' *N,N,O,C*-BODIPY such as *N,N,O,C*-BODIPY **2.38**, we suggest that a more electron deficient boronic acid should be used.

With our series of *N,N,O,C*-BODIPYs in hand, we turned our attention to the resolution of the enantiomers of each *N,N,O,C*-BODIPY, in order to investigate the chiroptical properties of the series.

2.3.3 Resolution of the enantiomers of *N,N,O,C*-BODIPYs **2.32**-**2.35**

Resolution of the racemic mixtures of *N,N,O,C*-BODIPYs **2.32**-**2.35** was performed by semi-preparative chiral HPLC (table 2.8). After combining multiple runs, we were able to isolate approximately 20 µg of each enantiomer of *N,N,O,C*-BODIPYs **2.32**-**2.35**. We then assigned the enantiomers of the *N,N,O,C*-BODIPYs as (+)-**2.32**-**2.35** and (-)-**2.32**-**2.35** by measuring the specific optical rotation ($[\alpha]_D$).

The enantiomeric excess (*ee*) of the isolated enantiomers was then assessed by resubmitting them to the chiral HPLC conditions. Once we confirmed that we had isolated enantiopure (%*ee* = >95%) samples, we then turned our attention to the measurement of the chiroptical properties of the series.

Column / Conditions		Retention time / min	
		(+)-**X**	(-)-**X**
2.32	Daicel Chiralpak® IA / 85:15 Hexane : DCM, 1 mL/min	14.95	17.36
2.33	Daicel Chiralpak® IA / Toluene, 1 mL/min	5.51	3.77
2.34	Daicel Chiralpak® IA / 80 : 20 Toluene : Hexane, 1 mL/min	5.82	4.46
2.35	Daicel Chiralpak® OD-H / 95 : 5 Hexane : IPA, 1 mL/min	18.07	21.19

Table 2.8: Retention times and column conditions for the separation by chiral HPLC of compounds **2.32**-**2.35**.

2.3.4 Chiroptical properties of the series

2.3.4.1 ECD spectroscopy of *N,N,O,C*-BODIPYs **2.32**-**2.35**

With our set of single enantiomers of *N,N,O,C*-BODIPYs **2.32**-**2.35** in hand, our next step was to measure ECD spectra (performed by Jonathan Bogaerts). As previously discussed (section 2.2.2), we would expect to observe equal and opposite (or 'mirror image') ECD spectra for each pair of enantiomers.

As we had anticipated, mirror image ECD spectra were obtained for each set of enantiomers (figures 2.18a-2.21a). The ECD spectra of each enantiomer of *N,N,O,O*-BODIPYs **2.32**-**2.35** showed strong Cotton effects corresponding to the S_0-S_1 transition of each *N,N,O,O*-BODIPY **2.32**-**2.35** (table 2.9). Once we had recorded the experimental ECD spectra, we looked to assign each enantiomer as either (*P*) or (*M*) through a comparison of experimental to calculated ECD spectra.

Therefore Boltzmann-weighted ECD spectra were obtained from TD-DFT calculations at the cam-B3LYP/6-311++G(3df,2pd) level for the (*P*) enantiomer of each *N,N,O,C*-BODIPY ((b), blue, figures 2.18-2.21, calculations performed by Jonathan Bogaerts). By comparison of the calculated ECD spectra and the experimental ECD spectra, we were able to assign the (*P*) and (*M*) isomers of *N,N,O,C*-BODIPYs **2.32**-**2.35** (figures 2.18c-2.21c). Our next step was to measure the CPL spectra of each enantiomer and assess the g_{lum} values across the series.
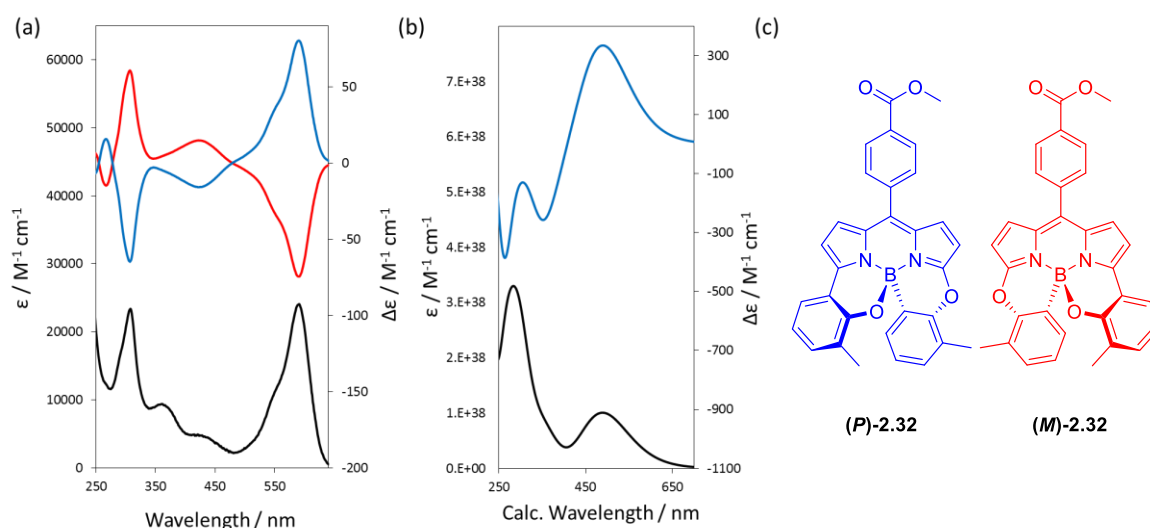
Figure 2.18: (a) Experimental ECD spectra (red – (*M*)-**2.32**, blue – (*P*)-**2.32**) and UV/Vis absorption spectrum (black) measured in DCM; (b) Calculated Boltzmann-weighted spectra, ECD (blue – postulated (*P*)-**2.32** (wavelength uncorrected) and UV/Vis absorption spectra (black – postulated (*P*)-**2.32** (wavelength uncorrected); c) (*P*)-**2.32** and (*M*)-**2.32**.
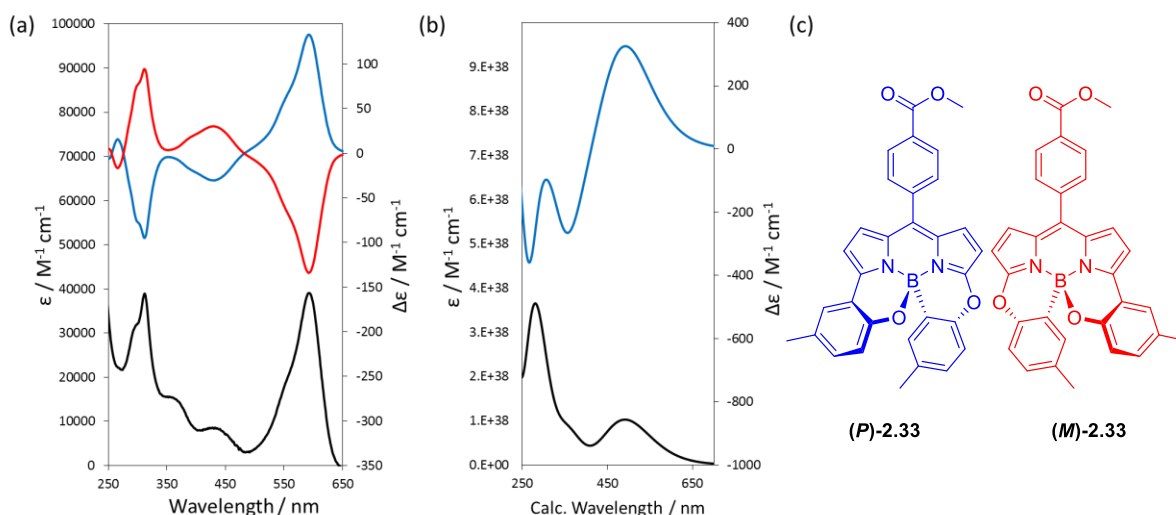
Figure 2.19: (a) Experimental ECD spectra (red – (*M*)-**2.33**, blue – (*P*)-**2.33**) and UV/Vis absorption spectrum (black) measured in DCM; (b) Calculated Boltzmann-weighted spectra, ECD (blue – postulated (*P*)-**2.33** (wavelength uncorrected) and UV/Vis absorption spectra (black – postulated (*P*)-**2.33** (wavelength uncorrected); c) (*P*)-**2.33** and (*M*)-**2.33**.
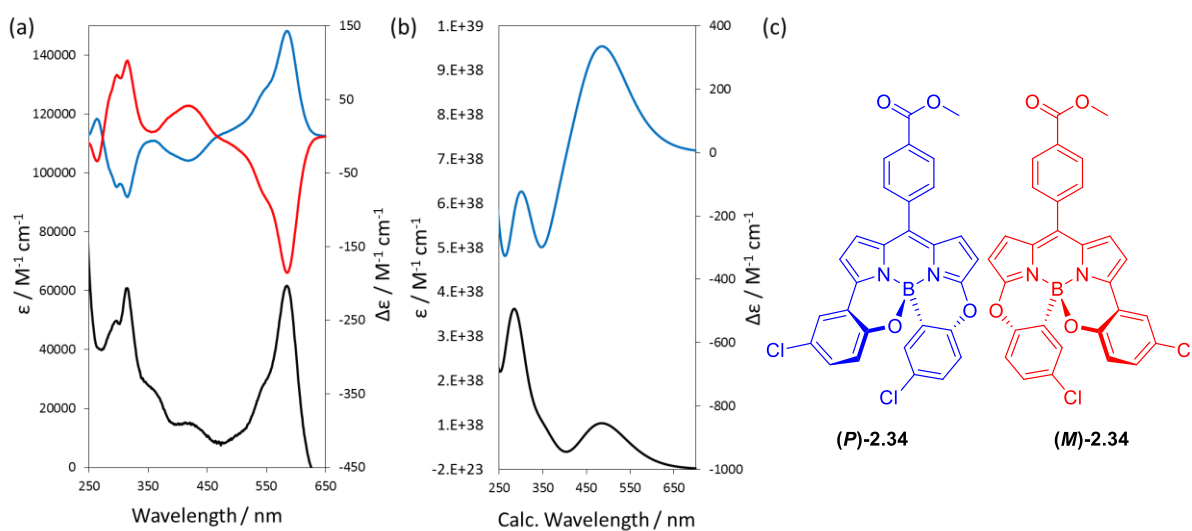
Figure 2.20: (a) Experimental ECD spectra (red – (*M*)-**2.34**, blue – (*P*)-**2.34**) and UV/Vis absorption spectrum (black) measured in DCM; (b) Calculated Boltzmann-weighted spectra, ECD (blue – postulated (*P*)-**2.34** (wavelength uncorrected) and UV/Vis absorption spectra (black – postulated (*P*)-**2.34** (wavelength uncorrected); c) (*P*)-**2.34** and (*M*)-**2.34**.
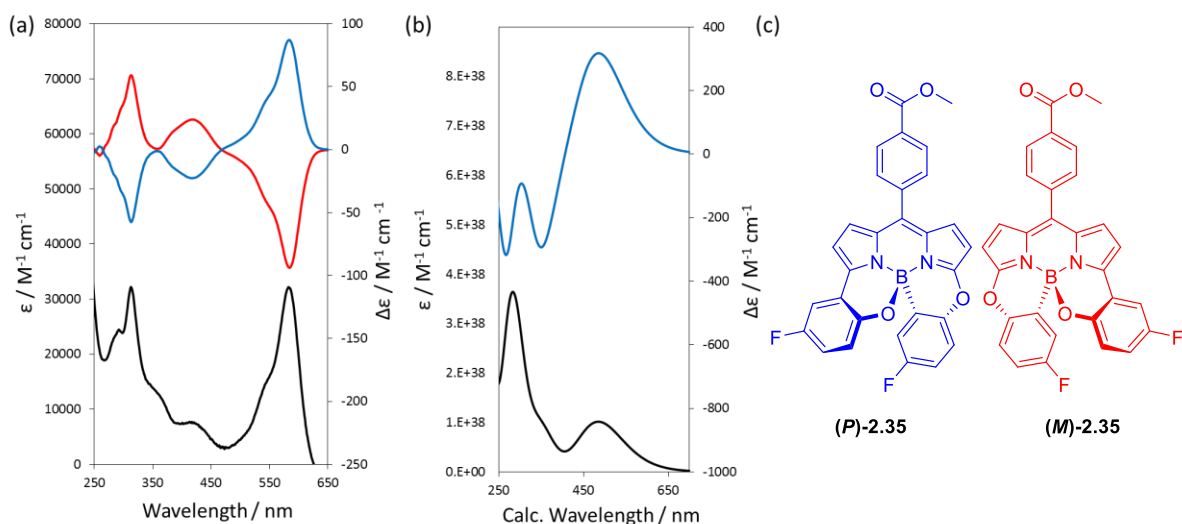
Figure 2.21: (a) Experimental ECD spectra (red – (*M*)-**2.35**, blue – (*P*)-**2.35**) and UV/Vis absorption spectrum (black) measured in DCM; (b) Calculated Boltzmann-weighted spectra, ECD (blue – postulated (*P*)-**2.35** (wavelength uncorrected) and UV/Vis absorption spectra (black – postulated (*P*)-**2.35** (wavelength uncorrected); c) (*P*)-**2.35** and (*M*)-**2.35**.

	Solvent	λ_{abs} /nm	ε /mol^{-1} cm^{-1}	$|g_{abs}|$	$\Delta\varepsilon_{max}$ / L mol^{-1}cm^{-1}
2.18	hexane	593	30 000	3.1×10^{-3}	±92
2.32	DCM	590	24 000	3.2×10^{-3}	±80
2.33	DCM	594	39 000	3.4×10^{-3}	±133
2.34	DCM	586	52 000	2.9×10^{-3}	±142
2.35	DCM	585	32 000	2.8×10^{-3}	±87

Table 2.9: Photophysical and chiroptical data for *N,N,O,C*-BODIPYs **2.18** and **2.32**-**2.35**.

2.3.4.2 CPL spectroscopy of *N,N,O,C*-BODIPYs **2.32**-**2.35**

Lastly CPL spectra of the (*P*) and (*M*) enantiomers of *N,N,O,C*-BODIPYs **2.32**-**2.35** were obtained (figure 2.22). Mirror image CPL spectra were obtained for all four BODIPYs, with g_{lum} values ranging between 2.1-2.6×10^{-3} (table 2.10).
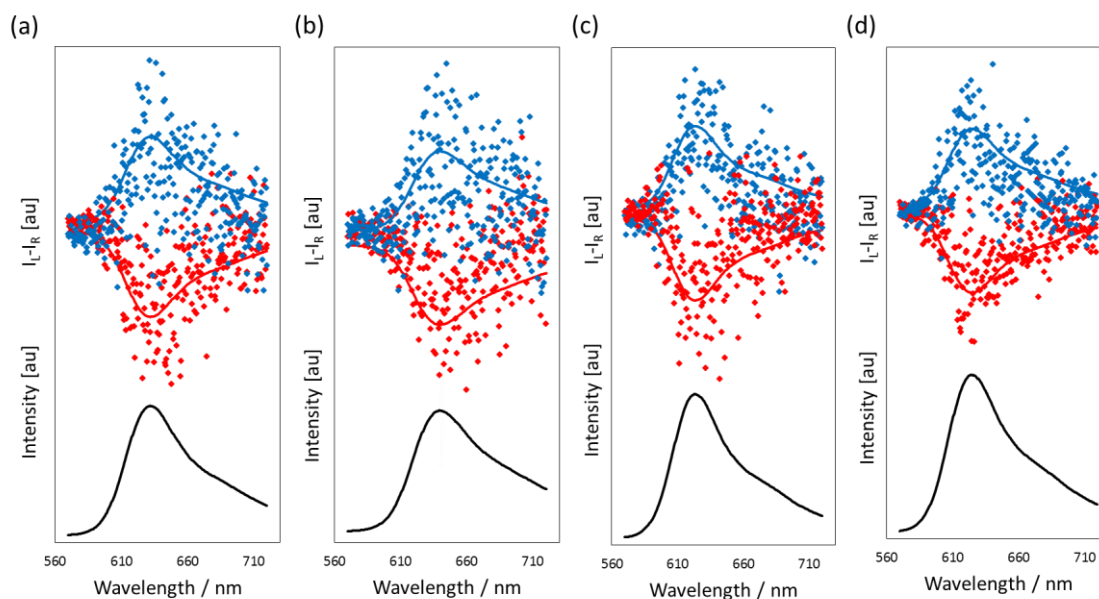
Figure 2.22: (a) Normalised CPL (I_L-I_R) (red – (*M*)-**2.32**, blue – (*P*)-**2.32** and fluorescence spectra (black – (*rac*)-**2.32**) measured in DCM; (b) Normalised CPL (I_L-I_R) (red – (*M*)-**2.33**, blue – (*P*)-**2.33** and fluorescence spectra (black – (*rac*)-**2.33**) measured in DCM; (c) Normalised CPL (I_L-I_R) (red – (*M*)-**2.34**, blue – (*P*)-**2.34** and fluorescence spectra (black – (*rac*)-**2.34**) measured in DCM; (d) Normalised CPL (I_L-I_R) (red – (*M*)-**2.35**, blue – (*P*)-**2.35** and fluorescence spectra (black – (*rac*)-**2.35**) measured in DCM.

Interestingly it can be observed in this series of dyes that if one enantiomer absorbs circularly polarised light with a particular handedness, then it also emits light with the same handedness. In the case of all of the helically chiral BODIPY dyes which have been hitherto reported, including *N,N,O,C*-BODIPYs **2.18** and **2.32**-**2.35**,[8,84] the *P*-isomer both absorbs and emits mostly left handed circularly polarised light.

An improved |g_{lum}| value from that observed from *N,N,O,C*-BODIPY **2.18** was not found among the four derivatives **2.32**-**2.35**. However the g_{lum} values obtained are typical when compared to the g_{lum} values usually observed from CPL-SOMs. Additionally the g_{lum} values obtained for *N,N,O,C*-BODIPYs **2.18** and **2.32**-**2.35** are consistent across the series, which suggests that modifications to the 3,5-aryl rings can be made without detriment to the CPL capability of the dye. This opens up the possibility of maintaining a predictable CPL output, while introducing functionality to the system.

	Solvent	λ_{abs} /nm	$\Delta\varepsilon_{max}$ / L mol^{-1} cm^{-1}	λ_{lum} /nm	ϕ_F	$|g_{lum}|$	$|g_{abs}|$	$|g_{lum}|/|g_{abs}|$	$(|g_{lum}|\cdot\phi_F)$
2.18	hexane	593	±92	622	0.49	3.7×10^{-3}	3.1×10^{-3}	1.19	1.8×10^{-3}
2.32	DCM	590	±80	633	0.41	2.3×10^{-3}	3.2×10^{-3}	0.72	9.4×10^{-4}
2.33	DCM	594	±133	637	0.25	2.6×10^{-3}	3.4×10^{-3}	0.76	6.5×10^{-4}
2.34	DCM	586	±142	622	0.37	2.1×10^{-3}	2.9×10^{-3}	0.72	7.8×10^{-4}
2.35	DCM	585	±87	623	0.43	2.2×10^{-3}	2.8×10^{-3}	0.79	9.46×10^{-4}

Table 2.10: Photophysical and chiroptical properties of *N,N,O,C*-BODIPYs **2.18** and **2.32**-**2.35**.

2.3.4.3 Assessing the correlation between g_{abs} and g_{lum} for the *N,N,O,C*-BODIPY series

As discussed in section 2.1.1.3 Mori *et al*.[134] have assessed the relationship between g_{abs} and g_{lum} for a range of CPL-SOMs, including BODIPYs. It was found that for rigid BODIPY systems, a good linear correlation was observed ($|g_{lum}|$ = 1.02×$|g_{abs}|$ (r^2=0.90)). Since one of our chapter aims was to corroborate this observation, we correlated the g_{lum} and g_{abs} values recorded for our *N,N,O,C*-BODIPY series (in red, figure 2.23) along with the rigid CPL-active BODIPYs studied by Mori *et al*. (in black, figure 2.23).
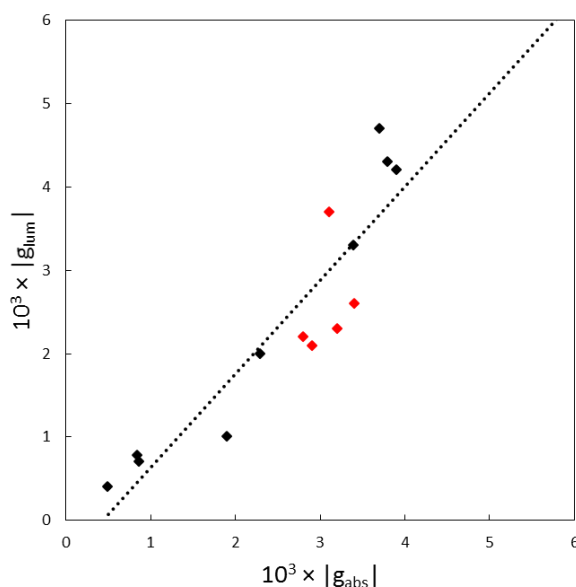
Figure 2.23: Correlation between g_{abs} and g_{lum} for the rigid CPL-active BODIPYs studied by Mori (black) and the *N,N,O,C*-BODIPYs **2.18** and **2.32**-**2.35** (red).

We found that the good linear correlation between g_{lum} and g_{abs} was maintained ($|g_{lum}|$ = 1.18×$|g_{abs}|$ (r^2=0.80)) when we included our new *N,N,O,C*-BODIPY systems. Although we observe a decrease in the r^2 value of the trend line (r^2 = 0.80 vs. 0.90), we can still consider this to be a good linear correlation.

2.4 Conclusions and Future work

In this chapter we aimed to synthesise new chiral BODIPYs according to two main design principles: a chirally perturbed BODIPY core (section 2.1.1.1), and a rigidified structure (section 2.1.1.3). We have considered these design principles in the examination of new chiral BODIPYs for use as CPL-SOMs.

The serendipitous discovery of *N,N,O,C*-BODIPY **2.18** has led to the identification of a new class of helically chiral BODIPYs, the *N,N,O,C*-BODIPYs. Chiroptical characterisation of *N,N,O,C*-BODIPY **2.18**, including the measurement of CPL (g_{lum} = 3.7×10^{-3}) confirmed that *N,N,O,C*-BODIPY **2.18** is a CPL-active BODIPY. Furthermore comparison of our experimental g_{lum} values and those obtained through computational modelling has allowed us to validate a computational method for the prediction of g_{lum}. By establishing the validity of computational modelling, we have gained valuable insight into the design of CPL-active BODIPYs.

Through a mechanistic investigation into the synthesis of *N,N,O,C*-BODIPY **2.18** we have designed and validated a new, reliable synthetic route to the *N,N,O,C*-BODIPYs. Subsequently, we have expanded the *N,N,O,C*-BODIPY series and have completed the chiroptical characterisation of all *N,N,O,C*-BODIPYs **2.32**-**2.35**.

We have thus shown that it is possible to include additional functionality into the 3,5-aryl rings of *N,N,O,C*-BODIPYs, without detriment to CPL emission. This opens up the possibility of creating more complex BODIPY systems based upon the *N,N,O,C*-BODIPY architecture, in order to synthesise highly functionalised CPL-active BODIPYs.

The validation of computational modelling to predict g_{lum} has promising applications to the future design of CPL-active BODIPYs. So far we have identified two possible strategies to increase the g_{lum} of these helically chiral BODIPY systems. The first of which is the inclusion of sulfur atoms (chapter 3), and the second is the extension of the BODIPY π-system to increase the helical pitch (chapter 4).

Chapter 3. Investigation of Sulfur Atom Inclusion on CPL Activity

3.1 Introduction

3.1.1 Effect of sulfur atom inclusion on g_{lum}

In this chapter, we will discuss our investigations into synthetic methodologies to introduce sulfur atoms to chiral BODIPY systems. We will then assess the effect of sulfur atom inclusion on CPL emission.

As discussed in section 2.2.4.1, we can control the $|g_{lum}|$ of a CPL-SOM by controlling the magnitudes of the magnetic ($|\mathbf{m}|$) and electric ($|\boldsymbol{\mu}|$) dipole moments. The equation which relates g_{lum} to $\mathbf{m}$ and $\boldsymbol{\mu}$ is as follows:

$$g_{lum} = \frac{4(\boldsymbol{\mu} \cdot \boldsymbol{m} \cdot cos\tau)}{(\boldsymbol{\mu}^2 + \boldsymbol{m}^2)}$$

In small organic molecules $\boldsymbol{\mu}$ is typically several orders of magnitude larger than $\mathbf{m}$, resulting in low g_{lum} values. In order to achieve a maximum g_{lum} value, we would look to increase $|\mathbf{m}|$ or decrease $|\boldsymbol{\mu}|$ in order to result in more similar magnitudes for these vectors. In chapter 2 we examined the effect of increased charge-transfer character in the excited state on the $|g_{lum}|$ of *N,N,O,C*-BODIPY **2.18**. Although the increased charge-transfer character did result in a reduced $|\boldsymbol{\mu}|$ as we had hoped, we found that a detrimental change in the angle τ resulted in a slight overall decrease in $|g_{lum}|$. We therefore looked to examine an alternative strategy to increase $|g_{lum}|$.

We thought that instead of attempting to decrease $|\boldsymbol{\mu}|$, we could instead attempt to increase $|\mathbf{m}|$ to result in a higher $|g_{lum}|$. The equation which describes the magnetic transition dipole moment is as follows:

$$\boldsymbol{\epsilon} \cdot \boldsymbol{d}_{if} = \frac{1}{2m_e c} \boldsymbol{b} \cdot \langle i|L + 2S|f \rangle$$

Where the term ϵ is the unity vector and $\mathbf{d}_{if}$ is the dipole matrix, together these terms describe the magnetic ($\mathbf{m}$) dipole moment vector. Furthermore m_e is the mass of an electron, c is the speed of light, $\mathbf{b}$ is the polarisation direction of the magnetic component and **S** is the electron spin. Pertinently the term **L** represents the orbital angular momentum. Thus we can conclude that if we increase the orbital angular momentum (**L**), we can increase $|\mathbf{m}|$.

Chiral lanthanide complexes have been shown to be efficient emitters of CPL,[5,6,153] with typically high g_{lum} values (≤1.38).[7,154] The success of chiral lanthanide complexes as CPL-emitters arises from the involvement of *f*-orbital character in their optical transitions. This *f*-orbital character results in higher

orbital angular momentum, which in turn increases $|\mathbf{m}|$. Small organic molecules typically only have *p*-orbital character in their optical transitions, which results in lower orbital angular momentum and thus small $|\mathbf{m}|$.

Sulfur has been shown to increase angular momentum,[155] due to the increased *d*-orbital character imparted by sulfur atoms. One strategy to achieve this increase in $|\mathbf{m}|$ was identified by computational modelling (performed by Dr Thomas Penfold). Thus *N,N,S,S*-BODIPY **3.1** was proposed as a sulfur containing, helically chiral BODIPY with an increased g_{lum}. Preliminary computational modelling of *N,N,S,S*-BODIPY **3.1** gave a predicted g_{um} value of 9×10^{-3}.

3.1
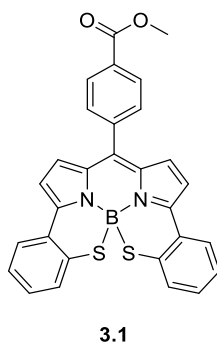
Figure 3.1: *N,N,S,S*-BODIPY **3.1**.

3.1.2 Chapter Aims

Thus our aim for this chapter is the synthesis of *N,N,S,S*-BODIPY **3.1**, in order to examine the effect of sulfur atom inclusion on g_{lum}.

We considered an approach towards *N,N,S,S*-BODIPY **3.1** which involves a late-stage Suzuki coupling between the intermediate 3,5-dibromo-BODIPY **2.11** and (2-(methylthio)phenyl)boronic acid. The resulting 3,5-diaryl-BODIPY **3.2** will then undergo a double demethylation reaction and *in situ* intramolecular double B-S bond formation to form the target *N,N,S,S*-BODIPY **3.1**.
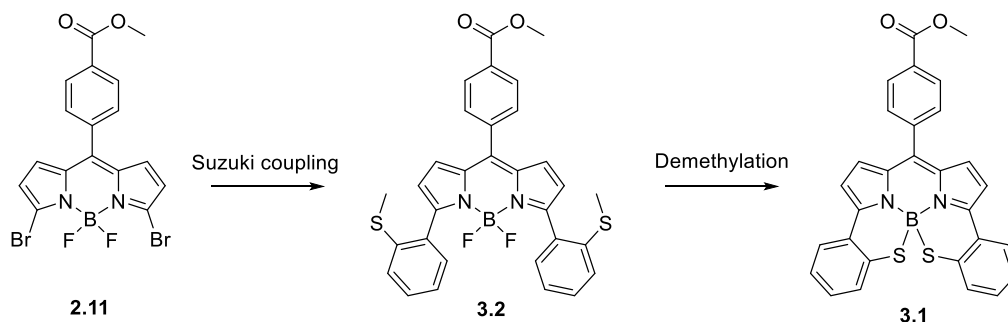
Scheme 3.1: First planned approach towards *N,N,S,S*-BODIPY **3.1**.

3.2 Results and Discussion

3.2.1 Synthesis of *N,N,S,S*-BODIPY **3.1** *via* a late-stage Suzuki-Miyaura coupling approach

3.2.1.1 Synthesis of 3,5-diaryl-BODIPY **3.2**

Our first step was the synthesis of the intermediate 3,5-dibromo-BODIPY **2.11**. To do this, we followed the same procedure described in section 2.1.2.2. For the next step, we planned to use a Suzuki-Miyaura cross-coupling between 3,5-dibromo-BODIPY **2.11** and 2-(methylthio)phenyl boronic acid to synthesise 3,5-diaryl-BODIPY **3.2**.

Thus we performed a Suzuki-Miyaura cross-coupling between 3,5-dibromo-BODIPY **2.11** and 2-(methylthio)phenyl boronic acid, catalysed by Pd(PPh₃)₄ (5 mol%). Following purification by silica gel chromatography, we were able to isolate 3,5-diaryl-BODIPY **3.2** in a good yield of 63%. We confirmed the formation of 3,5-diaryl-BODIPY **3.2** by analysis of the ^{1}H NMR spectrum, which showed a signal corresponding to the hydrogens of the thiomethyl groups (δ_H 2.39 ppm, s, 6H) and signals corresponding to the pyrrolic hydrogens (δ_H 6.84 ppm, d, 2H, *J* = 4.3 Hz; 6.64 ppm, d, 2H, *J* = 4.3 Hz).

2.11   **3.2**
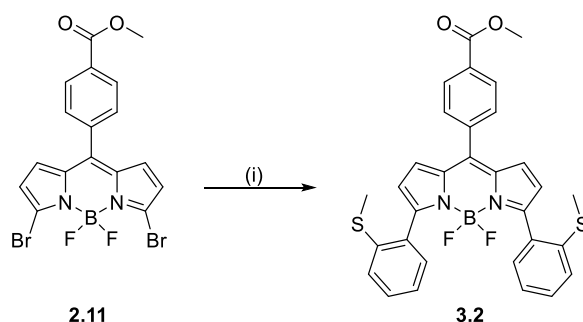
Scheme 3.2: Reagents and conditions: (i) 2-(methylthio)phenyl boronic acid (4 eq.), Pd(PPh₃)₄ (5 mol%), Na₂CO₃, toluene, 1,4-dioxane, 90 °C, 18 h (63%).

3.2.1.2 Examination of the double demethylation reaction of 3,5-diaryl-BODIPY **3.2**

Our next planned step in our synthetic pathway was the double demethylation of 3,5-diaryl-BODIPY **3.2** and *in situ* intramolecular double B-S bond formation, resulting in the formation of *N,N,S,S*-BODIPY **3.1**. To achieve this, we planned to use boron tribromide at low temperatures.[84]

Therefore we reacted 3,5-diaryl-BODIPY **3.2** with boron tribromide at 0 °C. After 80 minutes, we observed the appearance of a new compound by TLC analysis. Purification of the crude reaction mixture by silica gel chromatography was challenging, due to poor solubility. Despite this challenging purification, we were able to analyse the ^{11}B NMR and ^{1}H NMR spectra of the impure product. Examination of the ^{1}H NMR spectrum suggested the loss of one methyl group of one of the thiol moieties (δ_H 2.30 ppm, s, 3H), however the ^{11}B NMR spectrum showed that boron had been lost during the course of the reaction. We thought that the demethylation was failing due to the boron tribromide

preferentially mediating the loss of BF_2 from 3,5-diaryl-BODIPY **3.2** instead of mediating the loss of the methyl groups of the thiol moieties.[156] We decided to first remove the BF_2 moiety from 3,5-diaryl-BODIPY **3.2**, and then repeat the demethylation procedure.
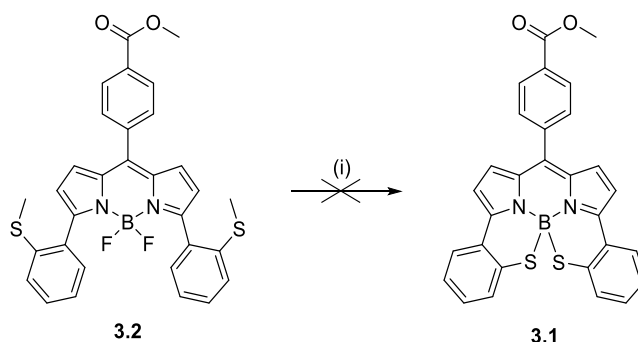
Scheme 3.3: Reagents and conditions: (i) BBr_3 (10 eq.), DCM, 0 °C, 1h.

We elected to use a BODIPY deprotection strategy described by Sánchez *et al.*, which involves the use of a Lewis acid (trifluoroacetic acid) to mediate the loss of BF_2 from the BODIPY core.[146] Therefore we dissolved 3,5-diaryl-BODIPY **3.2** in a solution of DCM:methanol:trifluoroacetic acid (90:5:5). Simple purification by removal of the reaction solvents under reduced pressure led to the isolation of dipyrromethene **3.3** in an almost quantitative yield (99%). Analysis of the ^{11}B NMR spectrum confirmed that we had successfully removed the BF_2 moiety. Thus we were then able to attempt the double demethylation of dipyrromethene **3.3**.
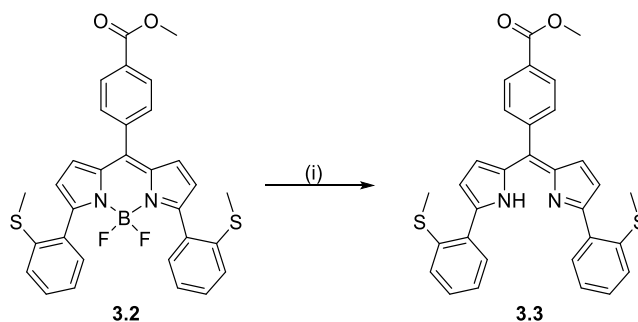
Scheme 3.4: Reagents and conditions: (i) DCM:MeOH:TFA (90:5:5), R.T., 1 h (99%).

In our first attempt at the double demethylation of dipyrromethene **3.3**, we added boron tribromide to a solution of dipyrromethene **3.3** at 0 °C and then allowed the reaction mixture to reach room temperature before work-up (entry 1, table 3.1). Analysis of the crude ^{1}H NMR spectrum showed that we had retained the methyl groups of the thiol moieties (δ_H 2.31 ppm, s, 6H), and had instead lost the methyl group of the methyl ester (δ_H 3.98 ppm, s, 3H). Extending the reaction time (entry 2, table 3.1) and increasing the reaction temperature (entry 3, table 3.1) did not result in the loss of the methyl groups of the thiol moieties, and again the methyl group of the methyl ester was removed.

We decided to examine the use of an alternative source of boron tribromide. Therefore we repeated the demethylation procedure using boron tribromide dimethyl sulfide. Our first attempt at this transformation resulted in the recovery of starting material dipyrromethene **3.3**, and increasing the reaction temperature resulted again in the loss of the methyl group from the methyl ester.

3.3
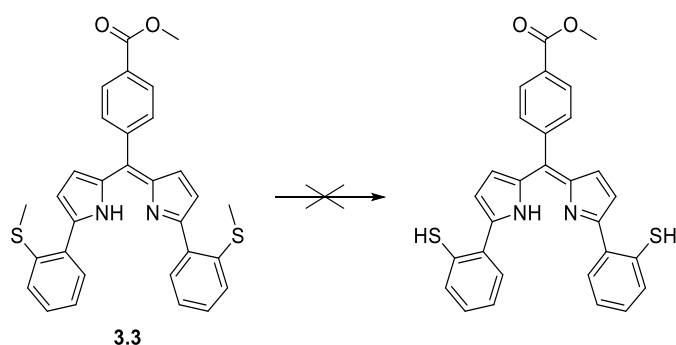
Entry	Reagent	Reaction Solvent	Reaction time /h	Reaction temperature	Reaction outcome
1	BBr$_3$ (1 M in hexane, 10 eq.)	DCM	1	0 °C to R.T.	loss of methyl group from methyl ester
2	BBr$_3$ (1 M in hexane, 10 eq.))	DCM	24	0 °C to R.T.	loss of methyl group from methyl ester
3	BBr$_3$ (1 M in DCM, 10 eq.))	CHCl$_3$	2	reflux	loss of methyl group from methyl ester
4	BBr$_3$SMe$_2$ (1 M in DCM, 10 eq.))	DCM	21	R.T.	starting material dipyrromethene **3.3** recovered
5	BBr$_3$SMe$_2$ (1 M in DCM, 10 eq.))	CHCl$_3$	19	reflux	loss of methyl group from methyl ester

Table 3.1: Examination of the reaction conditions to achieve the double demethylation of dipyrromethene **3.3**, reaction outcomes determined by analysis of the crude ^{1}H NMR spectra.

Given the difficulties we encountered in our attempts to remove the methyl groups of the thiol moieties of 3,5-diaryl-BODIPY **3.2** and dipyrromethene **3.3**, we decided instead to examine a second approach towards *N,N,S,S*-BODIPY **3.1**.

3.2.2 Synthesis of *N,N,S,S*-BODIPY **3.1** via a prefunctionalisation route

3.2.2.1 Planned second approach towards the synthesis of *N,N,S,S*-BODIPY **3.1**

The second approach we examined to synthesise *N,N,S,S*-BODIPY **3.1** involves a pre-functionalisation strategy, whereby the pyrrole moiety is functionalised prior to the formation of the BODIPY architecture. We planned to use a Suzuki-Miyaura cross-coupling reaction to introduce the desired

functionality to the pyrrole. However thiols are known to poison palladium catalysts[157,158] thus requiring the use of more than stoichiometric amounts of catalyst.

We therefore planned to protect the sulfur of 2-bromothiophenol prior to the Suzuki-Miyaura cross-coupling reaction (step A, scheme 3.5).[159] The resulting protected benzenethiol **3.4** will then be used in a Suzuki-Miyaura cross-coupling reaction with *N*-Boc-2-pyrroleboronic acid to produce Boc-protected 2-arylpyrrole **3.5** (step B).[160] A subsequent Boc deprotection (step C) allows for the next step, in which a condensation reaction between 2-arylpyrrole **3.6** and methyl 4-formylbenzoate is followed immediately by oxidation in a one-pot procedure to form dipyrromethene **3.7** (step D). A sulfur double deprotection (step E) and subsequent boron chelation (step F) would then form the target *N,N,S,S*-BODIPY **3.1**.
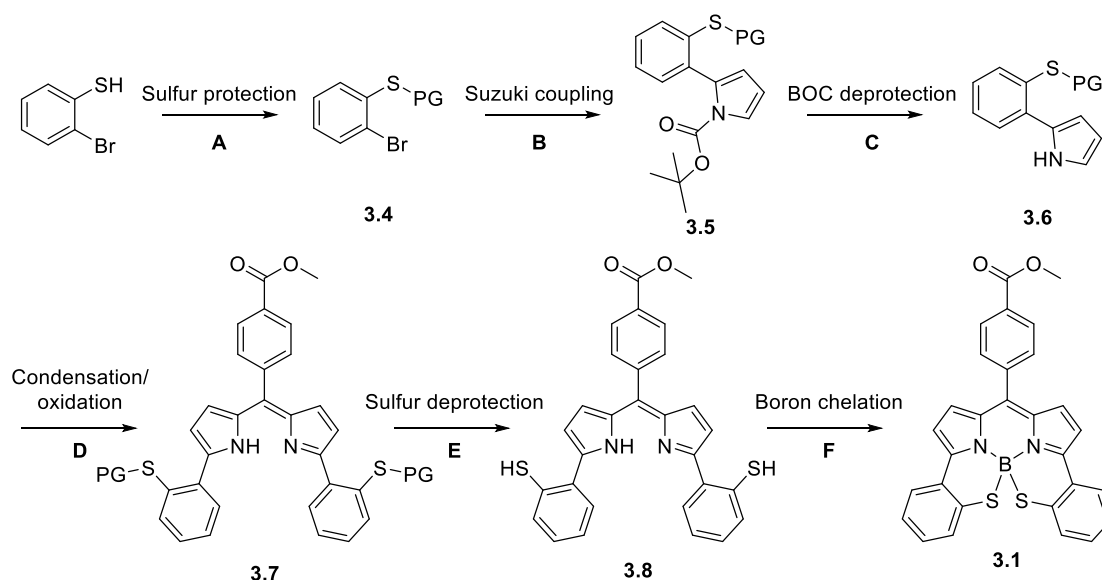
Scheme 3.5: Second planned approach towards *N,N,S,S*-BODIPY **3.1**.

3.2.2.2 Synthesis of MOM-protected dipyrromethene **3.7a**

The first step in our second approach to *N,N,S,S*-BODIPY **3.1** is the protection of the sulfur atom of 2-bromothiophenol. Protection of the sulfur moiety is required at this stage to allow for the subsequent Suzuki-Miyaura coupling to produce the desired 2-arylpyrrole.

We chose to use a methoxymethyl ether (MOM) protecting group, which are typically removed using acidic conditions. Since we were not planning to use strongly acidic conditions for any of our subsequent synthetic steps, we concluded that a MOM protecting group is compatible with our planned synthetic route. Additionally Yamamoto *et al.* have shown that the MOM protected *ortho*-bromobenzenethiols undergo Sonogashira cross-couplings,[159] so we reasoned that we would observe

good reaction compatibility between this protecting group and our planned Suzuki-Miyaura cross-coupling reaction.

Therefore 2-bromothiophenol was reacted with methoxymethyl chloride in the presence of a suitable base (scheme 3.6). Disappearance of the starting material and the appearance of a new compound by TLC analysis indicated that the reaction was complete. Purification of the crude reaction mixture by silica gel chromatography allowed us to isolate benzenethiol **3.4a** in a quantitative yield. The successful protection of 2-bromothiophenol was confirmed by the appearance of two singlets in the ^{1}H NMR spectrum corresponding to the methoxymethyl moiety (δ_H 5.02 ppm, s, 2H; 3.45 ppm, s, 3H).

3.4a
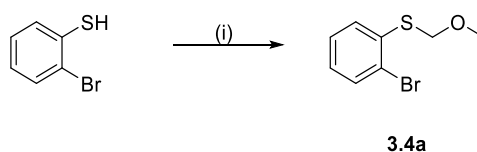
Scheme 3.6: Reagents and conditions: (i) NaO^{t}Bu (1 eq.), MOMCl (1.1 eq.), THF, R.T., 30 minutes (quant.).

The next step in our synthetic pathway involved a Suzuki-Miyaura cross-coupling between benzenethiol **3.4a** and *N*-Boc-2-pyrroleboronic acid. Thus a Suzuki-Miyaura cross-coupling reaction between benzenethiol **3.4a** and *N*-Boc-2-pyrroleboronic acid (catalysed by Pd(PPh$_3$)$_4$, 5 mol%), was followed by silica gel chromatography to give Boc-protected 2-arylpyrrole **3.5a** in a good yield of 77%. We confirmed the formation of **3.5a** by analysis of the FT-IR spectrum, which showed a peak at 1736 cm^{-1} corresponding to the C=O bond of the Boc protecting group.

3.4a   **3.5a**
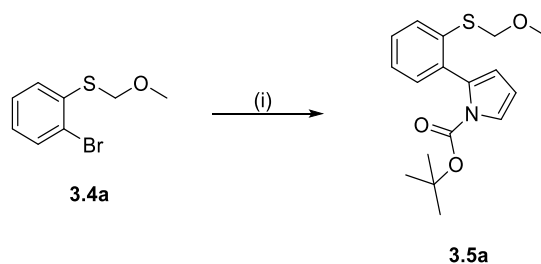
Scheme 3.7: Reagents and conditions: (i) *N*-Boc-2-pyrroleboronic acid (1.5 eq.), Pd(PPh$_3$)$_4$ (5 mol%), K$_3$PO$_4$, THF, H$_2$O, 75 °C, 24 h (77%).

In order to successfully form the dipyrromethene **3.7a**, we must first remove the sterically demanding Boc group. Thus next step we examined in our synthetic pathway was the Boc deprotection of 2-arylpyrrole **3.5a**.

The removal of the Boc protecting group was performed following a thermolytic deprotection procedure.[161] The advantage of this method are that there is no solvent, acid or base required.

We heated a round bottomed flask containing Boc-protected 2-arylpyrrole **3.5a** to 200 °C for 30 minutes. Examination of the FT-IR spectrum of the crude product showed that the peak at 1736 cm^{-1} corresponding to the C=O bond of the Boc protecting group was no longer present, confirming the successful deprotection of Boc-protected 2-arylpyrrole **3.5a**. Analysis of the crude ^{1}H NMR spectrum showed that Boc-deprotected 2-arylpyrrole **3.6a** had been formed in sufficient purity to continue with the next step in our synthetic pathway without further purification.
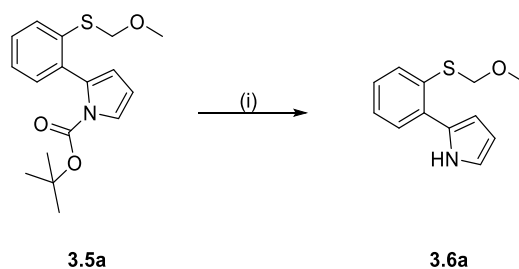
Scheme 3.8: Reagents and conditions: (i) 200 °C, 30 minutes.

Once we had synthesised 2-arylpyrrole **3.6a**, the next step we wished to examine was the one-pot condensation/oxidation procedure to form dipyrromethene **3.7a**. We opted to use a trifluoroacetic acid (TFA) catalysed condensation procedure, followed immediately by oxidation with *p*-chloranil.

We therefore reacted the 2-arylpyrrole **3.6a** together with methyl 4-formylbenzoate in the presence of a catalytic amount of TFA. After the disappearance of methyl 4-formylbenzoate was observed by TLC analysis, we added a solution of *p*-chloranil in DCM and saw an instant colour change. We were concerned that the oxidant (*p*-chloranil) may oxidise the sulfide groups to the corresponding sulfoxides or sulfones, so we left the reaction mixture to stir for only ten minutes after the addition of *p*-chloranil. The appearance of a new compound by TLC analysis indicated that we had formed dipyrromethene **3.7a**. After work up, dipyrromethene **3.7a** was isolated in an exceptional 87 % yield, and examination of the ^{1}H NMR spectrum indicated that **3.7a** did not require further purification. We confirmed the structure of dipyrromethene **3.7a** by the observation of signals in the ^{1}H NMR spectrum corresponding to the aryl methyl ester (δ_H 3.99 ppm, s, 3H) and signals corresponding to the MOM protecting groups (δ_H 4.80 ppm, s, 4H; 3.23 ppm, s, 6H).

3.6a   3.7a
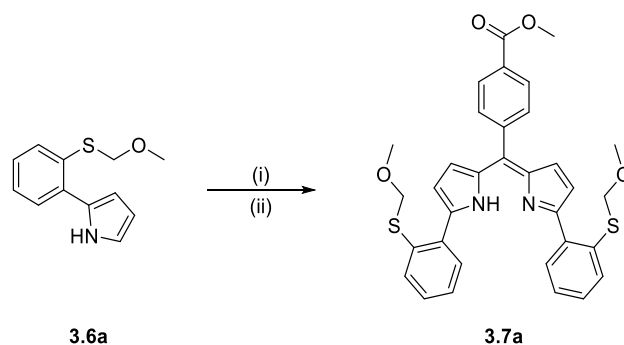
Scheme 3.9: Reagents and conditions: (i) methyl 4-formylbenzoate, TFA (cat.), DCM, R.T., 3.5 h; (ii) *p*-chloranil (1 eq.), R.T., 10 minutes (87%).

Once we had successfully synthesised dipyrromethene **3.7a**, we turned our attention to the MOM deprotection of the sulfide functional groups and subsequent chelation of boron, to form *N,N,S,S*-BODIPY **3.1**.

3.2.2.3 Attempts towards the MOM deprotection of dipyrromethene **3.7a**

MOM protecting groups are typically removed under acidic conditions. Therefore the first MOM deprotection approach we examined involved the treatment of dipyrromethene **3.7a** with acid. Following an adapted literature procedure,[162] we treated dipyrromethene **3.7a** with a solution of hydrochloric acid in methanol (generated by the slow addition of acetyl chloride to anhydrous methanol at 0 °C). However after 24 hours there was no indication by TLC analysis that any new products had been formed. Analysis of the crude ^{1}H NMR spectrum showed that we had recovered starting material dipyrromethene **3.7a**. We therefore looked to examine an alternative deprotection strategy.

3.7a   3.8a
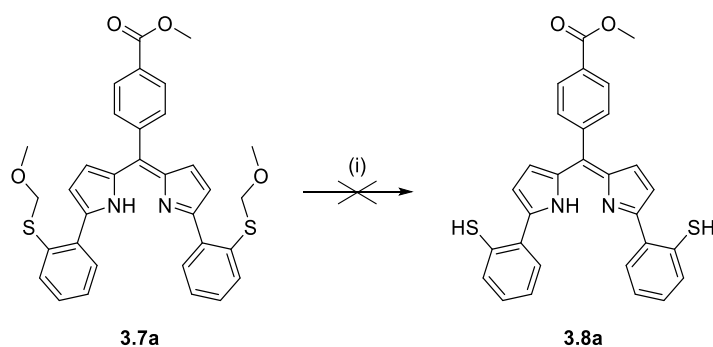
Scheme 3.10: Reagents and conditions: (i) HCl (1 M in MeOH), DCM, R.T., 24 h.

The second MOM deprotection strategy we examined was the treatment of dipyrromethene **3.7a** with boron trichloride.[163] We treated dipyrromethene **3.7a** with boron trichloride at room temperature and after 5 minutes, the disappearance of starting material and the appearance of a new compound by TLC suggested that the reaction was complete. However upon analysis of the crude ^{1}H NMR spectrum

we observed signals corresponding to the MOM protecting group (δ_H 4.76 ppm, s, 4H; 2.16 ppm, s, 6H). Since we had limited amounts of dipyrromethene **3.7a**, we decided to attempt optimisation of this procedure on the benzenethiol **3.4a**.
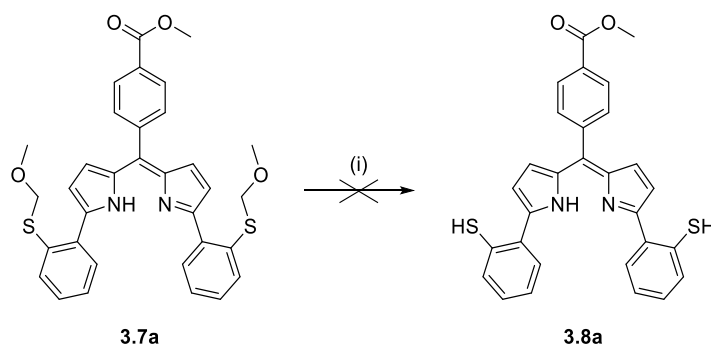
Scheme 3.11: Reagents and conditions: (i) BCl₃, DCM, R.T., 5 minutes.

Treatment of benzenethiol **3.4a** with boron trichloride at room temperature did not result in the formation of 2-bromothiophenol. Analysis of the crude ^{1}H NMR spectrum revealed that the peak corresponding to the methyl group of the MOM protecting group was no longer visible, indicating the loss of this methyl group. However the peak corresponding to the hydrogens of the methylene moiety were still visible (δ_H 5.00 ppm, s, 2H). Given the difficulties we encountered in our attempts towards this MOM deprotection, we decided to repeat this synthetic route using an alternative protecting group for 2-bromothiophenol.
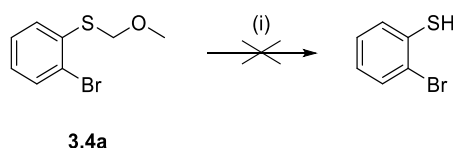
Scheme 3.12: Reagents and conditions: (i) BCl₃, DCM, R.T., 80 minutes.

3.2.2.4 Synthesis of TMSE-protected dipyrromethene **3.7b**

The second sulfur protecting group that we considered was ethyltrimethylsilane (TMSE). This protecting group can be removed using a fluoride source, for example tetra-*N*-butylammonium fluoride (TBAF).[164,165] The only step in our planned synthetic pathway which might generate a fluoride source is the boron chelation step, at which stage we would expect to have already performed the TMSE deprotection. Thus we considered TMSE to be an appropriate protecting group for this approach.

The first step we examined in this approach was the protection of the sulfur of 2-bromothiophenol. Therefore we performed a radical reaction between 2-bromothiophenol and vinyltrimethylsilane in the presence of azobisisobutyronitrile (AIBN) as the radical initiator.[166] After 2.5 hours the

disappearance of the starting material 2-bromothiophenol and the appearance of a new compound by TLC analysis indicated that the reaction was complete. Purification by dry column flash chromatography, using petrol as the eluent, allowed for the isolation of benzenethiol **3.4b** in a quantitative yield. We confirmed the formation of the benzenethiol **3.4b** by analysis of the ^{1}H NMR spectrum, which showed a distinctive AA'BB' spin system arising from the ethyl moiety of the TMSE protecting group of **3.4b** (figure 3.2).
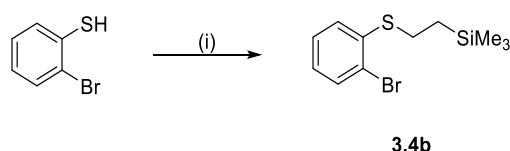
Scheme 3.13: Reagents and conditions: (i) vinyltrimethylsilane (1.2 eq.), AIBN (5 mol%), 100 °C, 2.5h (quant.).
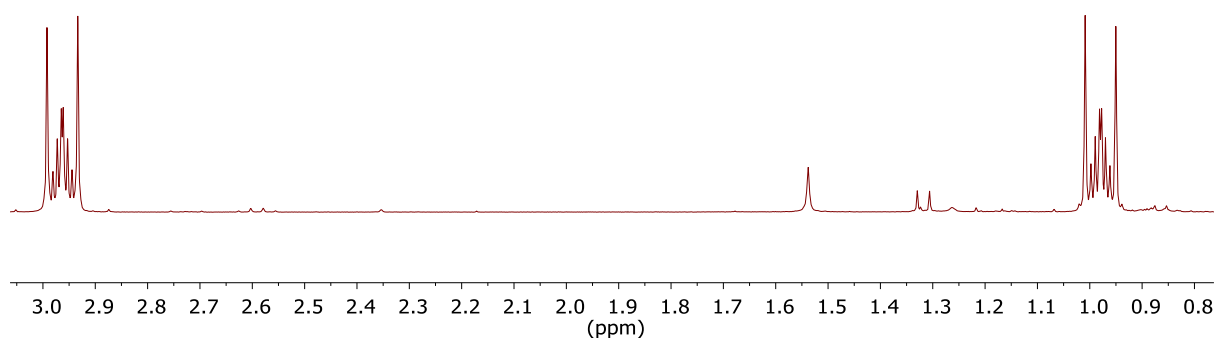
Figure 3.2: ^{1}H NMR spectrum of benzenethiol **3.4b** showing the AA'BB' spin system corresponding to the ethyl moiety.

The next step in our planned approach was the Suzuki-Miyaura cross-coupling reaction between benzenethiol **3.4b** and *N*-Boc-2-pyrroleboronic acid. Thus following the cross-coupling reaction between **3.4b** and *N*-Boc-2-pyrroleboronic acid (catalysed by Pd(PPh$_3$)$_4$, 5 mol %) and purification by silica gel chromatography, we isolated Boc- protected 2-arylpyrrole **3.5b** in an excellent yield of 93%. We confirmed the synthesis of **3.5b** through analysis of the FT-IR spectrum, which showed a peak at 1737 cm^{-1} corresponding to the C=O bond of the Boc protecting group.

3.4b   (i)   3.5b
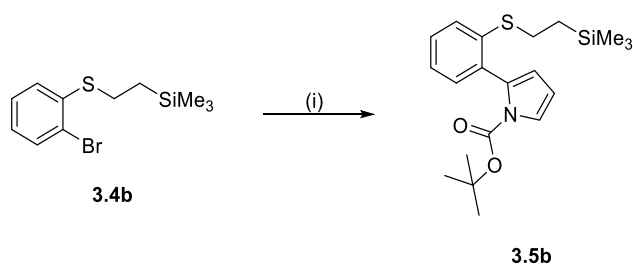
Scheme 3.14: Reagents and conditions: (i) *N*-Boc-2-pyrroleboronic acid (1.5 eq.), Pd(PPh$_3$)$_4$ (5 mol%), K$_3$PO$_4$, THF, H$_2$O, 75 °C, 24 h (93%).

Using the same approach as that employed in section 3.2.2.1, we elected to remove the Boc protecting group by a thermolytic deprotection procedure.[161]

We heated a round bottomed flask containing Boc-protected 2-arylpyrrole **3.5b** to 200 °C for 30 minutes. Examination of the FT-IR spectrum of the crude product indicated the loss of the Boc protecting group, due to the absence of the peak at 1737 cm^{-1} corresponding to the C=O bond of the Boc moiety. Pleasingly the ^{1}H NMR spectrum of the crude product showed that we had formed **3.6b** in sufficient purity to continue with the next step of our synthetic pathway without further purification.

3.5b   (i)   3.6b
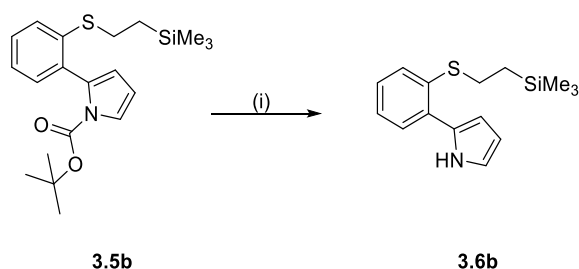
Scheme 3.15: Reagents and conditions: (i) 200 °C, 30 minutes.

With our Boc-deprotected 2-arylpyrrole in hand, we next examined the one-pot condensation/oxidation procedure to form dipyrromethene **3.7b**.

We therefore performed a TFA-catalysed condensation reaction between 2-arylpyrrole **3.7b** and 4-methyl-4-formylbenzoate. After 30 minutes the disappearance of 4-methyl-4-formylbenzoate was observed by TLC analysis, and so a solution of *p*-chloranil in DCM was added. The appearance of a new compound, observed by TLC analysis, indicated that we had formed dipyrromethene **3.7b**. Purification by silica gel chromatography gave dipyrromethene **3.7b** in a good yield of 64%. We confirmed the structure of dipyrromethene **3.7b** through the observation of a signal in the ^{1}H NMR spectrum corresponding to the methyl groups of the TMSE protecting group (δ_H -0.01 ppm, s, 18H) and signals corresponding to the methyl group of the aryl methyl ester (δ_H 3.98 ppm, s, 3H).
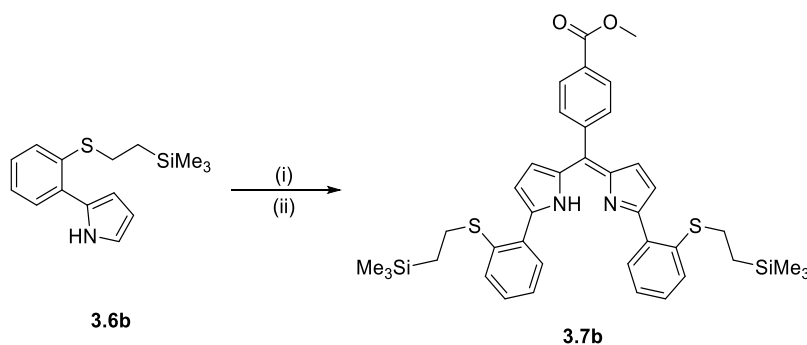
Scheme 3.16: Reagents and conditions: (i) methyl 4-formylbenzoate, TFA (cat.), DCM, R.T., 30 minutes; (ii) *p*-chloranil, R.T., 10 minutes (64%).

Once we had successfully synthesised dipyrromethene **3.7b**, we turned our attention to the TMSE double deprotection of **3.7b**.

3.2.2.5 Attempts towards the TMSE deprotection of dipyrromethene **3.7b**

The TMSE protecting group may be removed using a fluoride source, such as tetra-*N*-butylammonium fluoride (TBAF).[164,165] Due to the difficulties we had previously encountered in our attempts towards the MOM deprotection of dipyrromethene **3.7a**, we decided to test our deprotection procedure on the benzenethiol **3.4b** before attempting the double deprotection of dipyrromethene **3.7b**.

Therefore we treated benzenethiol **3.4b** with an excess of TBAF in THF. After two hours at room temperature, the appearance of 2-bromothiophenol was observed by TLC analysis. Furthermore, examination of the crude ^{1}H NMR spectrum suggested the formation of 2-bromothiophenol, due to the presence of a peak corresponding to the hydrogen of the thiol functional group (δ_H 4.00 ppm, s, 1H).[167] Once we had determined that our deprotection strategy should be successful, we decided to examine the double TMSE deprotection of dipyrromethene **3.7b**.
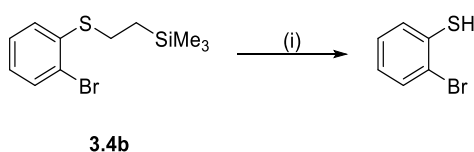
Scheme 3.17: Reagents and conditions: (i) TBAF (6.7 eq.), THF, R.T., 2 h.

We treated dipyrromethene **3.7b** with an excess of TBAF, and after 21 hours we observed the disappearance of starting material and the appearance of a new compound by TLC analysis. However we were unable to determine whether we had formed dipyrromethene **3.7b**, because examination of the crude ^{1}H NMR spectrum only showed peaks corresponding to TBAF. We chose to avoid silica gel chromatography because we thought that dipyrromethene **3.7b** would chelate the trace metals in the silica, leading to a significant loss of product. Therefore we chose to proceed and continue with the

next step in our synthetic pathway, and perform the boron chelation step on the crude reaction mixture.

Treatment of the crude reaction mixture, arising from the attempted double TMSE deprotection step, using our standard boron chelation procedure resulted in a colour change. However TLC analysis suggested that purification by silica gel chromatography would not be workable, due to the high polarity of the crude reaction mixture. Analysis of the ^{11}B NMR spectrum of the crude reaction mixture revealed that the only boron containing species present was residual boron triflouride diethyl etherate, suggesting that boron chelation had been unsuccessful.
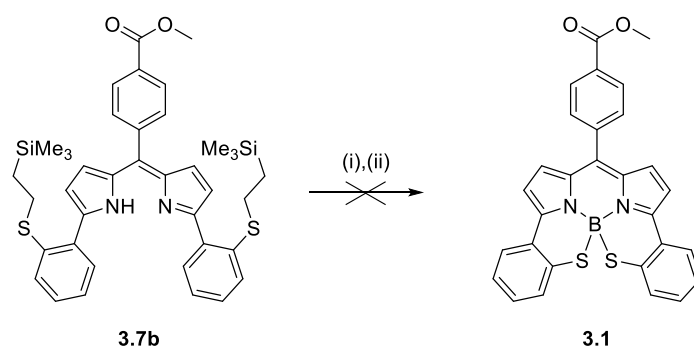
Scheme 3.18: Reagents and conditions: (i) TBAF (13.4 eq.), THF, R.T., 21 h; (ii) BF$_2$.OEt$_2$, N^{i}Pr$_2$Et, DCM, R.T., 1h.

We concluded that this approach was not workable. Due to our inability to confirm the loss of the TMSE protecting groups from **3.7b**, we were unable to rationalise the unsuccessful boron chelation step. We suggest that this approach (i.e. the protection of 2-bromothiophenol and the successive steps to build dipyrromethene **3.7**) is still viable, however future work would include repeating this synthetic pathway using an alternative sulfur protecting group.

3.2.3 New sulfur-containing chiral BODIPY targets

Due to the difficulties presented by the synthesis of *N,N,S,S*-BODIPY **3.1**, we decided to re-examine our design of sulfur containing chiral BODIPYs. We wanted to retain the helically chiral architecture, along with the chirally induced twist to the planar BODIPY core.

We envisioned three helically chiral, sulfur containing BODIPY targets: *N,N,O,O*-BODIPY **3.9** bearing 3,5-dithiophenyl rings, *N,N,O,F*-BODIPY **3.10** bearing a 5-benzothiophene ring system and a 3-phenolic ring, and finally *N,N,O,F*-BODIPY **3.11** which contains a 5-thiophenol substituent and a 3-phenolic ring. All three of these targets are tri- or tetradentate dipyrromethene ligands, and so should have rigid structures. They should also be helically chiral, due to the inclusion of 3-aryl or 3,5-diaryl substituents

containing a B-O bond. We therefore thought that these BODIPYs would be good examples of helically chiral, sulfur containing BODIPYs to examine the effect the inclusion of sulfur atoms has on g_{lum}.

3.9   **3.10**   **3.11**
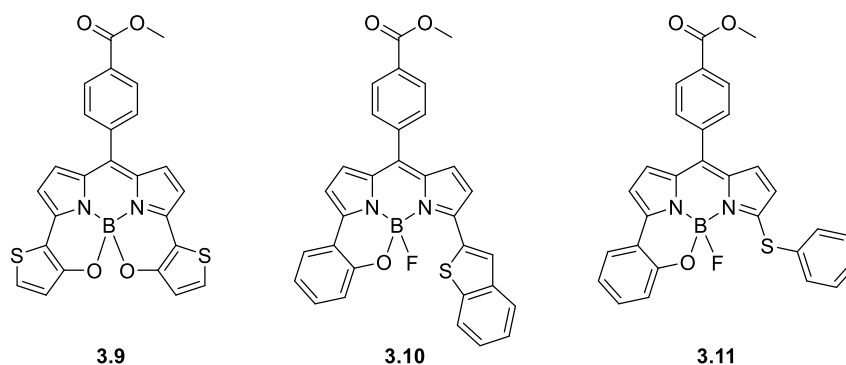
Figure 3.3: *N,N,O,O*-BODIPY **3.9**, *N,N,O,F*-BODIPY **3.10** and *N,N,O,F*-BODIPY **3.11**.

3.2.4 Synthesis of *N,N,O,O*-BODIPY **3.9**

3.2.4.1 Planned synthetic approach towards *N,N,O,O*-BODIPY **3.9**

Our approach towards *N,N,O,O*-BODIPY **3.9** involves a late-stage Suzuki-Miyaura cross-coupling between 3,5-dibromo-BODIPY **2.11** and 3-methoxythiophene-2-boronic acid to form 3,5-dithiophene-BODIPY **3.12**. A subsequent double demethylation and *in situ* double B-O bond formation would then produce the target *N,N,O,O*-BODIPY **3.9**.

Suzuki coupling

Demethylation

2.11   **3.12**   **3.9**
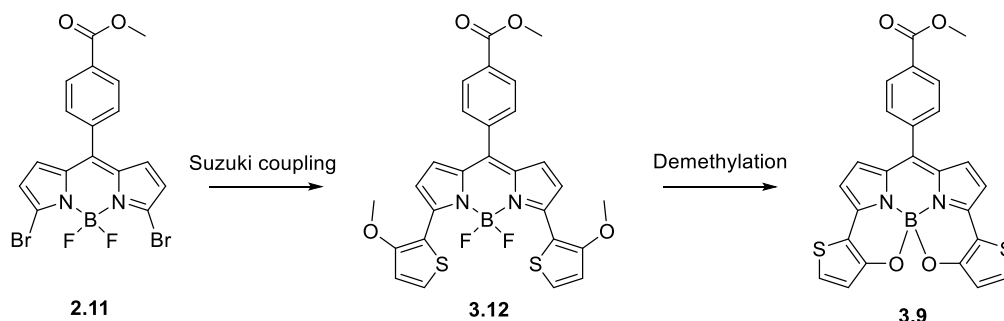
Scheme 3.19: Planned synthetic pathway to *N,N,O,O*-BODIPY **3.9**.

3.2.4.2 Synthesis of 3,5-dithiophene-BODIPY **3.12**

Our procedure for the synthesis of 3,5-dibromo-BODIPY **2.11** has been previously described in section 2.1.2.2, and was followed without modification. Therefore the first step we attempted in the synthesis of *N,N,O,O*-BODIPY **3.9** was the Suzuki-Miyaura cross-coupling reaction between 3,5-dibromo-BODIPY **2.11** and 3-methoxythiophene-2-boronic acid.

We performed a Suzuki-Miyaura cross-coupling, catalysed by Pd(PPh$_3$)$_4$ (5 mol%), between 3,5-dibromo-BODIPY **2.11** and 3-methoxythiophene-2-boronic acid. The disappearance of starting material 3,5-dibromo-BODIPY **2.11** indicated that the reaction was complete. Following purification

by silica gel chromatography, 3,5-dithiophene-BODIPY **3.12** was isolated in an excellent yield of 84%. We confirmed the synthesis of 3,5-dithiophene-BODIPY **3.12** by analysis of the ^{1}H NMR spectrum, which showed a pair of doublets with coupling constants consistent with a thiophene moiety (δ_H 7.48 ppm, d, 2H, J = 5.6 Hz; 6.89 ppm, d, 2H, J = 5.6 Hz).
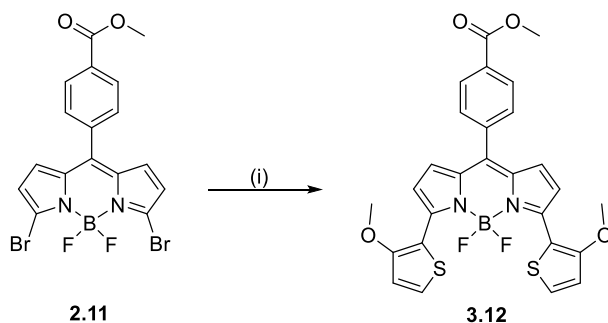
Scheme 3.20: Reagents and conditions: (i) 3-methoxythiophene-2-boronic acid pinacol ester (4 eq.), Pd(PPh$_3$)$_4$ (5 mol%), Na$_2$CO$_3$, toluene, 1,4-dioxane, 90 °C, 23 h (84%).

3.2.4.3 Attempts towards the double demethylation of 3,5-dithiophene-BODIPY **3.12**

Once we had completed the synthesis of 3,5-dithiophene-BODIPY **3.12**, we turned our attention to the boron tribromide mediated double demethylation reaction of **3.12**. This double demethylation reaction would be followed by *in situ* double B-O bond formation to form *N,N,O,O*-BODIPY **3.9**.

Therefore we treated 3,5-dithiophene-BODIPY **3.12** with boron tribromide at 0 °C. The disappearance of starting material **3.12** was observed by TLC analysis, which indicated that the reaction was complete. Examination of the crude ^{1}H NMR spectrum indicated that the double demethylation had been successful, due to the absence of the peak at δ_H 3.94 ppm (s, 6H) corresponding to the methoxy functional groups. If we had formed *N,N,O,O*-BODIPY **3.9** we would observe a singlet in the ^{11}B NMR spectrum, however examination of the crude ^{11}B NMR spectrum showed a doublet at δ_B 0.98 ppm (*J* = 48.5 Hz, figure 3.4). This suggested to us that only one of the B-O bonds had been formed. We suggest that the substructure of this major product **3.13** contains only one B-O bond (scheme 3.21b).
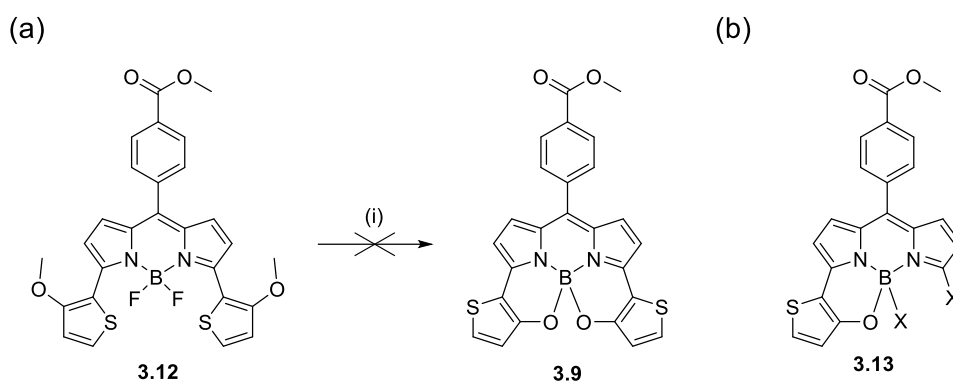
Scheme 3.21: (a) Reagents and conditions: (i) BBr$_3$ (10 eq.), DCM, 0 °C to R.T.; (b) Proposed substructure of the major compound arising from the boron tribromide mediated double demethylation reaction of 3,5-dithiophene-BODIPY **3.12**.
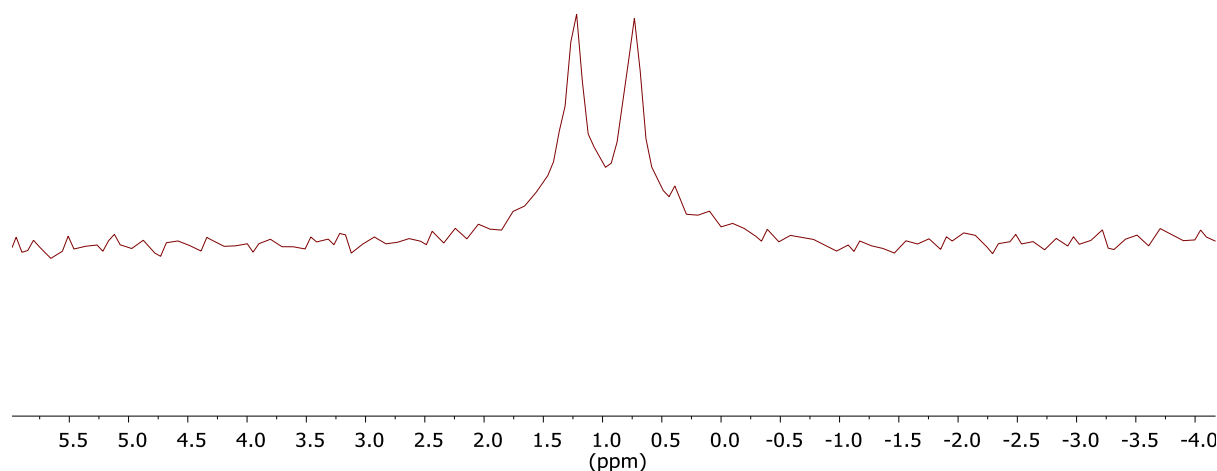
Figure 3.4: ^{11}B NMR spectrum of the crude reaction mixture arising from the boron tribromide mediated double demethylation reaction of 3,5-dithiophene-BODIPY **3.12**.

Purification of this major product was difficult due to its poor solubility, which prevented further analysis. Since this reaction had been initially performed on a small scale (0.018 mmol of starting material 3,5-dithiophene-BODIPY **3.12**), we decided to scale up the reaction to make analysis of the resulting crude reaction mixtures more facile. We also decided that in future repeats of the double demethylation reaction, we would treat the resulting crude reaction mixture with boron triflouride diethyletherate in the presence of Hunig's base. We hoped that this would encourage the second B-O bond formation event to occur, and thereby improve the solubility of the resulting reaction mixtures.

We attempted the double demethylation of 3,5-dithiophene-BODIPY **3.12** multiple times at scales of up to 177 mg (0.32 mmol) of starting material **3.12**. Unfortunately we were unable to detect *N,N,O,O-*BODIPY **3.9** from any these reactions. Instead we consistently observed a doublet at δ$_B$ 0.98 ppm (*J* =

48.5 Hz) in the ^{11}B NMR spectra of the crude reaction mixtures. Despite our attempts to improve the solubility of the crude reaction mixtures by treating them with boron triflouride diethyletherate, the resulting crude mixtures remained insoluble and difficult to purify. Similarly our attempts to encourage the formation of the second B-O bond by treatment of these reaction mixtures with tin tetrachloride[168] did not form *N,N,O,O*-BODIPY **3.9**.

3.12   **3.9**
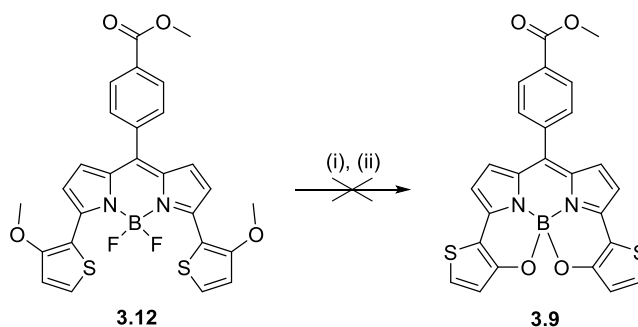
Scheme 3.22: Reagents and conditions: (i) BBr$_3$ (10 eq.), DCM, 0 °C to R.T., (ii) BF$_3$.OEt$_2$, N^{i}PrEt$_2$, DCM, R.T.

We concluded that the synthesis of *N,N,O,O*-BODIPY **3.9** may not be possible. We only found evidence that one of the required B-O bonds was formed, even after treatment with boron triflouride diethyletherate or treatment with tin tetrachloride. We have concluded that the proposed ring system might be too constrained, due to the smaller size of the thiophene rings as compared to the phenyl rings of *N,N,O,O*-BODIPY **2.13**. We decided to focus instead on the synthesis of our other sulfur containing BODIPY targets.

3.2.5 Synthesis of *N,N,O,F*-BODIPY **3.10**

3.2.5.1 Planned synthesis of *N,N,O,F*-BODIPY **3.10**

In order to synthesise *N,N,O,F*-BODIPY **3.10**, we planned to use a late-stage Suzuki-Miyaura cross-coupling reaction between 3,5-dibromo-BODIPY **2.11** and benzo[*b*]thiophene-2-boronic acid to form intermediate BODIPY **3.14**. A further Suzuki-Miyaura cross-coupling reaction between BODIPY **3.14** and 2-hydroxyphenyl boronic acid to install the phenolic ring would then be used to form *N,N,O,F*-BODIPY **3.10**.
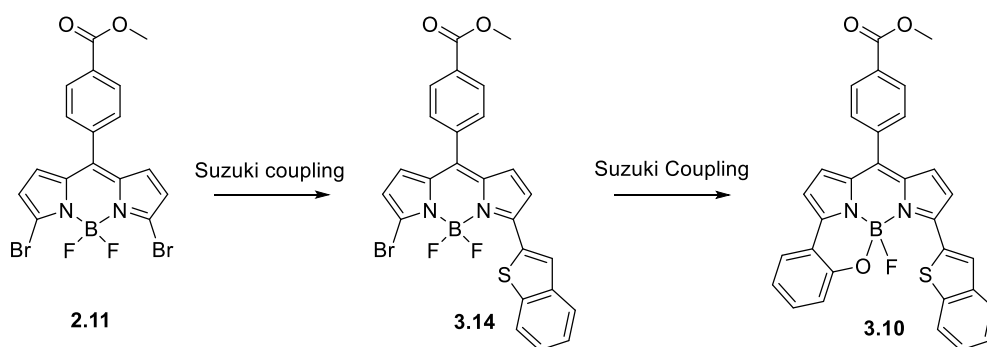
Scheme 3.23: Planned synthetic pathway to *N,N,O,F*-BODIPY **3.10**.

3.2.5.2 Synthesis of 3-benzo[*b*]thiophene-BODIPY **3.14**

Our first planned synthetic step towards *N,N,O,F*-BODIPY **3.10** was the Suzuki-Miyaura cross-coupling reaction between 3,5-dibromo-BODIPY **2.11** and benzo[*b*]thiophene-2-boronic acid to form the 3-benzo[*b*]thiophene-BODIPY **3.14**. We wanted to discourage the occurrence of the double Suzuki-Miyaura cross-coupling reaction, which would produce 3,5-dibenzo[*b*]thiophene-BODIPY **3.15**. We therefore chose to use fewer equivalents of benzo[*b*]thiophene-2-boronic acid than of 3,5-dibromo-BODIPY **2.11**.

We performed a Suzuki-Miyaura cross-coupling reaction between 3,5-dibromo-BODIPY **2.11** and 0.8 equivalents of benzo[*b*]thiophene-2-boronic acid, catalysed by Pd(PPh$_3$)$_4$ (entry 1, table 3.2). After 2 hours we observed by TLC analysis that two new compounds had been formed. After purification by silica gel chromatography, we were able to isolate an impure sample of 3-benzo[*b*]thiophene-BODIPY **3.14**. We were able to confirm the structure of 3-benzo[*b*]thiophene-BODIPY **3.14** by the presence of peaks in the ^{1}H NMR spectrum corresponding to one benzo[*b*]thiophene moiety (δ_H 8.56 ppm, s, 1H; 7.99-7.93 ppm, m, 1H; 7.87-7.81 ppm, m, 1H; 7.45-7.36 ppm, m, 2H). However we also observed in the ^{1}H NMR spectrum that 3-benzo[*b*]thiophene-BODIPY **3.14** was contaminated with a small amount of 3,5-dibenzo[*b*]thiophene-BODIPY **3.15**, and with starting material 3,5-dibromo-BODIPY **2.11**.

Our approximate yield of 3-benzo[*b*]thiophene-BODIPY **3.14** was <5%. The low yield obtained over this step was due to the presence of a large amount of unreacted starting material in the crude reaction mixture. We decided to repeat this Suzuki-Miyaura cross-coupling reaction with an increased number of equivalents of benzo[*b*]thiophene-2-boronic acid, in order to improve the conversion of 3,5-dibromo-BODIPY **2.11** to 3-benzo[*b*]thiophene-BODIPY **3.14** (table 3.2).

In all of the crude ^{1}H NMR spectra arising from these Suzuki-Miyaura cross-coupling reactions, we observed two singlet peaks at δ_H 8.57 ppm and δ_H 8.50 ppm, corresponding to the hydrogen of the thiophene moiety of BODIPYs **3.14** and **3.15** respectively. Thus we were able to estimate the ratio of 3-benzo[*b*]thiophene-BODIPY **3.14** to 3,5-dibenzo[*b*]thiophene-BODIPY **3.15** through analysis of the

^{1}H NMR spectra of the crude reaction mixtures generated from the Suzuki-Miyaura cross-coupling reactions between 3,5-dibromo-BODIPY **2.11** and benzo[*b*]thiophene-2-boronic acid.
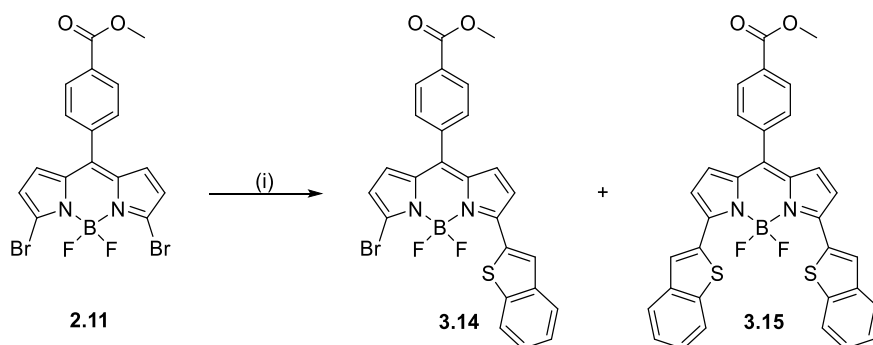
Scheme 3.24: Reagents and conditions: (i) benzo[*b*]thiophene-2-boronic acid, Pd(PPh$_3$)$_4$ (5 mol%), Na$_2$CO$_3$, toluene, 1,4-dioxane, 90 °C.

Entry	Reaction scale /mmol	Equivalents of boronic acid	Reaction time /h	Ratio of **3.14**:**3.15**[a]
1	0.041	0.8	2	1:0.15
2	0.10	1.2	2	1:1.04
3	0.10	1.0	3	1:1.5
4	0.13	1.0	2	1:0.40

Table 3.2: Reaction conditions of the Suzuki-Miyaura cross-coupling reaction between 3,5-dibromo-BODIPY **2.11** and benzo[*b*]thiophene-2-boronic acid examined. [a]Ratio of products determined by ^{1}H NMR.

After some reaction optimisation, we found that the best ratio of BODIPYs **3.14**:**3.15** (i.e. the highest ratio of the desired 3-benzo[*b*]thiophene-BODIPY **3.14**) was attained when using 1 equivalent of benzo[*b*]thiophene-2-boronic acid and a reaction time of 2 hours. However despite multiple attempts to purify 3-benzo[*b*]thiophene-BODIPY **3.14** by silica gel chromatography, we were unable to separate 3-benzo[*b*]thiophene-BODIPY **3.14** from 3,5-dibenzo[*b*]thiophene-BODIPY **3.15** due to mixed column fractions. To overcome this, we decided to continue with the second Suzuki-Miyaura cross-coupling reaction (with 2-hydroxyphenyl boronic acid) on a mixture of 3-benzo[*b*]thiophene-BODIPY **3.14** and 3,5-dibenzo[*b*]thiophene-BODIPY **3.15**. We postulated that the R$_f$ of the target *N,N,O,F*-BODIPY **3.10** would be sufficiently different from the R$_f$ of 3,5-dibenzo[*b*]thiophene-BODIPY **3.15** to allow for separation by silica gel chromatography.

3.2.5.3 Synthesis of *N,N,O,F*-BODIPY **3.10**

We performed a Suzuki-Miyaura cross-coupling reaction on a mixture of 3-benzo[*b*]thiophene-BODIPY **3.14** and 3,5-dibenzo[*b*]thiophene-BODIPY **3.15**, using 2-hydroxyphenyl boronic acid as the coupling

partner. After 24 hours the disappearance of 3-benzo[*b*]thiophene-BODIPY **3.14** and the appearance of a new compound was observed by TLC analysis. Gratifyingly the R*f* of the new compound was sufficiently different from the R*f* of 3,5-dibenzo[*b*]thiophene-BODIPY **3.15** to allow for separation of these two compounds by silica gel chromatography.

Following purification by silica gel chromatography, initial analysis of the ^{1}H NMR spectrum of the new compound indicated that we had formed *N,N,O,F*-BODIPY **3.10**. This was due to the observation of signals in the ^{1}H NMR spectrum corresponding to the hydrogens of the phenolic ring (δ_H 7.49-7.41 ppm, m, 2H; 7.38-7.28, m, 4H) and the absence of a broad singlet peak corresponding to a phenolic OH. However the observation of a triplet in the ^{11}B NMR spectrum (δ_B 1.19 ppm, t, J_{B-F} = 29.8 Hz) suggested to us that we had instead synthesised BODIPY **3.16**.
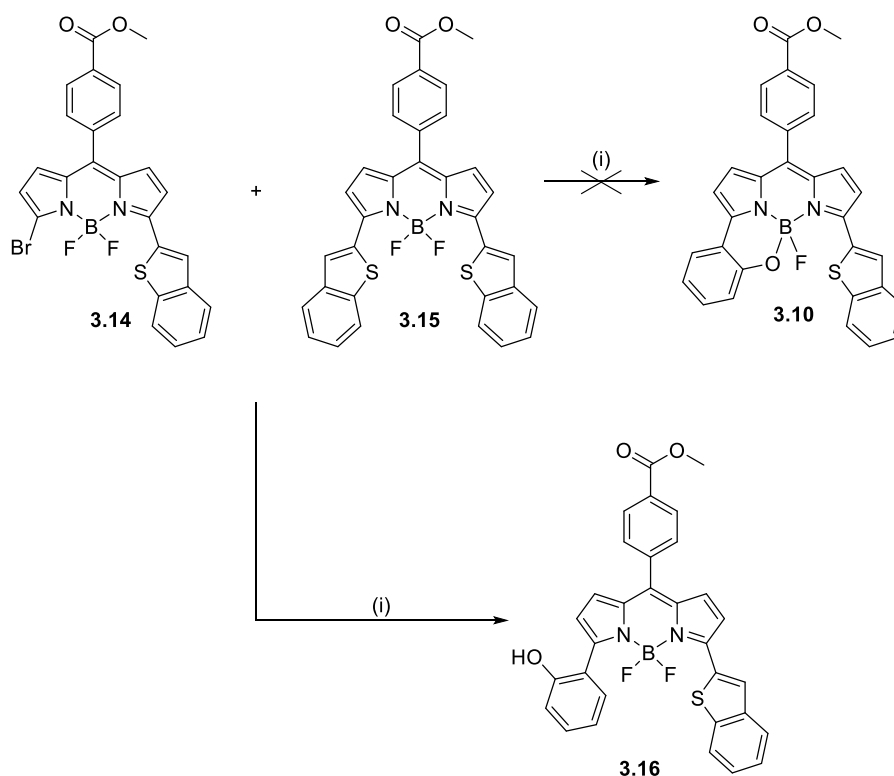
Scheme 3.25: Reagents and conditions: (i) 2-hydroxyphenyl boronic acid , Pd(PPh$_3$)$_4$ (5 mol%), Na$_2$CO$_3$, toluene, 1,4-dioxane, 90 °C, 24 h (17% over two steps).

In order to encourage the B-O bond formation event to occur, we decided to treat BODIPY **3.16** with tin tetrachloride. Therefore we treated BODIPY **3.16** with tin tetrachloride in a solution of deuterated chloroform. Analysis of the resulting ^{11}B NMR spectra revealed that there had been no change to the boron environment of BODIPY **3.16**, as we could still observe a triplet signal (δ_B 1.19 ppm, t, *J* = 29.8 Hz).

Given the difficulties we encountered in our attempted synthesis of *N,N,O,F*-BODIPY **3.10**, we decided to focus instead on the synthesis of our final sulfur containing chiral BODIPY, *N,N,O,F*-BODIPY **3.1**.

3.2.6 Synthesis of *N,N,O,F*-BODIPY **3.11**

3.2.6.1 Planned synthesis of *N,N,O,F*-BODIPY **3.11**

In order to install the thiophenol ring of our target *N,N,O,F*-BODIPY **3.11**, we envisioned using a nucleophilic aromatic substitution (S_NAr) reaction with thiophenol. Due to the increased reactivity of chloride functional groups to S_NAr chemistry, we decided to first synthesise 3,5-dichloro-BODIPY **3.19**. Our planned synthesis of 3,5-dichloro-BODIPY **3.19** involved the oxidation of dipyrromethane **2.9** to form dipyrromethene **3.17**. Subsequent chelation of boron would then form BODIPY **3.18**. In order to chlorinate the 3,5-positions, we then planned to use a regioselective chlorination procedure described by Jiao *et al.*[169] to form 3,5-dichloro-BODIPY **3.19**.
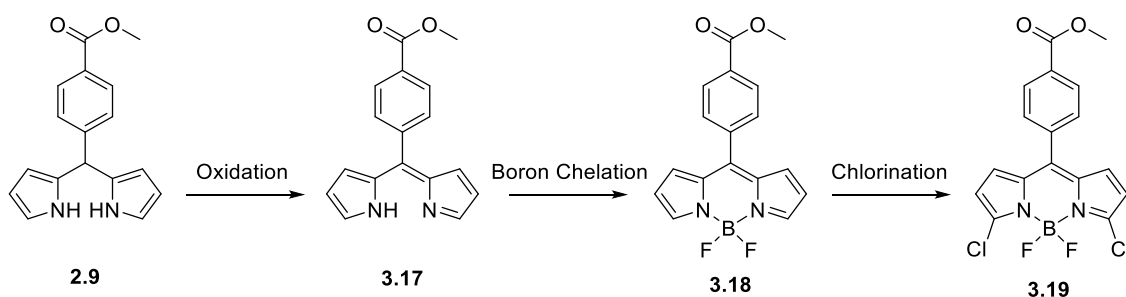
Scheme 3.26: Planned synthetic pathway to 3,5-dichloro-BODIPY **3.19**.

We then planned to synthesise *N,N,O,F*-BODIPY **3.11** via a nucleophilic aromatic substitution reaction between thiophenol and 3,5-dichloro-BODIPY **3.19** to form 3-thiophenol-BODIPY **3.20**. A Suzuki-Miyaura coupling between 3-thiophenol-BODIPY **3.20** and 2-hydroxyphenyl boronic acid would then be used to form *N,N,O,F*-BODIPY **3.11**.
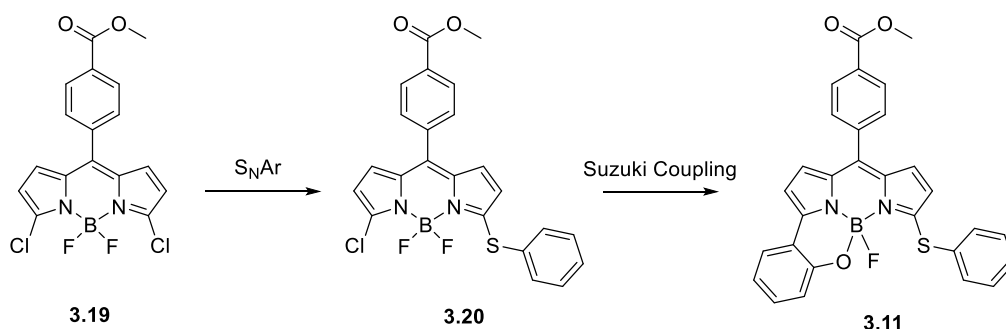
Scheme 3.27: Planned synthetic pathway to *N,N,O,F*-BODIPY **3.11**.

3.2.6.2 Synthesis of 3,5-dichloro-BODIPY **3.19**

The first step in the synthesis of 3,5-dichloro-BODIPY **3.19** was the synthesis of dipyrromethane **2.9**. We synthesised dipyrromethene **2.9** according to the same procedure as described in section 2.1.2.2.

Thus the first reaction we examined in the synthesis of 3,5-dichloro-BODIPY **3.19** was the oxidation of dipyrromethane **2.9**. We planned to test two different oxidants, DDQ and *p*-chloranil, in order to determine which oxidant gives the cleanest conversion of dipyrromethane **2.9** to dipyrromethene **3.17**.

Therefore we reacted dipyrromethane **2.9** together with 1.1 equivalents of DDQ for one hour. Analysis of the crude ^{1}H NMR spectrum showed that dipyrromethene **3.17** was the major product from the oxidation, and the purity of dipyrromethene **3.17** was high (figure 3.5). We confirmed the successful oxidation of dipyrromethene **2.9** by the absence of a signal at δ_H 5.56 ppm (s, 1H) corresponding to the *meso*-proton of **2.9**, which is lost during the oxidation of dipyrromethane **2.9**. Signals in the ^{1}H NMR spectrum of dipyrromethene **3.17** corresponding to the pyrrolic (δ_H 7.68 ppm, s, 2H; 6.53 ppm, d, 2H, *J* = 4.2 Hz; 6.41 ppm, d, 2H, *J* = 4.2 Hz) and aryl (δ_H 8.13 ppm, d, 2H, *J* = 8.4 Hz; 7.57 ppm, d, 2H, *J* = 8.4 Hz) protons further confirmed the synthesis of dipyrromethene **3.17**.

We then repeated the oxidation procedure using *p*-chloranil as the oxidant in DCM for 18 hours. Examination of the crude ^{1}H NMR spectrum showed that dipyrromethene **3.17** was again the major product from the oxidation, and was formed in exceptional purity (figure 3.5). Although the reaction time using *p*-chloranil is longer, the higher purity offered by using this milder oxidising agent led us to use *p*-chloranil for all further oxidations of dipyrromethene **2.9**. Owing to the exceptional purity offered using *p*-chloranil, we continued with the next step in our synthetic pathway without further purification of dipyrromethene **3.17**.
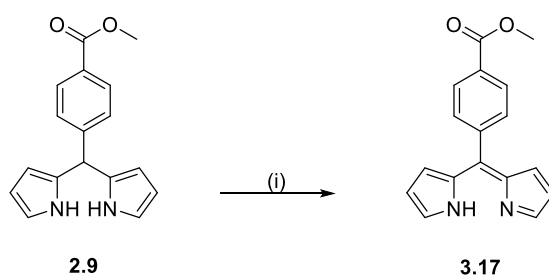
Scheme 3.28: Reagents and conditions: (i) DDQ, THF, R.T., 1 hour; or *p*-chloranil, DCM, R.T., 18 hours.
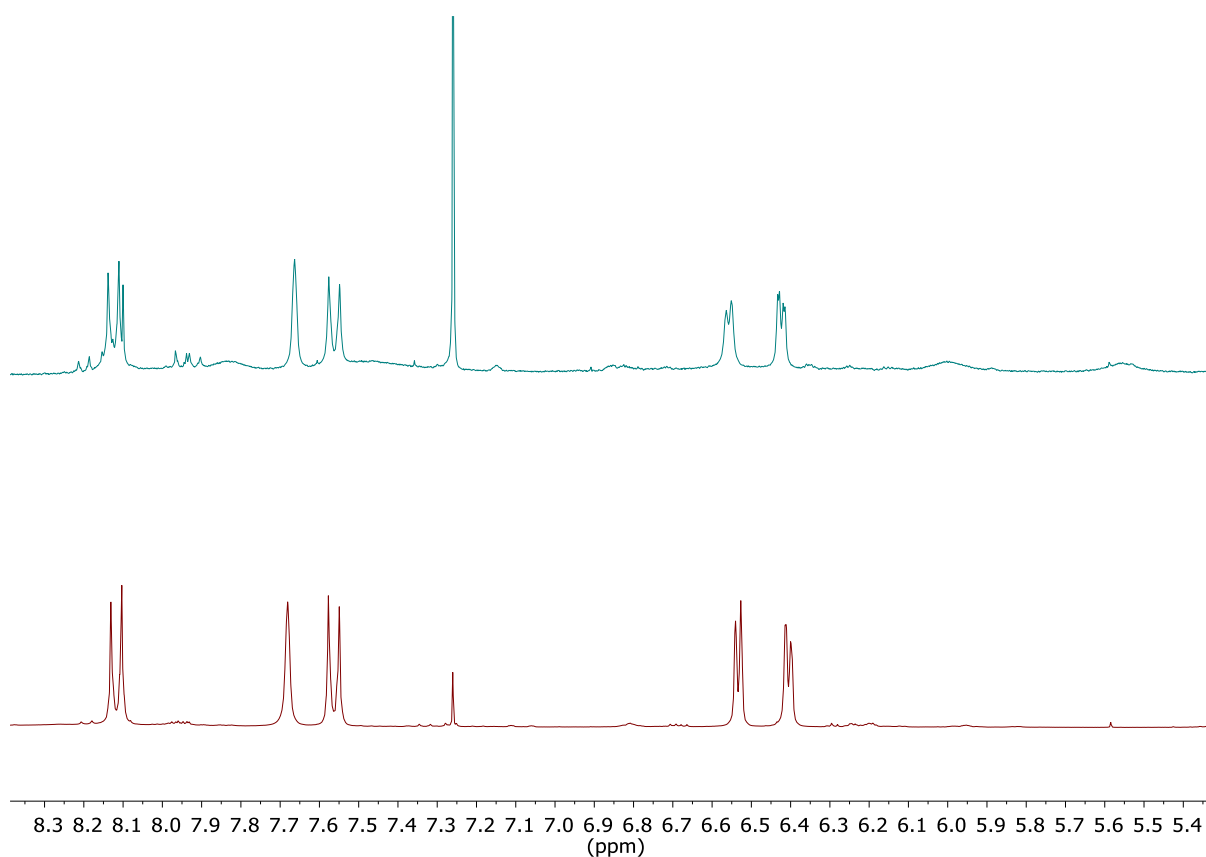
Figure 3.5: ^{1}H NMR spectrum of a typical crude reaction mixture of the oxidation of dipyrromethane **2.9** with DDQ (green, top) and *p*-chloranil (red, bottom) showing the *meso*-aryl and pyrrolic protons.

The next step we examined was the boron chelation of dipyrromethene **3.17** to form BODIPY **3.18**. We therefore treated dipyrromethene **3.17** with boron triflouride diethyl etherate in the presence of Hunig's base. After purification by silica gel chromatography, using DCM as eluent, BODIPY **3.18** was isolated in a 41% yield over two steps. Analysis of the ^{11}B NMR spectrum showed a triplet peak (δ_B 0.25 ppm, t, *J* = 28.5 Hz), indicating the successful inclusion of a BF$_2$ moiety.
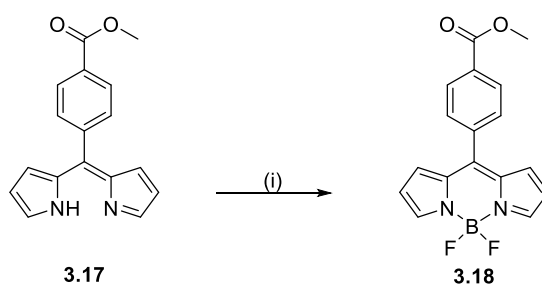
Scheme 3.29: Reagents and conditions: (i) BF$_2$.OEt$_2$, N^{i}Pr$_2$Et, DCM, R.T., 1 hour (41% over two steps).

The final step we examined in the synthesis of 3,5-dichloro-BODIPY **3.19** was the regioselective chlorination of BODIPY **3.18**, following a modified procedure described by Jiao *et al.*.[169] This chlorination is thought to proceed through a single electron transfer (SET) from copper(II) to the

BODIPY, which forms a radical cation. This is followed by nucleophilic attack of a chloride ion to form 3-chloro-BODIPY. This process is then repeated on the 5-position to form 3,5-dichloro-BODIPY.

We reacted BODIPY **3.18** together with copper(II) chloride dihydrate in acetonitrile. After one hour, we observed the disappearance of starting material BODIPY **3.18** by TLC analysis. However after purification by silica gel chromatography we isolated 3,5-dichloro-BODIPY **3.19** in a low yield (9%). This chlorination reaction is performed in the presence of air, which oxidises the reduced copper species (produced from each SET event) to the active copper(II) species. We thought that by reducing the scale of the reaction we would increase the surface area/volume ratio of the reaction mixture, thus allowing more efficient oxidation by air. We postulated that this would in turn result in an improved yield of 3,5-dichloro-BODIPY **3.19**.

By reducing the scale of the reaction (0.31 mmol of BOIDPY **3.18**) we saw a marked increase in the yield of 3,5-dichloro-BODIPY **3.19** from 9% to 32%. However the yields of 3,5-dichloro-BODIPY **3.19** remained low, so we looked to further improve the chlorination. We postulated that the low yields were due to the poor solubility of copper(II) chloride dihydrate in acetonitrile. Therefore we chose to use 5 equivalents of copper(II) triflate as a more soluble source of copper(II). Additionally we added 2 equivalents of ethanolamine, which we thought would improve the solubility of the copper(II) chloride dihydrate. These changes to the reaction conditions led to an improved yield of 52% of 3,5-dichloro-BODIPY **3.19** (entry 5, table 3.3).
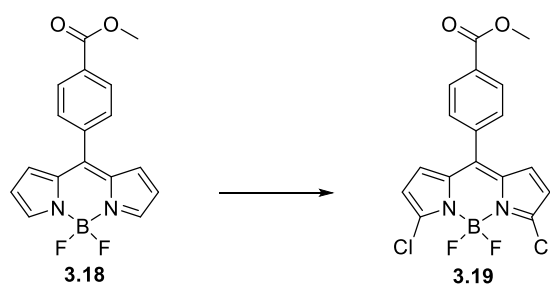
Entry	Scale / mmol of BODIPY **3.18**	Reaction conditions	Yield /%
1	2.68	CuCl$_2$.2H$_2$O (9.8 eq.), MeCN, reflux, 1.5 h	9
2	0.55	CuCl$_2$.2H$_2$O (9.8 eq.), MeCN, reflux, 1 h	8
3	0.40	CuCl$_2$.2H$_2$O (9.8 eq.), MeCN, reflux, 1 h	22
4	0.31	CuCl$_2$.2H$_2$O (9.8 eq.), MeCN, reflux, 1 h	32
5	0.15	CuOTf$_2$ (5 eq.), CuCl$_2$.2H$_2$O (5 eq.), ethanolamine (2 eq.), MeCN, reflux, 1.5 h	52

Table 3.3: Reaction conditions of the regioselective chlorination of BODIPY **3.18** examined.

With our improved reaction conditions, we were then able to isolate sufficient amounts of 3,5-dichloro-BODIPY **3.19** to continue with the next step in our synthetic pathway.

3.2.6.3 S_NAr reaction of 3,5-dichloro-BODIPY **3.19** and thiophenol

The next step we wished to examine in the synthesis of *N,N,O,F*-BODIPY **3.11** was the S_NAr reaction of 3,5-dichloro-BODIPY **3.19** and thiophenol. Adapting a procedure described by Dehaen *et al.*[55], we reacted together 3,5-dichloro-BODIPY **3.19** and two equivalents of thiophenol in the presence of triethylamine. However upon examination of the crude ^{1}H NMR spectrum, we discovered that the only product formed under the reaction conditions was 3,5-dithiophenol-BODIPY **3.21**. We confirmed the structure of 3,5-dithiophenol-BODIPY **3.21** by the observation of two equivalent doublets in the ^{1}H NMR spectrum corresponding to the pyrrolic protons (6.54 ppm, d, 2H, *J* = 4.4 Hz; 5.88 ppm, d, 2H, *J* = 4.4 Hz).
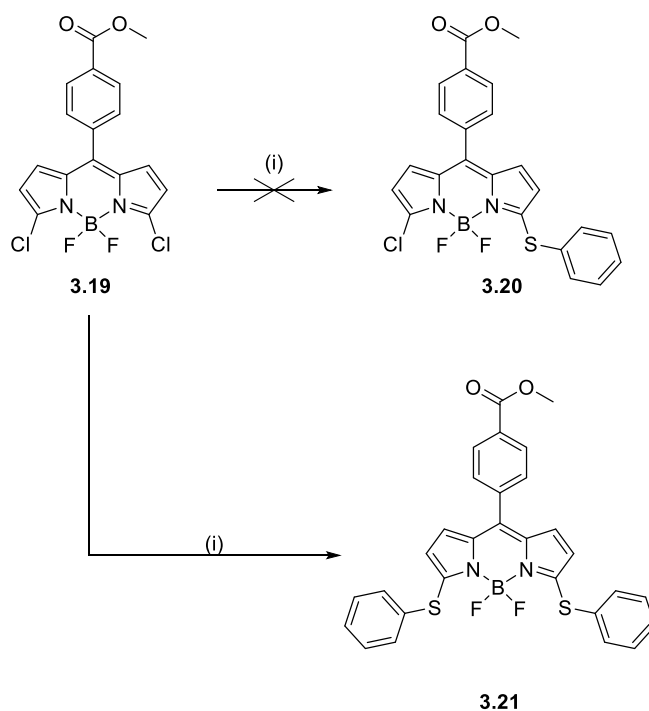
Scheme 3.30: Reagents and conditions: (i) thiophenol (2 eq.), Et$_3$N (2 eq.), MeCN, R.T., 30 minutes (92%).

Due to this unexpected result, we looked to reduce the equivalents of thiophenol used to minimise the formation of 3,5-dithiophenol-BODIPY **3.21** and thereby isolate 3-thiophenol-BODIPY **3.20**.

We therefore repeated the S_NAr reaction between 3,5-dichloro-BODIPY **3.19** and thiophenol, using fewer equivalents of thiophenol and a lower reaction temperature. Analysis of the crude reaction mixture by TLC indicated that starting material 3,5-dichloro-BODIPY **3.19**, 3,5-thiophenol-BODIPY **3.21** and a third compound were present.

Analysis of the crude ^{1}H NMR spectrum confirmed that there were at least three BODIPY species present, owing to the observation of three signals corresponding to at least three aryl methyl groups (figure 3.6). Comparison of the crude ^{1}H NMR spectrum and the ^{1}H NMR spectra of 3,5-dichloro-BODIPY **3.19** and of 3,5-dithiophenol BODIPY **3.21** confirmed that these two BODIPYs were present in the crude reaction mixture.
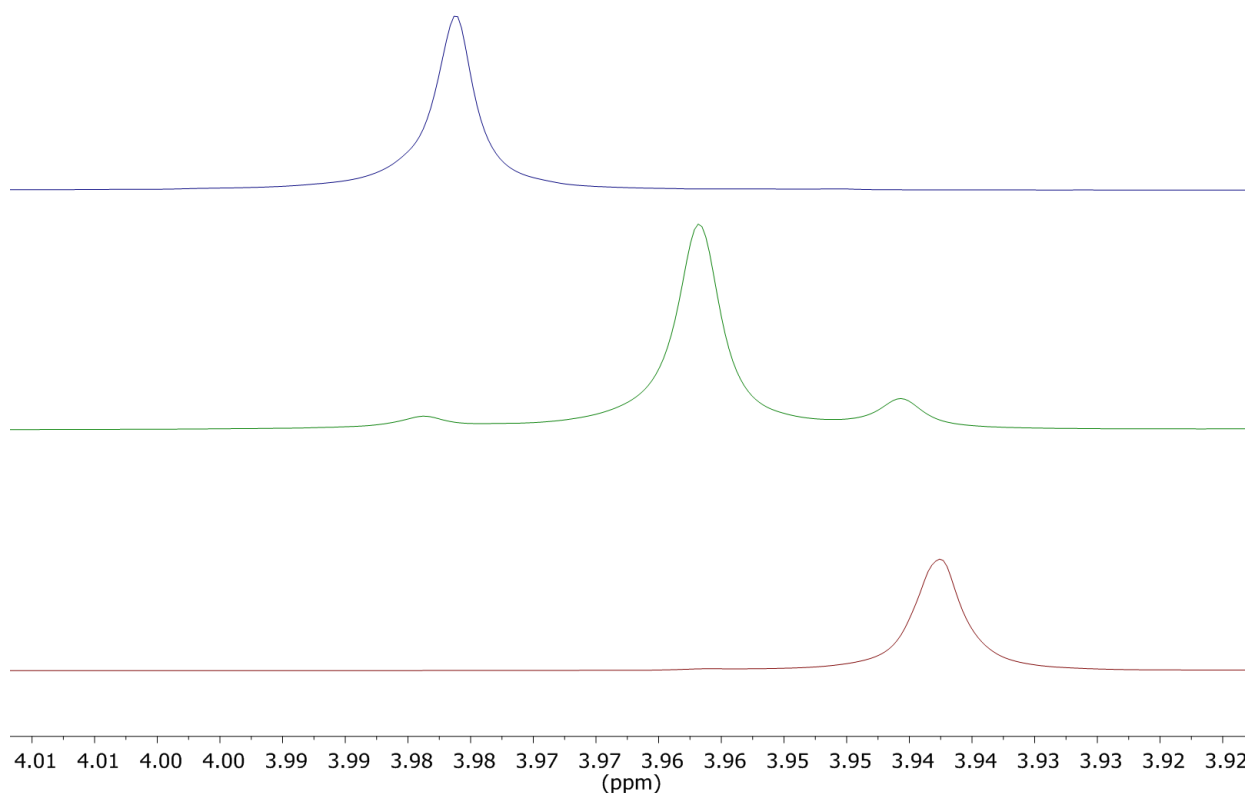
Figure 3.6: ^{1}H NMR spectra of 3,5-dichloro-BODIPY **3.19** (top, blue), a typical crude reaction mixture arising from the S$_N$Ar reaction between 3,5-dichloro-BODIPY **3.19** and thiophenol (green, middle) and 3,5-dithiophenol BODIPY **3.21** (red, bottom), showing the signals corresponding to the methyl groups of the aryl methyl esters.

We concluded that the third compound, which is the major product, is therefore 3-thiophenol BODIPY **3.21**. This hypothesis was supported by the observation of a set of signals in the crude ^{1}H NMR spectrum corresponding to two inequivalent C-2,5-substituted pyrrolic moieties (δ_H 6.65 ppm, d, 1H, J = 4.7 Hz; 6.60 ppm, d, 1H, J = 4.4 Hz; 6.34 ppm, d, 1H, J = 4.4 Hz; 5.89 ppm, d, 1H, J = 4.7 Hz).

Separation of 3,5-dichloro-BODIPY **3.19**, 3,5- and 3-thiophenol-BODIPYs **3.20** and **3.21** by silica gel chromatography was not possible, due to mixed column fractions. Consequently we looked to

optimise the reaction further to minimise the formation of 3,5-dithiophenol-BODIPY **3.21** whilst maximising the conversion from 3,5-dichloro-BODIPY **3.19** to 3-thiophenol-BODIPY **3.20**.

Reducing the number of equivalents of thiophenol and the reaction temperature led to a decrease in the amount of 3,5-dithiophenol-BODIPY **3.21** generated. However these changes to the reaction conditions led to an increase in the amount of starting material 3,5-dichloro-BODIPY **3.19** present in the crude reaction mixtures.
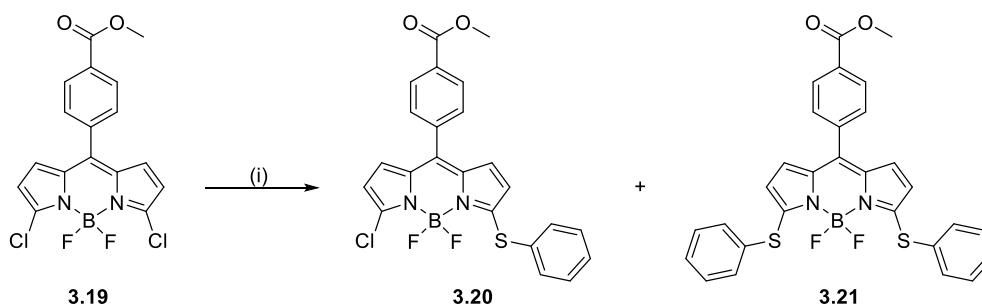
Entry	Reaction solvent	Equivalents of thiophenol	Reaction temperature	Reaction time / minutes	Ratio of BODIPYs **3.19**:**3.20**:**3.21**[a]
1	MeCN	2	R.T.	30	0:0:1
2	MeCN	1.1	0 ° - R.T.	20	0.5:1:0.2
3	MeCN	1.2	0 ° - R.T.	300	0.3:1:0.3
4	MeCN	1.8	0 ° - R.T.	120	0.1:1:0.3
5	THF	0.99	-78 °C	180	0.1:1:0.2
6	THF	1	-78 °C	120	1:1:0
7	THF	1	-90 °C	120	1:0:0
8	THF	0.99	-110 °C	120	0.8:1:0

Table 3.4: Reaction conditions of the S_NAr reaction between 3,5-dichloro-BODIPY **3.19** and thiophenol examined. [a]Ratios determined by ^{1}H NMR.

Due to the challenging separation of 3,5-dichloro-BODIPY **3.19**, 3,5-dithiophenol-BODIPY **3.21** and 3-thiophenol-BODIPY **3.20** by silica gel chromatography, we decided to examine instead the S_NAr reaction between 3,5-dibromo-BODIPY **2.11** and thiophenol. We reasoned that since bromide functional groups have lowered reactivity towards S_NAr chemistry, we may be able to control the addition of thiophenol to 3,5-dibromo-BODIPY **2.11** in order to selectively synthesise the brominated analogue of 3-thiophenol-BODIPY **3.20**.

3.2.6.4 S$_N$Ar reaction of 3,5-dibromo-BODIPY **2.11** and thiophenol

In order to synthesise 3-thiophenol-BODIPY **3.22**, we reacted 3,5-dibromo-BODIPY **2.11** together with two equivalents of thiophenol in the presence of triethylamine. Upon the addition of thiophenol an immediate colour change was observed. Analysis of the TLC of the crude reaction mixture indicated the presence of starting material 3,5-dibromo-BODIPY **2.11** and two new compounds.

Comparison of the crude ^{1}H NMR spectrum with those of 3,5-dithiophenol-BODIPY **3.21** and 3,5-dibromo-BODIPY **2.11** confirmed that these species were present in the crude reaction mixture, due to the presence of signals corresponding to their corresponding aryl methyl groups (figure 3.7). We concluded that 3-thiophenol-BODIPY **3.22** was also present as a minor compound, due to the presence of a set of signals corresponding to two inequivalent C-2,5-substituted pyrrolic moieties in the crude ^{1}H NMR spectrum (δ_H 6.66 ppm, d, 1H, J = 4.5 Hz; 6.55 ppm, m; 6.45 ppm, d, 1H, J = 3.9 Hz; 5.90 ppm, d, 1H, J = 3.9 Hz).
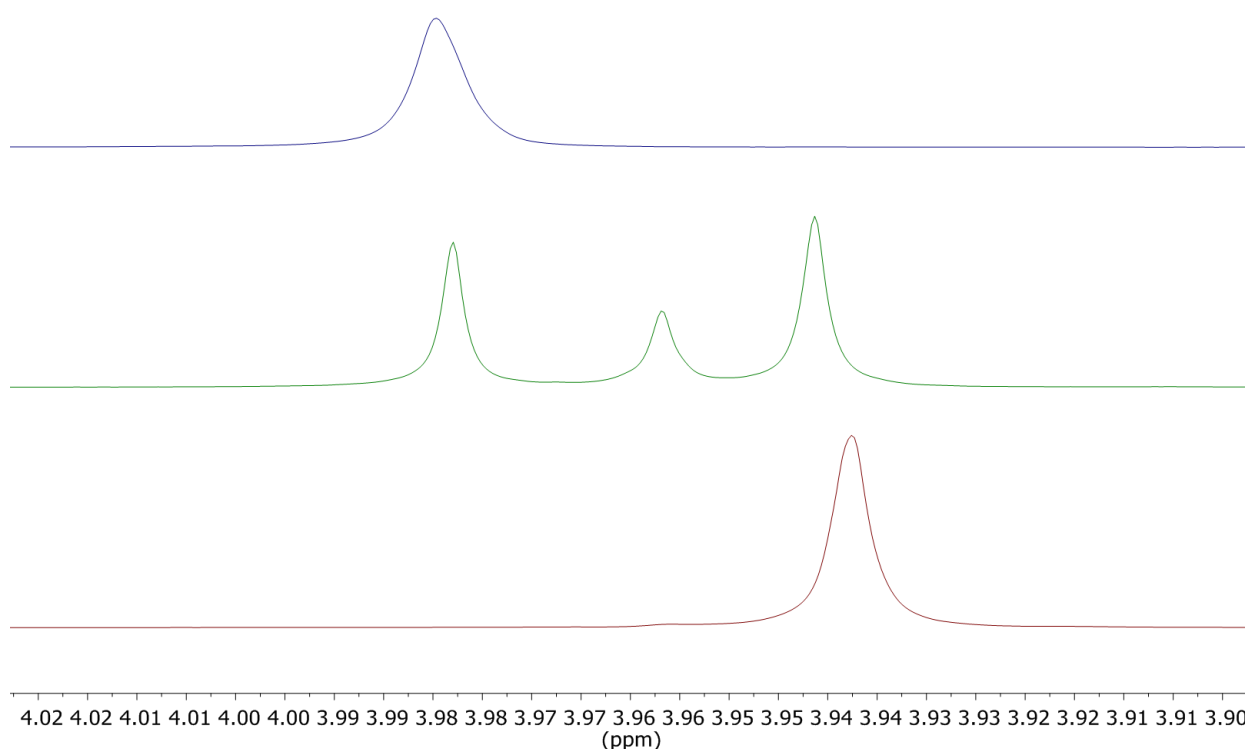
Figure 3.7: ^{1}H NMR spectra of 3,5-dibromo-BODIPY **2.11** (top, blue), a typical crude reaction mixture arising from the S$_N$Ar reaction between 3,5-dibromo-BODIPY **2.11** and thiophenol (green, middle) and 3,5-dithiophenol BODIPY **3.21** (red, bottom), showing the signals corresponding to the methyl groups of the aryl methyl esters.

Separation of these three BODIPYs by silica gel chromatography was challenging, so we looked to optimise the reaction to minimise the formation of 3,5-dithiophenol-BODIPY **3.21** (table 3.5). However we found that decreasing the reaction temperature and using a lower number of equivalents of thiophenol did not improve the ratio of BODIPYs **2.11**:**3.22**:**3.21**. We concluded that the selective synthesis of 3-thiophenol-BODIPYs **3.20** or **3.22** was not possible using this strategy.
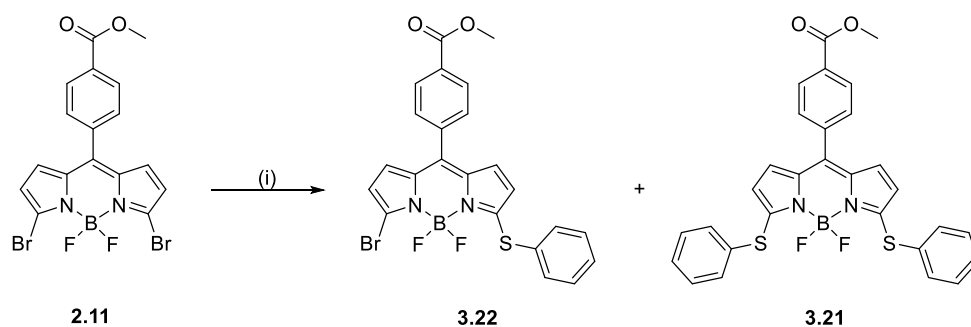
Entry	Equivalents of thiophenol	Equivalents of NEt$_2$	Reaction temperature /°C	Reaction time /minutes	Ratio of **2.11**:**3.22**:**3.21**[a]
1	2	1	R.T.	120	2:1:2
2	1	0.5	R.T.	15	3:1:2
3	1	0.5	0 °C	25	8:1:5

Table 3.5: Reaction conditions for the S$_N$Ar reaction between 3,5-dibromo-BODIPY **2.11** and thiophenol examined. [a]Ratio determined by analysis of the crude ^{1}H NMR spectra.

We decided to examine the use of a thiophenol derivative. We thought that by using a thiophenol derivative with an electron withdrawing group, the resulting mixture of BODIPYs would be sufficiently different in polarity to allow for purification by silica gel chromatography.

3.2.7 Synthesis of *N,N,O,F*-BODIPY **3.23**

We chose the thiophenol derivative 4-(trifluoromethyl)thiophenol, due to its strongly electron withdrawing group. Our new sulfur-containing BODIPY target was therefore *N,N,O,F*-BODIPY **3.23**.

We elected to use 3,5-dibromo-BODIPY **2.11** in our attempts towards the synthesis of the new target *N,N,O,F*-BODIPY **3.23**. This was due to the low overall yield to 3,5-dichloro-BODIPY **3.19** (19% over four steps) as compared to the overall yield to 3,5-dibromo-BODIPY **2.11** (66% over three steps). Combined with the poor scalability of the regioselective chlorination step, we were unable to produce sufficient amounts of 3,5-dichloro-BODIPY **3.19** to complete the synthesis of *N,N,O,F*-BODIPY **3.23**.
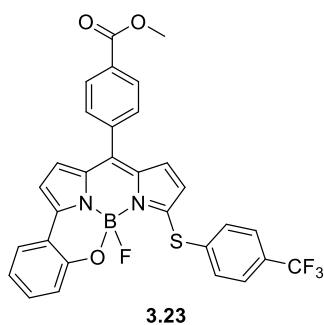
Figure 3.6: *N,N,O,F*-BODIPY **3.23**.

3.2.7.1 S$_N$Ar reaction of 3,5-dibromo-BODIPY **2.11** and 4-(trifluoromethyl)thiophenol

The first step we examined in the synthesis of *N,N,O,F*-BODIPY **3.23** was the S$_N$Ar reaction between 4-(trifluoromethyl)thiophenol and 3,5-dibromo-BODIPY **2.11**.

We therefore reacted 3,5-dibromo-BODIPY **2.11** together with 4-(trifluoromethyl)thiophenol (1 equivalent) at -78 °C. After 90 minutes, the presence of starting material 3,5-dibromo-BODIPY **2.11** and the formation of two new compounds was observed by TLC analysis. Comparison of the crude ^{1}H NMR spectrum and the ^{1}H NMR spectrum of 3,5-dibromo-BODIPY **2.11** confirmed that starting material **2.11** was present in the crude reaction mixture. We postulated that the remaining two compounds were 3-thiophenol-BODIPY **3.24** and 3,5-dithiophenol-BODIPY **3.25**.

Gratifyingly the three compounds formed during the S$_N$Ar reaction between 3,5-dibromo-BODIPY **2.11** and 4-(trifluoromethyl)thiophenol had polarities which were sufficiently different to allow for purification by silica gel chromatography. Thus we were able to isolate 3-thiophenol-BODIPY **3.24** in a 43% yield following purification by silica gel chromatography. We confirmed the structure of 3-thiophenol-BODIPY **3.24** by the observation of four doublet signals in the ^{1}H NMR spectrum corresponding to two inequivalent C-2,5 substituted pyrrolic moieties (δ_H 6.71 ppm, d, 1H, *J* = 4.6 Hz; 6.62 ppm, d, 1H, *J* = 4.2 Hz; 6.49 ppm, d, 1H, *J* = 4.2 Hz; 5.98 ppm, d, 1H, *J* = 4.6 Hz).
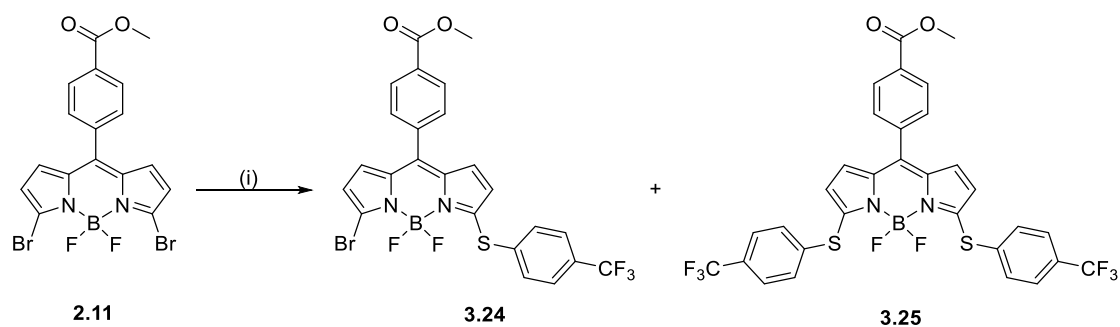
Scheme 3.31: Reagents and conditions: (i) 4-(trifluoromethyl)thiophenol (1 eq.), Et$_3$N (0.5 eq.), THF, -78 °C, 90 minutes (**3.24** 43%).

Comparison of the ^{1}H NMR spectra of 3,5-dibromo-BODIPY **2.11**, 3-thiophenol-BODIPY **3.24** and of the crude reaction mixture allowed us to assign the third compound present in the crude reaction mixture. The presence of two doublet signals corresponding to two equivalent C-2,5 substituted pyrrolic moieties in the crude ^{1}H NMR spectrum indicated the formation of 3,5-dithiophenol-BODIPY **3.25**.
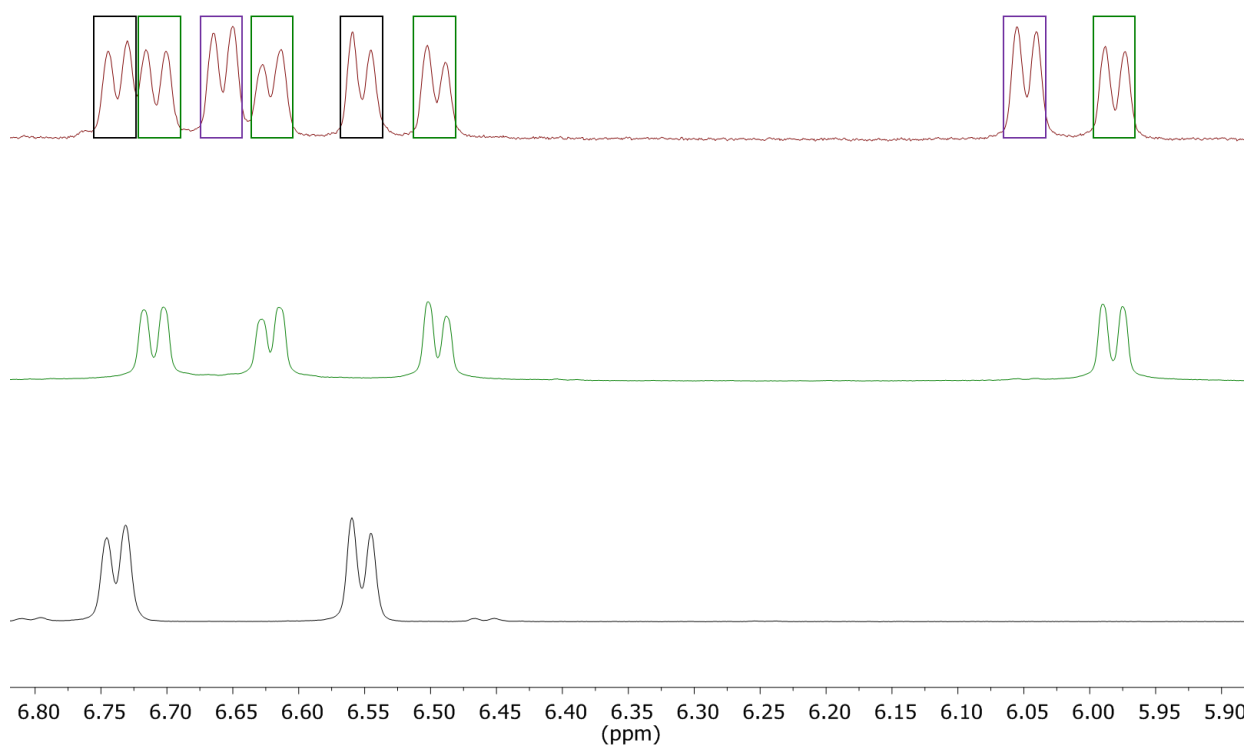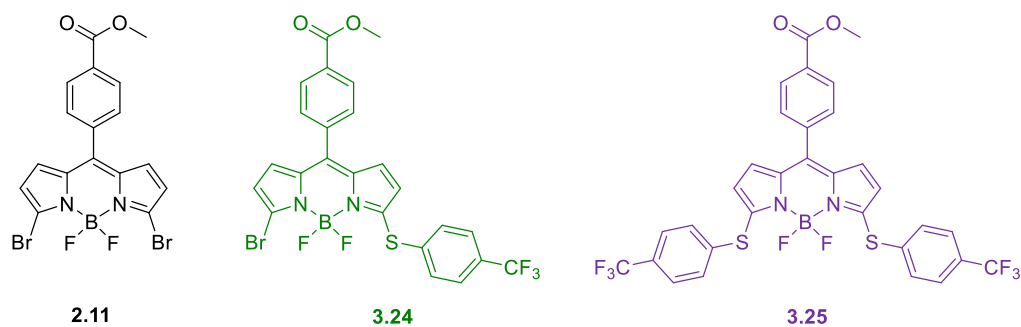
Figure 3.8: a) ^{1}H NMR spectra of a typical crude reaction mixture arising from the S$_N$Ar reaction between 3,5-dibromo-BODIPY **2.11** and 4-(trifluoromethyl)-thiophenol (red, top), 3-thiophenol BODIPY **3.24** (green, middle), and 3,5-dibromo-BODIPY **2.11** (bottom, blue), showing the signals corresponding to the pyrrolic hydrogens; b) 3,5-dibromo-BODIPY **2.11**, 3-thiophenol BODIPY **3.24** and 3,5-dithiophenol-BODIPY **3.25**.

Once we had synthesised sufficient amounts of 3-thiophenol-BODIPY **3.24**, we were then able to continue with the next step in our synthetic pathway.

3.2.7.2 Synthesis of *N,N,O,F*-BODIPY **3.23**

The next step in our synthesis of *N,N,O,F*-BODIPY **3.23** was the Suzuki-Miyaura cross-coupling reaction between 3-thiophenol-BODIPY **3.24** and 2-hydroxyphenyl boronic acid, followed by a subsequent *in situ* B-O bond formation to form *N,N,O,F*-BODIPY **3.23**.

We therefore performed a Suzuki-Miyaura cross-coupling reaction between 3-thiophenol-BODIPY **3.24** and 2-hydroxyphenyl boronic acid. After 20 minutes the formation of two new compounds was observed by TLC analysis of the crude reaction mixture. Interestingly analysis of the crude ^{1}H NMR spectrum showed that the major compound arising from this Suzuki-Miyaura cross-coupling reaction was 3,5-dithiophenol-BODIPY **3.25** (figure 3.9).
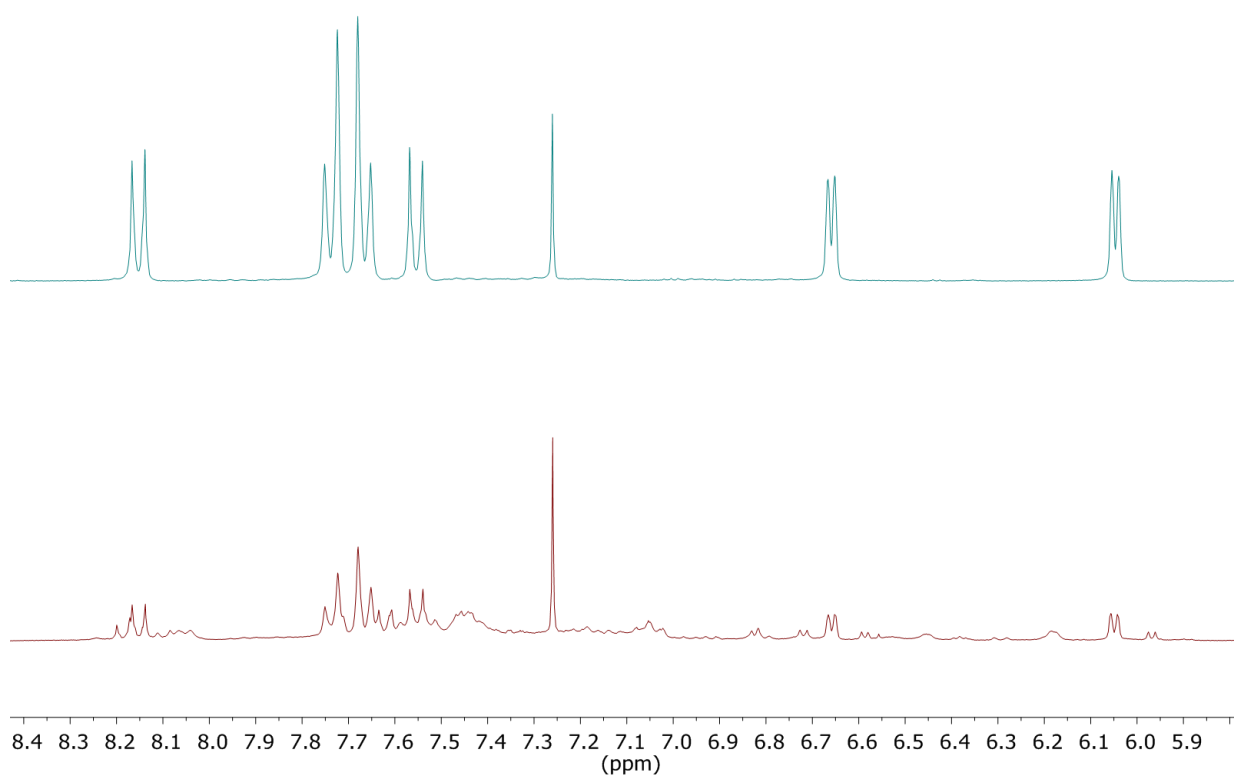
Figure 3.9: ^{1}H NMR spectra of 3,5-dithiophenol-BODIPY **3.25** (top, green) and of the crude reaction mixture arising from the Suzuki-Miyaura cross-coupling reaction between 3-thiophenol-BODIPY **3.24** and 2-hydroxyphenyl boronic acid (red, bottom), showing peaks corresponding to the pyrrolic and aryl hydrogens.

Despite this unexpected result, we continued with purification of the crude reaction mixture in order to elucidate the structure of the second compound formed under the reaction conditions. Following purification by silica gel chromatography, we isolated BODIPY **3.26** (20% yield) arising from the successful Suzuki-Miyaura cross-coupling reaction between 3-thiophenol-BODIPY **3.24** and 2-hydroxyphenyl boronic acid. However the isolation of BODIPY **3.26** indicated that the *in situ* B-O bond formation step had not taken place. The appearance of a broad singlet in the ^{1}H NMR spectrum corresponding to the hydrogen of the phenolic moiety (δ_H 5.74 ppm, br s, 1H) and the observation of a triplet signal in the ^{11}B NMR spectrum (δ_B 0.97 ppm, t, J_{B-F} = 32.0 Hz) corresponding to a BF$_2$ moiety confirmed that the B-O bond formation step had not occurred.
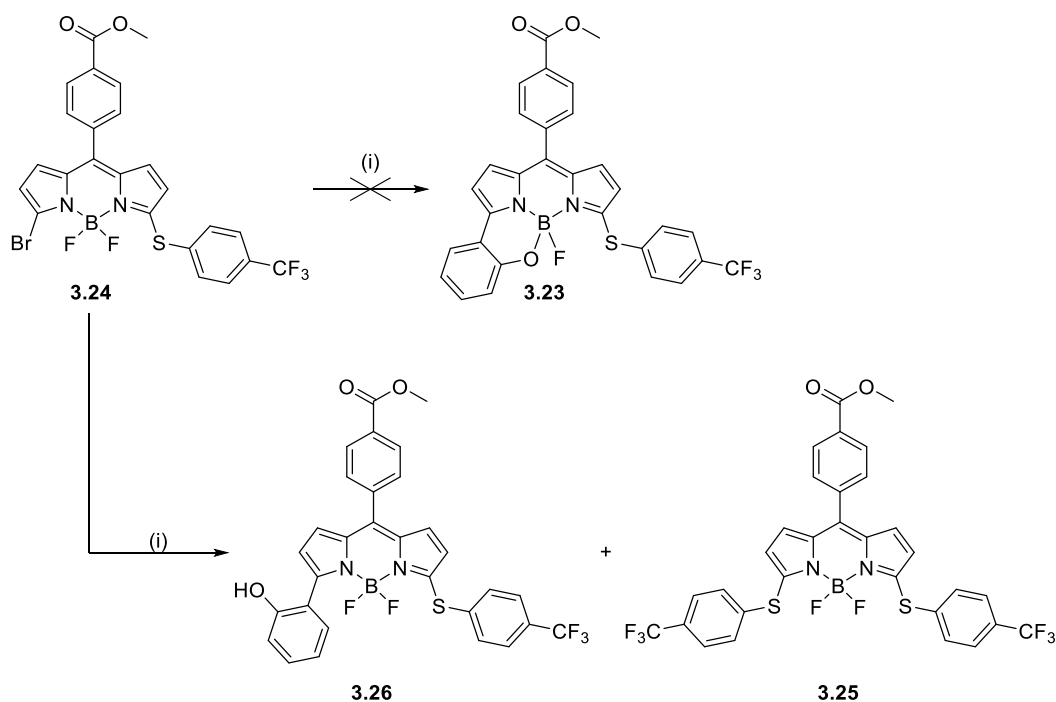
Scheme 3.32: Reagents and conditions: (i) 2-hydroxyphenyl boronic acid, Pd(PPh$_3$)$_4$ (5 mol%), Na$_2$CO$_3$, toluene, 1,4-dioxane, 90 °C, 20 minutes (20% **3.26**).

We decided to submit BODIPY **3.26** to our standard chelation conditions, in order to encourage the B-O bond formation step to occur. We treated BODIPY **3.26** with boron trifluoride diethyl etherate in the presence of Hunig's base, and after 75 minutes the formation of a new compound was observed by TLC analysis. Following purification by silica gel chromatography, we isolated *N,N,O,F*-BODIPY **3.23** (15% yield). We confirmed that we had successfully formed the B-O bond between the oxygen atom of the phenolic moiety and the central boron atom by the observation of a doublet signal in the ^{11}B NMR spectrum (δ_B 0.18 ppm, d, J_{B-F} = 46.5 Hz).
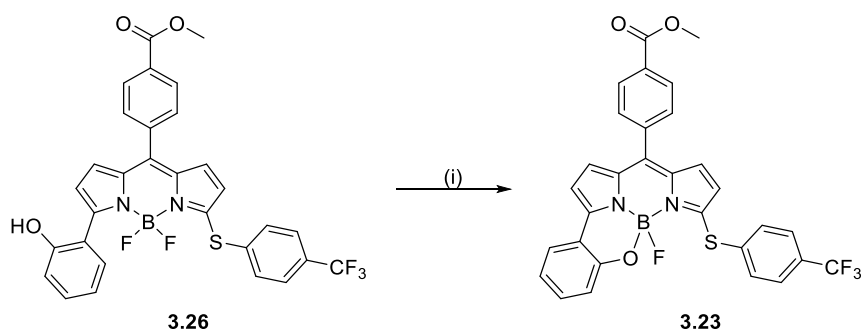
Scheme 3.33: Reagents and conditions: (i) $BF_3.OEt_2$, N^iPr_2Et, DCM, R.T., 75 minutes (15%).

We have identified a successful route to our one of our target sulfur-containing BODIPYs, *N,N,O,F*-BODIPY **3.23**. In order to study the chiroptical properties of *N,N,O,F*-BODIPY **3.23** including possible CPL emission, we first needed to resolve the racemic mixture of *N,N,O,F*-BODIPY **3.23** into its respective enantiomers.

3.2.8 Resolution of the enantiomers of *N,N,O,F*-BODIPY **3.23** and measurement of CPL emission

3.2.8.1 Resolution of the enantiomers of *N,N,O,F*-BODIPY **3.23**

To perform the resolution of the enantiomers of *N,N,O,F*-BODIPY **3.23**, we performed semi-preparative chiral HPLC on a racemic mixture of *N,N,O,F*-BODIPY **3.23** using a Daicel Chiralpak® IA column (1 mL/minute, toluene). After combining multiple runs, we were able to obtain approximately 20 µg of each enantiomer. We assigned the enantiomers as (-)-**3.23** and (+)-**3.23** respectively by retention time and by measuring the specific optical rotation ($[\alpha]_D$).
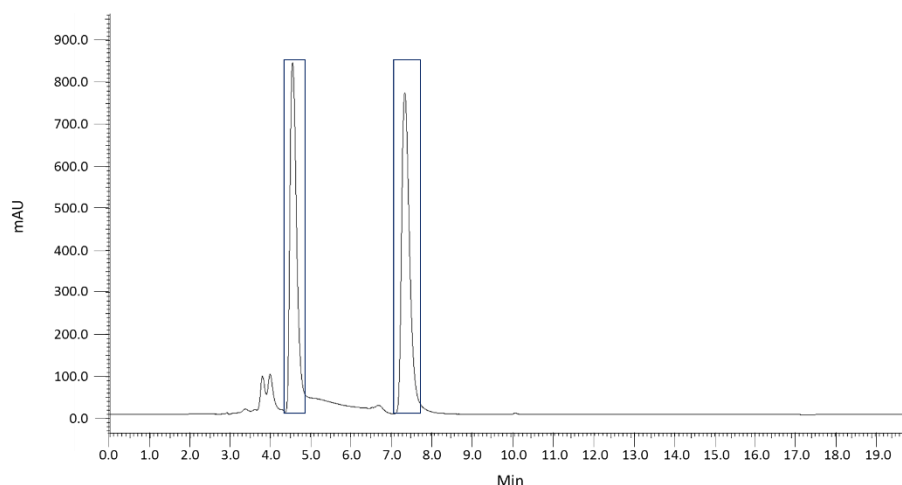
Figure 3.10: A typical chiral HPLC trace of a racemic sample of **3.23**. Daicel Chiralpak® IA column, 4.6 x 250 mm, 5µm particle size, toluene, 1 mL/min.

After separation of the enantiomers of *N,N,O,F*-BODIPY **3.23**, the enantiomeric excess (*ee*) of each enantiomer was measured by resubmitting the enantiomers to the chiral HPLC conditions ((+)-**3.23** %*ee* = >95%, (-)-**3.23** %*ee* = >95%). Once we were satisfied that we had isolated enantiopure samples of each enantiomer of *N,N,O,F*-BODIPY **3.23**, we focused on the measurement of the CPL spectra of the enantiomers of *N,N,O,F*-BODIPY **3.23**.

3.2.8.2 Measurement of CPL emission of *N,N,O,F*-BODIPY **3.23**

Our next step was to measure the CPL spectra of the enantiomers of *N,N,O,F*-BODIPY **3.23** (performed by Dr Lewis Mackenzie). However we did not observe an appreciable CPL signal from either enantiomer (+)-**3.23** or (-)-**3.23** at the emission maxima (λ = 635 nm) of (*rac*)-**3.23** (figure 3.11).
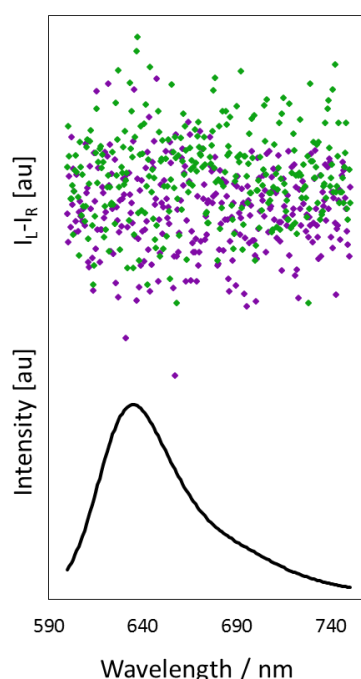
Figure 3.11: CPL data (I_L-I_R) for (+)-**3.23** (green) and (-)-**3.23** (purple), and fluorescence spectra of (*rac*)-**3.23** (black) measured in DCM.

As discussed in section 2.1.1.1, Gossauer *et al.* have proposed that chiral BODIPY dyes must contain a twisted planar core in order to produce a CPL output.[129] We suggest that the tridentate dipyrromethene ligand of *N,N,O,F*-BODIPY **3.23** does not induce a sufficiently pronounced twist to the planar core. This results in the lack of an appreciable CPL signal from the enantiomers of *N,N,O,F*-BODIPY **3.23**, and thus limits our investigations on the effect sulfur atom inclusion has on g_{lum}.

3.3 Conclusions and Future Work

We have successfully synthesised one of our target sulfur-containing chiral BODIPYs, *N,N,O,F*-BODIPY **3.23**. We were also able to successfully resolve (*rac*)-**3.23** into its respective enantiomers, however

there was no observable CPL emission from either enantiomer. We suggest that this is because the tridentate dipyrromethene ligand structure is not sufficient to induce a significant chiral twist to the planar BODIPY core. We therefore propose that the presence of a chirally perturbed core structure has a larger impact on CPL emission than the inclusion of sulfur atoms.

3.23
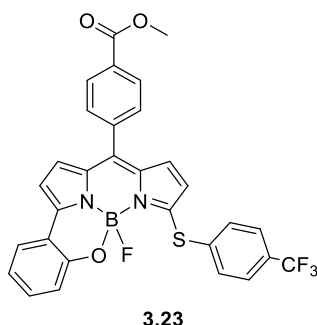
Figure 3.12: *N,N,O,F*-BODIPY **3.23**.

However we still would like to investigate the effect of sulfur atom inclusion on CPL emission, by synthesising a sulfur-containing, C_2-symmetric BODIPY such as *N,N,S,S*-BODIPY **3.1**. We have made significant progress towards the synthesis of *N,N,S,S*-BODIPY **3.1** in that we have synthesised two dipyrromethene precursors, dipyrromethene **3.7a** and **3.7b**. However we were unable to isolate and characterise the sulfur-deprotected dipyrromethene **3.8** or *N,N,S,S*-BODIPY **3.1**.

3.7a   **3.7b**   **3.8**   **3.1**
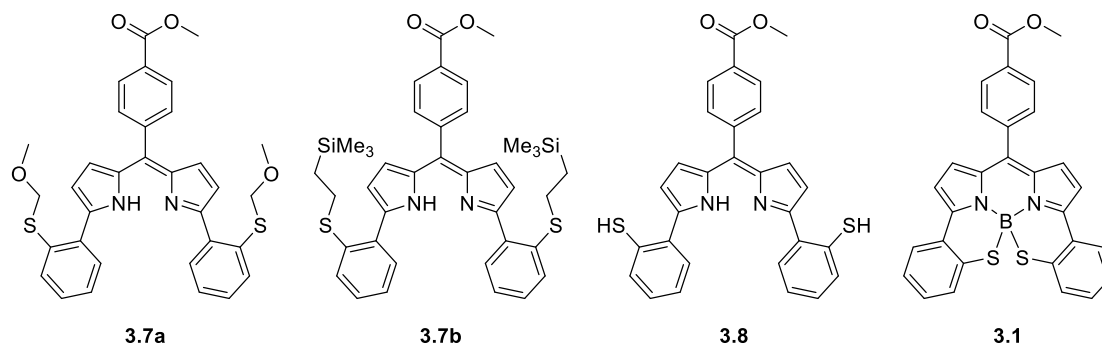
Figure 3.13: Sulfur-protected dipyrromethenes **3.7a** and **3.7b**, sulfur-deprotected dipyrromethene **3.8** and *N,N,S,S*-BODIPY **3.1**.

In the future we would like to revisit the synthetic pathway taken to dipyrromethenes **3.7a** and **3.7b** using an alternative sulfur protecting group. One such approach would involve the formation of a thioester, which can be removed by hydrolysis under basic conditions.[170]

Chapter 4. Modulation of the Helical Pitch of *N,N,O,O*-BODIPYs

4.1 Introduction

In this chapter we will discuss our investigations into the effect modulation of the helical pitch of *N,N,O,O*-BODIPYs has on the direction of the magnetic dipole moment (**m**), and thus the angle between the magnetic and electric dipole moments (τ).

4.1.1 Relationship between helical pitch and the direction of the magnetic transition dipole moment

As discussed in section 2.1.1.2, the theoretical equation by which the luminescence dissymmetry factor (g_{lum}) is defined is as follows:

$$g_{lum} = \frac{4(\boldsymbol{\mu} \cdot \boldsymbol{m} \cdot cos\tau)}{(\boldsymbol{\mu}^2 + \boldsymbol{m}^2)}$$

Where **m** is the magnetic transition dipole moment, **μ** is the electric transition dipole moment, and τ is the angle between these two vectors. From this equation, we can conclude that the highest value for g_{lum} can only be obtained when τ = 0° or 180°.

In *N,N,O,O*- and *N,N,O,C*-BODIPY architectures we observed that **m** aligns with the helical axis whilst **μ** aligns with the π-system (section 2.2.4.1). This is the same pattern as is observed in the carbo[n]helicene series. In a computational study of a series of carbo[*n*]helicenes conducted by Mori, Inoue *et al*., it was observed that increasing the helical pitch of a helicene through the extension of the π-system resulted in a reduction in the angle (τ) between the magnetic and electric transition dipole moments.[144] For the carbo[*n*]helicene with the most pronounced helical pitch (CH[10], figure 4.1) it was calculated that τ ≈ 0°, since the direction of the magnetic transition dipole moment is almost parallel with the direction of the electric transition dipole moment.
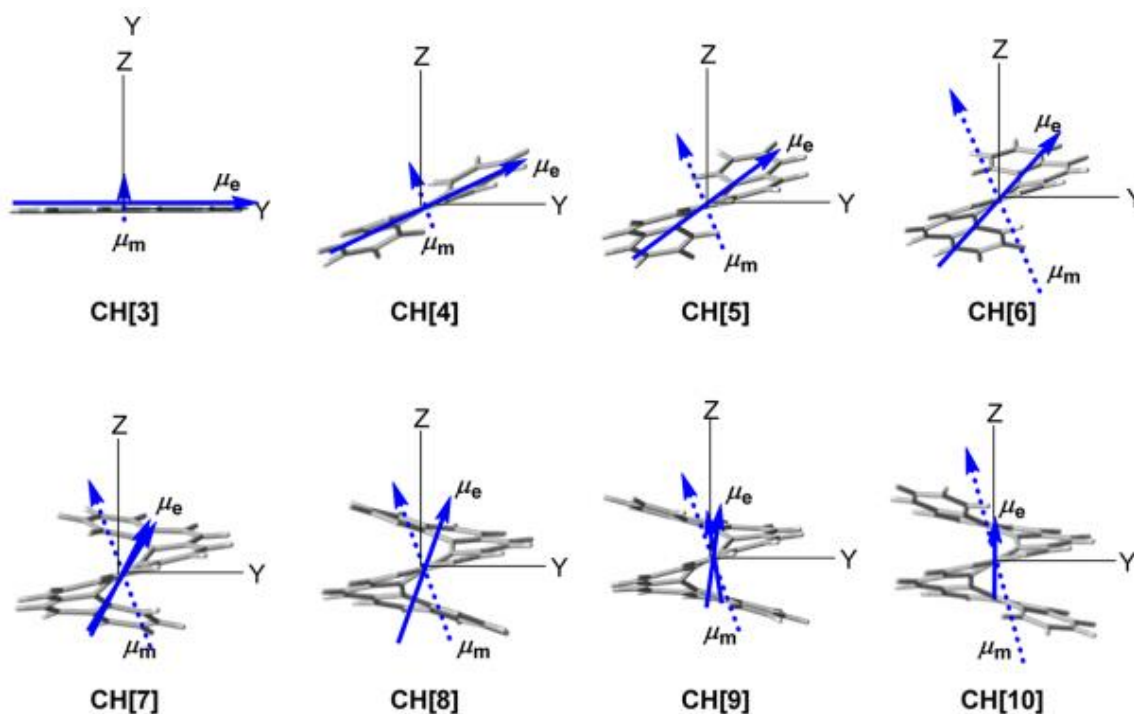
Figure 4.1: The calculated electric (solid arrow) and magnetic (dotted arrow) transition dipole moments of the carbo[*n*]helicenes CH[3]-CH[10] (reproduced from the report by Mori *et al.*).[144]

We thought that if we could mimic this effect in helically chiral *N,N,O,O*-BODIPYs then we could achieve control over the angle τ. Successful control and reduction of the angle τ (such that τ tends to 0°), would provide a route to high g_{lum} *N,N,O,O*-BODIPYs. Our new design principle is therefore the extension of the *N,N,O,O*-BODIPY π-system in order to increase the helical pitch, and thus foster a more favourable angle (τ) between the magnetic and electric transition dipole moments.

4.1.2 Chapter Aims

Our aim for this chapter was to examine the synthesis of a CPL-SOM BODIPY which will incorporate the design principles described in section 2.1.1 (i.e. chirally perturbed BODIPY core, rigid structure) along with an increase in the helical pitch. In this way we hoped to encourage a more favourable angle between the magnetic and electric transition dipole moments (i.e. τ < 65°).

N,N,O,O-BODIPY **1.93** contains a chirally perturbed BODIPY core, and it has been observed that **1.93** is an efficient emitter of CPL.[84] We have also observed that BODIPYs based on this architecture are efficient emitters of CPL, and as such we decided to use this architecture as our starting point for this work. We planned to achieve an increase in the helical pitch of *N,N,O,O*-BODIPY **1.93** by extending the π-system of the 3,5-diaryl substituents. We therefore designed our target *N,N,O,O*-BODIPY **4.1** with 3,5-dinapth-2-olic rings (figure 4.2).
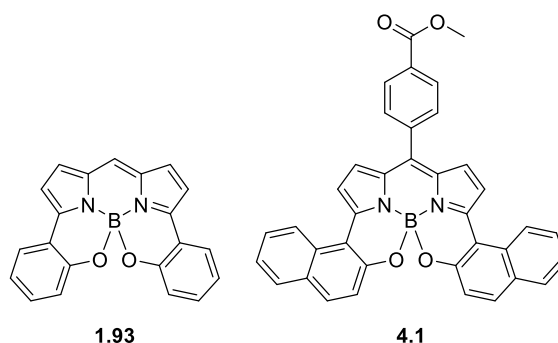
Figure 4.2: *N,N,O,O*-BODIPY **1.93** and target *N,N,O,O*-BODIPY **4.1**.

4.1.3 Synthetic strategy towards *N,N,O,O*-BODIPY **4.1**

Our planned synthesis of *N,N,O,O*-BODIPY **4.1** is outlined in scheme 4.1. This approach first involves a Suzuki-Miyaura cross-coupling reaction between 1-bromonaphthalen-2-ol **4.2** and *N*-Boc-2-pyrroleboronic acid to form Boc-protected 2-arylpyrrole **4.3**. A subsequent Boc deprotection would then afford Boc-deprotected 2-arylpyrrole **4.4**. Finally, we planned to use a one-pot condensation/oxidation/chelation procedure to synthesise *N,N,O,O*-BODIPY **4.1**.
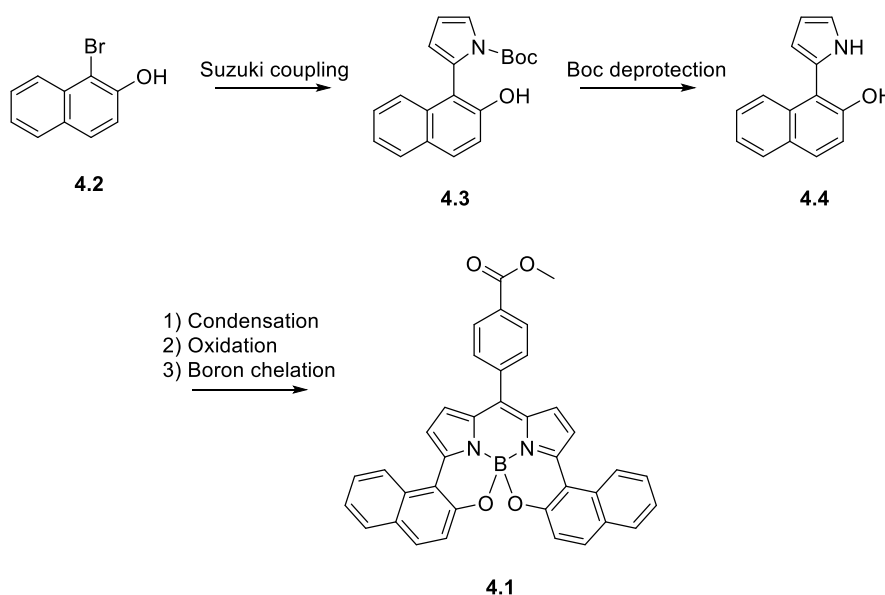
Scheme 4.1: Planned synthetic route to *N,N,O,O*-BODIPY **4.1**.

4.2 Results and Discussion

4.2.1 Synthesis of *N,N,O,O*-BODIPY **4.1**

The first step we examined in the synthesis of *N,N,O,O*-BODIPY **4.1** was the Suzuki-Miyaura cross-coupling reaction between 1-bromonaphthalen-2-ol **4.2** and *N*-Boc-2-pyrroleboronic acid, catalysed by Pd(PPh$_3$)$_4$ (5 mol%), adapted from a literature procedure.[171]

In our first attempt at the Suzuki-Miyaura cross-coupling between 1-bromonaphthalen-2-ol **4.2** and *N*-Boc-2-pyrroleboronic acid, we observed the appearance of two new compounds by TLC analysis of the crude reaction mixture. However after purification by silica gel chromatography, we discovered that the major product from this Suzuki-Miyaura cross-coupling reaction was not 2-arylpyrrole **4.3** as we had expected, but instead an unexpected compound which we will designate **4.5**.

Analysis of the ^{1}H NMR spectrum of **4.5** showed signals corresponding to pyrrolic hydrogens (δ_H 7.21 ppm, dd, 1H, *J* = 3.7, 1.3 Hz; 6.75 ppm, t, 1H, *J* = 3.7 Hz), and signals corresponding to the hydrogens of the napthyl moiety (δ_H 8.49 ppm, d, 1H, *J* = 8.6 Hz; 7.88 ppm, d, 1H, *J* = 8.1 Hz; 7.77 ppm, d, 1H, *J* = 8.9 Hz; 7.55 ppm, ddd, 1H, *J* = 8.1, 6.9, 1.2 Hz; 7.38 ppm, d, 1H, *J* = 8.9 Hz). This evidence led us to believe that the Suzuki-Miyaura cross-coupling reaction had been successful, in that a pyrrole to napthyl bond had been formed.

Analysis of the FT-IR spectrum of **4.5** showed a strong signal at 1754 cm^{-1}, corresponding to a carbonyl moiety contained in either a cyclic ketone or a cyclic carbamate. This was supported by analysis of the ^{13}C NMR spectrum of **4.5** which showed a signal at δ_c 146.3 corresponding to the carbon of a carbonyl moiety residing in either an amide or a carbamate. Therefore we postulated that **4.5** was in fact a carbamate (scheme 4.2), potentially formed via a successful Suzuki-Miyaura cross-coupling between 1-bromonaphthalen-2-ol **4.2** and *N*-Boc-2-pyrroleboronic acid followed by an attack from the naptholic OH into the carbonyl of the Boc protecting group and a loss of *tert*-butanol.

This observation is supported by the previous isolation of the phenolic analogue of **4.5** by Hall *et al.*,[84] which was synthesised by a Suzuki-Miyaura cross-coupling reaction between *N*-Boc-2-bromopyrrole and (2-hydroxyphenyl)boronic acid *en route* to *N,N,O,O*-BODIPY **1.93**.

Further analysis of the product mixture arising from the Pd(PPh$_3$)$_4$ catalysed by Suzuki-Miyaura cross-coupling between 1-bromonaphthalen-2-ol **4.2** and *N*-Boc-2-pyrroleboronic acid showed the presence of a second compound. Analysis of the ^{1}H NMR spectrum of this second compound suggested the formation of the deprotected 2-arylpyrrole **4.4**, due to the presence of two broadened signals in the ^{1}H NMR spectrum corresponding to the N-H moiety (δ_H 8.31 ppm, br s, 1H) and of the O-H moiety (δ_H 6.04 ppm, br s, 1H). We postulated that **4.4** arises from the basic hydrolysis of **4.5** under the Suzuki-Miyaura cross-coupling reaction conditions. It has been previously shown that similar carbamates can undergo clean hydrolysis under basic conditions to the desired deprotected arylpyrroles.[172]
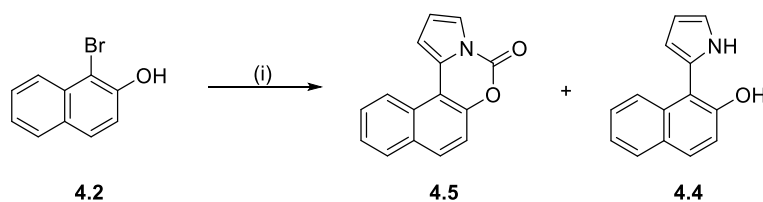
Scheme 4.2: Reagents and conditions: (i) *N*-Boc-2-pyrroleboronic acid (1.5 eq.), Pd(PPh$_3$)$_4$ (5 mol%), K$_3$PO$_4$, THF, H$_2$O, 90 °C, 20 h (**4.5** 32%, **4.4** 58% approx.).

Thus we attempted to optimise the coupling for the direct production of **4.5**, which we would then hydrolyse to cleanly produce deprotected 2-arylpyrrole **4.4**. We found that by using lower reaction temperatures (65 °C) for the Suzuki-Miyaura cross-coupling step, we were able improve the obtained yield of **4.5** from 32% to 64%. Once we had sufficiently improved the yield of **4.5**, we examined the next step in our synthetic pathway.
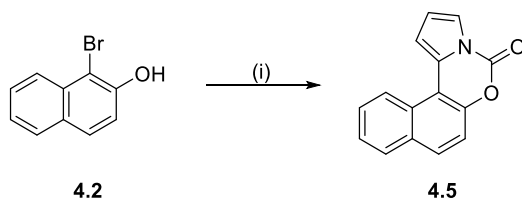
Scheme 4.3: Reagents and conditions: (i) *N*-Boc-2-pyrroleboronic acid (1.5 eq.), Pd(PPh$_3$)$_4$ (5 mol%), K$_3$PO$_4$, THF, H$_2$O, 65 °C, 20 h (**4.5** 64%).

The next step in our synthetic pathway was the hydrolysis of 2-arylpyrrole **4.5**. Following an adapted literature procedure,[172] we reacted 2-arylpyrrole **4.5** with a large excess of sodium hydroxide in ethanol. After one hour at room temperature, the formation of a new product was observed by TLC analysis. After purification by silica gel chromatography, we isolated the desired 2-arylpyrrole **4.4** in a good yield (74%). ^{1}H NMR data obtained for 2-arylpyrrole **4.4** matched previously obtained data for **4.4**. Furthermore analysis of the ^{13}C NMR spectrum of **4.4** showed the disappearance of the signal corresponding to the carbonyl carbon of carbamate **4.5** (δ_C 146.3).
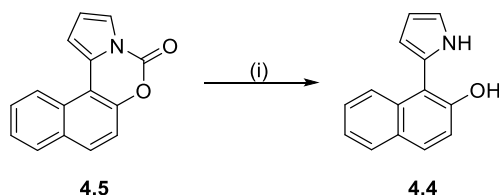
Scheme 4.4: Reagents and conditions: (i) NaOH (200 eq.), EtOH, R.T., 1 h (74%).

The final step in our synthesis was the one-pot condensation/oxidation/boron chelation procedure to form *N,N,O,O*-BODIPY **4.1**.

Following an adapted procedure from Boens *et al*.[173] we treated a solution of 2-arylpyrrole **4.4** and 4-methyl-4-formylbenzoate in DCM with a catalytic amount of TFA at room temperature. After one hour, the appearance of a new compound by TLC indicated the formation of the corresponding dipyrromethane. We then added one equivalent of *p*-chloranil in order to oxidise the dipyrromethane to the corresponding dipyrromethene. An immediate colour change was observed, and the formation of a new compound was confirmed by TLC analysis. Thus after a further 15 minutes diisopropylamine and boron triflouride diethyletherate were added, resulting in the appearance of a new, highly coloured compound by TLC analysis. After purification by silica gel chromatography, *N,N,O,O*-BODIPY **4.1** was isolated in a 16% yield over these three steps.

We confirmed the structure of *N,N,O,O*-BODIPY **4.1** by the observation of a singlet in the ^{11}B NMR spectrum with a chemical shift of δ_B 0.07 ppm. This result is in-keeping with the typical ^{11}B NMR shifts observed from constrained *N,N,O,O*-BODIPYs[79,84,138] (section 2.1.2.2), suggesting that we had formed *N,N,O,O*-BODIPY **4.1**. Furthermore, analysis of the ^{1}H NMR spectrum showed signals corresponding to the napthyl moiety (δ_H 8.47 ppm, d, 2H, *J* = 8.3 Hz; 7.53 ppm, d, 2H, *J* = 7.9 Hz; 7.22 ppm, ddd, 2H, *J* = 7.9, 6.8, 1.2 Hz) and a singlet peak corresponding to the methyl group of the aryl methyl ester (δ_H 3.56 ppm, s, 3H).
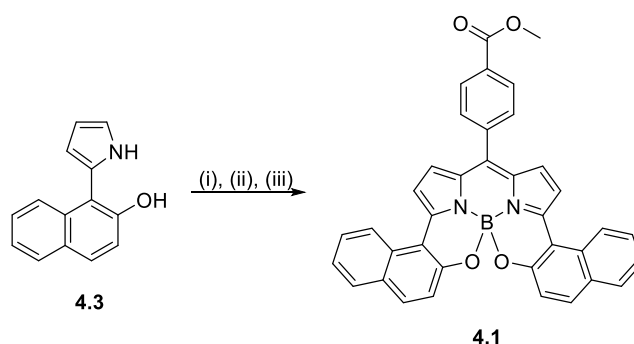
Scheme 4.5: Reagents and conditions: (i) 4-methyl-4-formylbenzoate, TFA, DCM, R.T., 1 h; (ii) *p*-chloranil, 15 minutes; (iii) N^{i}Pr$_2$, BF$_3$.OEt$_2$, 20 minutes (16%).

Further evidence to corroborate the formation of *N,N,O,O*-BODIPY **4.1** came from analysis of the UV/Visible and fluorescence spectra. The absorptive λ_{max} (687 nm) and emissive λ_{max} (730 nm) for *N,N,O,O*-BODIPY **4.1** are even more bathochromically shifted than those measured for *N,N,O,O*-BODIPY **2.13** (λ_{abs} = 632 nm, λ_{em} = 653 nm), suggesting extended conjugation in the fluorophore of **4.1**. The fluorescence quantum yield of *N,N,O,O*-BODIPY **4.1**(ϕ_F = 0.24) is lower than that of *N,N,O,O*-BODIPY **2.13** (ϕ_F = 0.58), which may arise from the additional flexibility imparted to the structure by the 3,5-dinapth-2-olic rings.

N,N,O,O-BODIPY **4.1** is a previously unreported helically chiral, tetradentate *N,N*-dipyrromethene ligand, of which there are limited examples in the literature.[8,79,84,124]

Now that we had identified a successful synthetic route to *N,N,O,O*-BODIPY **4.1**, we wished to resolve the racemic mixture of *N,N,O,O*-BODIPY **4.1** into its respective enantiomers in order to measure the ECD and CPL spectra.

4.2.2 Resolution of the enantiomers of *N,N,O,O*-BODIPY **4.1**

In order to separate the enantiomers of *N,N,O,O*-BODIPY **4.1**, we performed semi-preparative chiral HPLC on a racemic mixture of **4.1** using a Daicel Chiralpak® IA column (1 mL/ minute, toluene). After multiple runs, we were able to collect approximately 20 µg of each enantiomer, which were assigned as (-)-**4.1** and (+)-**4.1** respectively by retention time and by measurement of their specific optical rotation ($[\alpha]_D$).
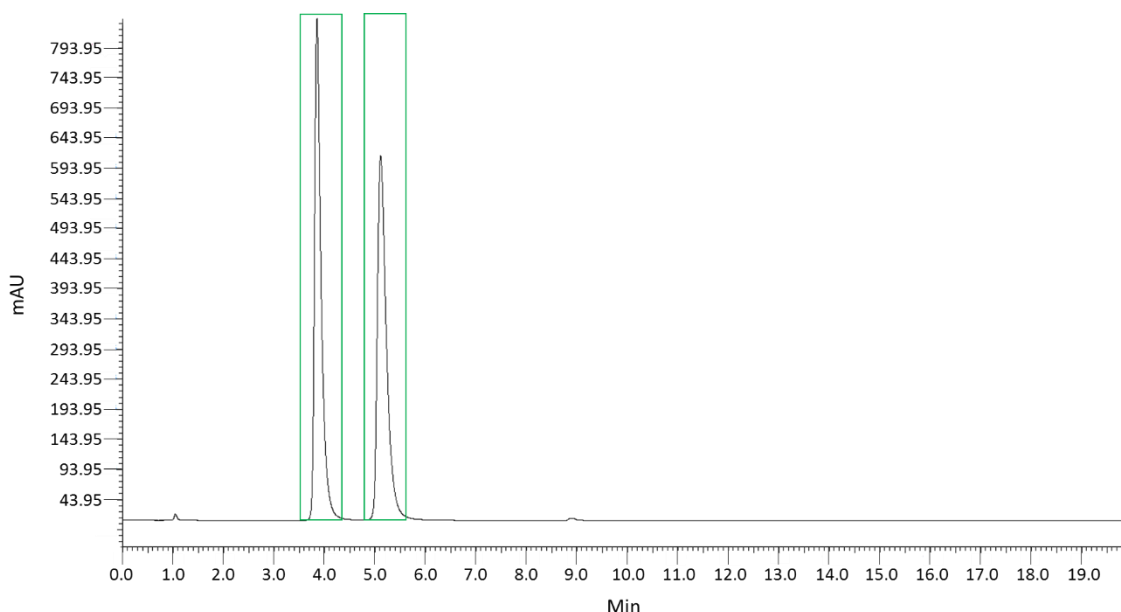
Figure 4.3: A typical chiral HPLC trace obtained from a racemic sample of **4.1**. Daicel Chiralpak® IA column, 4.6 x 250 mm, 5µm particle size,toluene, 1 mL/min.

In order to validate the enantiopurity of the resolved enantiomers of **4.1**, the *ee* of (-)-**4.1** and (+)-**4.1** was measured by resubmission to the same chiral HPLC conditions ((+)-**4.1** %*ee* = >95%, (-)-**4.1** %*ee* = >95%). Once we had confirmed that we had obtained enantiopure samples of each enantiomer of *N,N,O,O*-BODIPY **4.1**, we next studied the chiroptical properties of both (-)-**4.1** and (+)-**4.1**.

4.2.3 ECD spectroscopy of *N,N,O,O*-BODIPY **4.1**

We next measured the ECD spectra of both (+)-**4.1** and (-)-**4.1** (performed by Jonathan Bogaerts) and were pleased to observe that mirror image spectra were obtained. A strong Cotton effect was observed in the transition at 687 nm (±120 L mol^{-1}cm^{-1}), corresponding to the S_0-S_1 transition of *N,N,O,O*-BODIPY **4.1**.

Boltzmann-weighted ECD spectra for the postulated *M* enantiomer of **4.1** were then obtained from TD-DFT calculations at the B3LYP/6-311++G(3df,2pd) level (figure 4.4b, calculations performed by Jonathan Bogaerts). Through comparison of the theoretical ECD spectrum and the experimental ECD spectrum, we were able to assign the enantiomers as (*P*)-(-)-**4.1** (blue) and (*M*)-(+)-**4.1** (red). Interestingly in the case of *N,N,O,O*-BODIPY **4.1** the best agreement between the calculated and experimental ECD spectra was obtained using calculations at the B3LYP level, rather than calculations at the cam-B3LYP or B3PW91 level (see section 5.3.4.6).
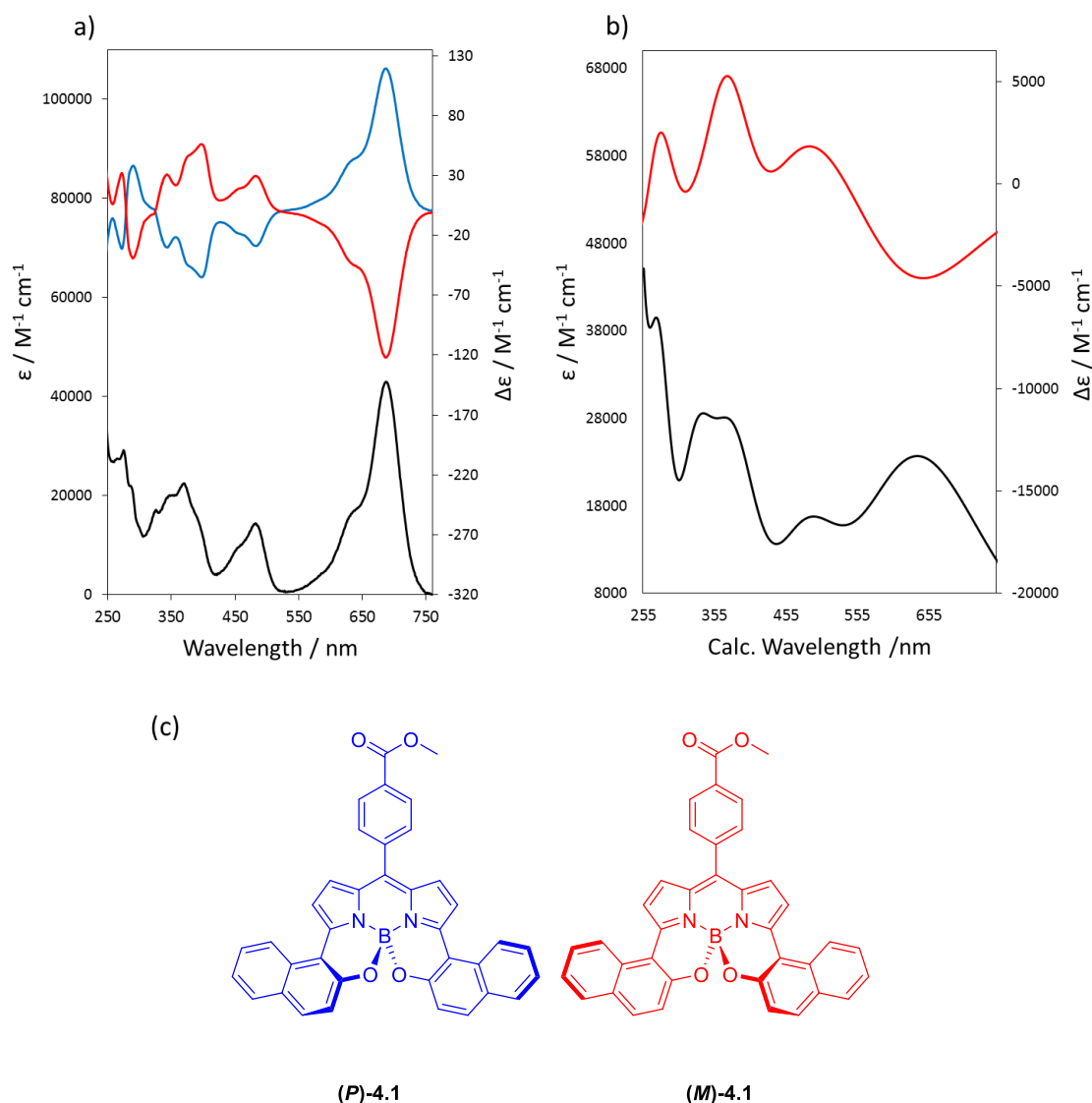
Figure 4.4: a) Experimental ECD spectrum (blue – (*P*)-(-)-**4.1**, red – (*M*)-(+)-**4.1**) and UV/Vis absorption spectrum (black) measured in DCM; b) Calculated Boltzmann-weighted spectra: ECD (red – postulated (*M*)-**4.1** (wavelength uncorrected) and UV/Vis absorption spectra (black – postulated (*M*)-**4.1**(wavelength uncorrected); (c) (*P*)-**4.1** and (*M*)-**4.1**.

	Solvent	λ_{abs} /nm	ε /mol^{-1} cm^{-1}	λ_{em} /nm	ϕ_F	$|g_{abs}|$	$\Delta\varepsilon_{max}$ / L mol^{-1}cm^{-1}
4.1	DCM	687	30 000	730	0.49	2.8×10^{-3}	±120

Table 4.1: Experimental photophysical and chiroptical properties of *N,N,O,O*-BODIPY **4.1**.

4.3.4 CPL spectroscopy of *N,N,O,O*-BODIPY **4.1**

Finally CPL spectra of the (*P*)-(-)-**4.1** and (*M*)-(+)-**4.1** enantiomers of *N,N,O,O*-BODIPY **4.1** were recorded (performed by Dr Lewis Mackenzie). The signals observed were opposite at the emission

maxima (λ_{em} = 730 nm) corresponding to the S_1-S_0 transition of *N,N,O,O*-BODIPY **4.1**, as we would expect for a pair of enantiomers.

We measured a g_{lum} of 1.7×10^{-3} from (*P*)-(-)-**4.1** and -1.5×10^{-3} from (*M*)-(+)-**4.1** (both measured at 730 nm in DCM), giving an average magnitude $|g_{lum}|$ of 1.6×10^{-3} (figure 4.4). To compare g_{lum} values to previously reported systems, we can calculate the overall CPL quantum efficiency ($|g_{lum}|\cdot\phi_F$). For *N,N,O,O*-BODIPY **4.1** the overall CPL quantum efficiency is 4.1×10^{-4}.
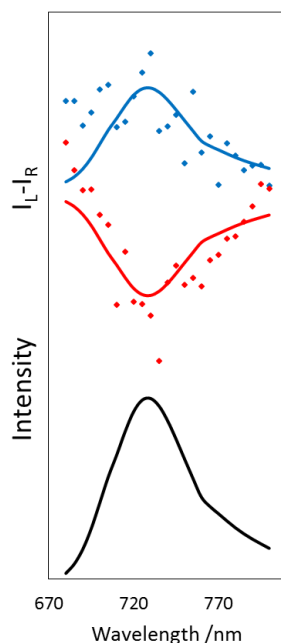
Figure 4.5: Normalised CPL (I_L-I_R) (blue – (*P*)-(-)-**4.1**, red – (*M*)-(+)-**4.1** and fluorescence spectra (black – (*rac*)-**4.1**) measured in DCM.

	Solvent	λ_{abs} /nm	ε /mol^{-1} cm^{-1}	λ_{em} /nm	ϕ_F	$|g_{abs}|$	$\Delta\varepsilon_{max}$ / L mol^{-1}cm^{-1}	$|g_{lum}|$	($|g_{lum}|\cdot\phi_F$)
4.1	DCM	687	43000	730	0.24	2.8×10^{-3}	±120	1.7×10^{-3}	4.1×10^{-4}

Table 4.2: Experimental photophysical and chiroptical properties of *N,N,O,O*-BODIPY **4.1**.

4.3.5 Theoretical calculations of *N,N,O,O*-BODIPY **4.1**

Since our aim in the synthesis of *N,N,O,O*-BODIPY **4.1** was to attempt to control the angle (τ) between the magnetic (**m**) and electric (**μ**) dipole moments, we elected to perform theoretical calculations to determine the magnitude and direction of **m**, **μ** and the angle τ, which are related to g_{lum} by the following equation:

$$g_{lum} = \frac{4(\boldsymbol{\mu}\cdot\boldsymbol{m}\cdot cos\tau)}{(\boldsymbol{\mu}^2 + \boldsymbol{m}^2)}$$

We would then be able to assess the effect the 3,5-dinapth-2-olic rings had on these molecular properties, and determine whether we had successfully exhibited control over the angle τ of *N,N,O,O-*BODIPY **4.1**.

Thus the excited states of *N,N,O,O-*BODIPY (*P*)-**4.1** were calculated (table 4.3) using DFT(PBE0) with a def2-TZVP basis set (table 4.3, performed by Dr Thomas Penfold) as implemented within the ORCA quantum chemistry package.[143]

1.93   **4.1**
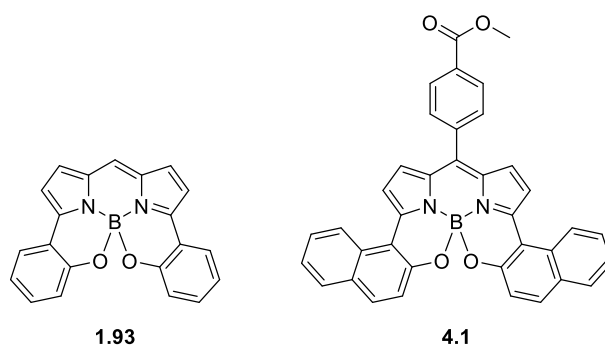
Compound	μ [au]	m [au]	τ [°]	$\lvert g_{lum}\rvert_{calc}$	$\lvert g_{lum}\rvert_{exp}$[a]
1.93	7.6×10^{-1}	1.4×10^{-3}	65	3.1×10^{-3}	4.7×10^{-3}
4.1	6.0×10^{-1}	9.6×10^{-6}	93	2.4×10^{-4}	1.7×10^{-3}

Table 4.3: Calculated magnitudes of the electric (**μ**) and magnetic (**m**) transition dipole moments, the angle between them (τ) and $\lvert g_{lum}\rvert_{calc}$ compared to $\lvert g_{lum}\rvert_{exp}$ for (*P*)-**1.93** and (*P*)-**4.1** [a] $\lvert g_{lum}\rvert_{exp}$ given at the respective λ_{max} value in hexane (**1.93**) and in DCM (**4.1**).

We can clearly observe through comparison of the calculated molecular properties of *N,N,O,O-*BODIPYs **1.93** and **4.1** that the introduction of 3,5-dinapth-2-olic rings to the *N,N,O,O-*BODIPY architecture has induced a significant change in the angle τ, as we had anticipated. We did not achieve a reduction in τ as we had hoped, instead we observe a detrimental increase from 65° in *N,N,O,O-*BODIPY **1.93** to 93° in *N,N,O,O-*BODIPY **4.1**. However we were able to confirm that the direction of the magnetic (**m**) transition dipole moment still aligns with the helical axis, and that the direction of the electric (**μ**) transition dipole moment still aligns with the BODIPY π-system (figure 4.6). Thus we can conclude that control over the angle τ can be achieved through modulation of the 3,5-aryl ring system of *N,N,O,O-*BODIPYs.
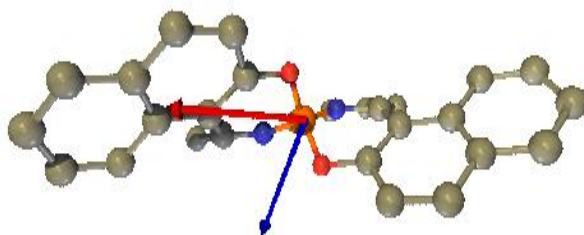
Figure 4.6: Electronic (red) and magnetic (blue) transition dipole moments for *N,N,O,O*-BODIPY **4.1** (magnetic transition dipole moment has been increased in scale by a factor of ten, H atoms and the 8-aryl ring have been omitted for clarity).

A slight decrease in $|\mathbf{\mu}|$ and a large reduction in $|\mathbf{m}|$ is also observed as a result of the inclusion of the 3,5-dinapth-2-olic rings. This along with the detrimental change in the angle τ resulted in a decrease in the calculated g_{lum} value of *N,N,O*,O-BODIPY **4.1** (2.4×10^{-4}) as compared to the calculated g_{lum} value of *N,N,O,O*-BODIPY **1.93** (3.1×10^{-3}). This reduction in calculated g_{lum} is mirrored in our experimental measurements of the g_{lum} of *N,N,O,O*-BODIPYs **4.1** (1.7×10^{-3}) and **1.93** (4.7×10^{-3}). This observation further supports our previous validation of the use of a computational method for the prediction of g_{lum}.

4.3 Conclusions and Future Work

In summary we have described a successful synthetic route to *N,N,O,O*-BODIPY **4.1**, which is a novel example of a tetradentate *N,N*-dipyrromethene ligand with helical chirality. We have characterised the chiroptical properties of **4.1**, including CPL emission. Through theoretical modelling of *N,N,O,O*-BODIPY **4.1** we have confirmed that the extension of the BODIPY π-system through the inclusion of 3,5-dinapth-2-olic rings induces a significant change to the angle τ. This result has promising applications to the future design of helically chiral, CPL-SOM BODIPYs, since exhibiting control over the angle τ is a key step in the development of high g_{lum} BODIPY systems.

In the future we would like to produce 3,5-diaryl-BODIPYs such as **4.6** and **4.7** (figure 4.6), whose aryl rings have structural similarity to the carbo[*n*]helicenes. We propose that the synthesis and study BODIPYs **4.6** and **4.7** (and further analogues) would enable us to recreate the trend observed in the carbo[*n*]helicene series, where an increase in helical pitch results in a decrease in the angle τ.
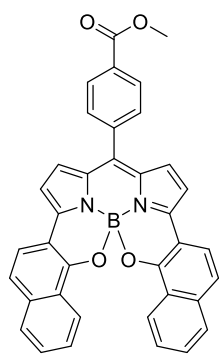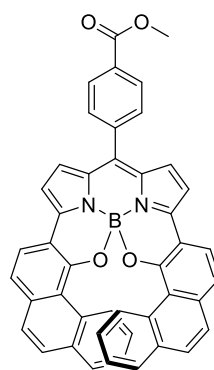
4.6   **4.7**

Figure 4.6: Molecular structures of proposed 3,5-diaryl-BODIPYs **4.6** and **4.7**.

Chapter 5. Experimental Methods and Characterisation

5.1 General Experimental Information

5.1.1 Analysis

Melting points were measured using Stuart SMP3 melting point apparatus. ^{1}H, ^{13}C, ^{11}B and ^{19}F NMR spectra were recorded directly with a Bruker Advance III HD 700 MHz, Jeol Lambda 500 MHz, Jeol ECS-400 MHz or Bruker Advance III 300 MHz spectrometer. Infrared (IR) spectra were recorded on either a Varian Scimitar 800 FT-IR spectrometer or a Perkin Elmer Spectrum Two FT-IR spectrometer. High resolution mass spectra (HRMS) were provided by the EPSRC National Mass Spectrometry Service (University of Swansea). UV/Vis absorption spectra were recorded on a Shimadzu UV-1800 UV spectrophotometer. Emission spectra were recorded on a Shimadzu RF-6000 spectro-fluorophotometer. ECD spectra were recorded on a Chirascan^{TM}-Plus instrument using a SUPRASIL® quartz sample cell with a path length of 10 mm, using a scan speed of 60 nm/min. Specific optical rotation ($[\alpha]_D$) was measured using an Optical Activity PolAAR 2001 automatic polarimeter.

5.1.2 Procedures

Standard Schlenk techniques were used for all experiments involving air-sensitive reagents, under an atmosphere of nitrogen. Solvents were distilled under an atmosphere of nitrogen and used directly, DCM was distilled from calcium hydride, THF was distilled from sodium/benzophenone, and toluene was distilled from sodium. Manual flash chromatography was performed using Geduran silicagel 60 (40-63 μm)

5.2 Experimental Procedures and Characterisation Data

<u>5.2.1 Chapter 2</u>

<u>5.2.1.1 Methyl 4-(di(1*H*-pyrrol-2-yl)methyl)benzoate (**2.9**)</u>
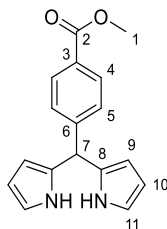
To a round bottomed flask was added an aqueous solution of HCl (0.05 M, 100 mL), followed by the addition of pyrrole (2.0 mL, 30 mmol) and methyl-4-formylbenzoate (1.64 g, 10 mmol). The reaction mixture was stirred for 4 hours under room temperature before the pink precipitate formed was filtered out and washed with water and petroleum ether. The crude product was then purified by column chromatography (Eluent system: DCM) to give methyl 4-(di(1*H*-pyrrol-2-yl)methyl)benzoate (2.52 g, 9 mmol, 90%).

Mp: 161-162 °C; R_f = 0.3 (DCM; UV light); ^{1}H NMR (300 MHz, CDCl$_3$): δ$_H$ 8.04 (d, 2H, *J* = 8.3 Hz, *4*), 7.31 (d, 2H, *J* = 8.3 Hz, *5*), 6.75 (m, 2H, *11*), 6.19 (dd, 2H, *J* = 3.2, 3.7 Hz, *10*), 5.92 (m, 2H, *9*), 5.56 (s, 1H, *7*), 3.93 (s, 3H, *1*); ^{13}C NMR (75 MHz, CDCl$_3$): δ$_C$ 167.0 (*2*), 147.5 (*6*), 131.7 (*8*), 130.0 (*4*), 129.0 (*3*), 128.5 (*5*), 117.7 (*11*), 108.7 (*10*), 107.6 (*9*), 52.3 (*1*), 44.1 (*7*); IR (neat): υ$_{max}$/cm^{-1} 3335 (*m*),1704 (*m*), 1607 (*w*), 1568 (*w*), 1434 (*m*), 1291 (*m*), 1197 (*w*), 1115 (*m*), 1031 (*m*), 961 (*w*), 866 (*w*), 820 (*w*), 730 (*s*); HRMS (pNSI) calcd for C$_{17}$H$_{16}$N$_2$O$_2$ [M+H]$^+$: 281.1285, found 281.1286.

<u>5.2.1.2 Methyl (Z)-4-((5-bromo-1*H*-pyrrol-2-yl)(5-bromo-2*H*-pyrrol-2-ylidene)methyl)benzoate (**2.10**)</u>
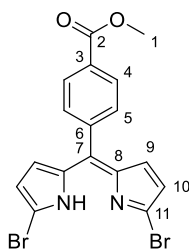
To a round bottomed flask under a nitrogen atmosphere was added methyl 4-(di(1*H*-pyrrol-2-yl)methyl)benzoate (1 g, 3.57 mmol) dissolved in THF (60 mL) and the reaction mixture was left to cool to -78 °C over 30 minutes. NBS (1.27 g, 7.14 mmol) was then added portion wise and the reaction mixture left to stir for 1 hour. DDQ (0.810 g, 3.57 mmol) was then added, and after 10 minutes the reaction mixture was warmed to room temperature. The reaction mixture was diluted with DCM (50 mL) and washed with sodium sulfite solution. The organic layers were combined and dried over MgSO$_4$ and the solvent removed under reduced pressure. The crude product was purified by column chromatography (eluent system: 1:1 DCM:petrol 40-60) to give methyl (Z)-4-((5-bromo-1*H*-pyrrol-2-yl)(5-bromo-2*H*-pyrrol-2-ylidene)methyl)benzoate (1.344 g, 3.08 mmol, 86%)

Mp: 128-130 °C; R$_f$ = 0.43 (1:1 DCM:petrol 40-60); ^{1}H NMR (300 MHz, CDCl$_3$): δ$_H$ 8.11 (d, 2H, *J* = 8.2 Hz, *4*), 7.51 (d, 2H, *J* = 8.2 Hz, *5*), 6.41 (d, 2H, *J* = 4.2, *9*), 6.35 (d, 2H, *J* = 4.2 Hz, *10*), 3.97 (s, 3H, *1*); ^{13}C NMR (75 MHz, CDCl$_3$): δ$_C$ 166.3 (*2*), 139.9 (*6*), 139.8 (*8*), 137.7 (*9*), 130.9 (*7*), 130.7 (*4*), 130.1 (*5*), 129.8 (*3*), 129.0 (*11*), 120.8 (*10*), 52.4 (*1*); IR (neat): υ$_{max}$/cm^{-1} 3329 (w), 3139 (w), 2950 (w), 1714 (m); HRMS (pNSI) calcd for C$_{17}$H$_{12}$N2O$_2$^{81}Br$_2$ [M+H]$^+$: 438.9298, found 438.9314.

5.2.1.3 Methyl 4-(3,7-dibromo-5,5-difluoro-5*H*-4λ^4,5λ^4-dipyrrolo[1,2-*c*:2',1'-*f*][1,3,2]diazaborinin-10-yl)benzoate (**2.11**)
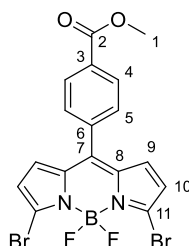
To a round bottomed flask under an inert atmosphere was added methyl (Z)-4-((5-bromo-1*H*-pyrrol-2-yl)(5-bromo-2*H*-pyrrol-2-ylidene)methyl)benzoate (2.54 g, 5.8 mmol) in DCM (10 mL) before adding ^{i}Pr$_2$NEt (2.52 mL, 14.5 mmol) and BF$_3$.OEt$_2$ (1.43 mL, 11.6 mmol). The reaction mixture was stirred at room temperature for 1 hour. The reaction mixture was then washed with sodium hydroxide solution (0.1 M, 115 mL) and HCl (0.1 M, 100 mL). The organic layers were then combined and dried over Na$_2$SO$_4$ and solvent removed under reduced pressure to give methyl 4-(3,7-dibromo-5,5-difluoro-5*H*-4λ^4,5λ^4-dipyrrolo[1,2-*c*:2',1'-*f*][1,3,2]diazaborinin-10-yl)benzoate (2.38 g, 4.90 mmol, 85%).

Mp: 249-251 °C; R$_f$ = 0.44 (1:1 DCM:toluene); ^{1}H NMR (300 MHz, CDCl$_3$): δ$_H$ 8.18 (d, 2H, *J* = 8.4 Hz, *4*), 7.57 (d, 2H, *J* = 8.4 Hz, *5*), 6.73 (d, 2H, *J* = 4.2 Hz, *9*), 6.55 (d, 2H, *J* = 4.2 Hz, *10*), 3.98 (s, 3H, *1*); ^{13}C NMR (75 MHz, CDCl$_3$): δ$_C$ 166.2 (*2*), 141.6 (*6*), 136.7 (*7*), 135.4 (*4*), 133.7 (*3*), 132.4 (*5*), 131.6 (*8*), 130.5 (*9*), 129.8 (*11*), 123.3 (*10*), 52.7 (*1*); ^{11}B NMR (96 MHz, CDCl$_3$): δ$_B$ 0.33 (t, J_{B-F} = 28 Hz); ^{19}F NMR (282MHz, CDCl$_3$): δ$_F$ -146.8 (q, J_{B-F} = 28.2 Hz); IR (neat): υ$_{max}$/cm^{-1} 1711 (*m*); HRMS (pNSI) calcd for C$_{17}$H$_{11}$N$_2$O$_2$^{81}Br$_2$^{11}BF$_2$ [M+H]$^+$: 486.9281, found 486.9277; ε = 84 000 M^{-1} cm^{-1} (DCM).

<u>5.2.1.4 Methyl 4-(5,5-difluoro-3,7-bis(2-methoxyphenyl)-5*H*-4λ⁴,5λ⁴-dipyrrolo[1,2-*c*:2',1'-*f*][1,3,2]diazaborinin-10-yl)benzoate (**2.12**)</u>
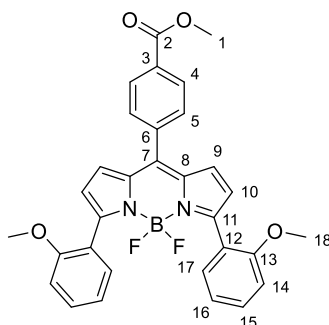
To a Schlenk flask under an inert atmosphere was added methyl 4-(3,7-dibromo-5,5-difluoro-5*H*-4λ⁴,5λ⁴-dipyrrolo[1,2-*c*:2',1'-*f*][1,3,2]diazaborinin-10-yl)benzoate (48 mg, 0.1 mmol), 2-methoxyphenylboronic acid (61 mg, 0.4 mmol), Pd(PPh$_3$)$_4$ (6 mg, 5 mol %) and potassium phosphate (54 mg, 0.4 mmol) in toluene (0.5 mL) and 1,4-dioxane (0.5 mL).The reaction mixture was then refluxed at 90 °C for 1 hour 20 min. The reaction mixture was then diluted with DCM (50 mL) and washed with water (50 mL). The organic layers were then combined and dried over MgSO$_4$ and solvent removed under reduced pressure. The crude product was then purified by column chromatography (eluent system: 5:1 petrol 40-60:EtOAc) to give methyl 4-(5,5-difluoro-3,7-bis(2-methoxyphenyl)-5*H*-4λ⁴,5λ⁴-dipyrrolo[1,2-*c*:2',1'-*f*][1,3,2]diazaborinin-10-yl)benzoate (31 mg, 0.058 mmol, 58%).

Mp: 118-120 °C; R$_f$ = 0.16 (1:1 petrol 40-60:DCM); ^{1}H NMR (300 MHz, CDCl$_3$): δ$_H$ 8.20 (d, 2H, *J* = 8.2 Hz, *4*), 7.74 (dd, 2H, *J* = 7.7, 1.7 Hz, *14*), 7.70 (d, 2H, *J* = 8.2 Hz, *5*), 7.34 (app. td, 2H, *J* = 8.2, 1.7 Hz, *16*), 7.00 (td, 2H, *J* = 7.7, 0.8 Hz, *15*), 6.92 (dd, 2H, *J* = 8.2, 0.8 Hz, *17*), 6.79 (d, 2H, *J* = 4.3 Hz, *9*), 6.61 (d, 2H, *J* = 4.3 Hz, *10*), 4.00 (s, 3H, *1*), 3.78 (s, 6H, *18*); ^{13}C NMR (176 MHz, CDCl$_3$): δ$_C$ 165.5 (*2*), 156.6, 154.9, 140.6, 138.0, 134.1, 130.8, 130.4, 129.7, 129.5, 128.3, 128.3, 121.6, 120.8, 119.2, 109.9, 54.7 (*1*), 51.4 (*18*); ^{11}B NMR (96 MHz, CDCl$_3$): δ$_B$ 1.06 (t, *J*$_{B-F}$ = 30.9 Hz); ^{19}F NMR (282 MHz, CDCl$_3$): δ$_F$ -135.05 (q, *J*$_{B-F}$ = 30.9 Hz); IR (neat): υ$_{max}$/cm^{-1} 2961 (w), 1721 (m), 1602 (w), 1570 (m); HRMS (pNSI) calcd for C$_{31}$H$_{25}$N$_2$O$_4$^{11}BF$_2$ [M+Na]$^+$: 561.1767, found 561.1761.

5.2.1.5 *N,N,O,O*-BODIPY **2.13**

To a Schlenk flask under an inert atmosphere was added methyl 4-(3,7-dibromo-5,5-difluoro-5*H*-4λ⁴,5λ⁴-dipyrrolo[1,2-*c*:2',1'-*f*][1,3,2]diazaborinin-10-yl)benzoate (48 mg, 0.1 mmol), 2-hydroxyphenolboronic acid (55 mg, 0.4 mmol), Pd(PPh$_3$)$_4$ (6 mg, 5 mol %) and sodium carbonate (114 mg, 0.4 mmol) in toluene (0.5 mL) and 1,4-dioxane (0.5 mL).The reaction mixture was then refluxed at 90 °C for 1 hour 20 min. The reaction mixture was then diluted with DCM (50 mL) and washed with water (50 mL). The organic layers were then combined and dried over MgSO$_4$ and solvent removed under reduced pressure. The crude product was then purified by column chromatography (eluent system: 5:1 petrol 40-60 : EtOAc) to give *N,N,O,O*-BODIPY **2.13** (20 mg, 0.043 mmol, 43%).

Mp: 276-278 °C; R$_f$ = 0.15 (5:1 petrol 40-60:EtOAc); ^{1}H NMR (300 MHz, CDCl$_3$): δ$_H$ 8.22 (d, 2H, *J* = 8.6 Hz, *4*), 7.83-7.78 (m, 4H, *5,15*), 7.35 (ddd, 2H, *J* = 8.3, 7.4, 1.5 Hz, *14*), 7.08 (dd, 2H, *J* = 7.4, 1.5 Hz, *16*), 7.05 (d, 2H, *J* = 4.4 Hz, *9*), 6.97 (dd, 2H, *J* = 8.3, 1.2 Hz, *13*), 6.93 (d, 2H, *J* = 4.4 Hz, *10*), 3.99 (s, 3H, *1*); ^{13}C NMR (75 MHz, CDCl$_3$): δ$_C$ 166.5 (*2*), 154.4 (*17*), 150.6 (*6*), 138.5 (*7*), 137.1 (*11*), 134.2 (*13*), 132.6 (*15*), 132.0 (*4*), 130.6 (*5*), 130.0 (*14*), 129.9 (*12*), 126.0 (*5*), 120.7 (*16*), 119.9 (*8*), 119.7 (*3*), 116.9 (*9*), 52.6 (*1*); ^{11}B NMR (96 MHz, CDCl$_3$): δ$_B$ -0.90 (s); IR (neat): υ$_{max}$/cm^{-1} 2923 (w), 2853 (w), 1713 (m); HRMS (TOF ASAP$^+$) calcd for C$_{29}$H$_{19}$N$_2$O$_4$^{11}B [M+H]$^+$: 471.1521, found 471.1519; ε = 24 000 M^{-1} cm^{-1} (DCM); ϕ$_F$ = 0.58 (DCM).

<u>5.2.1.6 3-(4-(methoxycarbonyl)phenyl)-10,15-dioxa-2a^1,3a^1-diaza-10a-borabenzo[5,6]indeno[1,7-</u>
<u>*ef*]aceanthrylen-2a^1-ium-16-uide (*N,N,O,C*-BODIPY **2.18**)</u>
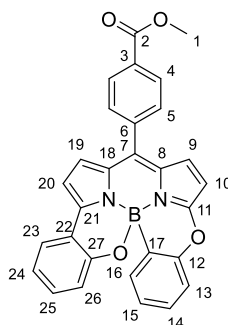
METHOD A: To a Schlenk flask under an inert atmosphere was added methyl 4-(3,7-dibromo-5,5-difluoro-5*H*-4λ^4,5λ^4-dipyrrolo[1,2-*c*:2',1'-*f*][1,3,2]diazaborinin-10-yl)benzoate (48 mg, 0.1 mmol), 2-hydroxyphenolboronic acid (55 mg, 0.4 mmol), Pd(PPh$_3$)$_4$ (6 mg, 5 mol %) and sodium carbonate (114 mg, 0.4 mmol) in toluene (0.5 mL) and 1,4-dioxane (0.5 mL).The reaction mixture was then refluxed at 90 °C for 16.5 hours. The reaction mixture was then diluted with DCM (50 mL) and washed with water (50 mL). The organic layers were then combined and dried over MgSO$_4$ and solvent removed under reduced pressure. The crude product was then purified by column chromatography (eluent system: 5:1 petrol 40-60:EtOAc) to give 3-(4-(methoxycarbonyl)phenyl)-10,15-dioxa-2a^1,3a^1-diaza-10a-borabenzo[5,6]indeno[1,7-*ef*]aceanthrylen-2a^1-ium-16-uide (17 mg, 0.036 mmol, 36%).

METHOD B: To a Schlenk flask under an inert atmosphere was added methyl (Z)-4-((5-bromo-1*H*-pyrrol-2-yl)(5-bromo-2*H*-pyrrol-2-ylidene)methyl)benzoate (150 mg, 0.34 mmol), 2-hydroxyphenylboronic acid (188 mg, 1.36 mmol), Pd(PPh$_3$)$_4$ (20 mg, 5 mol %) and sodium carbonate (389 mg, 1.36 mmol) in toluene (1.5 mL) and 1,4-dioxane (1.5 mL).The reaction mixture was then refluxed at 90 °C for 2 hours. The reaction mixture was then diluted with DCM (50 mL) and washed with water (50 mL). The organic layers were then combined and dried over MgSO$_4$ and solvent removed under reduced pressure. The crude product was then purified by column chromatography (eluent system: 5:1 petrol 40-60:EtOAc) to give 3-(4-(methoxycarbonyl)phenyl)-10,15-dioxa-2a^1,3a^1-diaza-10a-borabenzo[5,6]indeno[1,7-*ef*]aceanthrylen-2a^1-ium-16-uide (137 mg, 0.29 mmol, 85%).

Mp: 173-175 °C; R$_f$ = 0.35 (5:1 petrol 40-60:EtOAc); ^{1}H NMR (300 MHz, CDCl$_3$): δ$_H$ 8.22 (d, 2H, *J* = 8.45 Hz, *4*), 7.77 − 7.72 (m, 3H, *5*, *13*), 7.31 (d, 1H, *J* = 8.91 Hz, *16*), 7.24 − 7.17 (m, 3H, *14*, *15*, *24*), 7.02 − 6.91 (m, 4H, *9*, *10*, *25*, *26*), 6.86 (d, 1H, *J* = 4.5 Hz, *19*), 6.77 (d, 1H, *J* = 8.1 Hz, *23*), 6.43 (d, 1H, *J* = 4.5 Hz, *20*), 3.99 (s, 3H, *1*); ^{13}C NMR (75 MHz, CDCl$_3$): δ$_C$ 166.6 (*2*), 163.2 (*11*), 156.9 (*12*), 154.6 (*27*), 148.4 (*6*), 138.2 (*8*), 137.3 (*9*), 132.3 (*16*), 131.9 (*7*), 131.5 (*21*), 130.4 (*5*), 129.9 (*4*), 129.5 (*15*), 128.4 (*25*), 127.7 (*3*), 127.5 (*24*), 125.2 (*22*), 124.6 (*10*), 121.5 (*20*), 120.4 (*26*), 120.3 (*13*), 117.0 (*18*), 115.7 (*14*), 107.9 (*19*), 52.6 (*1*); ^{11}B NMR (96 MHz, CDCl$_3$): δ$_B$ -2.21 (s); IR (neat): υ$_{max}$/cm^{-1} 2953 (*w*), 2921 (*w*), 2852

(*w*), 1721 (*m*); HRMS (pNSI) calcd for $C_{29}H_{19}N_2O_4{}^{11}B$ [M+H]: 471.1521, found 471.1517; ε = 30 000 M^{-1} cm^{-1} (hexane); ϕ_F = 0.49 (hexane).

5.2.1.7 Methyl 4-(9,14-dimethyl-10,15-dioxa-2a^{1}λ^4,3a^1-diaza-10aλ^4-borabenzo[5,6]indeno[3,4-*ef*]aceanthrylen-3-yl)benzoate (*N,N,O,C*-BODIPY **2.32**)
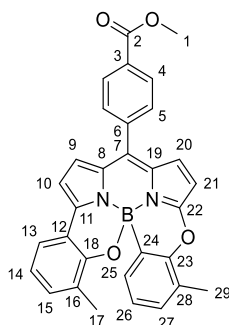
To a Schlenk flask under an inert atmosphere was added added methyl (Z)-4-((5-bromo-1*H*-pyrrol-2-yl)(5-bromo-2*H*-pyrrol-2-ylidene)methyl)benzoate (151 mg, 0.35 mmol), 3-methyl-2-hydroxyphenyl boronic acid (213 mg, 1.4 mmol), Pd(PPh$_3$)$_4$ (21 mg, 5 mol %) and sodium carbonate (401 mg, 1.4 mmol) in toluene (1.5 mL) and 1,4-dioxane (1.5 mL).The reaction mixture was then refluxed at 90 °C for 18.5 hours. The reaction mixture was then diluted with DCM (50 mL) and washed with water (50 mL). The organic layers were then combined and dried over MgSO$_4$ and solvent removed under reduced pressure. The crude product was then purified by column chromatography (eluent system: 5:1 petrol 40-60:EtOAc) to give methyl 4-(9,14-dimethyl-10,15-dioxa-2a^{1}λ^4,3a^1-diaza-10aλ^4-borabenzo[5,6]indeno[3,4-*ef*]aceanthrylen-3-yl)benzoate (67 mg, 0.13 mmol, 38%).

Mp: 235-236 °C; R$_f$ = 0.61 (5:1 petrol 40-60:EtOAc); ^{1}H NMR (300 MHz, CDCl$_3$): δ$_H$ 8.18 (d, 2H, *J* = 8.6 Hz, *4*), 7.75 (d, 2H, *J* = 8.6 Hz, *5*), 7.57 (dd, 1H, *J* = 7.7, 1.7 Hz, *15*), 7.05 (m, 2H, *14, 26*), 7.01-6.96 (m, 3H, *9, 13, 20*), 6.90-6.78 (m, 3H, *10, 25, 27*), 6.43 (d, 1H, *J* = 4.6 Hz, *21*), 3.99 (s, 3H, *1*), 2.47 (s, 3H, *17*), 1.95 (s, 3H, *29*); ^{13}C NMR (176 MHz, CDCl$_3$): δ$_C$ 166.5 (*2*), 163.2 (*22*), 155.4 (*23*), 153.2 (*18*), 149.2 (*6*), 138.4 (*19*), 137.1 (*20*), 133.0 (*7*), 132.4 (*15*), 131.9 (*27*), 131.0 (*25*), 130.4 (*5*), 130.0 (*4*), 129.5 (*3*), 129.1 (*11*), 128.2 (*13*), 127.4 (*16*), 127.1 (*28*), 125.9 (*14*), 124.1 (*26*), 122.8 (*12*), 120.9 (*21*), 119.7 (*8*), 115.8 (*9*), 107.7 (*10*), 52.4 (*1*), 16.6 (*17*), 16.2 (*29*); ^{11}B NMR (96 MHz, CDCl$_3$): δ$_B$ -2.93 (s); IR (neat): υ$_{max}$/cm^{-1} 2981 (m), 2943 (w), 2936 (w), 1725 (m); HRMS (pNSI) calcd for C$_{31}$H$_{23}$^{11}BN$_2$O$_4$ [M+H]: 499.1835, found 499.1838; ε = 24 000 M^{-1} cm^{-1} (DCM); φ$_F$ = 0.41 (DCM).

5.2.1.8 Methyl 4-(7,12-dimethyl-10,15-dioxa-2a^{1}λ^4,3a^1-diaza-10aλ^4-borabenzo[5,6]indeno[3,4-*ef*]aceanthrylen-3-yl)benzoate (*N,N,O,C*-BODIPY **2.33**)
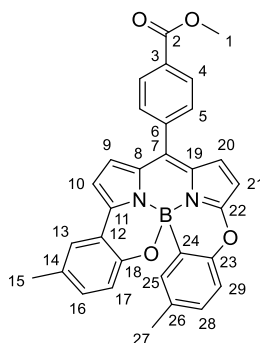
To a Schlenk flask under an inert atmosphere was added added methyl (Z)-4-((5-bromo-1*H*-pyrrol-2-yl)(5-bromo-2*H*-pyrrol-2-ylidene)methyl)benzoate (200 mg, 0.46 mmol), 5-methyl-2-hydroxyphenyl boronic acid (280 mg, 1.84 mmol), Pd(PPh$_3$)$_4$ (27 mg, 5 mol %) and sodium carbonate (526 mg, 1.84 mmol) in toluene (2 mL) and 1,4-dioxane (2 mL).The reaction mixture was then refluxed at 90 °C for 2 hours. The reaction mixture was then diluted with DCM (50 mL) and washed with water (50 mL). The organic layers were then combined and dried over MgSO$_4$ and solvent removed under reduced pressure. The crude product was then purified by column chromatography (eluent system: 5:1:1 petrol 40-60:toluene:EtOAc) to give methyl 4-(7,12-dimethyl-10,15-dioxa-2a^{1}λ^4,3a^1-diaza-10aλ^4-borabenzo[5,6]indeno[3,4-*ef*]aceanthrylen-3-yl)benzoate (127 mg, 0.25 mmol, 55%).

Mp: 249-250 °C; R$_f$ = 0.39 (5:1:1 petrol 40-60:toluene:EtOAc); ^{1}H NMR (300 MHz, CDCl$_3$): δ$_H$ 8.19 (d, 2H, *J* = 8.3 Hz, *4*), 7.74 (d, 2H, *J* = 8.3 Hz, *5*), 7.55 (d, 2H, *J* = 2.2 Hz, *13*), 7.21 (d, 1H, *J* = 8.1 Hz, *28*), 7.05-6.95 (m, 5H, *9, 10, 16, 17, 25*), 6.86 (d, 1H, *J* = 4.5 Hz, *20*), 6.70 (d, 2H, *J* = 8.1 Hz, *29*), 6.40 (d, 1H, *J* = 4.5 Hz, *21*), 3.99 (s, 3H, *1*), 2.36 (s, 3H, *27*), 2.16 (s, 3H, *15*); ^{13}C NMR (176 MHz, CDCl$_3$): δ$_C$ 166.5 (*2*), 163.5 (*22*), 155.4 (*23*), 152.7 (*18*), 148.7 (*6*), 138.4 (*25*), 136.9 (*19*), 133.8 (*20*), 133.2 (*7*), 132.4 (*13*), 131.9 (*14*), 131.1 (*11*), 130.4 (*5*), 129.9 (*26*), 129.9 (*28*), 129.3 (*16*), 128.2 (*4*), 128.1 (*3*), 127.5 (*12*), 125.2 (*21*), 121.1 (*17*), 120.0 (*8*), 116.7 (*29*), 115.6 (*10*), 107.7 (*9*), 52.5 (*1*), 21.0 (*15*), 20.8 (*27*); ^{11}B NMR (96 MHz, CDCl$_3$): δ$_B$ – 2.39 (s); IR (neat): υ$_{max}$/cm^{-1} 2981 (m), 2933 (w), 1718 (m); HRMS (pNSI) calcd for C$_{31}$H$_{23}$^{11}BN$_2$O$_4$ [M+H]: 499.1835, found 499.1846; ε = 39 000 M^{-1} cm^{-1} (DCM); ϕ$_F$ = 0.25 (DCM).

5.2.1.9 Methyl 4-(7,12-dichloro-10,15-dioxa-2a$^1\lambda^4$,3a^1-diaza-10aλ^4-borabenzo[5,6]indeno[3,4-*ef*]aceanthrylen-3-yl)benzoate (*N,N,O,C*-BODIPY **2.34**)
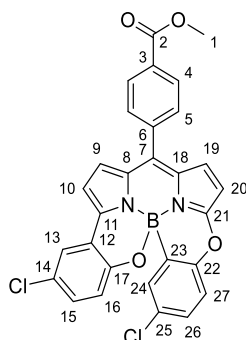
To a Schlenk flask under an inert atmosphere was added methyl (Z)-4-((5-bromo-1*H*-pyrrol-2-yl)(5-bromo-2*H*-pyrrol-2-ylidene)methyl)benzoate (200 mg, 0.46 mmol), 5-chloro-2-hydroxyphenyl boronic acid (317 mg, 1.84 mmol), Pd(PPh$_3$)$_4$ (27 mg, 5 mol %) and sodium carbonate (526 mg, 1.84 mmol) in toluene (2 mL) and 1,4-dioxane (2 mL).The reaction mixture was then refluxed at 90 °C for 2 hours. The reaction mixture was then diluted with DCM (50 mL) and washed with water (50 mL). The organic layers were then combined and dried over MgSO$_4$ and solvent removed under reduced pressure. The crude product was then purified by column chromatography (eluent system: 5:1:1 petrol 40-60:EtOAc:toluene) to give methyl 4-(7,12-dichloro-10,15-dioxa-2a$^1\lambda^4$,3a^1-diaza-10aλ^4-borabenzo[5,6]indeno[3,4-*ef*]aceanthrylen-3-yl)benzoate (177 mg, 0.33 mmol, 71%).

Mp: 126-127 °C; R_f = 0.30 (5:1:1 petrol 40-60:EtOAc:toluene); ^{1}H NMR (300 MHz, CDCl$_3$): δ_H 8.12 (d, 2H, *J* = 8.5 Hz, *4*), 7.67 (d, 2H, *J* = 8.5 Hz, *5*), 7.63 (d, 1H, *J* = 2.6 Hz, *24*), 7.18 (m, 1H, *27*), 7.10 (m, 1H, *15*), 7.07 (m, 1H, *26*), 7.02 (d, 1H, *J* = 2.5 Hz, *13*), 6.97 (d, 1H, *J* = 4.7 Hz, *19*), 6.94 (d, 1H, *J* = 4.3 Hz, *9*), 6.78 (d, 1H, *J* = 4.3 Hz, *10*), 6.64 (d, 1H, *J* = 8.5 Hz, *16*), 6.37 (d, 1H, *J* = 4.7 Hz, *20*), 3.91 (s, 3H, *1*); ^{13}C NMR (176 MHz, CDCl$_3$): δ_C 166.6 (*2*), 163.4 (*21*), 155.3 (*22*), 154.7 (*17*), 152.7 (*6*), 146.9 (*18*), 137.8 (*19*), 132.5 (*7*), 132.3 (*11*), 132.1 (*26*), 130.4 (*5*), 130.0 (*15*), 129.5 (*16*), 129.0 (*4*), 128.6 (*3*), 127.7 (*13*), 125.6 (*14*), 125.5 (*25*), 124.7 (*24*), 122.2 (*12*), 121.6 (*20*), 118.6 (*27*), 116.9 (*8*), 115.9 (*9*), 108.4 (*10*), 52.6 (*1*); ^{11}B NMR (96 MHz, CDCl$_3$): δ_B -3.26 (s); IR (neat): υ_{max}/cm^{-1} 2981 (w), 2970 (w), 1719 (m); HRMS (pNSI) calcd for C$_{29}$H$_{17}$^{11}B^{35}Cl$_2$N$_2$O$_4$ [M+H]: 539.0742, found 539.0746; ε = 52 000 M^{-1} cm^{-1} (DCM); ϕ_F = 0.37 (DCM).

5.2.1.10 Methyl 4-(7,12-difluoro-10,15-dioxa-2a^{1}λ^4,3a^1-diaza-10aλ^4-borabenzo[5,6]indeno[3,4-*ef*]aceanthrylen-3-yl)benzoate (*N,N,O,C*-BODIPY **2.35**)
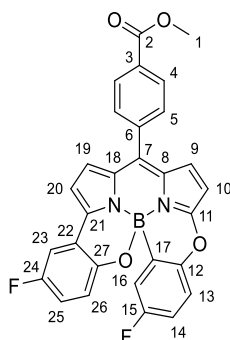
To a Schlenk flask under an inert atmosphere was added added methyl (Z)-4-((5-bromo-1*H*-pyrrol-2-yl)(5-bromo-2*H*-pyrrol-2-ylidene)methyl)benzoate (169 mg, 0.39 mmol), 5-fluoro-2-hydroxyphenyl boronic acid (242 mg, 1.55 mmol), Pd(PPh$_3$)$_4$ (23 mg, 5 mol %) and sodium carbonate (444 mg, 1.55 mmol) in toluene (1.5 mL) and 1,4-dioxane (1.5 mL).The reaction mixture was then refluxed at 90 °C for 2 hours. The reaction mixture was then diluted with DCM (50 mL) and washed with water (50 mL). The organic layers were then combined and dried over MgSO$_4$ and solvent removed under reduced pressure. The crude product was then purified by column chromatography (eluent system: 6:1:1 petrol 40-60:EtOAc:toluene) to give methyl 4-(7,12-difluoro-10,15-dioxa-2a^{1}λ^4,3a^1-diaza-10aλ^4-borabenzo[5,6]indeno[3,4-*ef*]aceanthrylen-3-yl)benzoate (67 mg, 0.13 mmol, 73%).

Mp: 122-123 °C; R$_f$ = 0.30 (6:1:1 petrol 40-60:EtOAc:toluene);

^{1}H NMR (700 MHz, CDCl$_3$): δ$_H$ 8.19 (d, 2H, *J* = 8.6 Hz, *4*), 7.74 (br s 2H, *5*), 7.42 (dd, 1H, *J* = 8.5, 3.5 Hz, *23*), 7.28 (dd, 1H, *J* = 8.6, 4.0 Hz, *13*), 7.03 (d, 1H, *J* = 4.6 Hz, *9*), 7.00 (d, 1H, *J* = 4.2 Hz, *19*), 6.92 (app. td, 1H, *J* = 8.5, 3.9 Hz, *25*), 6.89 (app. td, 1H, *J* = 8.6, 3.1 Hz, *14*), 6.84 (d, 1H, *J* = 4.2 Hz, *20*), 6.79 (dd, 1H, *J* = 8.0, 3.1 Hz, *16*), 6.72 (dd, 1H, *J* = 9.0, 3.5 Hz, *26*), 6.44 (d, 1H, *J* = 4.6 Hz, *10*), 3.99 (s, 3H, *1*); ^{13}C NMR (75 MHz, CDCl$_3$): δ$_C$ 166.4 (*2*), 163.6 (*11*), 159.3 (d, *J$_{C-F}$* = 245.5 Hz, *15*), 156.8 (d, *J$_{C-F}$* = 238.0 Hz, *24*), 152.5 (*12*), 150.3 (*27*), 146.8 (d, *J$_{C-F}$* = 2.9 Hz, *22*), 137.8 (*6*), 137.5 (*7*), 132.3 (*9*), 132.3 (*21*), 132.0 (*3*), 130.5 (*5*), 130.0 (*4*), 128.3 (*19*), 127.6 (*8*), 121.4 (*18*), 121.2 (d, *J$_{C-F}$* = 8.0 Hz, *26*), 119.0 (d, *J$_{C-F}$* = 23.2 Hz, *25*), 118.5 (d, *J$_{C-F}$* = 7.9 Hz, *13*), 115.7 (*20*), 115.2 (d, *J$_{C-F}$* = 21.4 Hz, *16*), 114.4 (d, *J$_{C-F}$* = 24.5 Hz, *14*), 110.8 (d, *J$_{C-F}$* = 24.1 Hz, *23*), 108.5 (*10*), 52.6 (*1*); ^{11}B NMR (96 MHz, CDCl$_3$): δ$_B$ -3.22 (s); ^{19}F NMR (282 MHz, CDCl$_3$): δ$_F$ -177.0 (s), -123.1 (s); IR (neat): υ$_{max}$/cm^{-1} 2951 (w), 2939 (w), 1723 (m); HRMS (pNSI) calcd for C$_{29}$H$_{17}$^{11}BF$_2$N$_2$O$_4$ [M+H]: 507.1333, found 507.1333; ε = 32 000 M^{-1} cm^{-1} (DCM); φ$_F$ = 0.43 (DCM).

<u>5.2.2 Chapter 3</u>

<u>5.2.2.1 Methyl 4-(5,5-difluoro-3,7-bis(2-(methylthio)phenyl)-5*H*-4λ⁴,5λ⁴-dipyrrolo[1,2-*c*:2',1'-*f*][1,3,2]diazaborinin-10-yl)benzoate (**3.2**)</u>
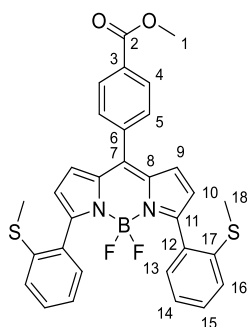
To a Schlenk flask under an inert atmosphere was added methyl 4-(3,7-dibromo-5,5-difluoro-5*H*-4λ⁴,5λ⁴-dipyrrolo[1,2-*c*:2',1'-*f*][1,3,2]diazaborinin-10-yl)benzoate (242 mg, 0.5 mmol), 2-(methylthio)phenyl boronic acid (336 mg, 2 mmol), Pd(PPh₃)₄ (29 mg, 5 mol %) and sodium carbonate (572 mg, 2 mmol) in toluene (2 mL) and 1,4-dioxane (2 mL).The reaction mixture was then refluxed at 90 °C for 18 h. The reaction mixture was then diluted with DCM and washed with water. The organic layers were then combined and dried over MgSO₄ and solvent removed under reduced pressure. The crude product was then purified by column chromatography (eluent system: 3:1 petrol 40-60:EtOAc) to give methyl 4-(5,5-difluoro-3,7-bis(2-(methylthio)phenyl)-5*H*-4λ⁴,5λ⁴-dipyrrolo[1,2-*c*:2',1'-*f*][1,3,2]diazaborinin-10-yl)benzoate (180 mg, 0.32 mmol, 63%).

Mp: 117-118 °C; R*f* = 0.43 (3:1 petrol 40-60:EtOAc); ¹H NMR (700 MHz, CDCl₃): δ_H 8.22 (d, 2H, *J* = 8.5 Hz, *4*), 7.74 (d, 2H, *J* = 8.5 Hz, *5*), 7.58 (d, 2H, *J* = 7.5 Hz, *13*), 7.33 (ddd, 2H, *J* = 8.0, 7.4, 1.5 Hz, *15*), 7.28-7.26 (m, 2H, *16*), 7.18 (ddd, 2H, *J* = 7.5, 7.4, 1.2 Hz, *14*), 6.84 (d, 2H, *J* = 4.3 Hz, *9*), 6.64 (d, 2H, *J* = 4.3 Hz, *10*), 4.00 (s, 3H, *1*), 2.39 (s, 6H, *18*); ¹³C NMR (176 MHz, CDCl₃): δ_C 166.5 (*2*), 157.4 (*11*), 143.1 (*6*), 138.8 (*17*), 138.4 (*15*), 135.4 (*12*), 131.9 (*7*), 131.8 (*3*), 131.1 (*5*), 130.7 (*4*), 130.5 (*8*), 129.8 (*9*), 129.6 (*13*), 126.1 (*16*), 124.7 (*14*), 122.6 (10), 52.6 (*1*), 16.6 (*18*); ¹¹B NMR (96 MHz, CDCl₃): δ_B 0.83 (t, *J*_{B-F} = 30.3 Hz); ¹⁹F NMR (282 MHz, CDCl₃): δ_F -147.0 (q, *J*_{B-F} = 30.3 Hz), -147.3 (q, *J*_{B-F} = 30.3 Hz); IR (neat): υ_max/cm⁻¹ 1714 (m), 2989 (w); HRMS (pAPCI) calcd for C₃₁H₂₅¹¹BF₂N₂O₂S₂ [M+H]⁺ 571.1497, found 571.1479; ε = 49 000 M⁻¹ cm⁻¹ (DCM).

5.2.2.2 Methyl (Z)-4-((5-(2-(methylthio)phenyl)-1*H*-pyrrol-2-yl)(5-(2-(methylthio)phenyl)-2*H*-pyrrol-2-ylidene)methyl)benzoate (**3.3**)
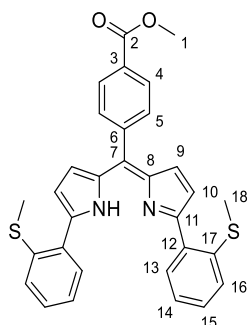
To a round bottomed flask under an inert atmosphere was added methyl 4-(5,5-difluoro-3,7-bis(2-(methylthio)phenyl)-5*H*-4λ^4,5λ^4-dipyrrolo[1,2-*c*:2',1'-*f*][1,3,2]diazaborinin-10-yl)benzoate (414 mg, 0.73 mmol), DCM (3.7 mL), MeOH (3.7 mL) and TFA (65.7 mL) were then added, and the reaction mixture stirred at room temperature for 1 hour. The solvent was removed under reduced pressure, and the residue redissolved in DCM (100 mL) and washed with water (200 mL). The organic layers were then combined and dried over MgSO$_4$ and solvent removed under reduced pressure, to give methyl (Z)-4-((5-(2-(methylthio)phenyl)-1*H*-pyrrol-2-yl)(5-(2-(methylthio)phenyl)-2*H*-pyrrol-2-ylidene)methyl)benzoate without the need for further purification (377 mg, 0.72 mmol, 99 %).

Mp: 198-200 °C; ^{1}H NMR (700 MHz, CDCl$_3$): δ_H 8.15 (d, 2H, *J* = 8.1 Hz, *4*), 7.76 (d, 2H, *J* = 7.6 Hz, *13*), 7.65 (d, 2H, *J* = 8.1 Hz, *5*), 7.35 (app. t, 2H, *J* = 8.2 Hz, *15*), 7.28 (d, 2H, *J* = 8.2 Hz, *16*), 7.21 (app. t, 2H, *J* = 7.6 Hz, *14*), 6.86 (br s, 2H, *9*), 6.60 (br s, 2H, *10*), 3.98 (s, 3H, *1*), 2.31 (s, 6H, *18*); ^{13}C NMR (176 MHz, CDCl$_3$): δ_C 166.9 (*2*), 153.9 (*11*), 142.3 (*6*), 140.7 (*17*), 138.6 (*8*), 131.2 (*7*), 131.1 (*15*), 130.5 (*3*), 130.2 (*4*), 129.2 (*13*), 129.1 (*16*), 129.0 (*9*), 128.7 (*5*), 125.4 (*14*), 124.5 (*10*), 119.0 (*12*), 52.5 (*1*), 16.1 (*18*); IR (neat): υ_{max}/cm^{-1} 1716 (m); HRMS (TOF MS ASAP+) calcd for C$_{31}$H$_{26}$N$_2$O$_2$S$_2$ [M+H]$^+$ 523.1514, found 523.1516.

5.2.2.3 (2-bromophenyl)(methoxymethyl)sulfane (**3.4a**)
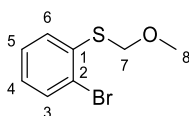
In a round bottomed flask under an inert atmosphere was added NaO^{t}Bu (961 mg, 10 mmol) and THF (25 mL). 2-bromobenzenethiol (1.2 mL, 10 mmol) was added to the resulting suspension, and the reaction mixture was stirred for 15 minutes. MOMCl (0.84 mL, 11 mmol) was then added and the reaction mixture stirred for a further 15 minutes. The reaction mixture was diluted with diethyl ether (50 mL) and washed with water (100 mL) and brine (100 mL). The organic layers were then combined and dried over MgSO$_4$ and solvent removed under reduced pressure. The crude product was then purified by column chromatography (eluent system: 10:1 petrol 40-60:EtOAc) to give (2-bromophenyl)(methoxymethyl)sulfane (2.33 g, 10 mmol, 100 %).

R$_f$ = 0.71 (10:1 petrol 40-60:EtOAc; UV light); ^{1}H NMR (500 MHz, CDCl$_3$): δ$_H$ 7.60 (dd, 1H, J = 8.0, 1.6 Hz, *3*), 7.54 (dd, 1H, J = 8.0, 1.4, *6*), 7.28 (td, 1H, J = 7.7, 1.4 Hz, *4*), 7.06 (td, 1H, J = 7.7, 1.6 Hz, *5*), 5.02 (s, 2H, *7*), 3.45 (s, 3H, *8*); ^{13}C NMR (126 MHz, CDCl$_3$): δ$_C$ 137.6 (*1*), 133.0 (*3*), 129.8 (*6*), 128.1 (*5*), 127.5 (*4*), 123.9 (*2*), 76.6 (*7*), 56.4 (*8*); IR (neat): υ$_{max}$/cm^{-1} 3058 (w), 2981 (w), 2927 (w), 2893 (w), 282.0 (w); HRMS (TOF MS ASAP$^+$) calcd for C$_8$H$_9$^{79}BrOS [M+H]$^+$ 232.9458, found 232.9463.

<u>5.2.2.4 1-(2-(2-((methoxymethyl)thio)phenyl)-1H-pyrrol-1-yl)-2,2-dimethylpropan-1-one (**3.5a**)</u>
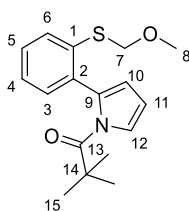
To a Schlenk flask under an inert atmosphere was added (2-bromophenyl)(methoxymethyl)sulfane (500 mg, 2.14 mmol), N-Boc-2-pyrrole boronic acid (677 mg, 3.21 mmol), Pd(PPh$_3$)$_4$ (124 mg, 5 mol %) and potassium phosphate (681 mg, 3.21 mmol) in THF (7.5 mL) and water (3.5 mL).The reaction mixture was then stirred at 75°C for 24 hours. The reaction mixture was then diluted with DCM and washed with water. The organic layers were then combined and dried over MgSO$_4$ and solvent removed under reduced pressure. The crude product was then purified by column chromatography (eluent system: 10:1 petrol 40-60:EtOAc) to give 1-(2-(2-((methoxymethyl)thio)phenyl)-1*H*-pyrrol-1-yl)-2,2-dimethylpropan-1-one (499 mg, 1.64 mmol, 77%).

R$_f$ = 0.60 (10:1 petrol 40-60:EtOAc; UV light); ^{1}H NMR (400 MHz, CDCl$_3$): δ$_H$ 7.60 (ddd, 1H, *J* = 7.8, 1.3, 0.5 Hz, *6*), 7.41 (dd, 1H, *J* = 3.3, 1.8 Hz, *12*), 7.30 (ddd, 1H, *J* = 7.8, 6.8, 2.2 Hz, *5*), 7.25-7.20 (m, 2H, *3,4*), 6.26 (app. t, 1H, *J* = 3.3 Hz, *11*), 6.14 (dd, 1H, *J* = 3.3, 1.8 Hz, *10*), 4.82 (s, 2H, *7*), 3.32 (s, 3H, *8*), 1.27 (s, 9H, *15*); ^{13}C NMR (126 MHz, CDCl$_3$): δ$_C$ 149.3 (*13*), 137.5 (*1*), 136.1 (*5*), 132.5 (*9*), 130.6 (*6*), 129.4 (*3*), 128.6 (*4*), 126.1 (*2*), 121.7 (*12*), 114.6 (*10*), 110.5 (*11*), 83.4 (*7*), 77.1 (*8*), 56.0 (*14*); IR (neat): υ$_{max}$/cm^{-1} 2980 (w), 2932 (w), 2820 (w), 1736 (s).

5.2.2.5 1-(2-(2-((methoxymethyl)thio)phenyl)-1*H*-pyrrol-1-yl)-2,2-dimethylpropan-1-one (**3.6a**)
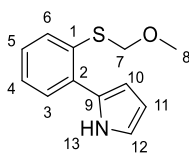
1-(2-(2-((methoxymethyl)thio)phenyl)-1*H*-pyrrol-1-yl)-2,2-dimethylpropan-1-one was placed in a 100 mL round bottomed flask under an inert atmosphere. Subsequently the flask was heated to 200 °C resulting in the evolution of gas (CO_2, isobutene), and rapid colour change of the oil. After 30 minutes the flask was allowed to cool to room temperature. The dark purple oil was used immediately for the next reaction without purification.

^{1}H NMR (400 MHz, CDCl$_3$): δ_H 9.63 (s, 1H, *13*), 7.63 (dd, 1H, *J* = 7.7, 1.4 Hz, *6*), 7.53 (dd, 1H, *J* = 7.7, 1.6 Hz, *3*), 7.29 (m, 1H, *4*), 7.20 (m, 1H, *5*), 6.90 (m, 1H, *12*), 6.51 (ddd, 1H, *J* = 3.5, 2.7, 1.5 Hz, *10*), 6.30 (m, 1H, *11*), 4.85 (s, 2H, *7*), 3.38 (s, 3H, *8*); ^{13}C NMR (126 MHz, CDCl$_3$): δ_C 135.0 (*1*), 134.2 (*5*), 131.1 (*9*), 129.3 (*3*), 128.2 (*4*), 127.2 (*12*), 118.7 (*2*), 109.3 (*11*), 109.2 (*10*), 78.8 (*7*), 57.0 (*8*); IR (neat): υ_{max}/cm^{-1} 3381 (br, w), 2981 (w), 2821 (w); HRMS (TOF MS ASAP$^+$) calcd for C$_{12}$H$_{13}$NOS [M]$^+$ 219.0718, found 219.0713.

5.2.2.6 Methyl (Z)-4-((5-(2-((methoxymethyl)thio)phenyl)-1*H*-pyrrol-2-yl)(5-(2-((methoxymethyl)thio)phenyl)-2*H*-pyrrol-2-ylidene)methyl)benzoate (**3.7a**)
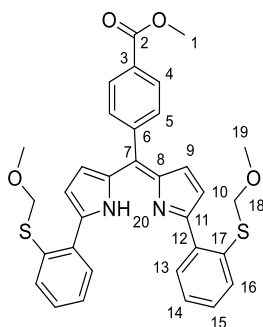
To a Schlenk flask under an inert atmosphere was added 1-(2-(2-((methoxymethyl)thio)phenyl)-1*H*-pyrrol-1-yl)-2,2-dimethylpropan-1-one (161 mg, 0.74 mmol) and 4-methyl-4-formyl benzoate (61 mg, 0.37 mmol). Dry DCM (6 mL) and TFA (*ca*. 0.1 mL) and the reaction mixure stirred for 3 hours 30 minutes. Then, *p*-chloranil (181 mg, 0.74 mmol) was added as a solution in DCM (3 mL), and the reaction stirred for 10 minutes. The reaction mixture was then diluted with DCM and washed with water. The organic layers were then combined and dried over MgSO₄ and solvent removed under reduced pressure to give methyl (Z)-4-((5-(2-((methoxymethyl)thio)phenyl)-1*H*-pyrrol-2-yl)(5-(2-((methoxymethyl)thio)phenyl)-2*H*-pyrrol-2-ylidene)methyl)benzoate without the need for further purification (374 mg, 87%).

Mp: 113-114 °C; R_f = 0.25 (10 :1 petrol 40-60:EtOAc); ^{1}H NMR (300 MHz, CDCl₃): δ_H 9.38 (br s, 1H, *20*), 8.14 (d, 2H, *J* = 8.3 Hz, *4*), 7.74-7.68 (m, 4H, *13*, *16*), 7.65 (d, 2H, *J* = 8.3 Hz, *5*), 7.35-7.24 (m, 4H, *14*, *15*), 6.79 (d, 2H, *J* = 4.3 Hz, *9*), 6.60 (d, 2H, *J* = 4.3 Hz, *10*), 4.80 (s, 4H, *18*), 3.99 (s, 3H, *1*), 3.23 (s, 6H, *19*); ^{13}C NMR (126 MHz, CDCl₃): δ_C 166.8 (*2*), 154.1 (*6*), 143.3 (*8*), 142.1 (*17*), 136.3 (*15*), 132.9 (*7*), 131.0 (*4*), 130.5 (*11*), 128.9 (*5*), 128.5 (*3*), 126.0 (*16*), 121.6 (*13*), 119.1 (*14*), 118.9 (*12*), 114.5 (*9*), 110.4 (*10*), 55.9 (*18*), 52.3 (*1*), 27.5 (*19*); IR (neat): υ_{max}/cm^{-1} 2993 (w), 2948 (w), 2820 (w), 1720 (m); HRMS (TOF MS ASAP$^+$) calcd for C₃₃H₃₀N₂O₄S₂ [M+H]$^+$ 583.1725, found 583.1734.

5.2.2.7 (2-((2-bromophenyl)thio)ethyl)trimethylsilane (**3.4b**)
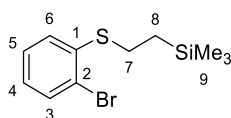
To a Schlenk flask under an inert atmosphere was added azobisisobutyronitrile (41 mg, 0.25 mmol), vinyltrimethylsilane (1.1 mL, 6 mmol) and 2-bromothiophenol (0.6 mL, 5 mmol). The reaction mixture was then stirred at 100 °C for 2 hours 30 minutes. The reaction mixture was diluted with petrol 40-60 and passed through a short silica pad to give (2-((2-bromophenyl)thio)ethyl)trimethylsilane in a quantitative yield.

R_f = 0.56 (petrol 40-60; UV light); ^{1}H NMR (300 MHz, CDCl$_3$): δ_H 7.54 (dd, 1H, *J* = 7.9, 1.3 Hz, *3*), 7.30-7.18 (m, 2H, *5,6*), 7.01 (ddd, 1H, *J* = 7.9, 7.1, 1.8 Hz, *4*), 3.00-2.92 (m, 2H, *7*), 1.03-0.93 (m, 2H, *8*), 0.07 (s, 9H, *9*); ^{13}C NMR (96 MHz, CDCl$_3$): δ_C 139.0 (*1*), 133.0 (*3*), 127.8 (*5*), 127.7 (*4*), 126.3 (*6*), 123.2 (*2*), 28.9 (*7*), 16.2 (*8*), -1.6 (*9*); IR (neat): υ_{max}/cm^{-1} 3059 (w), 2951 (w); HRMS (TOF MS ASAP$^+$) calcd for C$_{11}$H$_{17}$^{81}BrSSi [M+H]$^+$ 291.0061, found 291.0036.

<u>5.2.2.8 2,2-dimethyl-1-(2-(2-((2-(trimethylsilyl)ethyl)thio)phenyl)-1*H*-pyrrol-1-yl)propan-1-one (**3.5b**)</u>
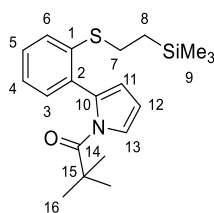
To a Schlenk flask under an inert atmosphere was added (2-((2-bromophenyl)thio)ethyl)trimethylsilane (289 mg, 1 mmol), N-Boc-2-pyrrole boronic acid (317 mg, 1.5 mmol), Pd(PPh$_3$)$_4$ (58 mg, 0.05 mmol) and K$_3$PO$_4$ (318 mg, 1.5 mmol). Solvent was added (THF : H$_2$O, 3.5 mL:1.5 mL) before heating to 75 °C and stirred for 24 hours. The reaction mixture was then diluted with DCM and washed with water. The organic layers were then combined and dried over MgSO$_4$ and solvent removed under reduced pressure. The crude product was then purified by column chromatography (eluent system: 15:1 petrol 40-60:EtOAc) to give 2,2-dimethyl-1-(2-(2-((2-(trimethylsilyl)ethyl)thio)phenyl)-1*H*-pyrrol-1-yl)propan-1-one (336 mg, 93%).

R$_f$ = 0.60 (10:1 petrol 40-60:EtOAc; UV light); ^{1}H NMR (300 MHz, CDCl$_3$): δ$_H$ 7.37 (dd, 1H, *J* = 3.3, 1.8 Hz, *13*), 7.28-7.10 (m, 4H, *3, 4, 5, 6*), 6.22 (app. t, 1H, *11*), 6.09 (dd, 1H, *J* = 3.3, 1.8 Hz, *12*), 2.76-2.68 (m, 2H, *7*), 1.23 (s, 9H, *16*), 0.82-0.74 (m, 2H, *8*), -0.05 (s, 9H, *9*); ^{13}C NMR (96 MHz, CDCl$_3$): δ$_C$ 149.3 (*14*), 138.7 (*1*), 135.5 (*5*), 132.4 (*10*), 130.6 (*6*), 128.2 (*3*), 127.8 (*4*), 125.1 (*2*), 121.7 (*13*), 114.4 (*11*), 110.5 (*12*), 83.1 (*15*), 28.7 (*7*), 27.6 (*16*), 16.8 (*8*), -1.7 (*9*); IR (neat): υ$_{max}$/cm^{-1} 2952 (w), 1737 (s); HRMS (TOF MS ASAP$^+$) calcd for C$_{20}$H$_{29}$NO$_2$SSi [M+H]$^+$ 376.1767, found 376.1753.

5.2.2.9 2-(2-((2-(trimethylsilyl)ethyl)thio)phenyl)-1*H*-pyrrole (**3.6b**)
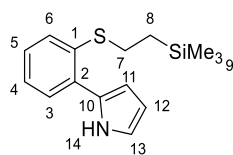
2,2-dimethyl-1-(2-(2-((2-(trimethylsilyl)ethyl)thio)phenyl)-1*H*-pyrrol-1-yl)propan-1-one was placed in a 100 mL round bottomed flask under an inert atmosphere. Subsequently the flask was heated to 200 °C resulting in the evolution of gas (CO_2, isobutene), and rapid colour change of the oil. After 30 minutes the flask was allowed to cool to room temperature. The dark purple oil was used immediately for the next reaction without purification.

^{1}H NMR (300 MHz, $CDCl_3$): δ_H 9.92 (s, 1H, *14*), 7.55 (dd, 1H, *J* = 7.8, 1.6 Hz, *3*), 7.42 (dd, 1H, *J* = 7.8, 1.5 Hz, *6*), 7.27-7.21 (m, 1H, *5*), 7.15 (app. td, 1H, *4*), 6.90 (app. td, 1H, *13*), 6.53 (ddd, 1H, *J* = 3.8, 2.6, 1.5 Hz, *11*), 6.29 (app. dt, 1H, *12*), 2.81-2.71 (m, 2H, *7*), 0.88-0.79 (m, 2H, *8*), -0.03 (s, 9H, *9*); ^{13}C NMR (75 MHz, $CDCl_3$): δ_C 134.0 (*1*), 133.2 (*5*), 131.6 (*10*), 131.1 (*6*), 128.9 (*3*), 127.4 (*4*), 126.6 (*13*), 118.5 (*2*), 109.2 (*12*), 108.8 (*11*), 30.8 (*7*), 17.0 (*8*), -1.7 (*9*); IR (neat): υ_{max}/cm^{-1} 3391 (br, w), 3057 (w), 2951 (w); HRMS (TOF MS ASAP[+]) calcd for $C_{15}H_{21}NSSi$ [M+H]$^+$ 276.1242, found 276.1240.

5.2.2.10 Methyl (Z)-4-((5-(2-((2-(trimethylsilyl)ethyl)thio)phenyl)-1*H*-pyrrol-2-yl)(5-(2-((2-(trimethylsilyl)ethyl)thio)phenyl)-2*H*-pyrrol-2-ylidene)methyl)benzoate (**3.7b**)
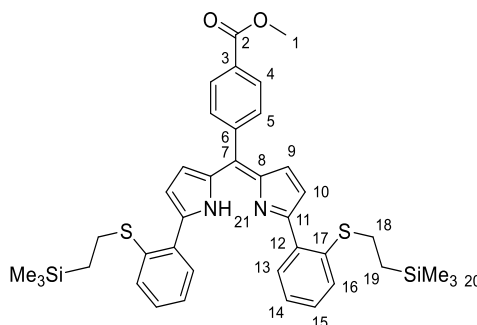
To a Schlenk flask under an inert atmosphere was added 2-(2-((2-(trimethylsilyl)ethyl)thio)phenyl)-1*H*-pyrrole (120 mg, 0.44 mmol) and 4-methyl-4-formyl benzoate (36 mg, 0.22 mmol). Dry DCM (3.5 mL) and TFA (10 μL) and the reaction mixure stirred for 30 minutes. Then, *p*-chloranil (108 mg, 0.44 mmol) was added and the reaction stirred for 10 minutes. The reaction mixture was then diluted with DCM and washed with water. The organic layers were then combined and dried over MgSO$_4$ and solvent removed under reduced pressure. The crude product was then purified by column chromatography (eluent system: 10:1 petrol 40-60:EtOAc) to give methyl (Z)-4-((5-(2-((2-(trimethylsilyl)ethyl)thio)phenyl)-1*H*-pyrrol-2-yl)(5-(2-((2-(trimethylsilyl)ethyl)thio)phenyl)-2*H*-pyrrol-2-ylidene)methyl)benzoate (96 mg, 64%).

Mp: 99-101 °C; R$_f$ = 0.50 (10:1 petrol 40-60:EtOAc); ^{1}H NMR (300 MHz, CDCl$_3$): δ$_H$ 13.31 (s, 1H, *21*), 8.14 (d, 2H, *J* = 8.4 Hz, *4*), 7.78 (d, 2H, *J* = 7.21 Hz, *13*), 7.65 (d, 2H, *J* = 8.41 Hz, *5*), 7.34-7.27 (m, 4H, *15*, *16*), 7.23-7.16 (m, 2H, *14*), 6.84 (d, 2H, *J* = 4.3 Hz, *9*), 6.57 (d, 2H, *J* = 4.3 Hz, *10*), 3.98 (s, 3H, *1*), 2.84-2.75 (m, 2H, *18*), 0.71-0.62 (m, 2H, *19*), -0.01 (s, 18H, *20*); ^{13}C NMR (75 MHz, CDCl$_3$): δ$_C$ 166.9 (*2*), 154.1 (*11*), 142.4 (*3*), 141.0 (*17*), 140.8 (*8*), 138.4 (*6*), 137.8 (*12*), 132.1 (*7*), 131.0 (*5*), 130.3 (*13*), 129.0 (*4*), 128.9 (*15*), 128.4 (*10*), 127.2 (*16*), 124.8 (*14*), 119.2 (*9*), 54.1 (*1*). 30.6 (*18*), 17.5 (*19*), 0.0 (*20*); IR (neat): υ$_{max}$/cm^{-1} 2951 (w), 1723 (m); HRMS (TOF ASAP+) calcd for C$_{39}$H$_{46}$N$_2$O$_2$S$_2$Si$_2$ [M+H]$^+$ 695.2617, found 695.2628.

<u>5.2.2.11 Methyl 4-(5,5-difluoro-3,7-bis(3-methoxythiophen-2-yl)-5*H*-4λ^4,5λ^4-dipyrrolo[1,2-*c*:2',1'-*f*][1,3,2]diazaborinin-10-yl)benzoate (**3.12**)</u>
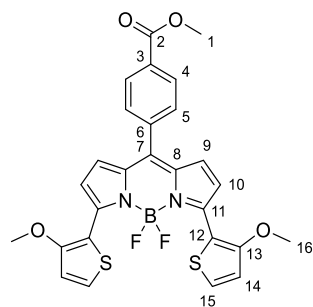
To a Schlenk flask under an inert atmosphere was added methyl 4-(3,7-dibromo-5,5-difluoro-5*H*-4λ^4,5λ^4-dipyrrolo[1,2-*c*:2',1'-*f*][1,3,2]diazaborinin-10-yl)benzoate (200 mg, 0.41 mmol), 3-methoxythiophene-2-boronic acid (394 mg, 1.64 mmol), Pd(PPh$_3$)$_4$ (24 mg, 5 mol %) and sodium carbonate (469 mg, 1.64 mmol) in toluene (2 mL) and 1,4-dioxane (2 mL).The reaction mixture was then refluxed at 90 °C for 23 hours. The reaction mixture was then diluted with DCM and washed with water. The organic layers were then combined and dried over MgSO$_4$ and solvent removed under reduced pressure. The crude product was then purified by column chromatography (eluent system: 4:1:1 petrol 40-60:EtOAc:toluene) to give methyl 4-(5,5-difluoro-3,7-bis(3-methoxythiophen-2-yl)-5*H*-4λ^4,5λ^4-dipyrrolo[1,2-*c*:2',1'-*f*][1,3,2]diazaborinin-10-yl)benzoate (190 mg, 0.35 mmol, 84%).

Mp: 118-119 °C; R$_f$ = 0.21 (3:1:1 petrol 40-60:EtOAc:toluene); ^{1}H NMR (300 MHz, CDCl$_3$): δ$_H$ 8.16 (d, 2H, *J* = 8.3 Hz, *4*), 7.60 (d, 2H, *J* = 8.3 Hz, *5*), 7.48 (d, 2H, *J* = 5.6 Hz, *15*), 7.20 (d, 2H, *J* = 4.5 Hz, *9*), 6.89 (d, 2H, *J* = 5.6 Hz, *14*), 6.69 (d, 2H, *J* = 4.5 Hz, *10*), 3.98 (s, 3H, *1*), 3.94 (s, 6H, *16*); ^{13}C NMR (75 MHz, CDCl$_3$): δ$_C$ 166.6 (*2*), 159.9 (*13*), 149.4 (*11*), 139.6 (*6*), 137.0 (*7*), 135.4 (*3*), 131.1 (*8*), 130.7 (*4*), 129.7 (*15*), 129.4 (*9*), 128.4 (*5*), 122.0 (*14*), 115.1 (*10*), 111.5 (*12*), 59.0 (*1*), 52.5(*16*); ^{11}B NMR (96 MHz, CDCl$_3$): δ$_B$ 1.51 (t, *J*$_{B-F}$ = 33.6 Hz); ^{19}F NMR (282 MHz, CDCl$_3$): δ$_F$ -132.4 (q, *J*$_{B-F}$ = 33.6 Hz); IR (neat): υ$_{max}$/cm^{-1} 1718 (m), 2991 (w), 3107 (w); HRMS (pNSI) calcd for C$_{27}$H$_{21}$^{11}BF$_2$N$_2$O$_4$S$_2$ [M+H]$^+$ 551.1082, found 551.1068.

5.2.2.12 Methyl 4-(3,7-bis(benzo[*b*]thiophen-2-yl)-5,5-difluoro-5*H*-4λ^4,5λ^4-dipyrrolo[1,2-*c*:2',1'-*f*][1,3,2]diazaborinin-10-yl)benzoate (**3.15**)
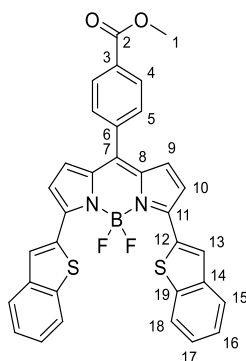
To a Schlenk flask under an inert atmosphere was added methyl 4-(3,7-dibromo-5,5-difluoro-5*H*-4λ^4,5λ^4-dipyrrolo[1,2-*c*:2',1'-*f*][1,3,2]diazaborinin-10-yl)benzoate (50 mg, 0.1 mmol), benzo[b]thien-2-ylboronic acid (71 mg, 0.4 mmol), Pd(PPh$_3$)$_4$ (6 mg, 5 mol %) and sodium carbonate (114 mg, 0.4 mmol) in toluene (0.5 mL) and 1,4-dioxane (0.5 mL).The reaction mixture was then refluxed at 90 °C for 2 hours. The reaction mixture was then diluted with DCM and washed with water. The organic layers were then combined and dried over MgSO$_4$ and solvent removed under reduced pressure. The crude product was then purified by column chromatography (eluent system: 3:1 petrol 40-60:EtOAc) to give methyl 4-(3,7-bis(benzo[*b*]thiophen-2-yl)-5,5-difluoro-5*H*-4λ^4,5λ^4-dipyrrolo[1,2-*c*:2',1'-*f*][1,3,2]diazaborinin-10-yl)benzoate (27 mg, 0.046 mmol, 46%).

Mp: 296-297 °C; R$_f$ = 0.35 (3:1 petrol 40-60:EtOAc); ^{1}H NMR (300 MHz, CDCl$_3$): δ$_H$ 8.50 (s, 2H, *13*), 8.21 (d, 2H, *J* = 8.3 Hz, *4*), 7.98-7.93 (m, 2H, *18*), 7.87-7.81 (m, 2H, *15*), 7.64 (d, 2H, *J* = 8.3 Hz, *5*), 7.45-7.36 (m, 4H, *16, 17*), 6.94 (d, 2H, *J* = 4.4 Hz, *9*), 6.81 (d, 2H, *J* = 4.4 Hz, *10*), 4.00 (s, 3H, *1*); ^{13}C NMR (75 MHz, CDCl$_3$): δ$_C$ 166.5 (*2*), 151.2 (*11*), 141.2 (*14*), 140.9 (*19*), 140.4 (*6*), 138.7 (*12*), 137.3 (*7*), 133.4 (*3*), 131.8 (*8*), 130.7 (*17*), 130.3 (*5*), 129.7 (*16*), 128.6 (*18*), 126.2 (*15*), 125.6 (*4*), 125.0 (*9*), 122.3 (*10*), 122.1 (*13*), 52.7(*1*); ^{11}B NMR (96 MHz, CDCl$_3$): δ$_B$ 1.80 (t, J_{B-F} = 32.8 Hz); ^{19}F NMR (282 MHz, CDCl$_3$): δ$_F$ -138.9 (q, J_{B-F} = 32.8 Hz); IR (neat): υ$_{max}$/cm^{-1} 1523 (s), 1722 (m), 2997 (w); HRMS (TOF MS ASAP+) calcd for C$_{33}$H$_{21}$^{11}BF$_2$N$_2$O$_2$S$_2$ [M+H] 591.1190, found 591.1191; ε = 100 000 M^{-1} cm^{-1} (DCM); φ$_F$ = 0.60 (DCM).

<u>5.2.2.13 Methyl 4-(10-(benzo[*b*]thiophen-2-yl)-10b-fluoro-10b*H*-11-oxa-4b^1,10aλ^4-diaza-10bλ^4-boracyclopenta[*e*]aceanthrylen-7-yl)benzoate (**3.16**)</u>
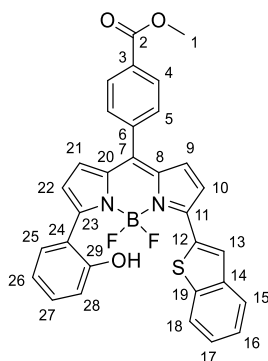
To a Schlenk flask under an inert atmosphere was added a mixture of methyl 4-(3,7-bis(benzo[*b*]thiophen-2-yl)-5,5-difluoro-5*H*-4λ^4,5λ^4-dipyrrolo[1,2-*c*:2',1'-*f*][1,3,2]diazaborinin-10-yl)benzoate and methyl 4-(3-(benzo[*b*]thiophen-2-yl)-7-bromo-5,5-difluoro-5*H*-4λ^4,5λ^4-dipyrrolo[1,2-*c*:2',1'-*f*][1,3,2]diazaborinin-10-yl)benzoate (31 mg), 2-hydroxybenzene boronic acid (17 mg, 0.12 mmol), Pd(PPh$_3$)$_4$ (4 mg, 5 mol %) and sodium carbonate (34 mg, 0.12 mmol) in toluene (0.5 mL) and 1,4-dioxane (0.5 mL).The reaction mixture was then refluxed at 90 °C for 24 hours. The reaction mixture was then diluted with DCM and washed with water. The organic layers were then combined and dried over MgSO$_4$ and solvent removed under reduced pressure. The crude product was then purified by column chromatography (eluent system: 6:5:0.5 petrol 40-60:toluene:EtOAc) to give methyl 4-(10-(benzo[*b*]thiophen-2-yl)-10b-fluoro-10b*H*-11-oxa-4b^1,10aλ^4-diaza-10bλ^4-boracyclopenta[*e*]aceanthrylen-7-yl)benzoate (12.1 mg, 0.022 mmol, 17% over two steps).

Mp: 267-269 °C; R$_f$ = 0.26 (6:5:0.5 petrol 40-60:toluene:EtOAc); ^{1}H NMR (300 MHz, CDCl$_3$): δ_H 8.41 (s, 1H, *13*), 8.18 (d, 2H, *J* = 8.3 Hz, *4*), 7.90-7.84 (m, 1H, *16*), 7.82-7.78 (m, 1H, *17*), 7.60 (d, 2H, *J* = 8.3 Hz, *5*), 7.49-7.41 (m, 2H, *25, 28*), 7.38-7.28 (m, 4H, *15, 18, 26, 27*), 6.84 (d, 1H, *J* = 4.3 Hz, *9*), 6.77 (d, 1H, *J* = 4.7 Hz, *21*), 6.69 (d, 1H, *J* = 4.3 Hz, *10*), 5.80 (d, 1H, *J* = 4.7 Hz, *22*), 3.98 (s, 3H, *1*); ^{13}C NMR (126 MHz, CDCl$_3$): δ_C 167.1 (*2*), 166.5 (*23*), 154.3 (*29*), 147.6 (*6*), 141.1 (*12*), 140.5 (*14*), 139.5 (*15*), 138.3 (*20*), 135.8 (*21*), 133.9 (*22*), 132.6 (*27*), 131.7 (*7*), 131.0 (*11*), 130.6 (*25*), 130.3 (*4*), 129.9 (*5*), 129.7 (*3*), 129.0 (*16*), 127.9 (*17*), 126.8 (*19*), 125.6 (*18*), 125.2 (*26*), 124.7 (*13*), 122.1 (*28*), 121.9 (*8*), 120.9 (*10*), 120.0 (*24*), 106.7 (*9*), 52.6 (*1*); ^{11}B NMR (96 MHz, CDCl$_3$): δ_B 1.19 (t, *J*$_{B-F}$ = 29.8 Hz); ^{19}F NMR (282 MHz, CDCl$_3$): δ_F -144.0 (q, *J*$_{B-F}$ = 29.8 Hz); IR (neat): υ_{max}/cm^{-1} 1523 (s), 1722 (m), 2997 (w); HRMS (TOF MS ASAP$^+$) calcd for C$_{31}$H$_{21}$^{11}BF$_2$N$_2$O$_3$S [M+H]$^+$ 551.1407, found 551.1401; ε = 52 000 M^{-1} cm^{-1} (DCM); ϕ_F = 0.85 (DCM).

5.2.2.14 Methyl (*Z*)-4-((1*H*-pyrrol-2-yl)(2*H*-pyrrol-2-ylidene)methyl)benzoate (**3.17**)
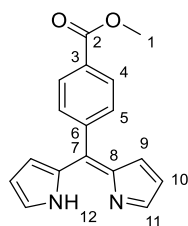
To a round bottomed flask, under an atmosphere of nitrogen, was added methyl 4-(di(1*H*-pyrrol-2-yl)methyl)benzoate (1 g, 3.57 mmol) and *p*-chloranil (966 mg, 3.93 mmol) followed by DCM (40 mL). The resulting reaction mixture was stirred at room temperature for 18 hours. Subsequently, the reaction mixture was diluted with DCM and washed with brine and water. The organic layer was dried over Na_2SO_4, filtered, and the solvent removed under reduced pressure to give a dark solid. The crude product was used in subsequent reactions without further purification.

Mp: = 128.4-129.8 °C [lit. 130-131 °C]; R$_f$ = 0.42 (DCM; UV light); ^{1}H NMR (300 MHz, CDCl$_3$): δ$_H$ 8.13 (d, 2H, *J* = 8.4 Hz, *4*), 7.68 (s, 2H, *11*), 7.57 (d, 2H, *J* = 8.4 Hz, *5*), 6.53 (d, 2H, *J* = 4.2 Hz, *9*), 6.41 (d, 2H, *J* = 4.2 Hz, *10*), 3.97 (s, 3H, *1*); ^{13}C NMR (75 MHz, CDCl$_3$): δ$_C$ 166.7 (*2*), 144.1 (*6*), 141.8 (*8*), 141.0 (*9*), 139.8 (*7*), 130.8 (*4*), 130.7 (*5*), 129.1 (*3*), 128.9 (*10*), 118.0 (*11*), 52.4 (*1*); IR(neat): υ$_{max}$/cm^{-1} 3143.9-2785.7 (CH, w), 1718.3 (CO, s).

5.2.2.15 Methyl 4-(5,5-difluoro-5H-4λ^4,5λ^4-dipyrrolo[1,2-*c*:2',1'-*f*][1,3,2]diazaborinin-10-yl)benzoate (**3.18**)
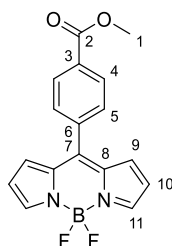
To a round bottom flask under an atmosphere of nitrogen was added methyl (*Z*)-4-((1*H*-pyrrol-2-yl)(2*H*-pyrrol-2-ylidene)methyl)benzoate (0.5304 g, 1.91 mmol) and DCM (10 mL), followed by *N,N*-diisopropylethylamine (0.92 mL, 5.27 mmol) and BF$_3$.OEt$_2$ (0.52 mL, 4.23 mmol). The resulting reaction mixture was stirred at room temperature for 1 hour, over which time the solution turned dark red. The reaction mixture was diluted with DCM (50 mL), washed with 0.1 M NaOH (100 mL), 0.1 M HCl (100 mL) and water (100 mL). The organic layer was dried over Na$_2$SO$_4$, filtered and the solvent removed under reduced pressure. The crude product was purified by silica gel column chromatography (DCM) to give methyl 4-(5,5-difluoro-5H-4λ^4,5λ^4-dipyrrolo[1,2-*c*:2',1'-*f*][1,3,2]diazaborinin-10-yl)benzoate (0.2543 g, 0.78 mmol, 41% over two steps) as an orange solid.

R$_f$ 0.58 (DCM); Mp = 204.5-204.8 °C; ^{1}H NMR (400 MHz, CDCl$_3$): δ$_H$ 8.20 (d, 1H, *J* = 8.6 Hz, *4*), 7.97 (s, 2H, *11*), 7.65 (d, 1H, *J* = 8.6 Hz, *5*), 6.89 (d, 2H, *J* = 4.3 Hz, *9*), 6.57 (d, 1H, *J* = 4.1 Hz, *10*), 3.99 (s, 3H, *1*); ^{13}C NMR (75 MHz, CDCl$_3$): δ$_C$ 166.2 (*2*), 145.7 (*6*), 144.8 (*8*), 137.9 (*9*), 134.7 (*7*), 132.2 (*4*), 131.4 (*5*), 130.4 (*3*), 129.6 (*10*), 119.0 (*11*), 52.5 (*1*); ^{11}B NMR (96 MHz, CDCl$_3$): δ$_B$ 0.25 (t, *J*$_{B-F}$ = 28.5 Hz); ^{19}F NMR (282MHz, CDCl$_3$): δ$_F$ -145.01 (q, *J*$_{B-F}$ = 28.5 Hz); IR(neat): υ$_{max}$/cm^{-1} 3142.9-2828.6 (CH, w), 1713.0 (CO, s). ε = 54 000 M^{-1} cm^{-1} (DCM).

5.2.2.16 Methyl 4-(3,7-dichloro-5,5-difluoro-5*H*-4λ^4,5λ^4-dipyrrolo[1,2-*c*:2',1'-*f*][1,3,2]diazaborinin-10-yl)benzoate (**3.19**)

Following a modified procedure from Jiao *et al.*, to a round bottomed flask was added methyl 4-(5,5-difluoro-5H-4λ^4,5λ^4-dipyrrolo[1,2-*c*:2',1'-*f*][1,3,2]diazaborinin-10-yl)benzoate (86.5 mg, 0.27 mmol) and MeCN (2.2 mL). The resulting orange solution was heated to reflux and CuCl$_2$.2H$_2$O (0.45 g, 2.65 mmol) was added. After 1 hour the reaction mixture was cooled to room temperature, diluted (DCM, 50 mL) and washed with H$_2$O (3x 30 mL). The organic layer was dried over Na$_2$SO$_4$, filtered, and the solvent removed under reduced pressure to a give a red solid. The crude product was purified by silica gel column chromatography (4:1 petrol 40-60:EtOAc) to give methyl 4-(3,7-dichloro-5,5-difluoro-5*H*-4λ^4,5λ^4-dipyrrolo[1,2-*c*:2',1'-*f*][1,3,2]diazaborinin-10-yl)benzoate (62.2 mg, 0.16 mmol, 59%) as a red/pink solid.

Mp = 207-208 °C; R$_f$ 0.65 (DCM); ^{1}H NMR (300 MHz, CDCl$_3$): δ_H 8.19 (d, 2H, *J* = 8.5 Hz, *4*), 7.57 (d, 2H, *J* = 8.5 Hz, *5*), 6.79 (d, 2H, *J* = 4.3 Hz, *9*), 6.45 (d, 2H, *J* = 4.4 Hz, *10*), 3.99 (s, 3H, *1*); ^{13}C NMR (176 MHz, CDCl$_3$): δ_C 166.2 (*2*), 145.9 (*6*), 142.4 (*7*), 136.7 (*4*), 133.7 (*5*), 132.5 (*3*), 131.6 (*8*), 130.5 (*9*), 129.8 (*11*), 119.5 (*10*), 52.7 (*1*); ^{11}B NMR (96 MHz, CDCl$_3$): δ_B 0.44 (t, *J*$_{B-F}$ = 27.9 Hz); ^{19}F NMR (282MHz, CDCl$_3$): δ_F -148.14 (q, *J*$_{B-F}$ = 27.9 Hz); IR(neat): υ_{max}/cm^{-1} 3133-2800 (w), 1722 (m); HRMS (pNSI) calcd for C$_{17}$H$_{12}$^{10}B^{35}Cl$_2$F$_2$N$_2$O$_2$ [M+H]$^+$: 394.0368, found 394.0361; ε = 39 000 M^{-1} cm^{-1} (DCM); φ$_F$ = 0.18 (DCM).

5.2.2.17 Methyl 4-(5,5-difluoro-3,7-bis(phenylthio)-5*H*-4λ^4,5λ^4-dipyrrolo[1,2-*c*:2',1'-*f*][1,3,2]diazaborinin-10-yl)benzoate (**3.21**)
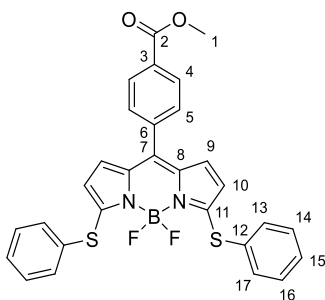
To a round bottomed flask under an inert atmosphere was added methyl 4-(3,7-dichloro-5,5-difluoro-5*H*-4λ^4,5λ^4-dipyrrolo[1,2-*c*:2',1'-*f*][1,3,2]diazaborinin-10 yl)benzoate (21 mg, 0.05 mmol), trimethylamine (14 μL 0.1 mmol) and MeCN (1 mL). Subsequently, thiophenol (10 μL, 0.1 mmol) was added slowly. The reaction mixture was then stirred at room temperature for 30 minutes. The reaction mixture was then diluted with ethyl acetate and washed with HCl (1 M, 50 mL). The organic layers were then combined and dried over MgSO$_4$ and solvent removed under reduced pressure. The crude product was then purified by column chromatography (eluent system: 4:1 petrol 40-60:EtOAc) to give methyl 4-(5,5-difluoro-3,7-bis(phenylthio)-5*H*-4λ^4,5λ^4-dipyrrolo[1,2-*c*:2',1'-*f*][1,3,2]diazaborinin-10-yl)benzoate (25 mg, 0.046 mmol, 92%).

Mp: 99-101 °C; R$_f$ = 0.23 (4:1 petrol 40-60:EtOAc); ^{1}H NMR (300 MHz, CDCl$_3$): δ$_H$ 8.11 (d, 2H, *J* = 8.3 Hz, *4*), 7.70 – 7.64 (m, 4H, *14, 16*), 7.52 (d, 2H, *J* = 8.3 Hz, *5*), 7.46 – 7.40 (m, 6H, *13, 15, 17*), 6.54 (d, 2H, *J* = 4.4 Hz, *9*), 5.88 (d, 2H, *J* = 4.4 Hz, *10*), 3.94 (s, 3H,*1*); ^{13}C NMR (176 MHz, CDCl$_3$): δ$_C$ 166.5 (*2*), 157.8 (*6*), 138.3 (*11*), 136.9 (*7*), 135.9 (*12*), 135.0 (*4*), 131.5 (*3*), 130.4 (*13*), 130.2 (*8*), 129.8 (*15*), 129.8 (*14*), 129.6 (*5*), 128.8 (*9*), 118.9 (*10*), 52.5 (*1*); ^{11}B NMR (96 MHz, CDCl$_3$): δ$_B$ 1.02 (t, *J*$_{B-F}$ = 32.3 Hz); ^{19}F NMR (282 MHz, CDCl$_3$): δ$_F$ -147.0 (q, *J*$_{B-F}$ = 32.3 Hz); IR (neat): υ$_{max}$/cm^{-1} 1542 (s), 1558 (m), 1712 (m), 2909 (w), 3033 (w); HRMS (TOF MS ASAP+) calcd for C$_{29}$H$_{21}$^{11}BF$_2$N$_2$O$_2$S$_2$ [M+H]$^+$ 543.1189, found 543.1190; ε = 79 000 M^{-1} cm^{-1} (DCM); ϕ$_F$ = 0.46 (DCM).

5.2.2.18 Methyl 4-(3-bromo-5,5-difluoro-7-((4-(trifluoromethyl)phenyl)thio)-5*H*-5λ^4,6λ^4-dipyrrolo[1,2-*c*:2',1'-*f*][1,3,2]diazaborinin-10-yl)benzoate (**3.24**)
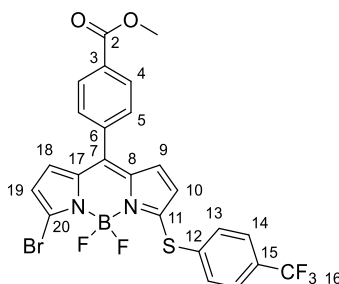
To a round bottomed flask under an inert atmosphere was added methyl 4-(3,7-dichloro-5,5-difluoro-5*H*-4λ^4,5λ^4-dipyrrolo[1,2-*c*:2',1'-*f*][1,3,2]diazaborinin-10 yl)benzoate (133 mg, 0.27 mmol), trimethylamine (20 µL 0.14 mmol) and THF (12 mL). The solution was then cooled to − 78 °C and 4-(trifluoromethyl)thiophenol (37 µL, 0.27 mmol) added slowly. The reaction mixture was then stirred at − 78 °C for 1.5 hours. The reaction mixture was then allowed to warm to room temperature for 20 minutes before it was diluted with ethyl acetate and washed with water. The organic layers were then combined and dried over MgSO$_4$ and solvent removed under reduced pressure. The crude product was then purified by column chromatography (eluent system: 10:5:0.5 toluene:petrol 40-60:diethyl ether) to give methyl 4-(3-bromo-5,5-difluoro-7-((4-(trifluoromethyl)phenyl)thio)-5*H*-5λ^4,6λ^4-dipyrrolo[1,2-*c*:2',1'-*f*][1,3,2]diazaborinin-10-yl)benzoate (67 mg, 0.12 mmol, 43%).

Mp: 167-169 °C; R$_f$ = 0.28 (10:5:0.5 toluene:petrol 40-60:diethyl ether); ^{1}H NMR (300 MHz, CDCl$_3$): δ$_H$ 8.16 (d, 2H, *J* = 8.3 Hz, *4*), 7.79 (d, 2H, *J* = 8.5 Hz, *14*), 7.70 (d, 2H, *J* = 8.5 Hz, *13*), 7.55 (d, 2H, *J* = 8.3 Hz, *5*), 6.71 (d, 1H, *J* = 4.6 Hz, *9*), 6.62 (d, 1H, *J* = 4.2 Hz, *18*), 6.49 (d, 1H, *J* = 4.2 Hz, *19*), 5.98 (d, 1H, *J* = 4.6 Hz, *10*), 3.97 (s, 3H, *1*); ^{13}C NMR (75 MHz, CDCl$_3$): δ$_C$ 166.2 (*2*), 160.3 (*15*), 139.3 (*6*), 137.2 (*16*), 136.5 (*4*), 134.8 (*8*), 134.7 (*7*), 134.2 (*3*), 133.8 (*12*), 132.0 (*13*), 131.5 (*5*), 130.3 (*17*), 129.6 (*18*), 129.0 (*18*), 129.0 (*19*), 128.9 (*9*), 126.7 (q, *J*$_{C-F}$ = 3.7 Hz, *20*), 121.5 (*10*), 120.4 (*11*), 52.5 (*1*); ^{11}B NMR (96 MHz, CDCl$_3$): δ$_B$ 0.77 (t, *J*$_{B-F}$ = 30.6 Hz); ^{19}F NMR (282 MHz, CDCl$_3$): δ$_F$ -62.9 (s), -146.7 (q, *J*$_{B-F}$ = 30.6 Hz); IR (neat): υ$_{max}$/cm^{-1} 3426 (w), 2954 (w), 1723 (m); HRMS (pNSI) calcd for C$_{24}$H$_{15}$^{10}B^{81}BrF$_5$N$_2$O$_2$^{32}S [M+H] 581.0134, found 581.0137.

5.2.2.19 Methyl 4-(5,5-difluoro-3-(2-hydroxyphenyl)-7-((4-(trifluoromethyl)phenyl)thio)-5*H*-5λ^4,6λ^4-dipyrrolo[1,2-*c*:2',1'-*f*][1,3,2]diazaborinin-10-yl)benzoate (**3.26**)
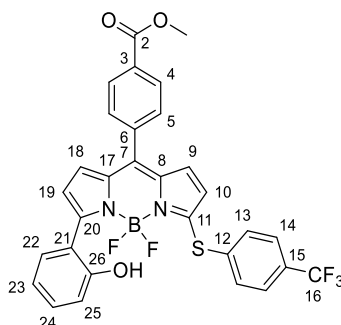

To a Schlenk flask under an inert atmosphere was added methyl 4-(3-bromo-5,5-difluoro-7-((4-(trifluoromethyl)phenyl)thio)-5*H*-5λ^4,6λ^4-dipyrrolo[1,2-*c*:2',1'-*f*][1,3,2]diazaborinin-10-yl)benzoate (97 mg, 0.17 mmol), 2-hydroxybenzene boronic acid (94 mg, 0.68 mmol), Pd(PPh$_3$)$_4$ (10 mg, 0.0083 mmol), Na$_2$CO$_3$ (195 mg, 0.68 mmol), toluene (1 mL) and 1,4-dioxane (1 mL).The reaction mixture was then refluxed at 90 °C for 20 min. The reaction mixture was then diluted with DCM (50 mL) and washed with water (50 mL). The organic layers were then combined and dried over MgSO$_4$ and solvent removed under reduced pressure. The crude product was then purified by column chromatography (eluent system: 10:5:0.5 toluene:petrol 40-60:diethyl ether) to give methyl 4-(5,5-difluoro-3-(2-hydroxyphenyl)-7-((4-(trifluoromethyl)phenyl)thio)-5*H*-5λ^4,6λ^4-dipyrrolo[1,2-*c*:2',1'-*f*][1,3,2]diazaborinin-10-yl)benzoate (20 mg, 0.034 mmol, 20%). This material was used immediately in the next step.

R$_f$ = 0.39 (5:1 petrol 40-60:EtOAc); ^{1}H NMR (300 MHz, CDCl$_3$): δ$_H$ 8.19 (d, 2H, *J* = 8.5 Hz, *4*), 7.73 (d, 2H, *J* = 8.4 Hz, *14*), 7.67 (d, 2H, *J* = 8.4 Hz, *13*), 7.63 (d, 2H, *J* = 8.5 Hz, *5*), 7.57 (dd, 1H, *J* = 7.6, 1.7 Hz, *22*), 7.40-7.33 (m, 1H, *24*), 7.09-7.02 (m, 2H, *25, 23*), 6.83 (d, 1H, *J* = 4.2 Hz, *18*), 6.73 (d, 1H, *J* = 4.5 Hz, *9*), 6.58 (d, 1H, *J* = 4.2 Hz, *19*), 5.97 (d, 1H, *J* = 4.5 Hz, *10*), 5.74 (br s, 1H, *26*), 3.98 (s, 3H, *1*); ^{11}B NMR (96 MHz, CDCl$_3$): δ$_B$ 0.97 (t, *J*$_{B-F}$ = 32.0 Hz); ^{19}F NMR (282 MHz, CDCl$_3$): δ$_F$ -62.9 (s), -142.3 (dd, *J*$_{B-F}$ = 32.0 Hz).

5.2.2.20 Methyl 4-(10b-fluoro-10-((4-(trifluoromethyl)phenyl)thio)-10b*H*-11-oxa-4b[1],10al[4]-diaza-10bl[4]-boracyclopenta[*e*]aceanthrylen-7-yl)benzoate (*N,N,O,F*-BODIPY **3.23**)
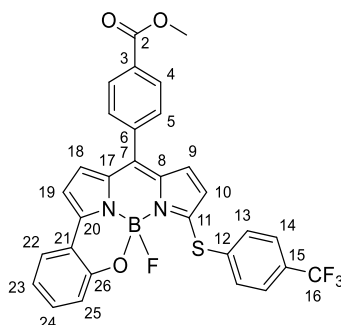

To a round bottomed flask under an inert atmosphere was added methyl 4-(5,5-difluoro-3-(2-hydroxyphenyl)-7-((4-(trifluoromethyl)phenyl)thio)-5*H*-5λ[4],6λ[4]-dipyrrolo[1,2-*c*:2',1'-*f*][1,3,2]diazaborinin-10-yl)benzoate (20 mg, 0.034 mmol) and dry DCM (2 mL). *N,N*-diisopropylethylamine (0.92 mL, 5.27 mmol) and BF$_3$.OEt$_2$ (0.52 mL, 4.23 mmol) were added, and the resulting reaction mixture was stirred at room temperature for 1 hour 15 minutes. The reaction mixture was diluted with DCM, and washed with water. The organic layer was dried over Na$_2$SO$_4$, filtered and the solvent removed under reduced pressure. The crude product was purified by silica gel column chromatography (5:1 petrol 40-60:EtOAc) to give methyl 4-(10b-fluoro-10-((4-(trifluoromethyl)phenyl)thio)-10b*H*-11-oxa-4b[1],10al[4]-diaza-10bl[4]-boracyclopenta[*e*]aceanthrylen-7-yl)benzoate (2.6 mg, 0.005 mmol, 15%).

Mp: 124-126 °C; R$_f$ = 0.36 (5:1 petrol 40-60:EtOAc); ^{1}H NMR (300 MHz, CDCl$_3$): δ$_H$ 8.19 (d, 2H, *J* = 8.5 Hz, *4*), 7.79-7.63 (m, 7H, *5, 24, 23, 16*), 7.47 (ddd, 1H, *J* = 8.6, 7.2, 1.7 Hz, *15*), 7.31-2.75 (m, 1H, *13*), 7.07 (m, 1H, *14*), 7.00-6.95 (m, 2H, *19, 20*), 6.83 (d, 1H, *J* = 4.3 Hz, *9*), 6.17 (d, 1H, *J* = 4.3 Hz, *10*), 4.00 (s, 3H, *1*); ^{13}C NMR (176 MHz, CDCl$_3$): δ$_C$ 166.5 (*2*), 155.5 (*21*), 151.5 (*17*), 150.3 (*6*), 138.6 (*22*), 138.3 (*8*), 137.0 (*9*), 136.9 (*7*), 133.6 (*13*), 133.4 (*11*), 133.1 (*15*), 131.9 (*4*), 131.1 (*23*), 130.9 (*3*), 130.6 (*5*), 129.9 (*25*), 127.0 (*24*), 124.7 (*26*), 126.5 (*14*), 123.2 (*18*), 120.9 (*12*), 120.5 (*10*), 119.1 (*16*), 116.7 (*20*), 116.2 (*19*), 52.6 (*1*); ^{11}B NMR (96 MHz, CDCl$_3$): δ$_B$ 0.18 (d, *J*$_{B-F}$ = 46.5 Hz); ^{19}F NMR (471 MHz, CDCl$_3$): δ$_F$ -62.75 (s), -141.68 (q, *J*$_{B-F}$ = 46.5 Hz); IR (neat): υ$_{max}$/cm^{-1} 2923 (w), 2852 (w), 1722 (m); HRMS (pAPCI) calcd for C$_{30}$H$_{19}$^{11}BF$_4$N$_2$O$_3$^{32}S [M$^+$] 574.1145, found 574.1151; ε = 48 000 M^{-1} cm^{-1} (DCM); φ$_F$ = 0.14 (DCM).

5.2.3 Chapter 4

5.2.3.1 5*H*-naphtho[1,2-*e*]pyrrolo[1,2-*c*][1,3]oxazin-5-one (**4.5**)
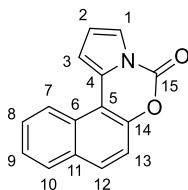
To a Schlenk flask under an inert atmosphere was added 1-bromo-2-napthol (578 mg, 2 mmol), N-Boc-2-pyrrole boronic acid (634 mg, 3 mmol), $Pd(PPh_3)_4$ (116 mg, 5 mol %) and K_3PO_4 (636 mg, 3 mmol). Solvent was added (THF:H_2O, 7 mL:3.6 mL) before heating to 65 °C and stirring for 20 hours. The reaction mixture was then diluted with DCM and washed with water. The organic layers were then combined and dried over $MgSO_4$ and solvent removed under reduced pressure. The crude product was then purified by column chromatography (eluent system: 15:1 petrol 40-60:EtOAc) to give 5*H*-naphtho[1,2-*e*]pyrrolo[1,2-*c*][1,3]oxazin-5-one (298 mg, 64%).

Mp: 153-154 °C; R_f = 0.40 (10:1 petrol 40-60:EtOAc; UV light); ^{1}H NMR (300 MHz, CDCl$_3$): δ_H 8.49 (d, 1H, *J* = 8.6 Hz, *7*), 7.88 (d, 1H, *J* = 8.1 Hz, *10*), 7.77 (d, 1H, *J* = 8.9 Hz, *12*), 7.70-7.64 (m, 2H, *1, 8*), 7.55 (ddd, 1H, *J* = 8.1, 6.9, 1.2 Hz, *9*), 7.38 (d, 1H, *J* = 8.9 Hz, *13*), 7.21 (dd, 1H, *J* = 3.7, 1.3 Hz, *3*), 6.75 (t, 1H, *J* = 3.7 Hz, *2*); ^{13}C NMR (75 MHz, CDCl$_3$): δ_C 146.3 (*15*), 144.1 (*14*), 131.4 (*4*), 129.7 (*12*), 129.3 (*10*), 128.1 (*8*), 127.9 (*6*), 127.4 (*11*), 125.9 (*9*), 124.2 (*7*), 118.2 (*1*), 116.7 (*13*), 116.0 (*2*), 110.5 (*3*), 109.0 (*5*); IR (neat): υ_{max}/cm^{-1} 1754 (s); HRMS (TOF MS ASAP$^+$) calcd for $C_{15}H_9NO_2$ [M+H]$^+$ 236.0712, found 236.0711.

5.2.3.2 1-(1*H*-pyrrol-2-yl)naphthalen-2-ol (**4.4**)
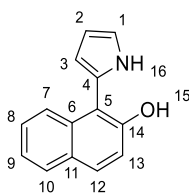
To a round bottomed flask were added 5*H*-naphtho[1,2-*e*]pyrrolo[1,2-*c*][1,3]oxazin-5-one (815 mg, 3.47 mmol), sodium hydroxide (27.76 g, 694 mmol), and ethanol (82 mL). The reaction mixture was stirred at room temperature for 1 hour. The reaction mixture was then neutralized with 2 M HCl, extracted with DCM and washed with water. The crude product was then purified by column chromatography (eluent system: 10:1 petrol 40-60:EtOAc) to give 1-(1*H*-pyrrol-2-yl)naphthalen-2-ol as a green oil (539 mg, 74%).

R_f = 0.16 (10:1 petrol 40-60:EtOAc; UV light); ^{1}H NMR (400 MHz, CDCl$_3$): δ_H 8.31 (br s, 1H, *16*), 7.82-7.77 (m, 2H, *1, 12*), 7.61 (d, 1H, *J* = 8.5 Hz, *7*), 7.40 (ddd, 1H, *J* = 8.5, 6.8, 1.5 Hz, *8*), 7.34 (ddd, 1H, *J* = 8.1, 6.8, 1.3 Hz, *9*), 7.25 (d, 1H, *J* = 8.9 Hz, *13*), 7.07 (m, 1H, *3*), 6.49-6.44 (m, 2H, *2, 10*), 6.04 (br s, 1H, *15*); ^{13}C NMR (101 MHz, CDCl$_3$): δ_C 152.2 (*14*), 134.0 (*6*), 130.3 (*12*), 129.0 (*4*), 128.3 (*1*), 127.0 (*8*), 124.4 (*7*), 123.6 (*11*), 123.3 (*9*), 120.1 (*3*), 117.3 (*13*), 112.6 (*5*), 110.4 (*10*), 110.0 (*2*); IR (neat): υ_{max}/cm^{-1} 3415 (m), 3056 (w); HRMS (TOF MS ASAP$^+$) calcd for C$_{14}$H$_{11}$NO [M+H]$^+$ 210.0919, found 210.0914.

<u>5.2.3.3 *N,N,O,O*-BODIPY **4.1**</u>
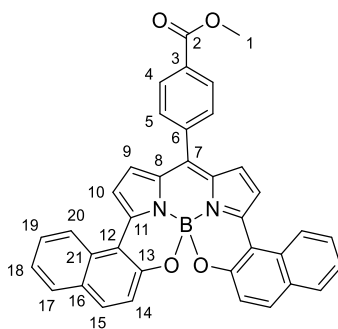
To a Schlenk flask under an inert atmosphere was added 1-(1*H*-pyrrol-2-yl)naphthalen-2-ol (100 mg, 0.36 mmol), 4-methyl-4-formyl benzoate (45 mg, 0.27 mmol) in DCM (2 mL). Then, TFA (5 μL) added dropwise, and the reaction mixture stirred for 1 hour at room temperature. Then *p*-chloranil (44 mg, 0.18 mmol) was added, and reaction mixture stirred for 15 minutes. Then diisopropyl amine (0.15 mL, 1.08 mmol) and boron triflouride diethyl etherate (0.16 mL, 1.26 mmol) were added and the reaction mixture stirred for 20 minutes. The reaction mixture was then diluted with DCM and washed with water. The organic layers were then combined and dried over $MgSO_4$ and solvent removed under reduced pressure. The crude product was then purified by column chromatography (eluent system: 4:1 toluene:DCM) to give *N,N,O,O*-BODIPY **4.1** (35 mg, 0.06 mmol, 16%).

Mp: 350 °C (decomposed); R_f = 0.31 (4:1 toluene:DCM); ^{1}H NMR (700 MHz, C_6D_6): δ_H 8.47 (d, 2H, *J* = 8.3 Hz, *20*), 8.10 (d, 2H, *J* = 8.3 Hz, *4*), 7.53 (d, 2H, *J* = 7.9 Hz, *17*), 7.42-7.37 (m, 4H, *19*, *15*), 7.34 (d, 2H, *J* = 8.3 Hz, *5*), 7.22 (ddd, 2H, *J* = 7.9, 6.8, 1.2 Hz, *18*), 7.05 (d, 2H, *J* = 4.4 Hz, *9*), 6.76 (d, 2H, *J* = 4.4 Hz, *10*), 3.56 (s, 3H, *1*); ^{13}C NMR (176 MHz, C_6D_6): δ_C 166.2 (*2*), 155.0 (*11*), 149.8 (*13*), 138.9 (*6*), 135.5 (*21*), 134.3 (*7*), 133.3 (*15*), 132.1 (*3*), 131.4 (*8*), 131.0 (*5*), 130.0 (*16*), 129.6 (*4*), 129.3 (*10*), 129.2 (*17*), 124.8 (*20*), 124.2 (*18*), 121.6 (*14*), 119.0 (*9*), 114.5 (*12*), 51.9 (*1*); ^{11}B NMR (128 MHz, C_6D_6): δ_B 0.07 (s); IR (neat): υ_{max}/cm^{-1} 1723 (m); HRMS (TOF MS ASAP$^+$) calcd for $C_{37}H_{23}{}^{11}BN_2O_4$ [M+H]$^+$ 571.1835, found 571.1827; ε = 43000 M^{-1} cm^{-1} (DCM); ϕ_F = 0.24 (DCM).

5.3 Photophysical and Chiroptical Measurements.

5.3.1 UV/Vis Absorption and Emission spectra.

5.3.1.1 Methyl 4-(3,7-dibromo-5,5-difluoro-5*H*-4λ⁴,5λ⁴-dipyrrolo[1,2-*c*:2',1'-*f*][1,3,2]diazaborinin-10-yl)benzoate (**2.11**)

Figure 5.1: Absorption and emission spectra of BODIPY **2.11**, measured in DCM. Excitation wavelength used for emission: 510 nm.

5.3.1.2 *N,N,O,O*-BODIPY **2.13**

Figure 5.2: Absorption and emission spectra of BODIPY **2.13**, measured in DCM. Excitation wavelength for emission: 570 nm (DCM).

5.3.1.3 Methyl 4-(9,14-dimethyl-10,15-dioxa-2a$^1\lambda^4$,3a^1-diaza-10aλ^4-borabenzo[5,6]indeno[3,4-*ef*]aceanthrylen-3-yl)benzoate (*N,N,O,C*-BODIPY **2.18**)

Figure 5.3: Absorption and emission spectra of BODIPY **2.18**, measured in DCM. Excitation wavelength for emission: 525 nm (DCM).

5.3.1.4 Methyl 4-(9,14-dimethyl-10,15-dioxa-2a$^1\lambda^4$,3a^1-diaza-10aλ^4-borabenzo[5,6]indeno[3,4-*ef*]aceanthrylen-3-yl)benzoate (*N,N,O,C*-BODIPY **2.32**)

Figure 5.4: Absorption and emission spectra of BODIPY **2.32**, measured in DCM. Excitation wavelength for emission: 575 nm (DCM).

5.3.1.5 Methyl 4-(7,12-dimethyl-10,15-dioxa-2a^{1}λ^4,3a^1-diaza-10aλ^4-borabenzo[5,6]indeno[3,4-*ef*]aceanthrylen-3-yl)benzoate (*N,N,O,C*-BODIPY **2.33**)

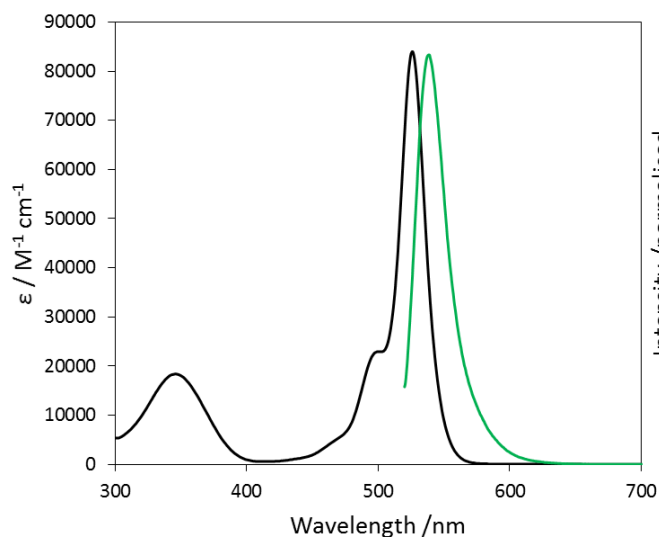**Figure 5.5**: Absorption and emission spectra of BODIPY **2.33**, measured in DCM. Excitation wavelength for emission: 555 nm (DCM).

5.3.1.6 Methyl 4-(7,12-dichloro-10,15-dioxa-2a^{1}λ^4,3a^1-diaza-10aλ^4-borabenzo[5,6]indeno[3,4-*ef*]aceanthrylen-3-yl)benzoate (*N,N,O,C*-BODIPY **2.34**)
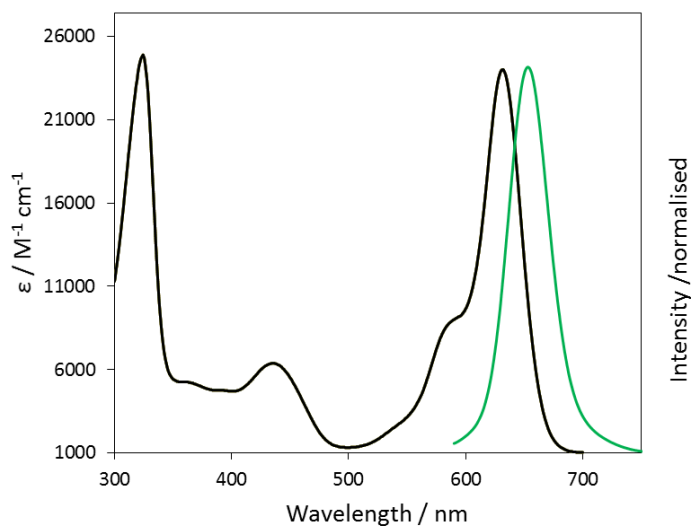

Figure 5.6: Absorption and emission spectra of BODIPY **2.34**, measured in DCM. Excitation wavelength for emission: 575 nm (DCM).

5.3.1.7 Methyl 4-(7,12-difluoro-10,15-dioxa-2a^{1}λ^4,3a^1-diaza-10aλ^4-borabenzo[5,6]indeno[3,4-*ef*]aceanthrylen-3-yl)benzoate (*N,N,O,C*-BODIPY **2.35**)
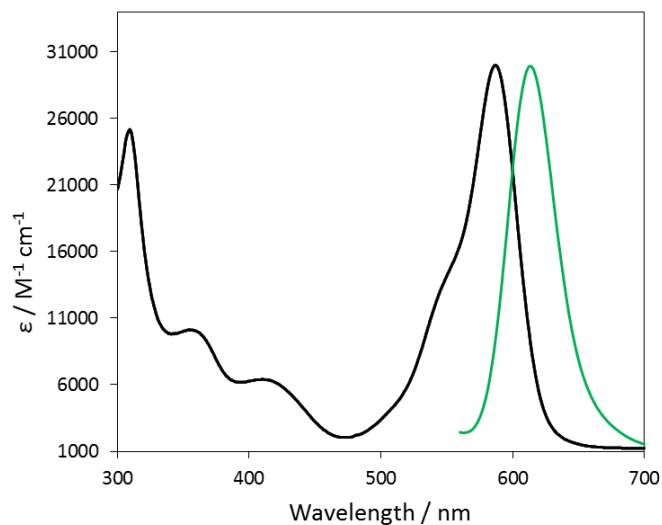

Figure 5.7: Absorption and emission spectra of BODIPY **2.35**, measured in DCM. Excitation wavelength for emission: 555 nm (DCM).

5.3.1.8 Methyl 4-(5,5-difluoro-3,7-bis(2-(methylthio)phenyl)-5*H*-4λ^4,5λ^4-dipyrrolo[1,2-*c*:2',1'-*f*][1,3,2]diazaborinin-10-yl)benzoate (**3.2**)

Figure 5.8: Absorption and emission spectra of BODIPY **3.2**, measured in DCM. Excitation wavelength for emission: 520 nm (DCM).

5.3.1.9 Methyl 4-(3,7-bis(benzo[*b*]thiophen-2-yl)-5,5-difluoro-5*H*-4λ⁴,5λ⁴-dipyrrolo[1,2-*c*:2',1'-*f*][1,3,2]diazaborinin-10-yl)benzoate (**3.15**)
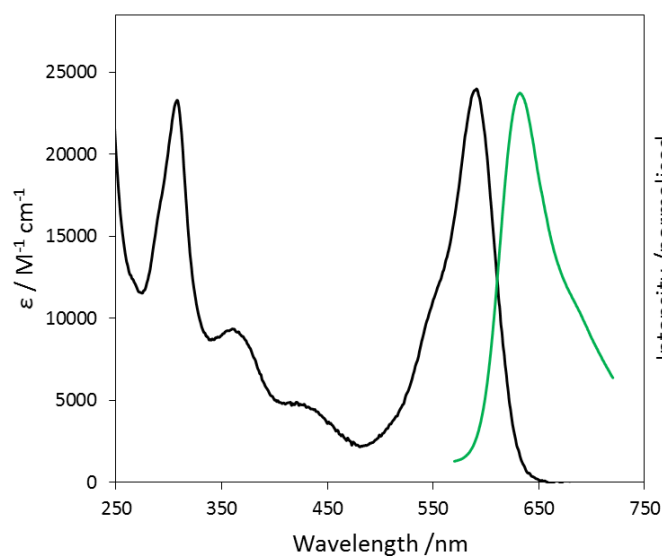

Figure 5.9: Absorption and emission spectra of BODIPY **3.15**, measured in DCM. Excitation wavelength for emission: 635 nm (DCM).

5.3.1.10 Methyl 4-(10-(benzo[*b*]thiophen-2-yl)-10b-fluoro-10b*H*-11-oxa-4b¹,10aλ⁴-diaza-10bλ⁴-boracyclopenta[*e*]aceanthrylen-7-yl)benzoate (**3.16**)
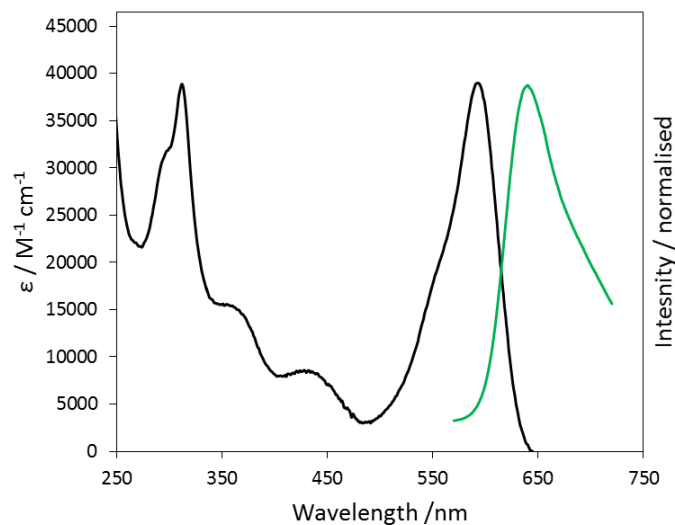

Figure 5.10: Absorption and emission spectra of BODIPY **3.16**, measured in DCM. Excitation wavelength for emission: 535 nm. (DCM).

<u>5.3.1.11 Methyl 4-(5,5-difluoro-5H-4λ⁴,5λ⁴-dipyrrolo[1,2-*c*:2',1'-*f*][1,3,2]diazaborinin-10-yl)benzoate (**3.18**)</u>
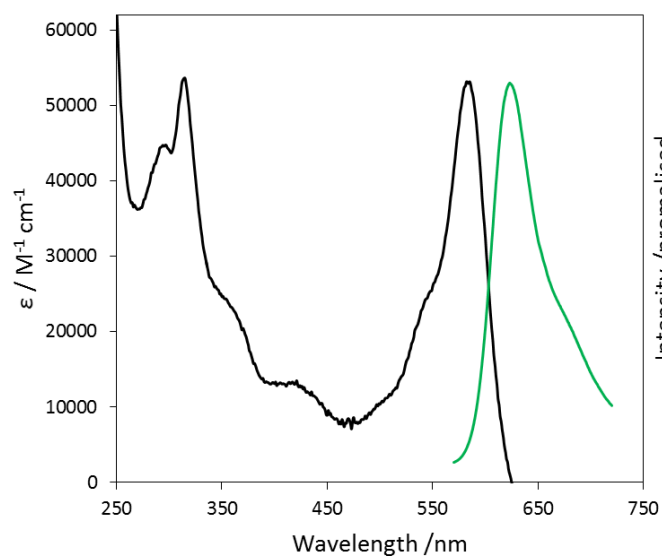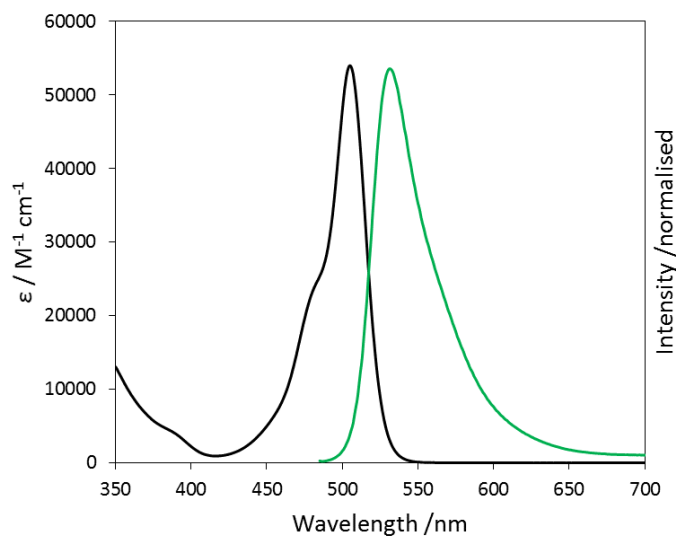

Figure 5.11: Absorption and emission spectra of BODIPY **3.18**, measured in DCM. Excitation wavelength for emission: 475 nm. (DCM).

<u>5.3.1.12 Methyl 4-(3,7-dichloro-5,5-difluoro-5*H*-4λ⁴,5λ⁴-dipyrrolo[1,2-*c*:2',1'-*f*][1,3,2]diazaborinin-10 yl)benzoate (**3.19**)</u>
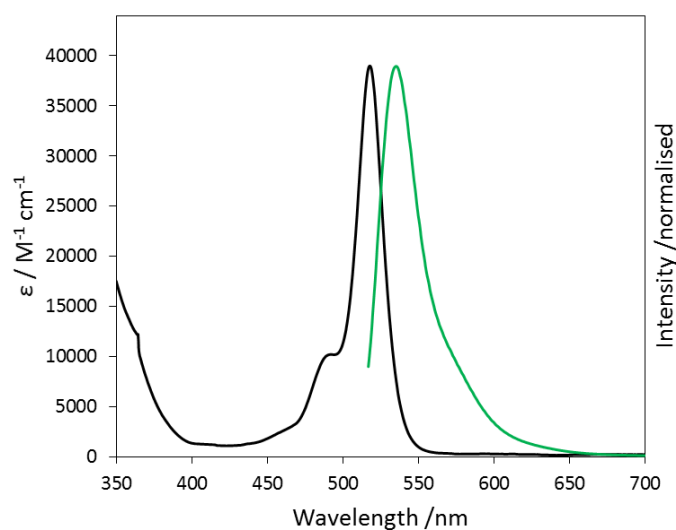
Figure 5.12: Absorption and emission spectra of BODIPY **3.19**, measured in DCM. Excitation wavelength for emission: 507 nm. (DCM).

5.3.1.13 Methyl 4-(5,5-difluoro-3,7-bis(phenylthio)-5*H*-4λ⁴,5λ⁴-dipyrrolo[1,2-*c*:2',1'-*f*][1,3,2]diazaborinin-10-yl)benzoate (**3.21**)
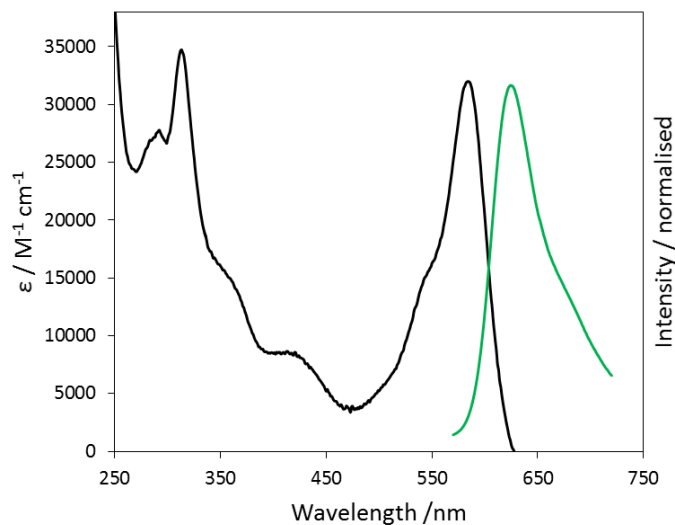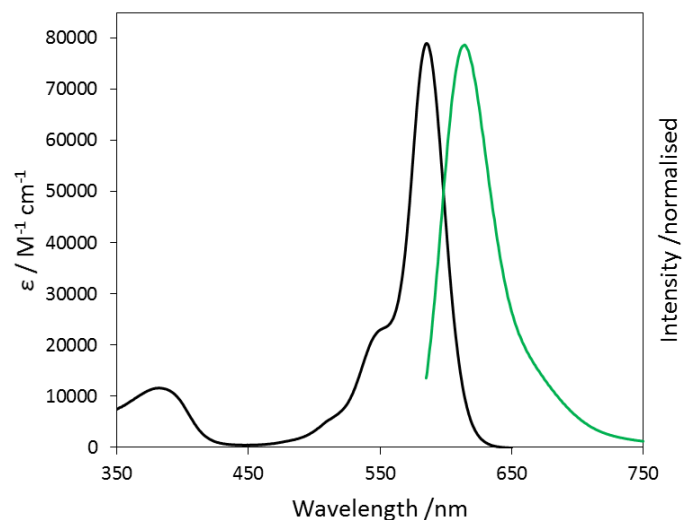

Figure 5.13: Absorption and emission spectra of BODIPY **3.21**, measured in DCM. Excitation wavelength for emission: 570 nm (DCM).

5.3.1.14 Methyl 4-(3-bromo-5,5-difluoro-7-((4-(trifluoromethyl)phenyl)thio)-5*H*-5λ⁴,6λ⁴-dipyrrolo[1,2-*c*:2',1'-*f*][1,3,2]diazaborinin-10-yl)benzoate (**3.24**)
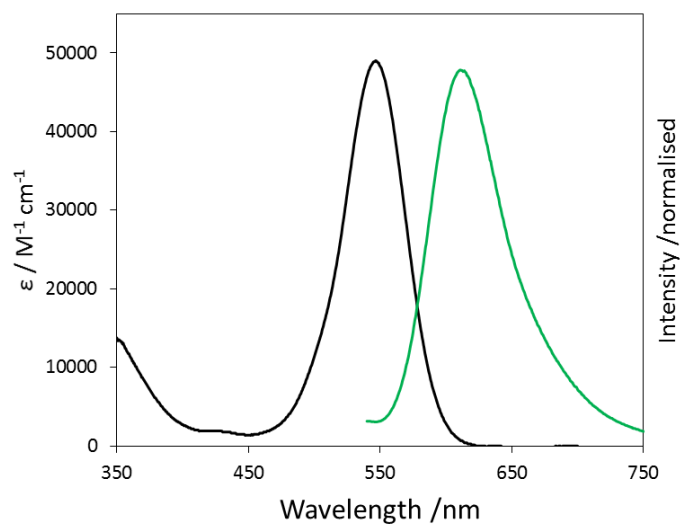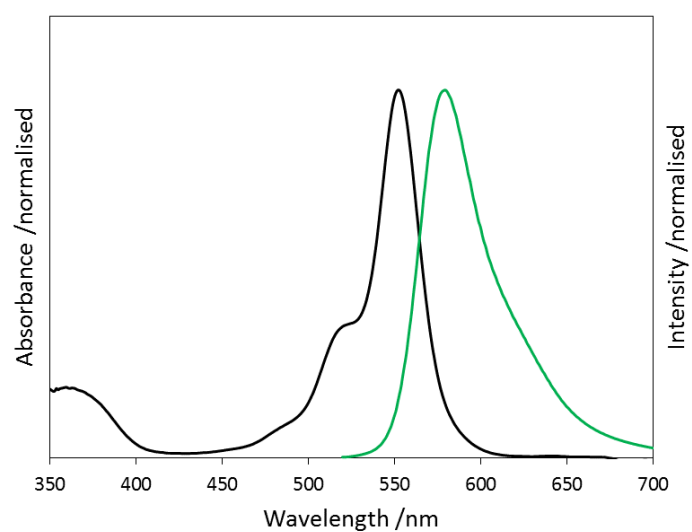

Figure 5.14: Absorption and emission spectra of BODIPY **3.24**, measured in DCM. Excitation wavelength for emission: 510 nm (DCM).

5.3.1.15 Methyl 4-(10b-fluoro-10-((4-(trifluoromethyl)phenyl)thio)-10b*H*-11-oxa-4b¹,10al⁴-diaza-

10bl⁴-boracyclopenta[*e*]aceanthrylen-7-yl)benzoate (*N,N,O,F*-BODIPY **3.23**)
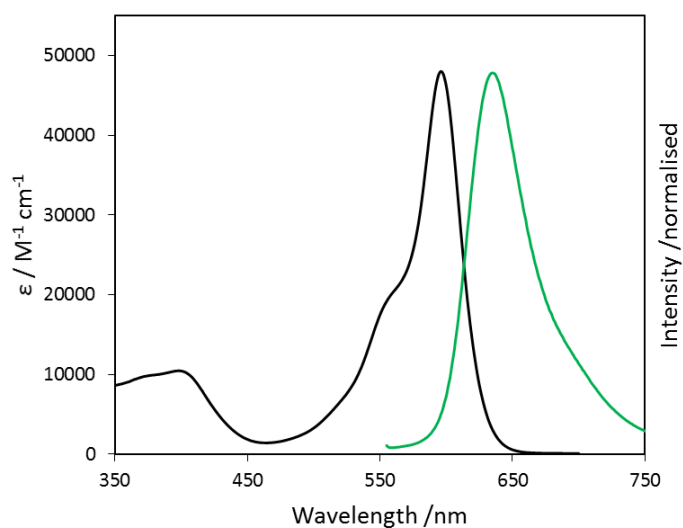
Figure 5.15: Absorption and emission spectra of BODIPY **3.23**, measured in DCM. Excitation wavelength for emission: 545 nm (DCM).
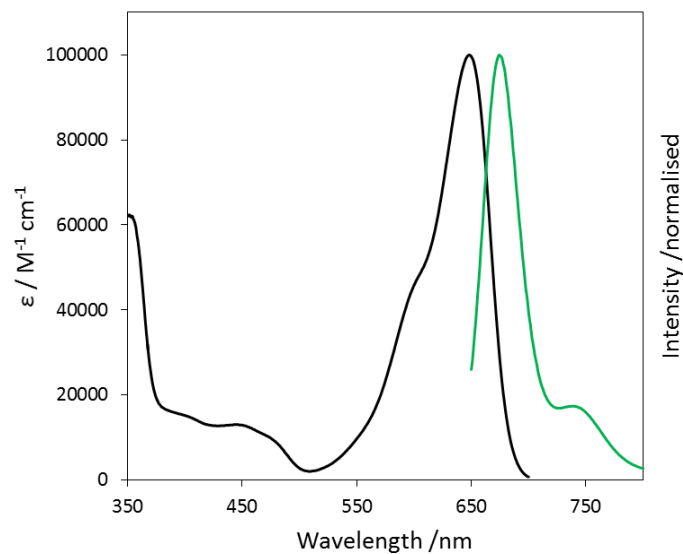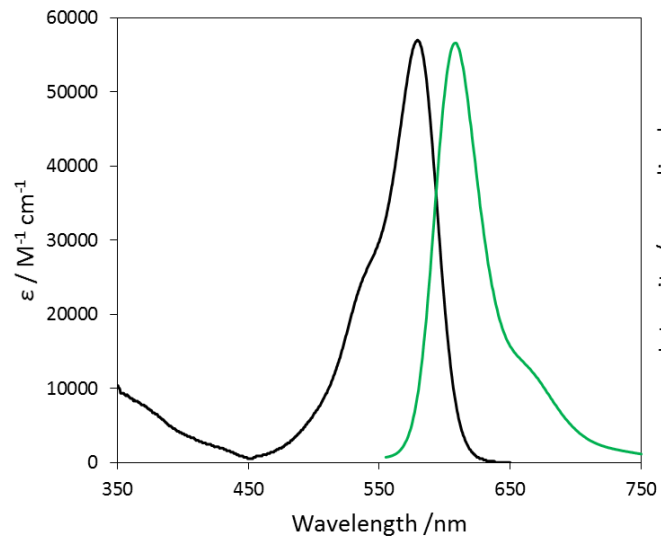
5.3.1.16 *N,N,O,O*-BODIPY **4.1**
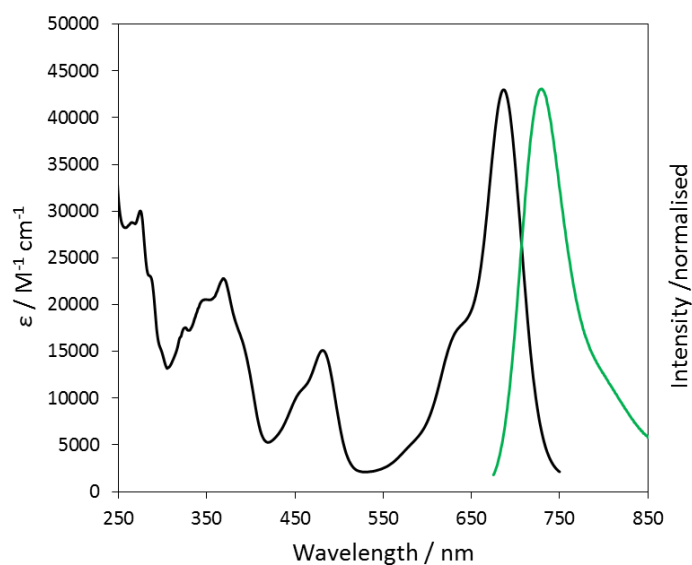
Figure 5.16: Absorption and emission spectra of BODIPY **4.1**, measured in DCM. Excitation wavelength for emission: 665 nm (DCM).

## 5.3.2 Molar Extinction Coefficients

Molar extinction coefficients were obtained by measuring the absorbance at the absorptive λ_{max} over a 4-10 point dilution series. The absorbance values for the series were then plotted against the molar concentrations of the series to calculate the molar extinction coefficient (ε) using the following equation:

$$A = \varepsilon l c$$

Where A is the absorbance ([au]), ε is the molar extinction coefficient ($M^{-1}\ cm^{-1}$), l is the path length (cm) and c is the molar concentration (M).

5.3.2.1 Methyl 4-(3,7-dibromo-5,5-difluoro-5H-4λ^4,5λ^4-dipyrrolo[1,2-c:2',1'-f][1,3,2]diazaborinin-10-yl)benzoate (**2.11**)

Figure 5.17: Absorbance at the absorptive λ_{max} plotted against molar concentration of a 8 point dilution series. Measured in DCM, ε = 84 000 $M^{-1}\ cm^{-1}$.

5.3.2.2 *N,N,O,O*-BODIPY **2.13**
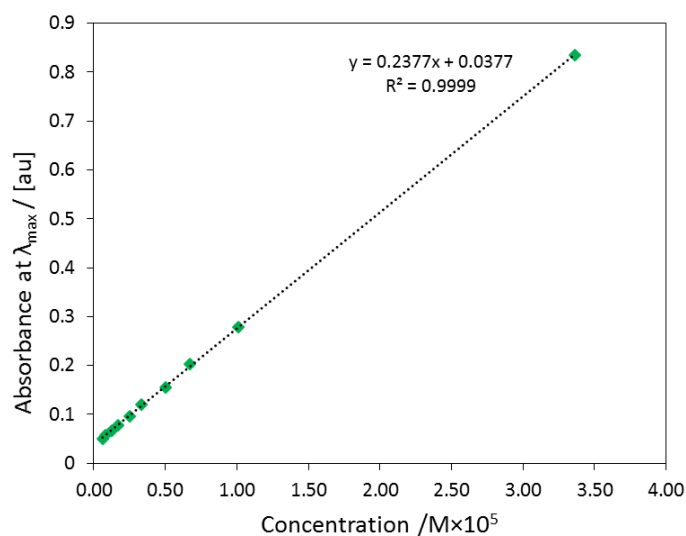
Figure 5.18: Absorbance at the absorptive λ_{max} plotted against molar concentration of a 10 point dilution series. Measured in DCM, $\varepsilon = 24\,000$ M^{-1} cm^{-1}.

5.3.2.3 Methyl 4-(9,14-dimethyl-10,15-dioxa-2a$^1\lambda^4$,3a^1-diaza-10aλ^4-borabenzo[5,6]indeno[3,4-*ef*]aceanthrylen-3-yl)benzoate (*N,N,O,C*-BODIPY **2.18**)
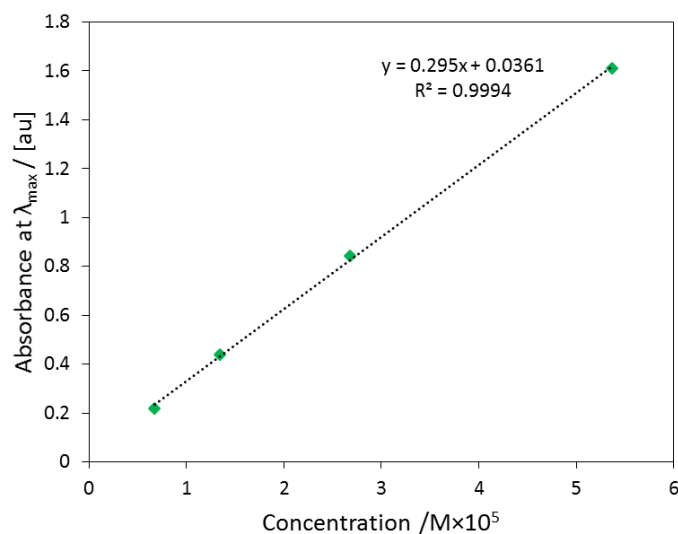
Figure 5.19: Absorbance at the absorptive λ_{max} plotted against molar concentration of a 4 point dilution series. Measured in hexane, $\varepsilon = 30\,000$ M^{-1} cm^{-1}.

5.3.2.4 Methyl 4-(9,14-dimethyl-10,15-dioxa-2a$^1\lambda^4$,3a^1-diaza-10aλ^4-borabenzo[5,6]indeno[3,4-*ef*]aceanthrylen-3-yl)benzoate (*N,N,O,C*-BODIPY **2.32**)

Figure 5.20: Absorbance at the absorptive λ_{max} plotted against molar concentration of a 7 point dilution series. Measured in DCM, ε = 24 000 M^{-1} cm^{-1}.

5.3.2.5 Methyl 4-(7,12-dimethyl-10,15-dioxa-2a$^1\lambda^4$,3a^1-diaza-10aλ^4-borabenzo[5,6]indeno[3,4-*ef*]aceanthrylen-3-yl)benzoate (*N,N,O,C*-BODIPY **2.33**)

Figure 5.21: Absorbance at the absorptive λ_{max} plotted against molar concentration of a 7 point dilution series. Measured in DCM, ε = 39 000 M^{-1} cm^{-1}.

5.3.2.6 Methyl 4-(7,12-dichloro-10,15-dioxa-2a^{1}λ^4,3a^1-diaza-10aλ^4-borabenzo[5,6]indeno[3,4-*ef*]aceanthrylen-3-yl)benzoate (*N,N,O,C*-BODIPY **2.34**)

Figure 5.22: Absorbance at the absorptive λ$_{max}$ plotted against molar concentration of a 7 point dilution series. Measured in DCM, ε = 52 000 M^{-1} cm^{-1}.

5.3.2.7 Methyl 4-(7,12-difluoro-10,15-dioxa-2a^{1}λ^4,3a^1-diaza-10aλ^4-borabenzo[5,6]indeno[3,4-*ef*]aceanthrylen-3-yl)benzoate (*N,N,O,C*-BODIPY **2.35**)

Figure 5.23: Absorbance at the absorptive λ$_{max}$ plotted against molar concentration of a 7 point dilution series. Measured in DCM, ε = 32 000 M^{-1} cm^{-1}.

5.3.2.8 Methyl 4-(5,5-difluoro-3,7-bis(2-(methylthio)phenyl)-5*H*-4λ^4,5λ^4-dipyrrolo[1,2-*c*:2',1'-*f*][1,3,2]diazaborinin-10-yl)benzoate (**3.2**)

Figure 5.24: Absorbance at the absorptive λ_{max} plotted against molar concentration of a 5 point dilution series. Measured in DCM, ε = 49 000 M^{-1} cm^{-1}.

5.3.2.9 Methyl 4-(3,7-bis(benzo[*b*]thiophen-2-yl)-5,5-difluoro-5*H*-4λ^4,5λ^4-dipyrrolo[1,2-*c*:2',1'-*f*][1,3,2]diazaborinin-10-yl)benzoate (**3.15**)
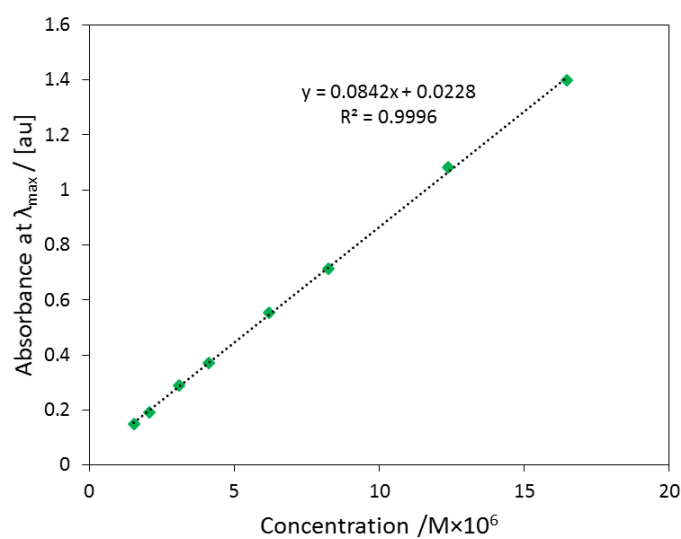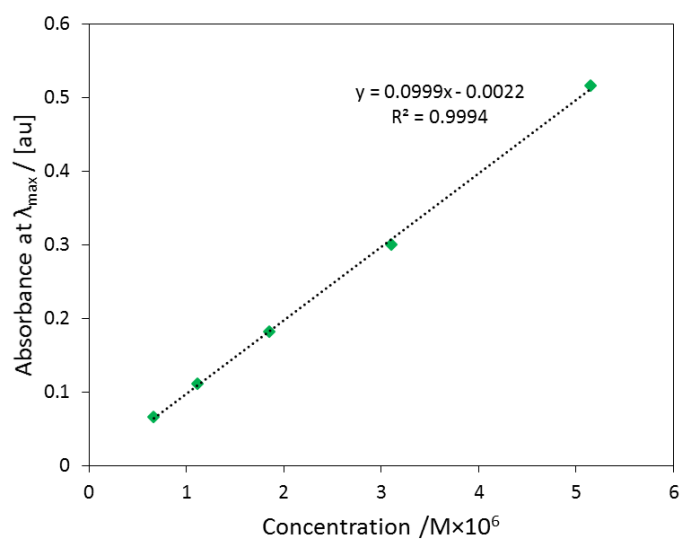

Figure 5.25: Absorbance at the absorptive λ_{max} plotted against molar concentration of a 5 point dilution series. Measured in DCM, ε = 100 000 M^{-1} cm^{-1}.

171

5.3.2.10 Methyl 4-(10-(benzo[*b*]thiophen-2-yl)-10b-fluoro-10b*H*-11-oxa-4b^1,10aλ^4-diaza-10bλ^4-boracyclopenta[*e*]aceanthrylen-7-yl)benzoate (**3.16**)
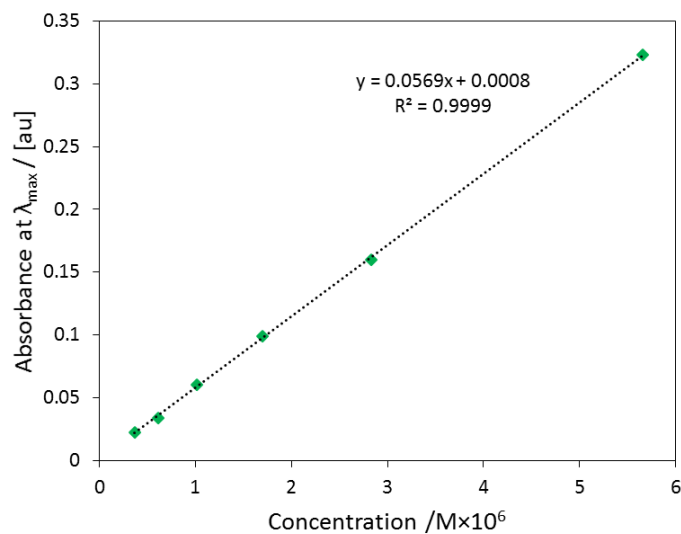
Figure 5.26: Absorbance at the absorptive λ_{max} plotted against molar concentration of a 6 point dilution series. Measured in DCM, ε = 57 000 M^{-1} cm^{-1}.

5.3.1.11 Methyl 4-(5,5-difluoro-5H-4λ^4,5λ^4-dipyrrolo[1,2-*c*:2',1'-*f*][1,3,2]diazaborinin-10-yl)benzoate (**3.18**)
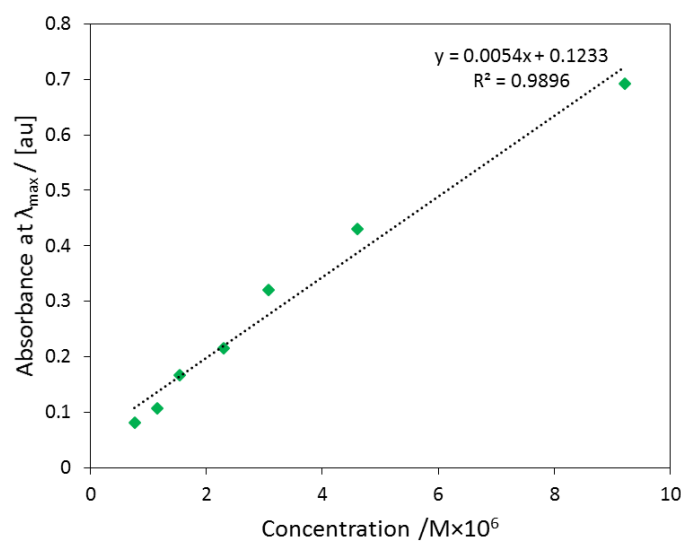
Figure 5.27: Absorbance at the absorptive λ_{max} plotted against molar concentration of a 7 point dilution series. Measured in DCM, ε = 54 000 M^{-1} cm^{-1}.

172

5.3.1.12 Methyl 4-(3,7-dichloro-5,5-difluoro-5*H*-4λ^4,5λ^4-dipyrrolo[1,2-*c*:2',1'-*f*][1,3,2]diazaborinin-10 yl)benzoate (**3.19**)
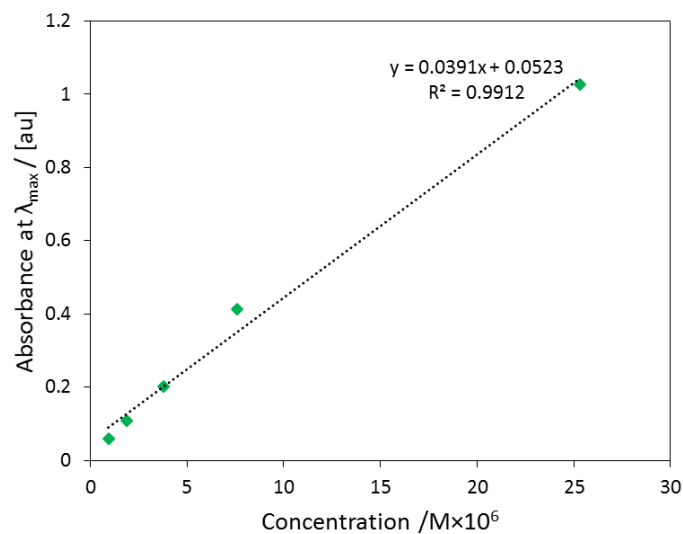
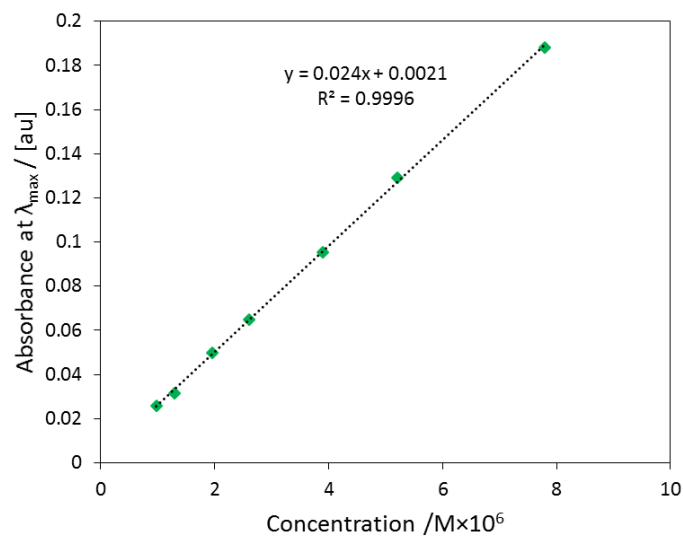**Figure 5.28**: Absorbance at the absorptive λ$_{max}$ plotted against molar concentration of a 5 point dilution series. Measured in DCM, ε = 39 000 M^{-1}cm^{-1}.

5.3.2.13 Methyl 4-(5,5-difluoro-3,7-bis(phenylthio)-5*H*-4λ^4,5λ^4-dipyrrolo[1,2-*c*:2',1'-*f*][1,3,2]diazaborinin-10-yl)benzoate (**3.21**)
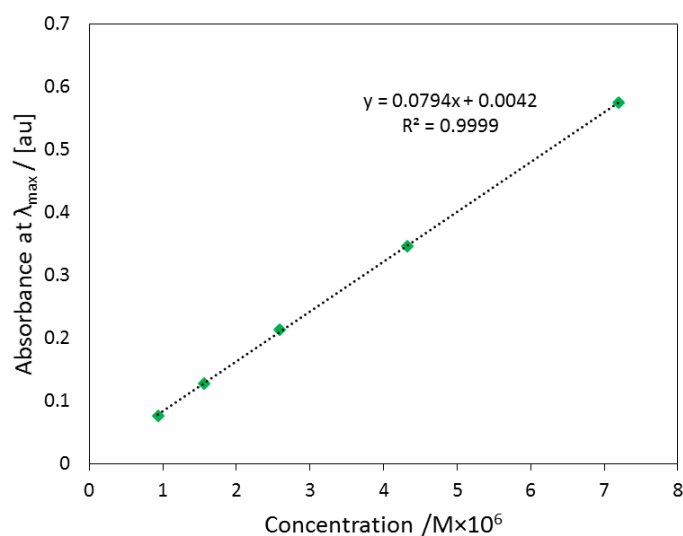
Figure 5.29: Absorbance at the absorptive λ$_{max}$ plotted against molar concentration of a 5 point dilution series. Measured in DCM, ε = 79 000 M^{-1} cm^{-1}.

173

5.3.2.14 Methyl 4-(10b-fluoro-10-((4-(trifluoromethyl)phenyl)thio)-10bH-11-oxa-4b^1,10al^4-diaza-10bl^4-boracyclopenta[e]aceanthrylen-7-yl)benzoate (N,N,O,F-BODIPY **3.23**)
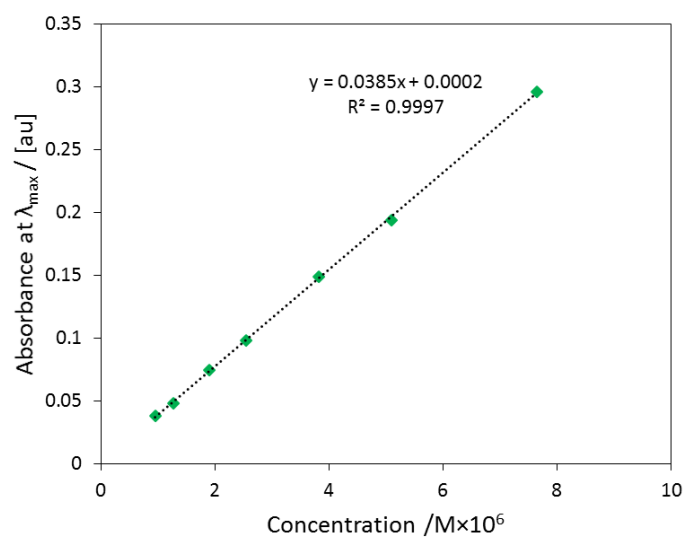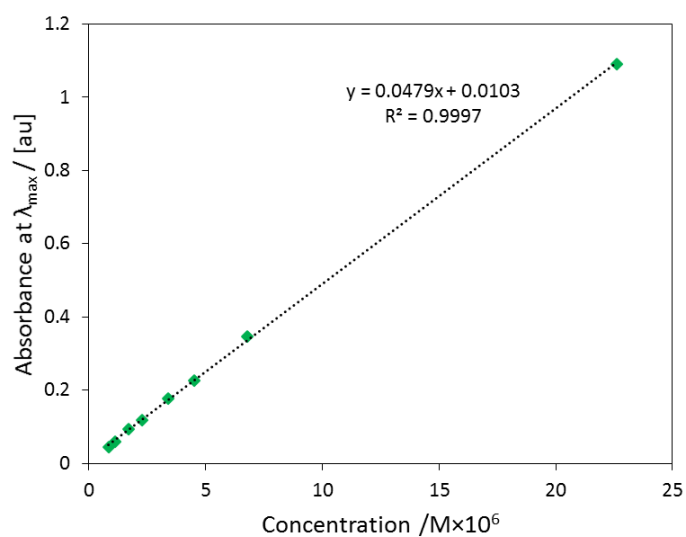

Figure 5.30: Absorbance at the absorptive λ$_{max}$ plotted against molar concentration of an 8 point dilution series. Measured in DCM, ε = 48 000 M^{-1} cm^{-1}.
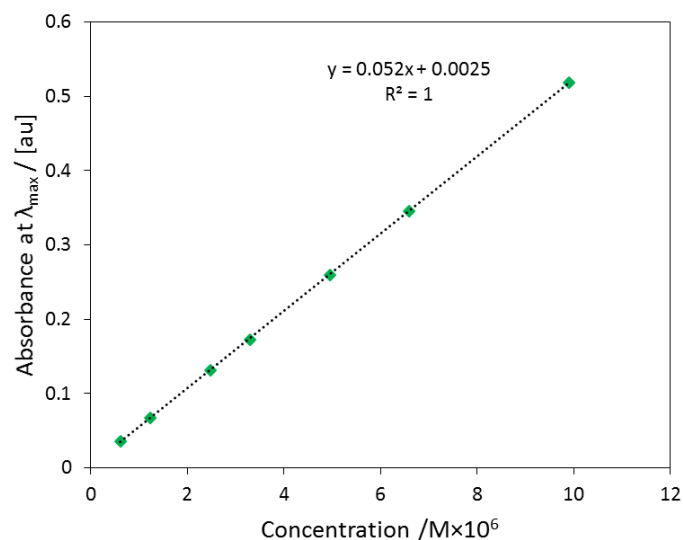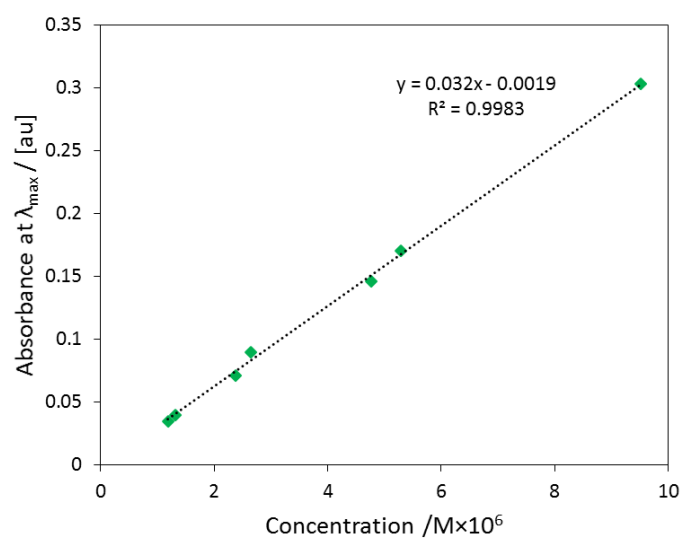
5.3.2.15 N,N,O,O-BODIPY **4.1**

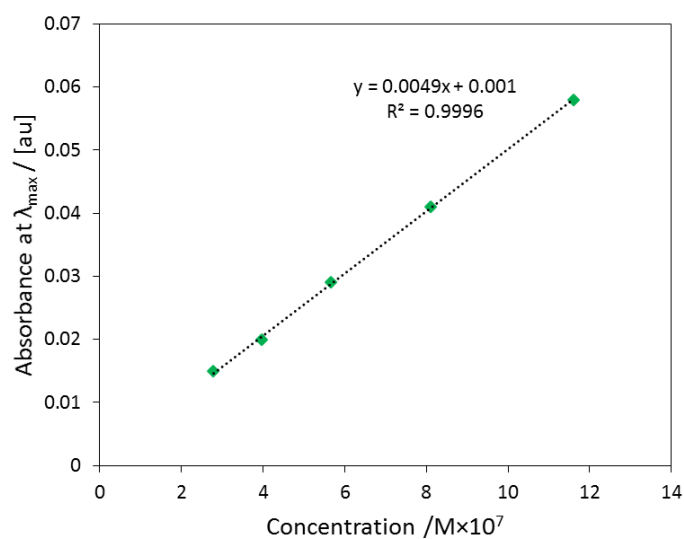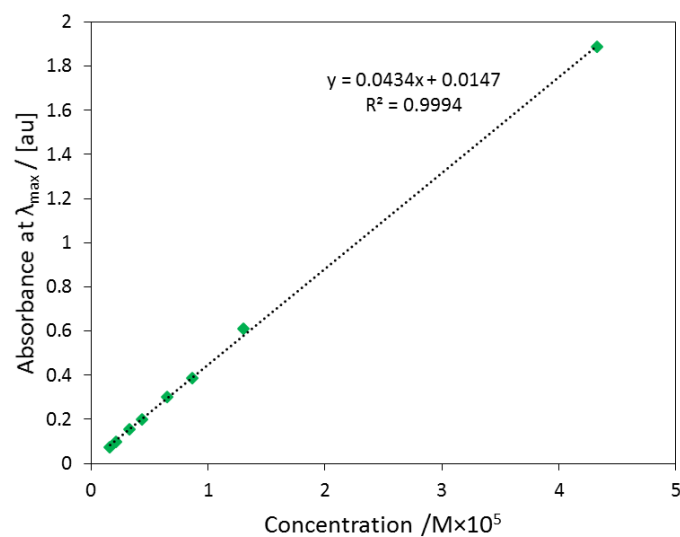**Figure 5.31**: Absorbance at the absorptive λ$_{max}$ plotted against molar concentration of an 8 point dilution series. Measured in DCM, ε = 43 000 M^{-1} cm^{-1}.

5.3.3 Fluorescence Quantum Yields

Fluorescence quantum yields (ϕ$_F$) were obtained by recording emission spectra of a suitable reference compound and emission spectra of the BODIPY. It is important that the emission peak of the reference compound has the maximum overlap possible with the emission peak of the BODIPY to ensure an accurate measurement of the ϕ$_F$. Furthermore the absorbance at the excitation wavelength of the reference sample should be as similar as possible to the absorbance at the excitation wavelength of the BODIPY sample, and the same excitation wavelength should be used for both measurements.

The fluorescence quantum yield was then calculated using the following equation:

$$\varphi_F = \varphi_{F\,ref}\left(\frac{I\eta^2 A_{ref}}{I_{ref}\eta_{ref}^2 A}\right)$$

Where $\varphi_{F\,ref}$ is the fluorescence quantum yield of the reference compound, I is the area under the emission peak, η is the refractive index of the solvent, and A is the absorbance at the excitation wavelength.

Compound	Quantum yield reference	$\phi_{F\,ref}$ (solvent)	Solvent	η	Reference solvent	η_{ref}	λ_{ex} /nm	A	A_{ref}	I	I_{ref}	ϕ_F
2.13	Oxazine 1	0.11 (MeOH)[174]	DCM	1.4125	MeOH	1.3145	590	0.05080	0.05138	7555728	1659292	0.58
2.18	Cresyl Violet	0.54 (MeOH)[175]	hexane	1.3741	MeOH	1.3145	520	0.0106	0.0106	8667874	10469931	0.49
2.32	Cresyl Violet	0.54 (MeOH)[175]	DCM	1.4125	MeOH	1.3145	528	0.010	0.010	870533	1877058	0.41
2.33	Cresyl Violet	0.54 (MeOH)[175]	DCM	1.4125	MeOH	1.3145	535	0.013	0.013	74234	1807890	0.25
2.34	Cresyl Violet	0.54 (MeOH)[175]	DCM	1.4125	MeOH	1.3145	545	0.017	0.017	1930163	3165515	0.37
2.35	Cresyl Violet	0.54 (MeOH)[175]	DCM	1.4125	MeOH	1.3145	535	0.013	0.013	1267511	1807890	0.43
3.15	Oxazine 1	0.11 (MeOH)[174]	DCM	1.4125	MeOH	1.3145	590	0.05321	0.05138	8219872	1659292	0.60
3.16	Cresyl Violet	0.54 (MeOH)[175]	DCM	1.4125	MeOH	1.3145	535	0.0207	0.0207	2163451	2053192	0.85
3.19	Rhodamine 6G	0.92 (H_2O)[176]	DCM	1.4125	H_2O	1.333	507	0.0427	0.0427	1303785	7450201	0.18
3.21	Cresyl Violet	0.54 (MeOH)[175]	DCM	1.4125	MeOH	1.3145	566	0.0408	0.0408	2360485	4141907	0.46
3.23	Cresyl Violet	0.54 (MeOH)[175]	DCM	1.4125	MeOH	1.3145	545	0.0270	0.0270	480311	2753627	0.14
4.1	Oxazine 1	0.11 (MeOH)[174]	DCM	1.4125	MeOH	1.3145	590	0.05138	0.05138	3222627	1659292	0.24

Table 5.1: Data used to calculate the fluorescence quantum yields of final BODIPY products.

5.3.4 Experimental and Calculated Electronic Circular Dichroism Spectra

5.3.4.1 3-(4-(methoxycarbonyl)phenyl)-10,15-dioxa-2a^1,3a^1-diaza-10a-borabenzo[5,6]indeno[1,7-*ef*]aceanthrylen-2a^1-ium-16-uide (*N,N,O,C*-BODIPY **2.18**)

Boltzmann-weighted UV-vis and ECD spectra for the postulated enantiomer (*M*)-(+)-**2.18** were obtained from TD-DFT calculations at the cam-B3LYP/6-311++G(3df,2pd) level.[177] First a low-energy conformation library was generated, followed by calculation of the individual ECD spectra for each of the low-energy conformations. The combined Boltzmann-weighted spectrum was blue-shift corrected by 10 nm, to compensate for the typical underestimation of transition energies by TD-DFT (Wouter Herrebout).[178]
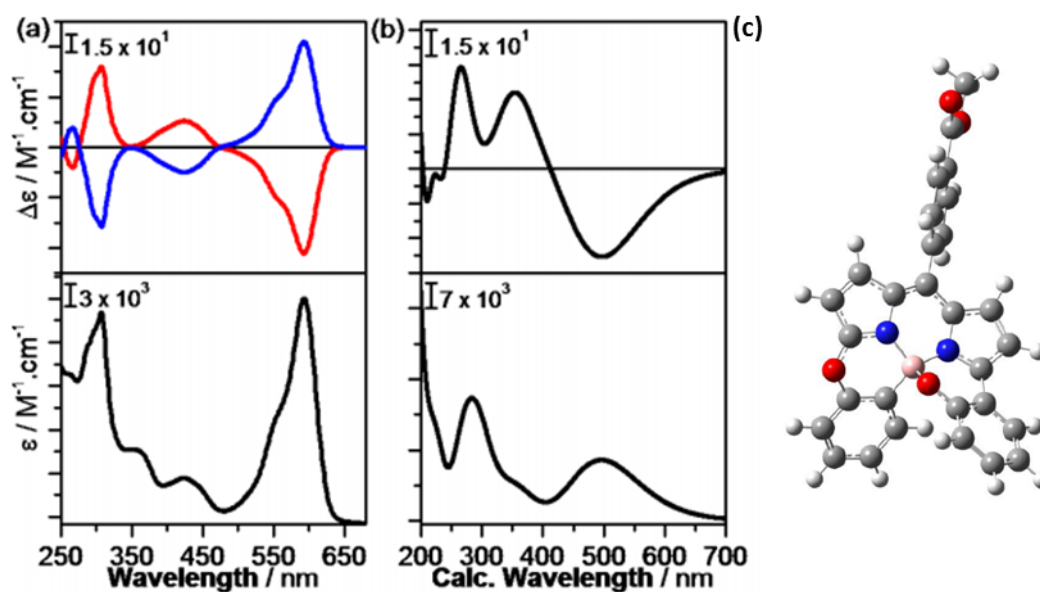
Figure 5.32: (a) Experimental ECD spectra for (*P*)-(-)-**2.18** (blue), (*M*)-(+)-**2.18** (red) and the experimental UV/Vis absorption spectra for (*rac*)-**2.18**; (b) Calculated ECD spectra for the postulated enantiomer (*M*)-(+)-**2.18** (top) and the calculated UV/Vis absorption spectra for (*rac*)-**2.18** (bottom); (c) Structure of the calculated lowest energy conformation of (*M*)-(+)-**2.18**.

<u>5.3.4.2 Methyl 4-(9,14-dimethyl-10,15-dioxa-2a^{1}λ^4,3a^1-diaza-10aλ^4-borabenzo[5,6]indeno[3,4-</u>

<u>*ef*]aceanthrylen-3-yl)benzoate (*N,N,O,C*-BODIPY **2.32**)</u>

Boltzmann-weighted UV-vis and ECD spectra for the postulated enantiomer (*P*)-(-)-**2.32** were obtained from TD-DFT calculations at the cam-B3LYP/6-311++G(3df,2pd) level.[179] First a low-energy conformation library was generated, followed by calculation of the individual ECD spectra for each of the low-energy conformations (Jonathan Bogaerts).

Figure 5.33: (a) Experimental ECD spectra for (*P*)-(-)-**2.32** (orange), (*M*)-(+)-**2.32** (blue) and the calculated ECD spectra for the postulated enantiomer (*P*)-(-)-**2.32**; (b) Structure of the calculated lowest energy conformation of (*P*)-(-)-**2.32**.

<u>5.3.4.3 Methyl 4-(7,12-dimethyl-10,15-dioxa-2a$^1\lambda^4$,3a^1-diaza-10aλ^4-borabenzo[5,6]indeno[3,4-</u>

<u>*ef*]aceanthrylen-3-yl)benzoate (*N,N,O,C*-BODIPY **2.33**)</u>

Boltzmann-weighted UV-vis and ECD spectra for the postulated enantiomer (*P*)-(-)-**2.33** were obtained from TD-DFT calculations at the cam-B3LYP/6-311++G(3df,2pd) level.[179] First a low-energy conformation library was generated, followed by calculation of the individual ECD spectra for each of the low-energy conformations (Jonathan Bogaerts).

Figure 5.34: (a) Experimental ECD spectra for (*P*)-(-)-**2.33** (orange), (*M*)-(+)-**2.33** (blue) and the calculated ECD spectra for the postulated enantiomer (*P*)-(-)-**2.33**; (b) Structure of the calculated lowest energy conformation of (*P*)-(-)-**2.33**.

5.3.4.4 Methyl 4-(7,12-dichloro-10,15-dioxa-2a$^1\lambda^4$,3a^1-diaza-10aλ^4-borabenzo[5,6]indeno[3,4-

ef]aceanthrylen-3-yl)benzoate (*N,N,O,C*-BODIPY **2.34**)

Boltzmann-weighted UV-vis and ECD spectra for the postulated enantiomer (*P*)-(-)-**2.34** were obtained from TD-DFT calculations at the cam-B3LYP/6-311++G(3df,2pd) level.[179] First a low-energy conformation library was generated, followed by calculation of the individual ECD spectra for each of the low-energy conformations (Jonathan Bogaerts).

Figure 5.35: (a) Experimental ECD spectra for (*P*)-(-)-**2.34** (orange), (*M*)-(+)-**2.34** (blue) and the calculated ECD spectra for the postulated enantiomer (*P*)-(-)-**2.34**; (b) Structure of the calculated lowest energy conformation of (*P*)-(-)-**2.34**.

<u>5.3.4.5 Methyl 4-(7,12-difluoro-10,15-dioxa-2a$^1\lambda^4$,3a^1-diaza-10aλ^4-borabenzo[5,6]indeno[3,4-</u>

<u>*ef*]aceanthrylen-3-yl)benzoate (*N,N,O,C*-BODIPY **2.35**)</u>

Boltzmann-weighted UV-vis and ECD spectra for the postulated enantiomer (*P*)-(-)-**2.35** were obtained from TD-DFT calculations at the cam-B3LYP/6-311++G(3df,2pd) level.[179] First a low-energy conformation library was generated, followed by calculation of the individual ECD spectra for each of the low-energy conformations (Jonathan Bogaerts).
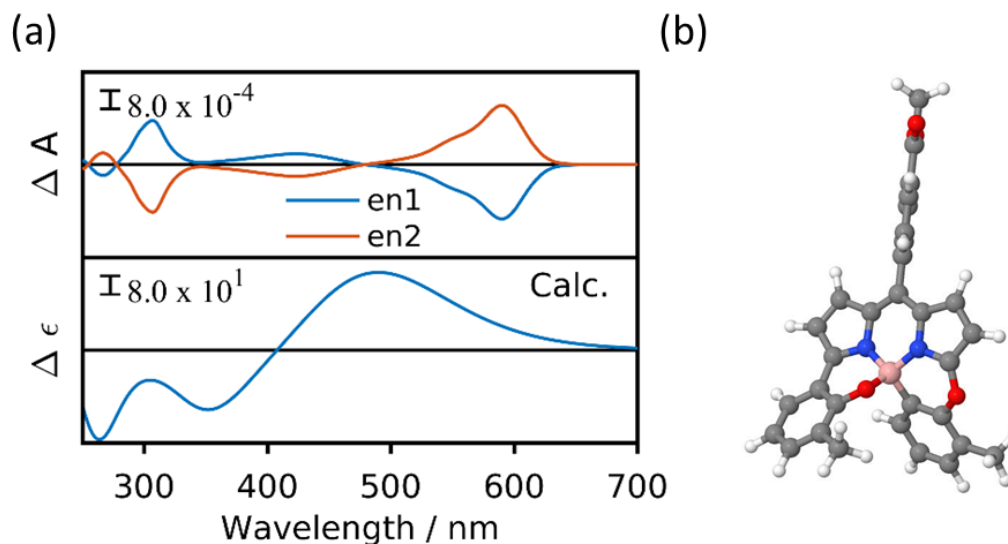

Figure 5.36: (a) Experimental ECD spectra for (*P*)-(-)-**2.35** (orange), (*M*)-(+)-**2.35** (blue) and the calculated ECD spectra for the postulated enantiomer (*P*)-(-)-**2.35**; (b) Structure of the calculated lowest energy conformation of (*P*)-(-)-**2.35**.

5.3.4.6 *N,N,O,O*-BODIPY **4.1**

Boltzmann-weighted UV-vis and ECD spectra for the postulated enantiomer (*M*)-(+)-**2.18** were obtained from TD-DFT calculations at the cam-B3LYP/6-311++G(3df,2pd) level.[177] First a low-energy conformation library was generated, followed by calculation of the individual ECD spectra for each of the low-energy conformations. Due to unsatisfactory agreement between the calculated and experimental ECD spectra using the TD-DFT calculations at the cam-B3LYP/6-311++G(3df,2pd) level, calculations were repeated at the B3LYP and B3PW91 levels. It was found that the best agreement between the experimental and calculated ECD spectra was obtained using TD-DFT calculations at the B3LYP level (Jonathan Bogaerts and Wouter Herrebout).
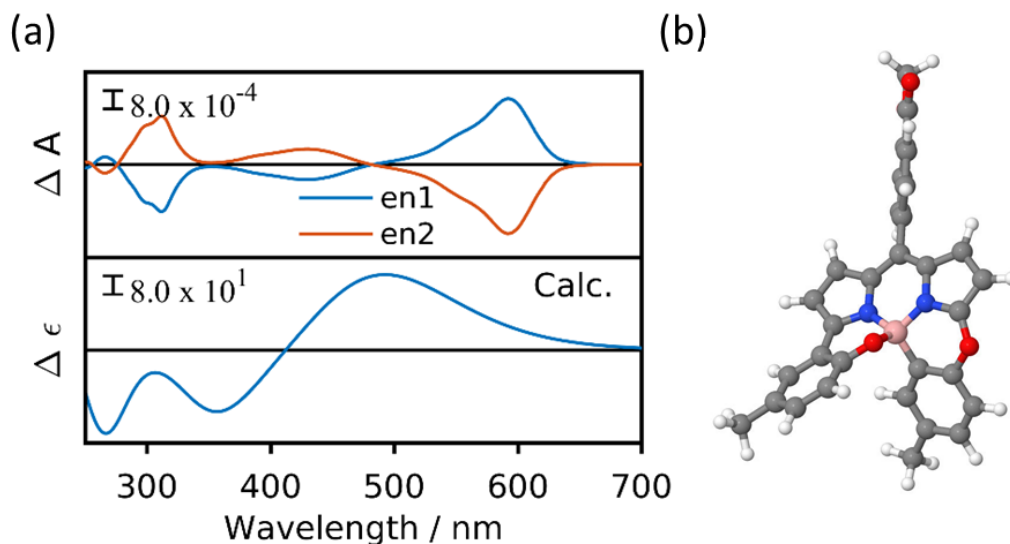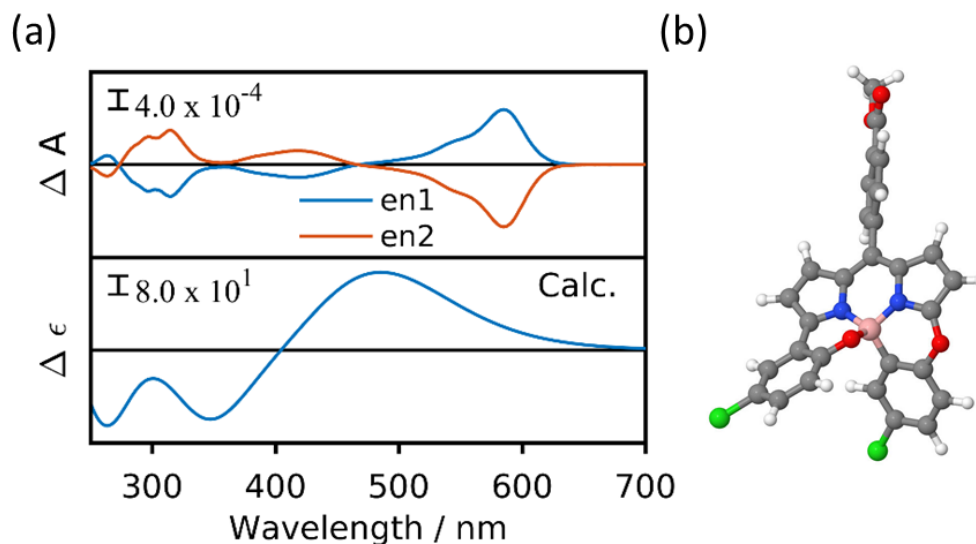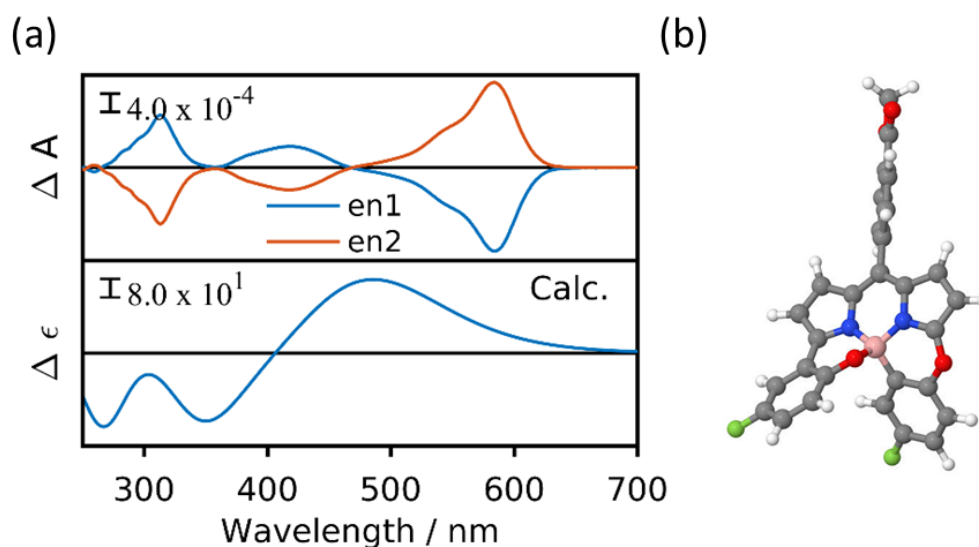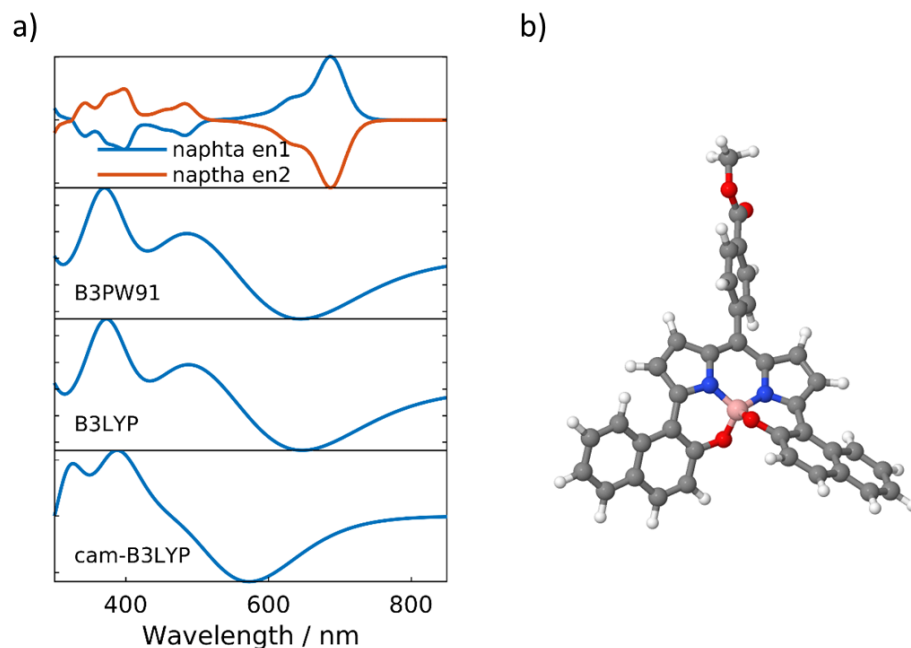

Figure 5.37: (a) Experimental ECD spectra for (*P*)-(-)-**4.1** (blue), (*M*)-(+)-**4.1** (orange) and the calculated ECD spectra for the postulated enantiomer (*M*)-(-)-**4.1**; (b) Structure of the calculated lowest energy conformation of (*M*)-(-)-**4.1**.

5.3.5 Circularly Polarised Luminescence Spectra

The CPL spectra were recorded on a custom built spectrometer 15 consisting of a laser driven light source (Energetiq EQ-99 LDLS, spectral range 170 to 2100 nm) coupled to an Acton SP2150 monochromator (600 g/nm, 300 nm Blaze) that allows excitation wavelengths to be selected with a 6 nm FWHM band-pass. The collection of the emitted light was facilitated (90° angle set up, 1 cm path length quartz cuvette) by a Lock-In Amplifier (Hinds Instruments Signaloc 2100) and Photoelastic Modulator (Hinds Instruments PEM-90). The differentiated light was focused onto an Acton SP2150 monochromator (1200 g/nm, 500 nm Blaze) equipped with a high sensitivity cooled Photo Multiplier Tube (Hamamatsu 10723-20 red corrected). The detection of the CPL signal was achieved using the field modulation lockin technique. The electronic signal from the PMT was fed into the lock-in amplifier (Hinds Instruments Signaloc 2100). The reference signal for the lock-in detection was provided by the PEM control unit. The monochromators, PEM control unit and lockin amplifier were interfaced with a desktop PC and controlled by Labview2013 code. A correction factor for the wavelength dependence of the detection system was constructed using a calibrated lamp (Ocean Optics, CAL_200). The measured raw data was subsequently corrected using this correction factor. The validation of the CPL detection systems was achieved using a light emitting diodes (LEDs) at v650 nm wavelength. The LED was mounted in the sample holder and the light from the LED was fed through a broad-band polarising filter and quarter wave plate (Thor Labs) to generate circularly polarised light. Prior to all measurements, this technique was used to set the phase of the lock-in amplifier correctly. Spectra were recorded using a 5 spectral average sequence in the range of 400-800 nm, with 0.5 nm spectral intervals and using a 500 microsecond integration time.

All CPL spectra were collected by either Dr Robert Pal (*N,N,O,C*-BODIPY **2.18**) or Dr Lewis Mackenzie.

5.3.5.1 3-(4-(methoxycarbonyl)phenyl)-10,15-dioxa-2a^1,3a^1-diaza-10a-borabenzo[5,6]indeno[1,7-*ef*]aceanthrylen-2a^1-ium-16-uide (*N,N,O,C*-BODIPY **2.18**)
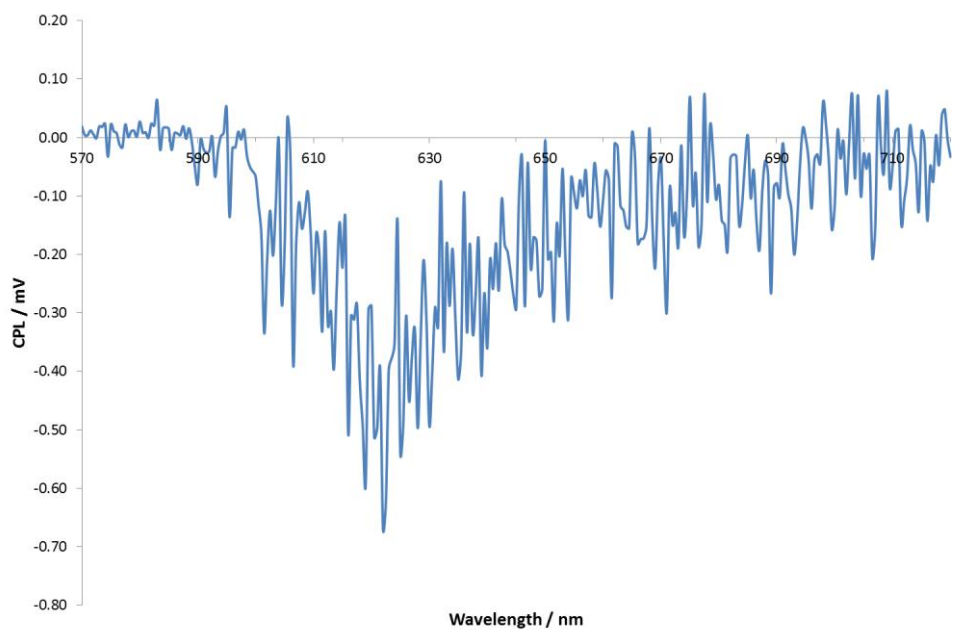
Figure 5.38: Experimental CPL spectra of (*M*)-(+)-**2.18**.
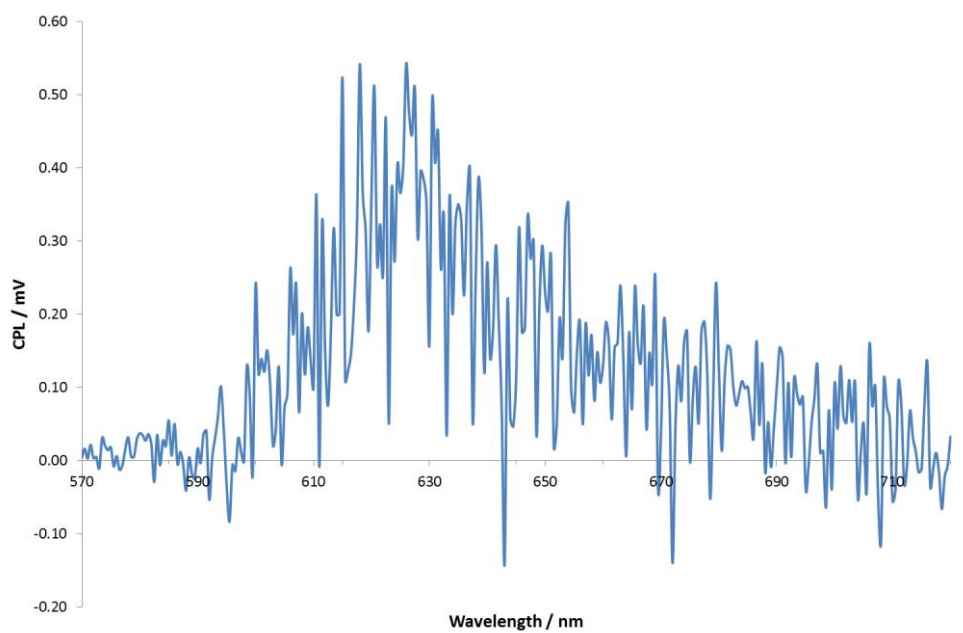
Figure 5.39: Experimental CPL spectra of (*P*)-(-)-**2.18**.

5.3.5.2 Methyl 4-(9,14-dimethyl-10,15-dioxa-2a^{1}λ^4,3a^1-diaza-10aλ^4-borabenzo[5,6]indeno[3,4-*ef*]aceanthrylen-3-yl)benzoate (*N,N,O,C*-BODIPY **2.32**)
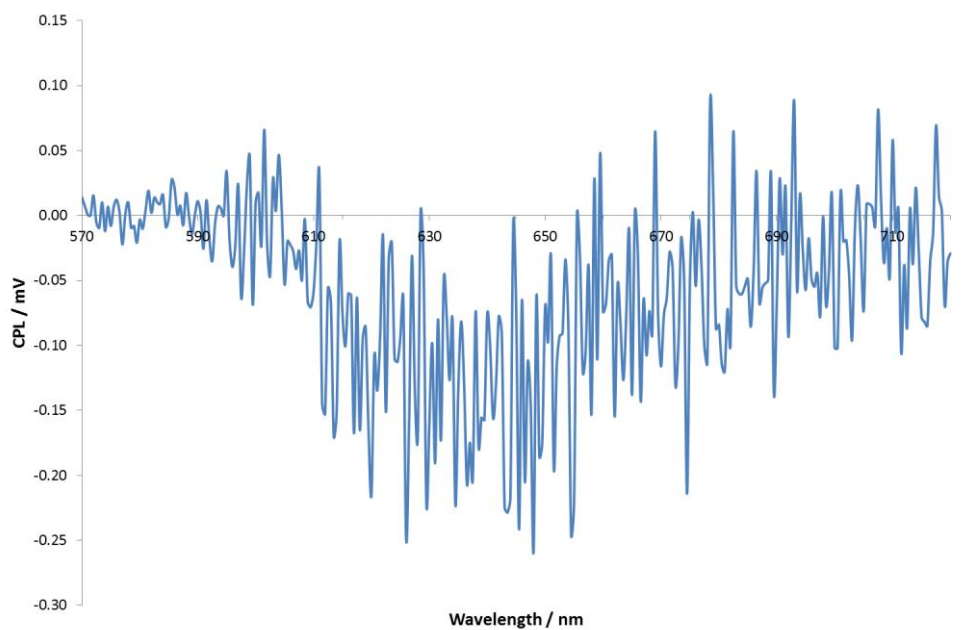
Figure 5.40: Experimental CPL spectra of (*M*)-(+)-**2.32**.
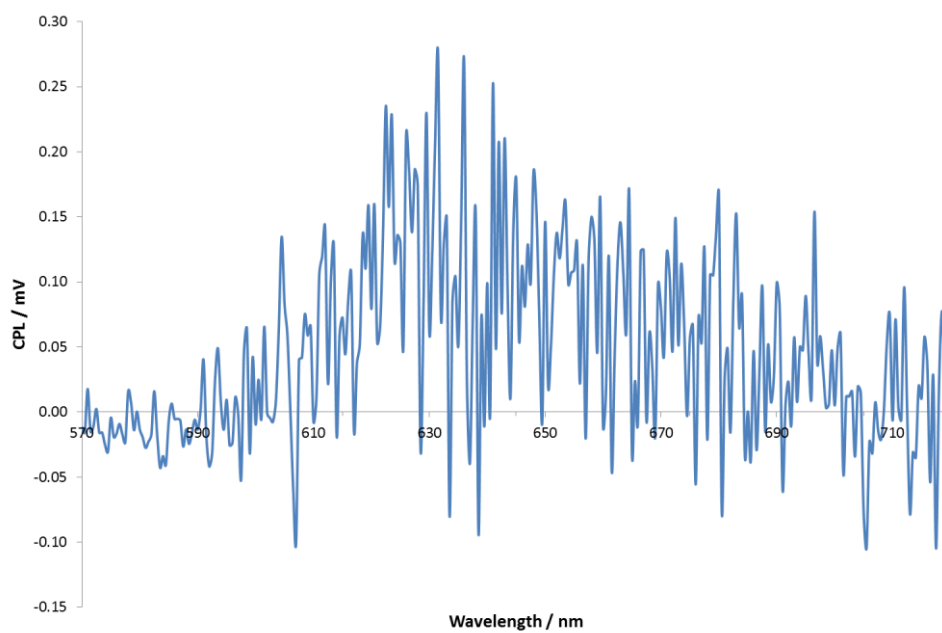
Figure 5.41: Experimental CPL spectra of (*P*)-(-)-**2.32**.

5.3.5.3 Methyl 4-(7,12-dimethyl-10,15-dioxa-2a$^1\lambda^4$,3a^1-diaza-10aλ^4-borabenzo[5,6]indeno[3,4-*ef*]aceanthrylen-3-yl)benzoate (*N,N,O,C*-BODIPY **2.33**)
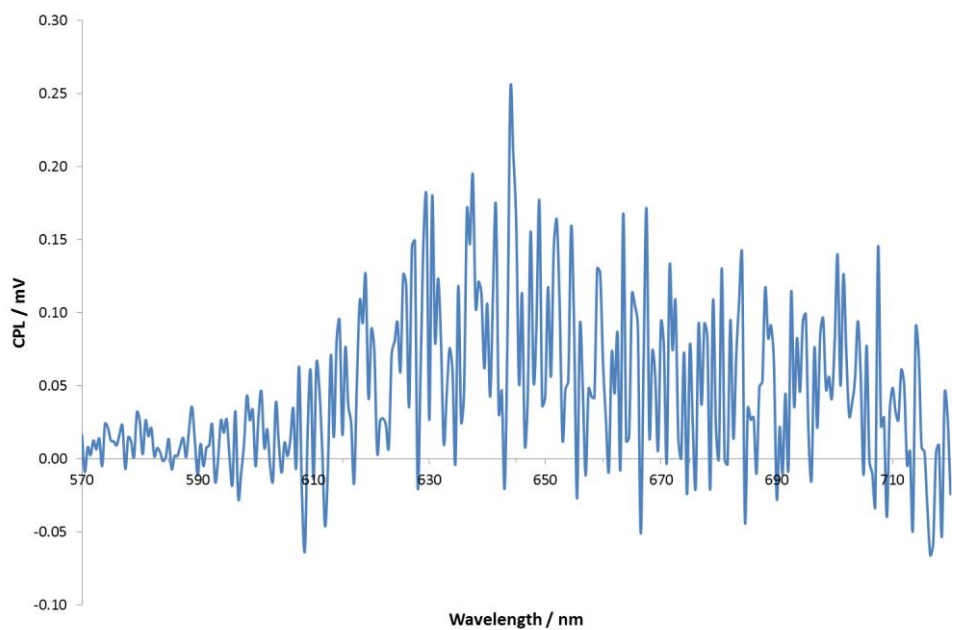
Figure 5.42: Experimental CPL spectra of (*P*)-(-)-**2.33**.
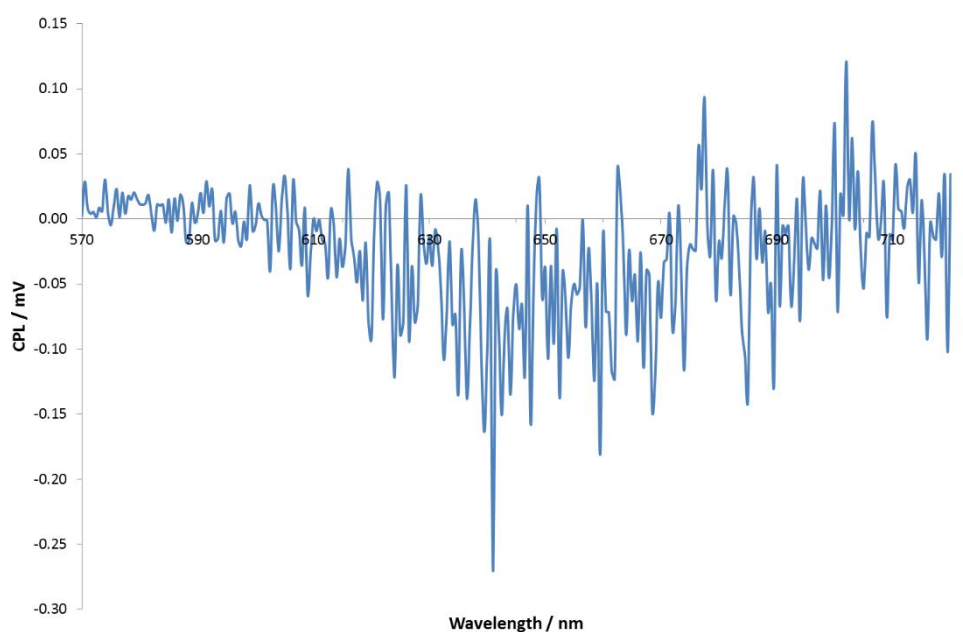
Figure 5.43: Experimental CPL spectra of (*M*)-(+)-**2.33**.

5.3.5.4 Methyl 4-(7,12-dichloro-10,15-dioxa-2a^{1}λ^4,3a^1-diaza-10aλ^4-borabenzo[5,6]indeno[3,4-*ef*]aceanthrylen-3-yl)benzoate (*N,N,O,C*-BODIPY **2.34**)
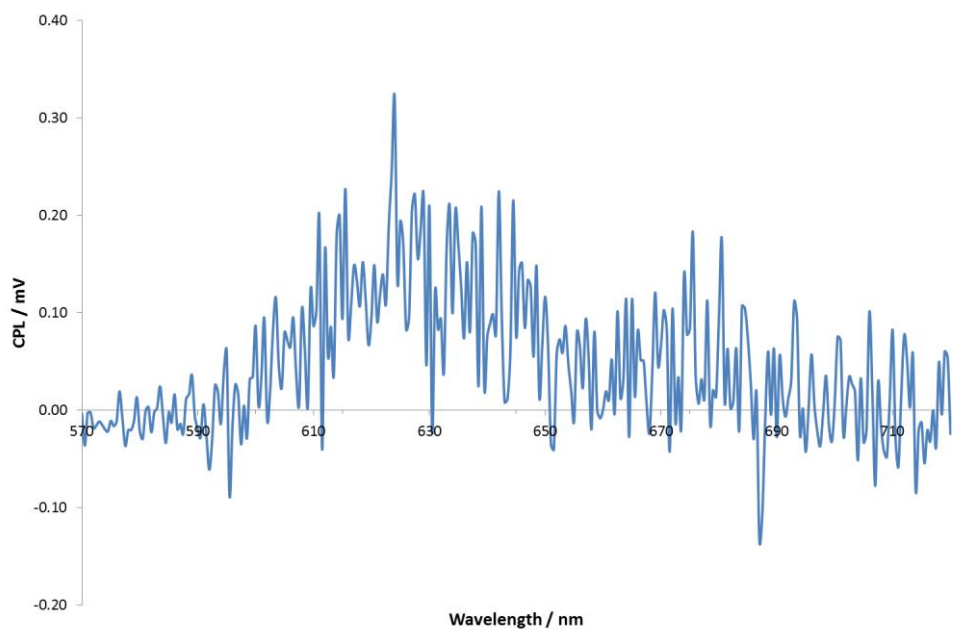
Figure 5.44: Experimental CPL spectra of (*P*)-(-)-**2.34**.
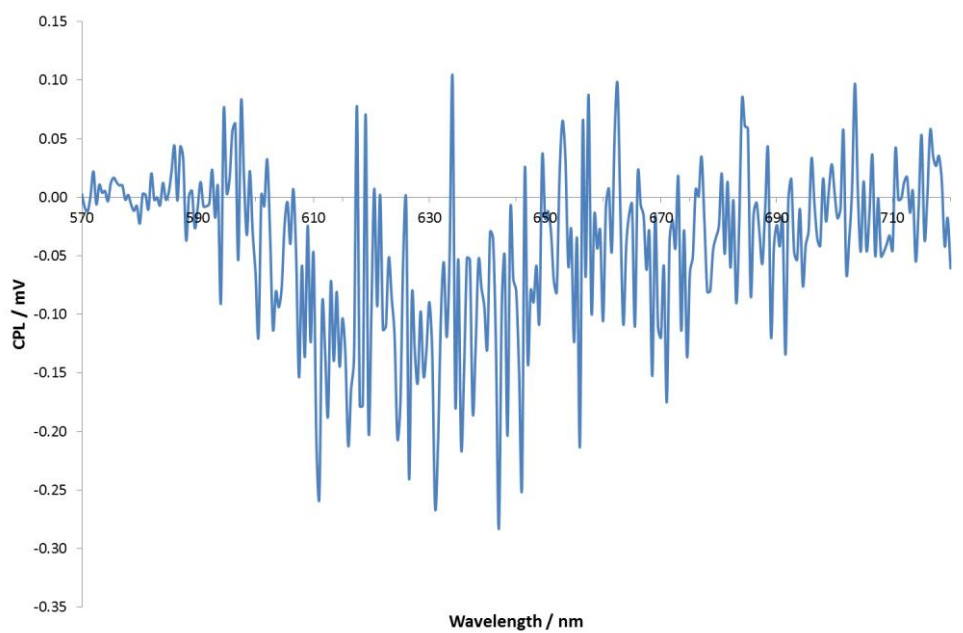
Figure 5.44: Experimental CPL spectra of (*M*)-(+)-**2.34**.

5.3.5.5 Methyl 4-(7,12-difluoro-10,15-dioxa-2a$^1\lambda^4$,3a^1-diaza-10aλ^4-borabenzo[5,6]indeno[3,4-*ef*]aceanthrylen-3-yl)benzoate (*N,N,O,C*-BODIPY **2.35**)
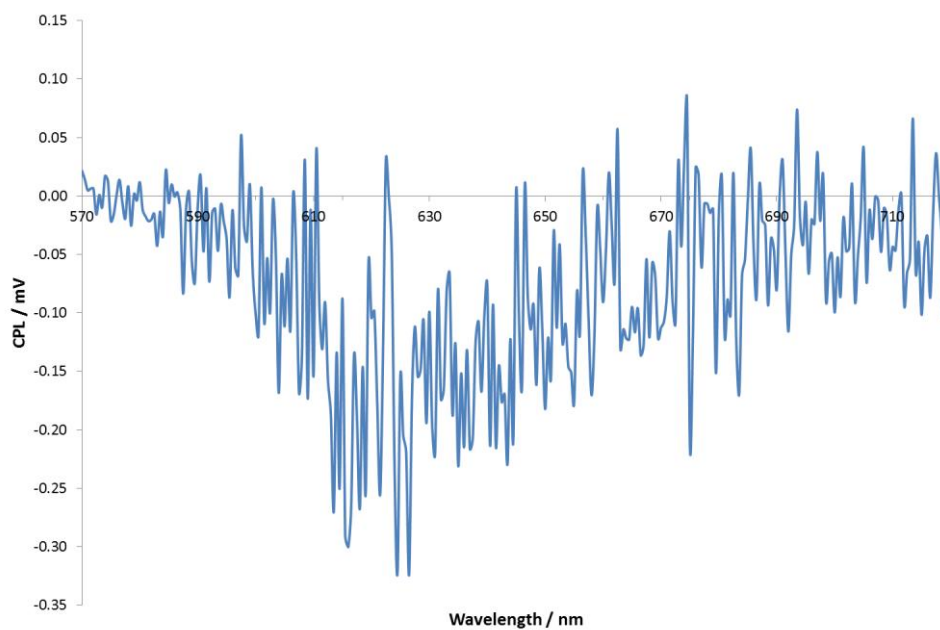
Figure 5.45: Experimental CPL spectra of (*M*)-(+)-**2.35**.
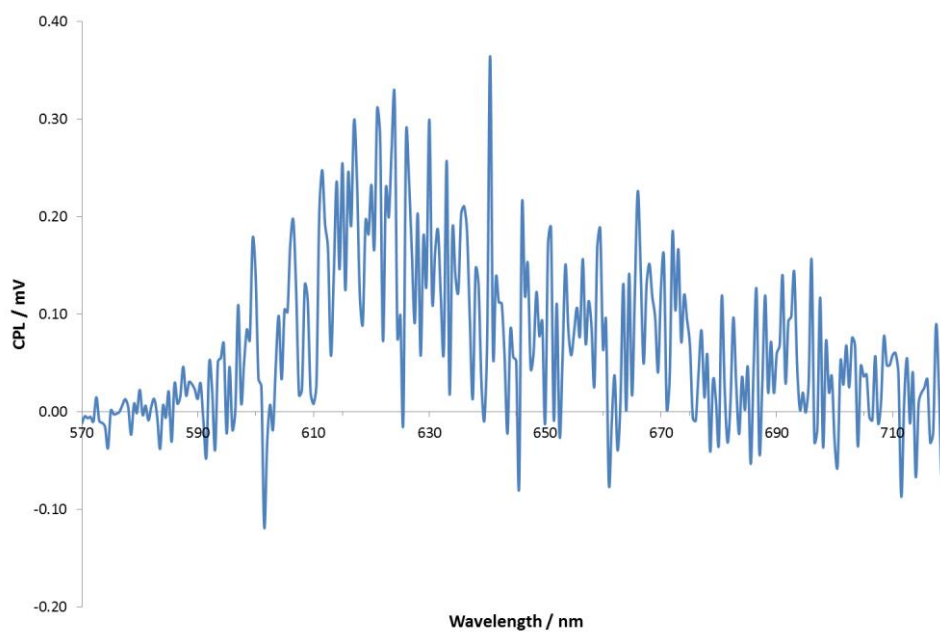
Figure 5.46: Experimental CPL spectra of (*P*)-(-)-**2.35**.

5.3.5.6 Methyl 4-(10b-fluoro-10-((4-(trifluoromethyl)phenyl)thio)-10bH-11-oxa-4b^1,10al^4-diaza-10bl^4-boracyclopenta[e]aceanthrylen-7-yl)benzoate (*N,N,O,F*-BODIPY **3.23**)
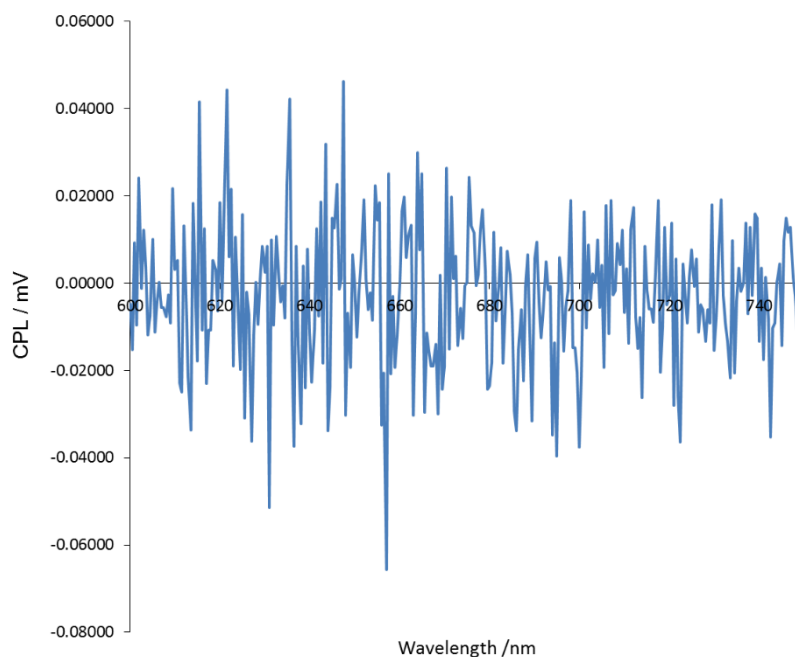
Figure 5.47: Experimental CPL spectra of (-)-**3.23**.
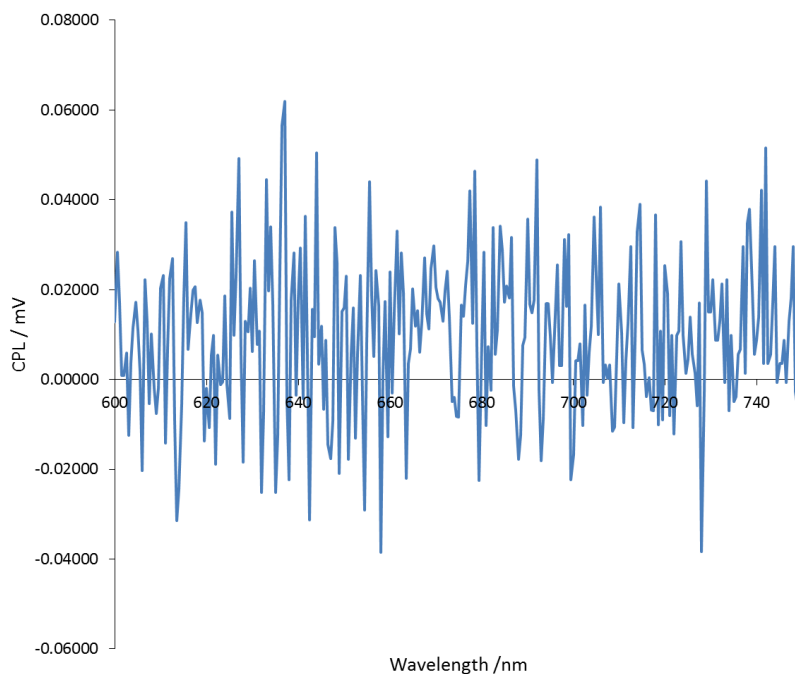
Figure 5.48: Experimental CPL spectra of (+)-**3.23**.

5.3.5.7 *N,N,O,O*-BODIPY **4.1**
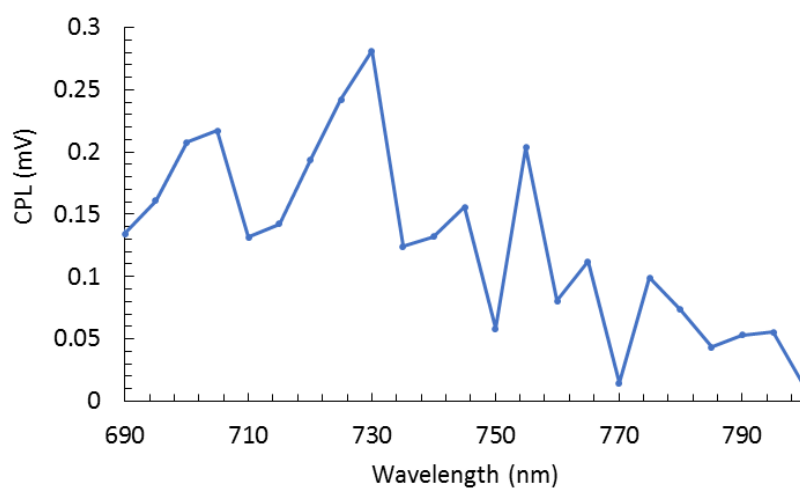
Figure 5.49: Experimental CPL spectra of (-)-**4.1**.
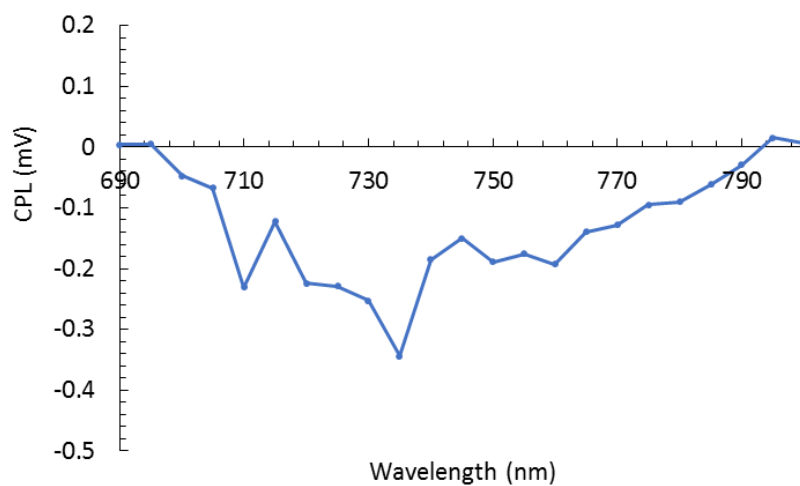
Figure 5.50: Experimental CPL spectra of (+)-**4.1**.

5.3.6 Specific Optical Rotation Measurements

The α_{obs} was calculated according to the following equation:

$$\alpha_{obs} = (R - B_2) - (S - B_1)$$

Where R is the reading for the sample, S is the reading for the solvent, and B_1 and B_2 are blank recordings made before and after the measurement of the sample. Then $[\alpha]_D$ was calculating using the following equation:

$$\alpha_D = \frac{\alpha_{obs}}{C \times d}$$

Where C is the concentration in g/mL, and d is the path length of the cell in dm. In all cases presented, the path length of the cell was 0.5 dm.

Compound	B_1	S	R	B_2	α_{obs}	C	$[\alpha]_D$
(*M*)-(+)-**2.18**	0.000	0.000	0.005	0.000	0.005	4.44×10^{-6}	2252°
(*P*)-(-)-**2.18**	0.000	0.002	-0.003	0.000	-0.005	4.76×10^{-6}	-2100°
(*M*)-(+)-**2.32**	0.005	0.005	0.024	0.010	0.014	5.56×10^{-6}	5034°
(*P*)-(-)-**2.32**	0.006	0.011	0.084	0.094	-0.015	6.19×10^{-6}	-4847°
(*P*)-(-)-**2.33**	0.000	-0.051	-0.072	-0.008	-0.013	4.60×10^{-6}	-5652°
(*M*)-(+)-**2.33**	-0.018	0.021	0.025	-0.028	0.014	6.43×10^{-6}	4355°
(*P*)-(-)-**2.34**	0.000	0.106	-0.020	-0.010	-0.116	1.88×10^{-6}	-123404°
(*M*)-(+)-**2.34**	0.000	-0.008	0.150	0.052	0.106	1.88×10^{-6}	112766°
(*M*)-(+)-**2.35**	-0.001	-0.011	0.050	-0.001	0.061	5.52×10^{-6}	22101°
(*P*)-(-)-**2.35**	-0.001	-0.018	-0.067	-0.009	-0.041	6.68×10^{-6}	-12275°
(-)-**3.23**	0.000	-0.037	-0.087	-0.019	-0.105	6.9×10^{-6}	-30434°
(+)-**3.23**	0.004	-0.020	0.023	-0.019	0.066	6.7×10^{-6}	19701°
(-)-**4.1**	0.054	0.079	0.045	0.110	-0.09	2.94×10^{-6}	-61224°
(+)-**4.1**	0.110	0.086	0.176	0.110	0.09	3.89×10^{-6}	46272°

Table 5.2: Measurements used to calculate the specific optical rotation ($[\alpha]_D$).

5.4 HPLC Methods and Chromatograms

5.4.1 Chapter 2

5.4.1.1 3-(4-(methoxycarbonyl)phenyl)-10,15-dioxa-2a^1,3a^1-diaza-10a-borabenzo[5,6]indeno[1,7-

ef]aceanthrylen-2a^1-ium-16-uide (*N,N,O,C*-BODIPY **2.18**)

Resolution of the enantiomers of *N,N,O,C*-BODIPY **2.18** was performed on a Varian ProStar HPLC, fitted with:

- Autosampler Model 410,
- two Pumps Model 200,
- Column Valve Module Model 500,
- Diode Array Detector Model 335,
- Daicel Chiralpak® IB column, 4.6×250 mm, 5 µm particle size.

A 1 mg/mL solution of *N,N,O,C*-BODIPY **2.18** (in 80:20 hexane:ethyl acetate) was prepared. Runs were performed at a flow rate of 1 mL/minute using 85:15 hexane:ethyl acetate as eluent and a run length of 23 minutes. The detection wavelength used was 580 nm. We performed 12 runs of 20 µL injections and combined the fractions from each run.

Figure 5.51: A typical chromatogram of the resolution of the enantiomers of *N,N,O,C*-BODIPY **2.18**.

After the runs were completed, we resubmitted the collected enantiomers to the same conditions to assess the enantiomeric excess (*ee*).

Figure 5.52: Chromatogram of enantiomer 1 (*M*)-(+)-**2.18** resubmitted to the separation conditions to assess the *ee*.

Figure 5.53: Chromatogram of enantiomer 2 (*P*)-(-)-**2.18** resubmitted to the separation conditions to assess the *ee*.

5.4.1.2 Methyl 4-(9,14-dimethyl-10,15-dioxa-2a$^1\lambda^4$,3a^1-diaza-10aλ^4-borabenzo[5,6]indeno[3,4-

ef]aceanthrylen-3-yl)benzoate (*N,N,O,C*-BODIPY **2.32**)

Resolution of the enantiomers of *N,N,O,C*-BODIPY **2.32** was performed on a Perkin Elmer HPLC, fitted with:

- Perkin Elmer Series 200 Autosampler,
- Perkin Elmer Series 200 Pump,
- Perkin Elmer Peltier Oven Selector Series 200,
- Perkin Elmer Diode Array Detector Series 200,
- Daicel Chiralpak® IA column, 4.6×250 mm, 5 µm particle size.

A 1 mg/mL solution of *N,N,O,C*-BODIPY **2.32** (in 80:20 hexane:DCM) was prepared. Runs were performed at a flow rate of 1 mL/minute using 85:15 hexane:DCM as eluent and a run length of 20 minutes. The detection wavelength used was 580 nm. We performed 6 runs of 20 µL injections and combined the fractions from each run.

Figure 5.54: A typical chromatogram of the resolution of the enantiomers of *N,N,O,C*-BODIPY **2.32**.

After the runs were completed, we resubmitted the collected enantiomers to the same conditions to assess the enantiomeric excess (*ee*).

Figure 5.55: Chromatogram of enantiomer 1 (*M*)-(+)-**2.32** resubmitted to the separation conditions to assess the *ee*.

Figure 5.56: Chromatogram of enantiomer 2 (*P*)-(-)-**2.32** resubmitted to the separation conditions to assess the *ee*.

5.4.1.3 Methyl 4-(7,12-dimethyl-10,15-dioxa-2a$^1\lambda^4$,3a^1-diaza-10aλ^4-borabenzo[5,6]indeno[3,4-*ef*]aceanthrylen-3-yl)benzoate (*N,N,O,C*-BODIPY **2.33**)

Resolution of the enantiomers of *N,N,O,C*-BODIPY **2.33** was performed on a Perkin Elmer HPLC, fitted with:

- Perkin Elmer Series 200 Autosampler,
- Perkin Elmer Series 200 Pump,
- Perkin Elmer Peltier Oven Selector Series 200,
- Perkin Elmer Diode Array Detector Series 200,
- Daicel Chiralpak® IA column, 4.6×250 mm, 5 μm particle size.

A 1 mg/mL solution of *N,N,O,C*-BODIPY **2.33** (in toluene) was prepared. Runs were performed at a flow rate of 1 mL/minute using toluene as eluent and a run length of 10 minutes. The detection wavelength used was 580 nm. We performed 6 runs of 20 μL injections and combined the fractions from each run.

Figure 5.57: A typical chromatogram of the resolution of the enantiomers of *N,N,O,C*-BODIPY **2.33**.

After the runs were completed, we resubmitted the collected enantiomers to the same conditions to assess the enantiomeric excess (*ee*).

Figure 5.58: Chromatogram of enantiomer 1 (*M*)-(+)-**2.33** resubmitted to the separation conditions to assess the *ee*.

Figure 5.59: Chromatogram of enantiomer 2 (*P*)-(-)-**2.33** resubmitted to the separation conditions to assess the *ee*.

5.4.1.4 Methyl 4-(7,12-dichloro-10,15-dioxa-2a$^1\lambda^4$,3a^1-diaza-10aλ^4-borabenzo[5,6]indeno[3,4-*ef*]aceanthrylen-3-yl)benzoate (*N,N,O,C*-BODIPY **2.34**)

Resolution of the enantiomers of *N,N,O,C*-BODIPY **2.34** was performed on a Perkin Elmer HPLC, fitted with:

- Perkin Elmer Series 200 Autosampler,
- Perkin Elmer Series 200 Pump,
- Perkin Elmer Peltier Oven Selector Series 200,
- Perkin Elmer Diode Array Detector Series 200,
- Daicel Chiralpak® IA column, 4.6×250 mm, 5 µm particle size.

A 1 mg/mL solution of *N,N,O,C*-BODIPY **2.34** (in 80:20 toluene:hexane) was prepared. Runs were performed at a flow rate of 1 mL/minute using 80:20 toluene:hexane as eluent and a run length of 10 minutes. The detection wavelength used was 580 nm. We performed 10 runs of 20 µL injections and combined the fractions from each run.
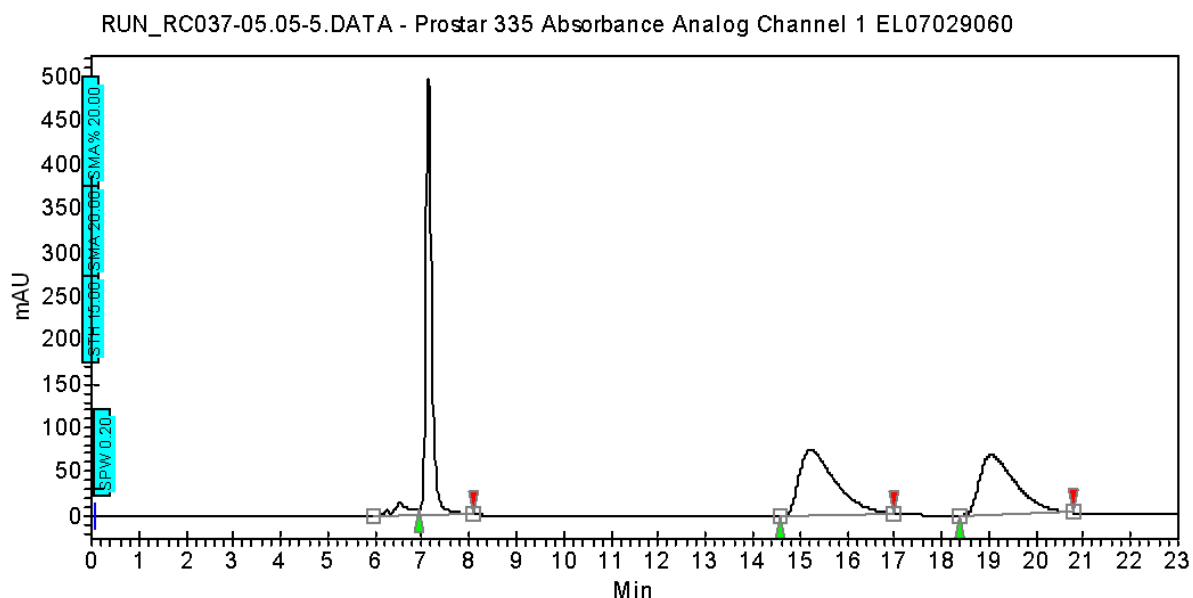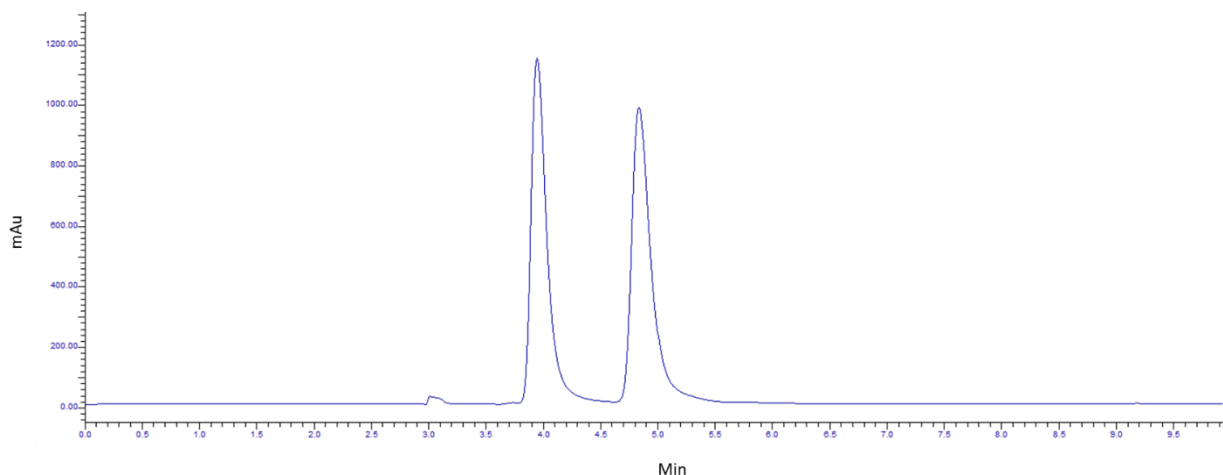

Figure 5.60: A typical chromatogram of the resolution of the enantiomers of *N,N,O,C*-BODIPY **2.34**.

After the runs were completed, we resubmitted the collected enantiomers to the same conditions to assess the enantiomeric excess (*ee*).
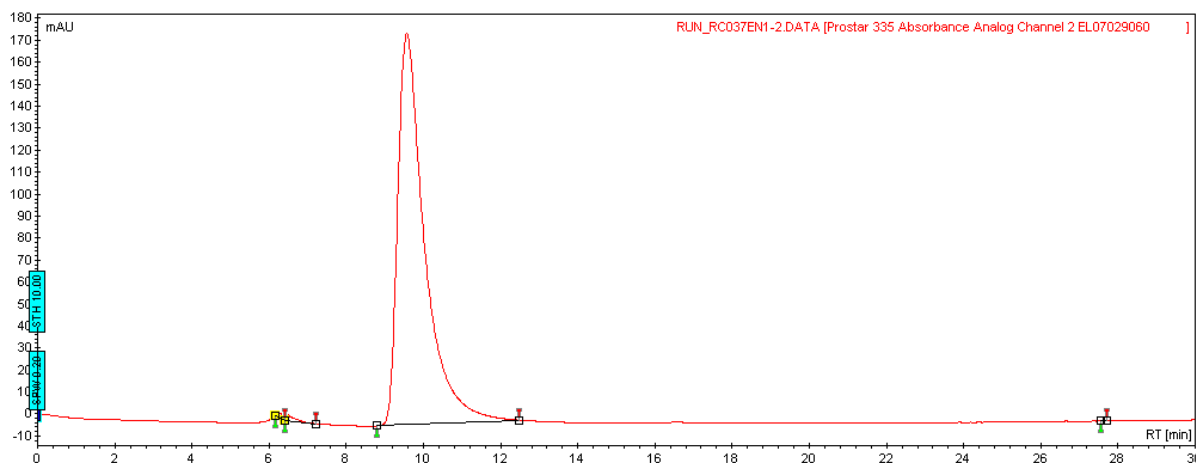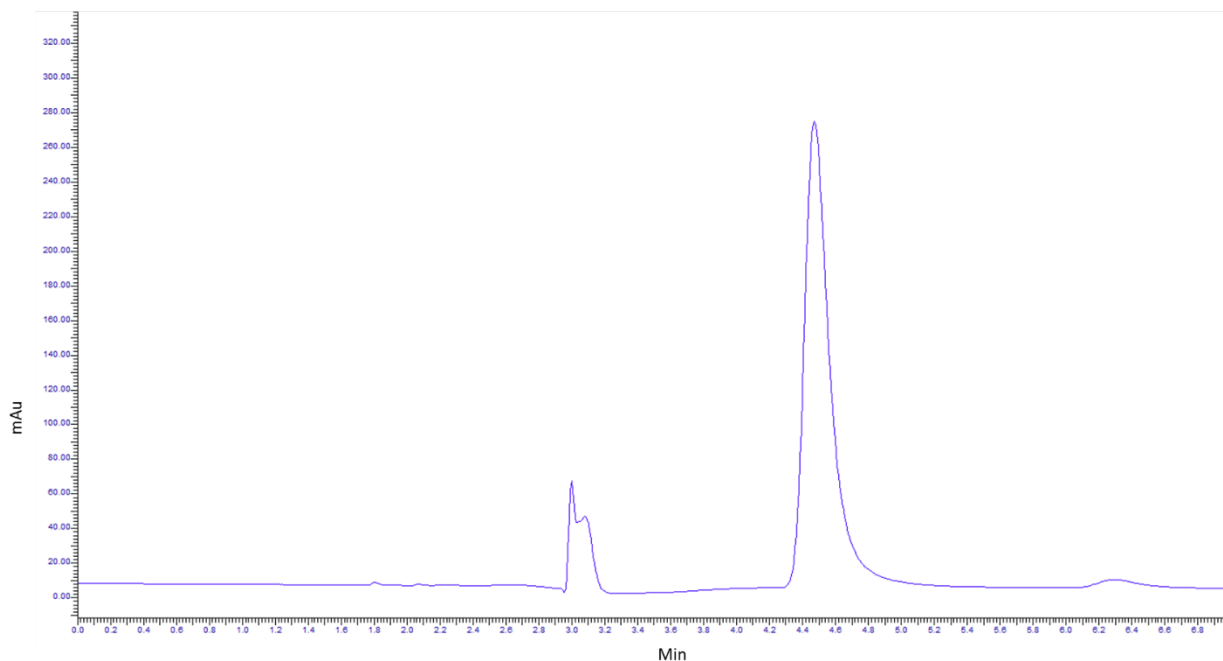

Figure 5.61: Chromatogram of enantiomer 1 (*M*)-(+)-**2.34** resubmitted to the separation conditions to assess the *ee*.
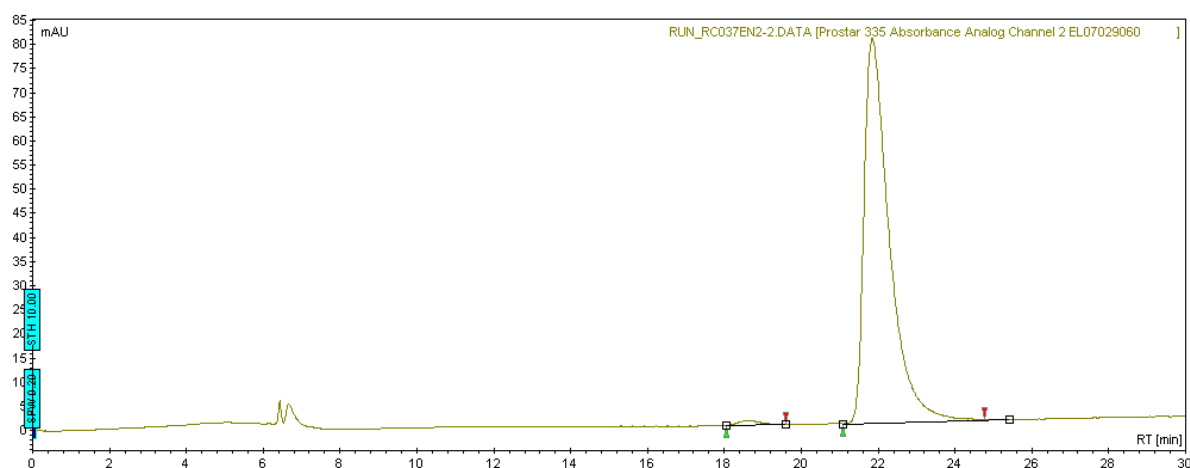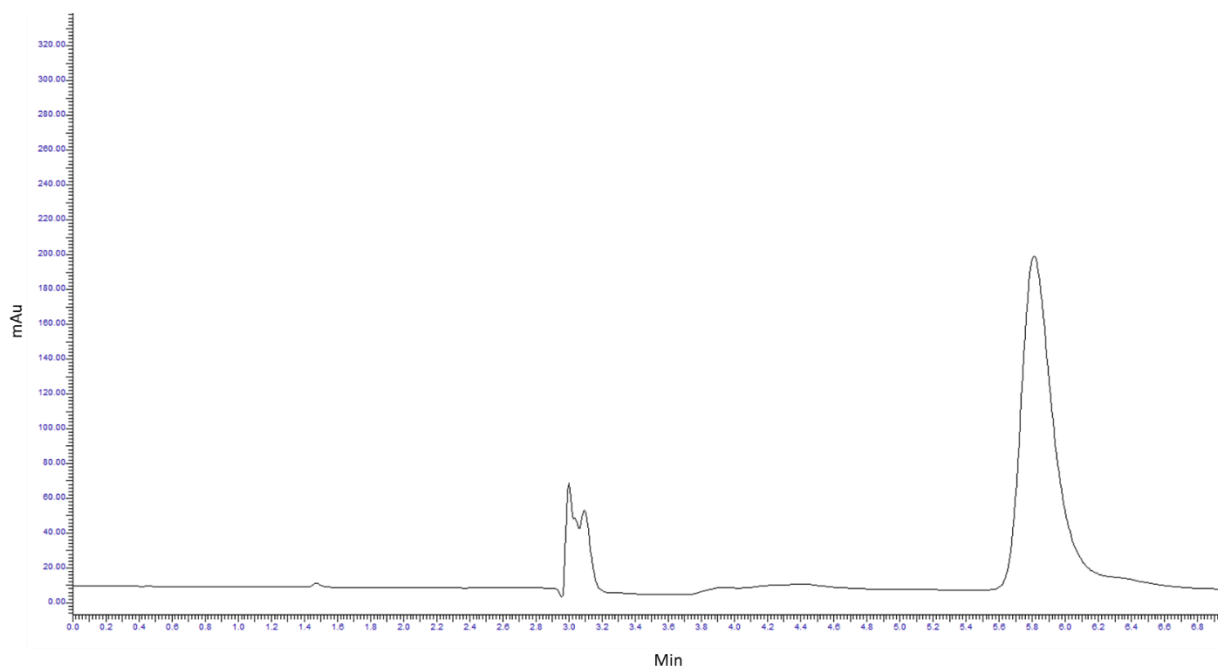
Figure 5.62: Chromatogram of enantiomer 2 (*P*)-(-)-**2.34** resubmitted to the separation conditions to assess the *ee*.

5.4.1.5 Methyl 4-(7,12-difluoro-10,15-dioxa-2a^{1}λ^4,3a^1-diaza-10aλ^4-borabenzo[5,6]indeno[3,4-*ef*]aceanthrylen-3-yl)benzoate (*N,N,O,C*-BODIPY **2.35**)

Resolution of the enantiomers of *N,N,O,C*-BODIPY **2.35** was performed on a Perkin Elmer HPLC, fitted with:

- Perkin Elmer Series 200 Autosampler,
- Perkin Elmer Series 200 Pump,
- Perkin Elmer Peltier Oven Selector Series 200,
- Perkin Elmer Diode Array Detector Series 200,
- Daicel Chiralpak® OD-H column, 4.6×250 mm, 5 μm particle size.

A 1 mg/mL solution of *N,N,O,C*-BODIPY **2.35** (in 95:5 hexane:IPA) was prepared. Runs were performed at a flow rate of 1 mL/minute using toluene as eluent and a run length of 25 minutes. The detection wavelength used was 580 nm. We performed 11 runs of 20 μL injections and combined the fractions from each run.
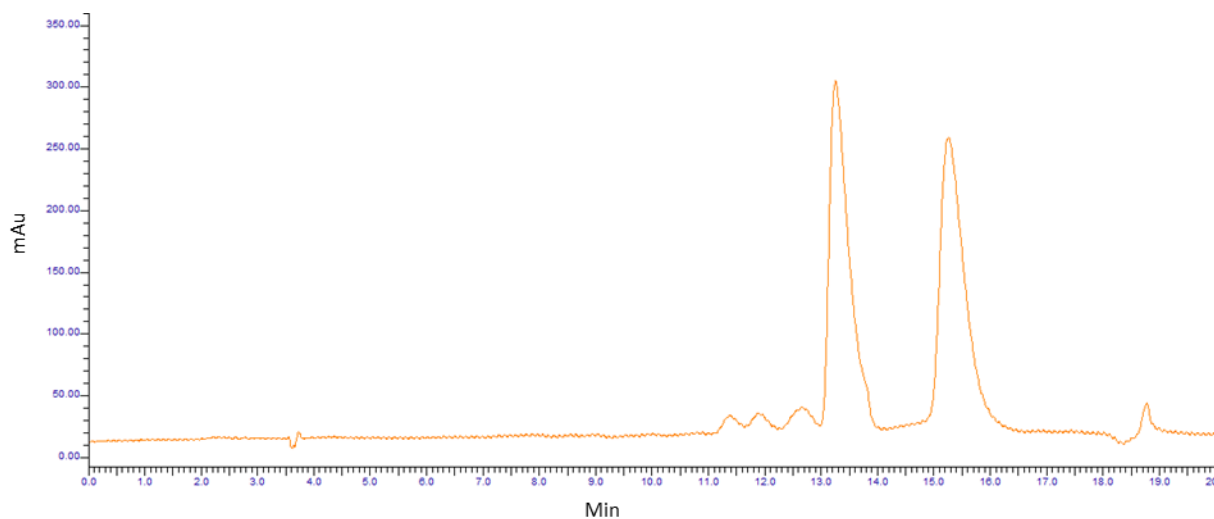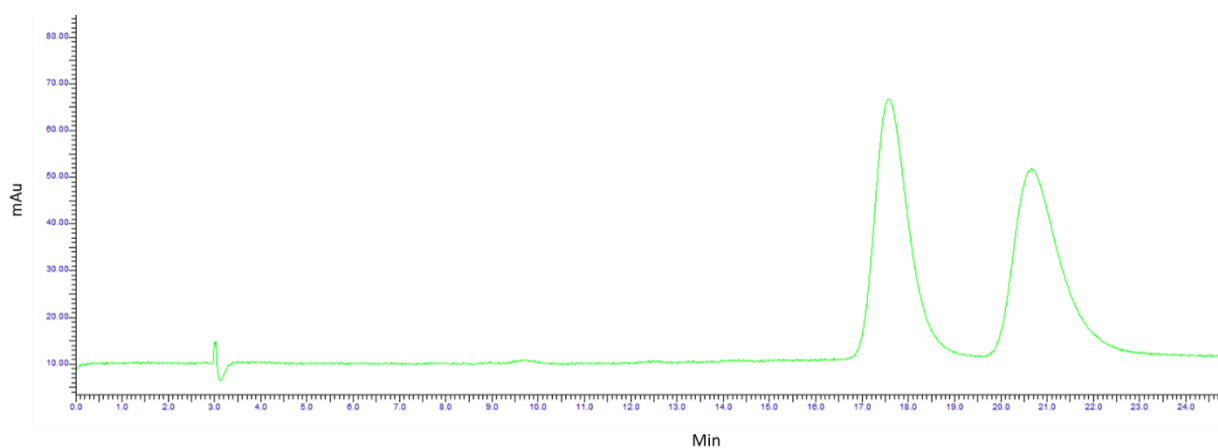

Figure 5.63: A typical chromatogram of the resolution of the enantiomers of *N,N,O,C*-BODIPY **2.35**.

After the runs were completed, we resubmitted the collected enantiomers to the same conditions to assess the enantiomeric excess (*ee*).
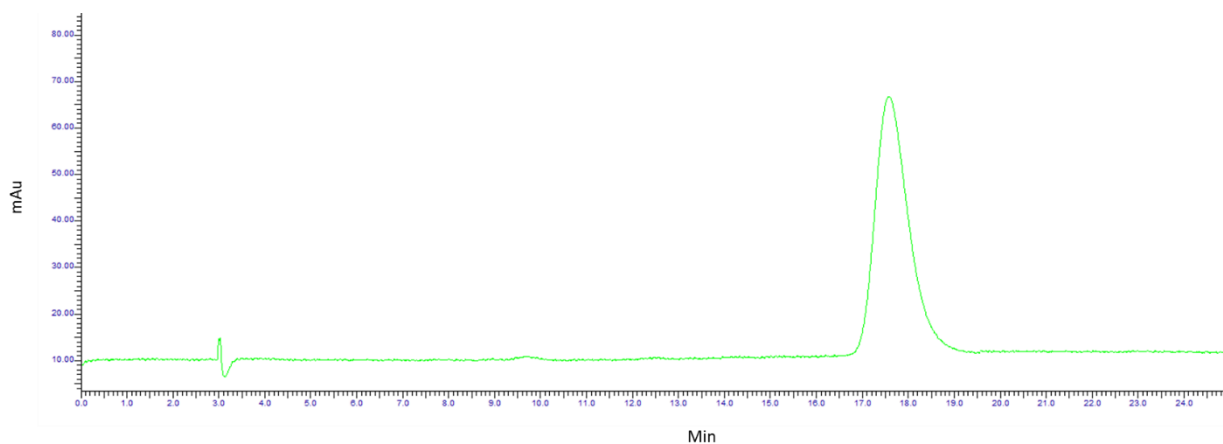
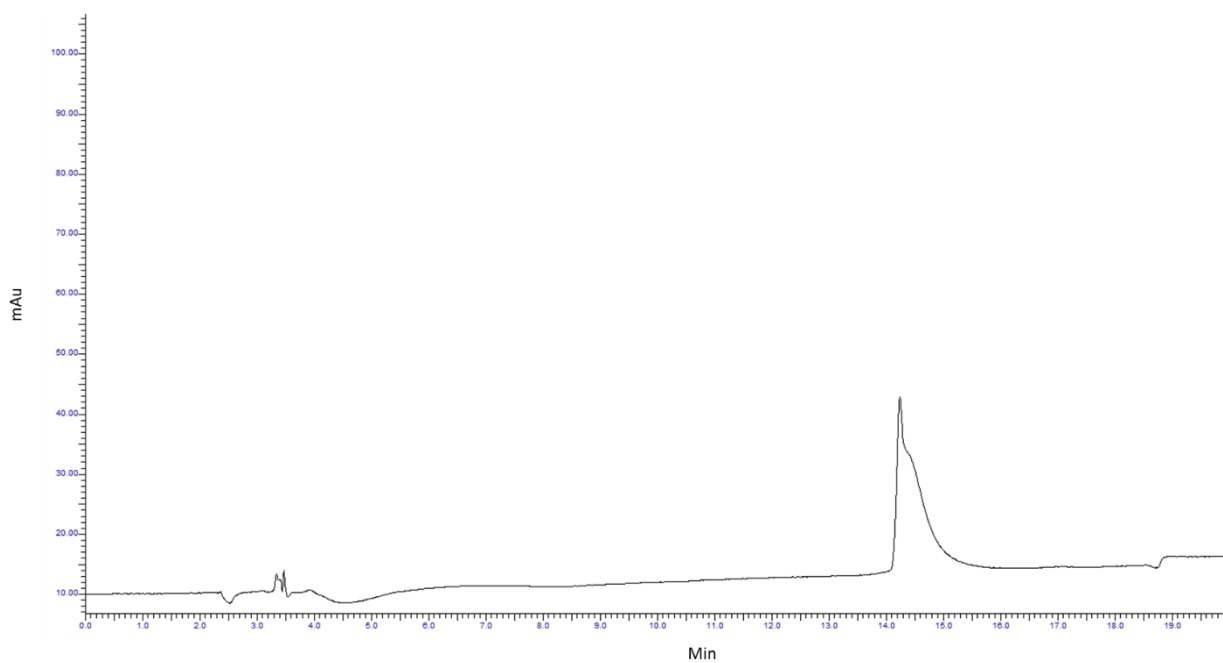**Figure 5.64**: Chromatogram of enantiomer 1 (*M*)-(+)-**2.35** resubmitted to the separation conditions to assess the *ee*.
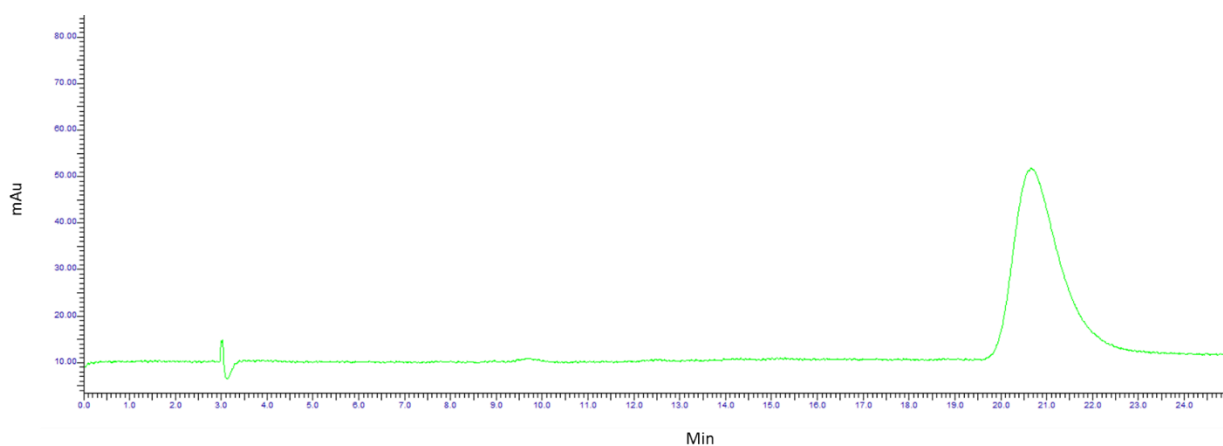
Figure 5.65: Chromatogram of enantiomer 2 (*P*)-(-)-**2.35** resubmitted to the separation conditions to assess the *ee*.

5.4.2 Chapter 3

5.4.2.1 Methyl 4-(10b-fluoro-10-((4-(trifluoromethyl)phenyl)thio)-10bH-11-oxa-4b^1,10al^4-diaza-10bl^4-boracyclopenta[e]aceanthrylen-7-yl)benzoate (N,N,O,F-BODIPY **3.23**)

Resolution of the enantiomers of N,N,O,F-BODIPY **X** was performed on a Perkin Elmer HPLC, fitted with:

- Perkin Elmer Series 200 Autosampler,
- Perkin Elmer Series 200 Pump,
- Perkin Elmer Peltier Oven Selector Series 200,
- Perkin Elmer Diode Array Detector Series 200,
- Daicel Chiralpak® IA column, 4.6×250 mm, 5 µm particle size.

A 1 mg/mL solution of N,N,O,F-BODIPY **3.23** (in toluene) was prepared. Runs were performed at a flow rate of 1 mL/minute using toluene as eluent and a run length of 20 minutes. The detection wavelength used was 604 nm. We performed 6 runs of 20 µL injections and combined the fractions from each run.
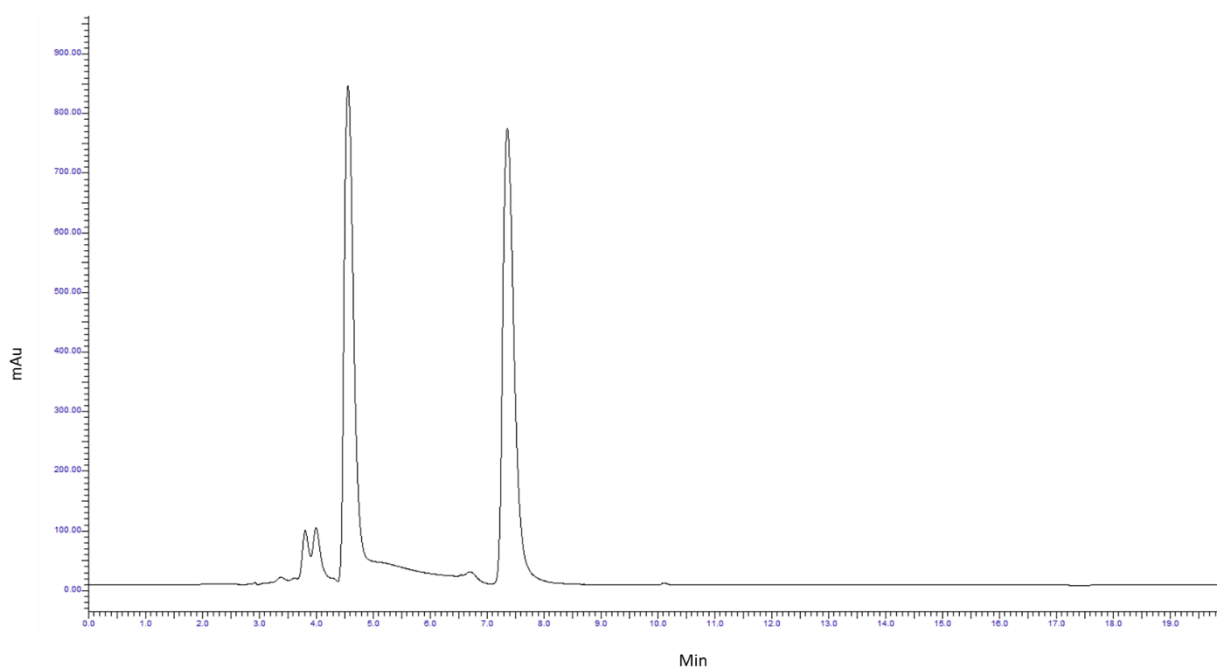
Figure 5.66: A typical chromatogram of the resolution of the enantiomers of N,N,O,F-BODIPY **3.23**.

After the runs were completed, we resubmitted the collected enantiomers to the same conditions to assess the enantiomeric excess (*ee*).
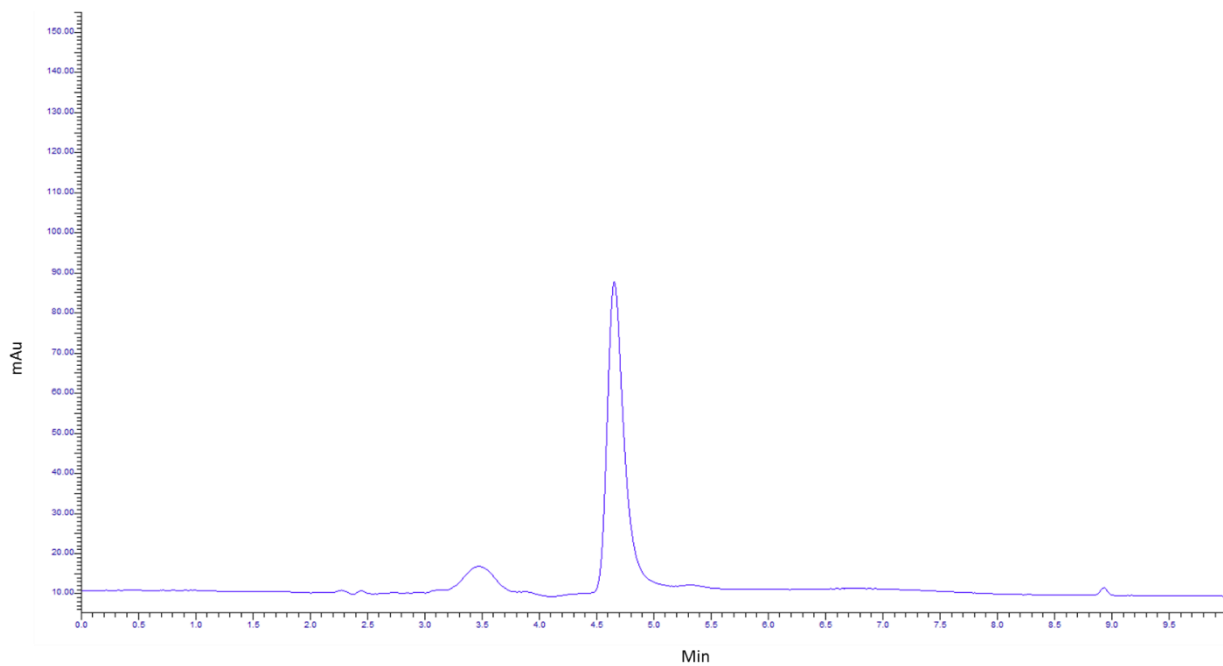
Figure 5.67: Chromatogram of enantiomer 1 (+)-**3.23** resubmitted to the separation conditions to assess the *ee*.
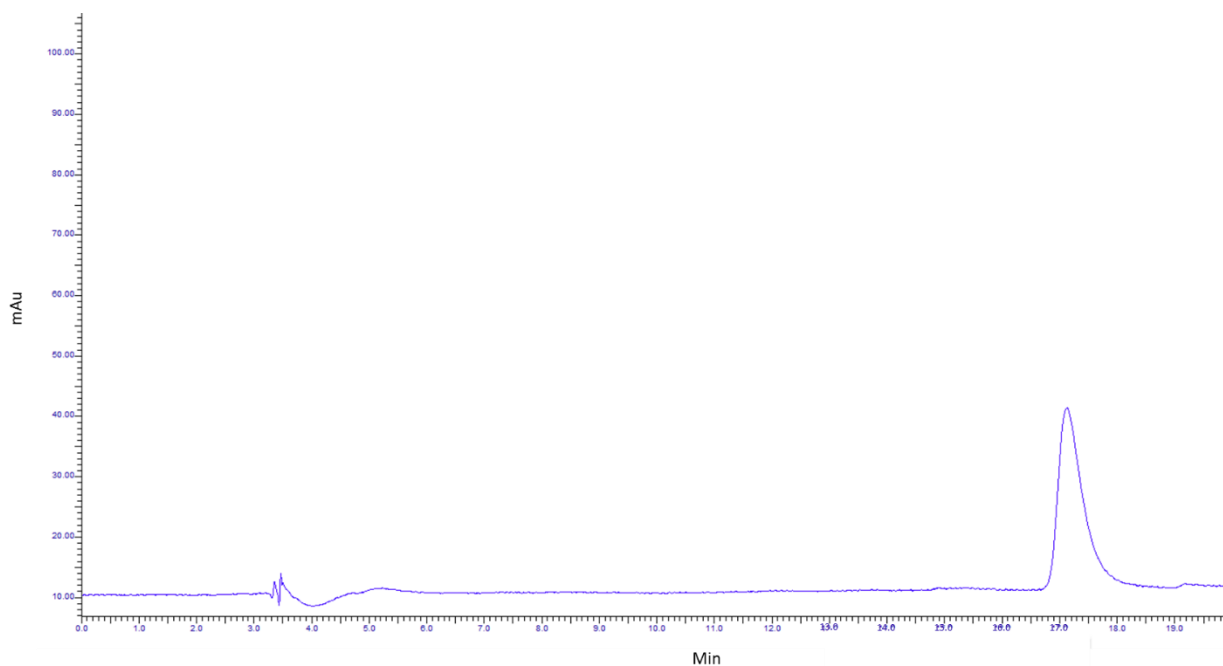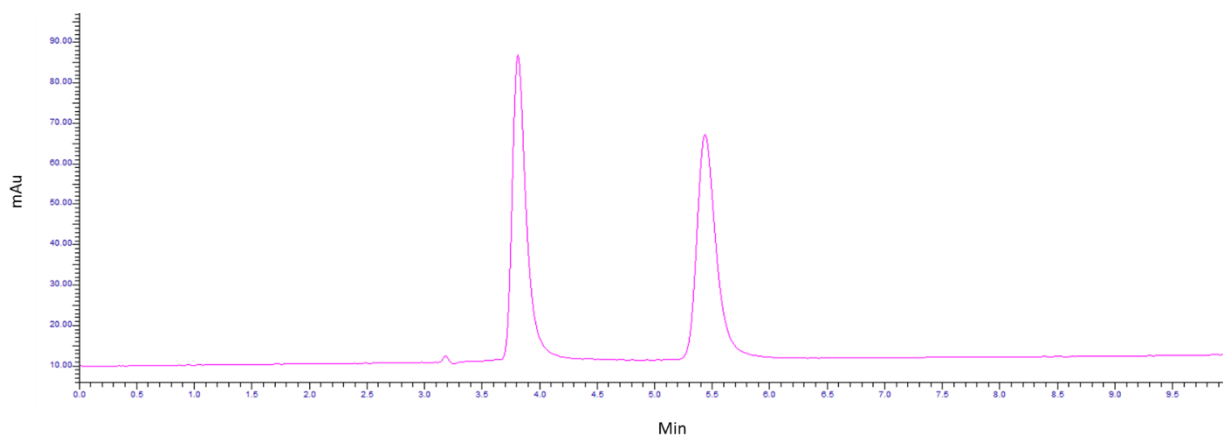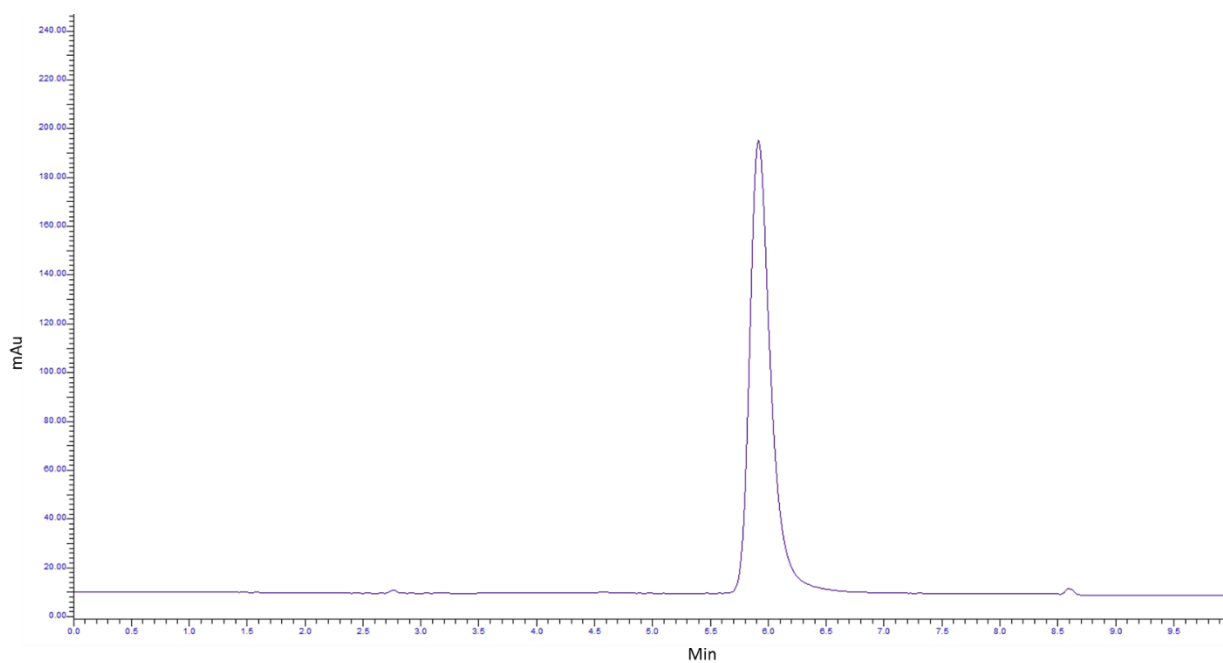

Figure 5.68: Chromatogram of enantiomer 2 (-)-**3.23** resubmitted to the separation conditions to assess the *ee*.

5.4.3 Chapter 4

5.4.3.1 *N,N,O,O*-BODIPY **4.1**

Resolution of the enantiomers of *N,N,O,O*-BODIPY **X** was performed on a Perkin Elmer HPLC, fitted with:

- Perkin Elmer Series 200 Autosampler,
- Perkin Elmer Series 200 Pump,
- Perkin Elmer Peltier Oven Selector Series 200,
- Perkin Elmer UV/Vis Detector Series 200,
- Daicel Chiralpak® IA column, 4.6×250 mm, 5 µm particle size.

A 1 mg/mL solution of *N,N,O,C*-BODIPY **4.1** (in toluene) was prepared. Runs were performed at a flow rate of 1 mL/minute using toluene as eluent and a run length of 20 minutes. The detection wavelength used was 360 nm. We performed 8 runs of 20 µL injections and combined the fractions from each run.
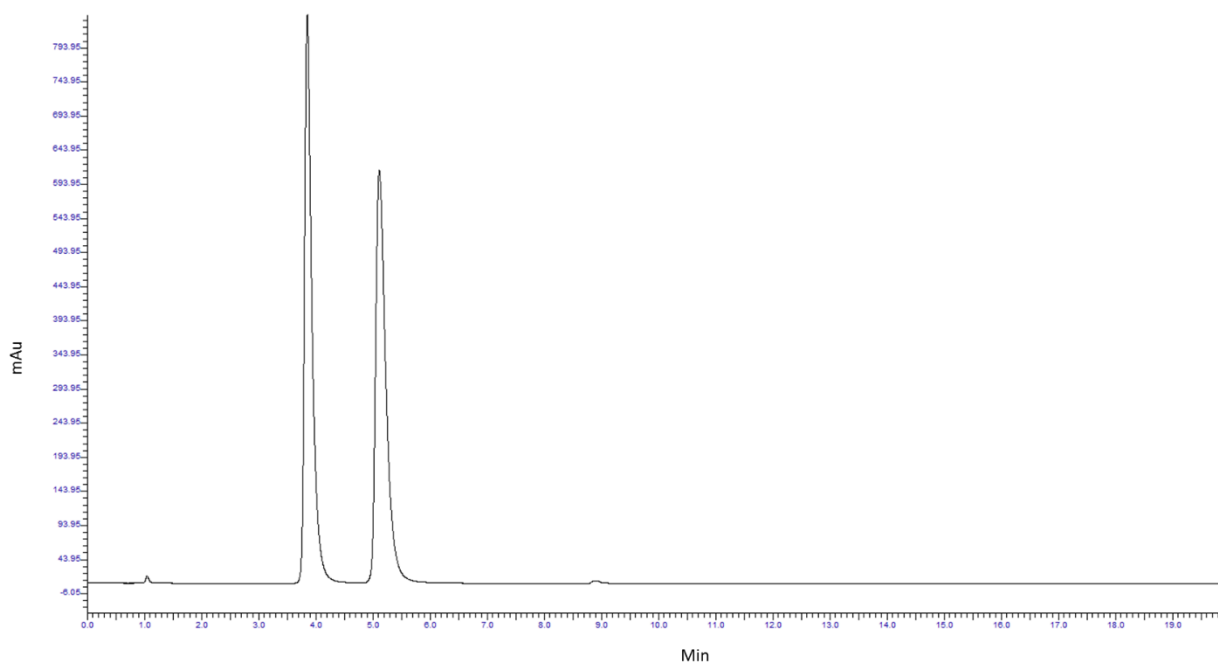
Figure 5.69: A typical chromatogram of the resolution of the enantiomers of *N,N,O,O*-BODIPY **4.1**.

After the runs were completed, we resubmitted the collected enantiomers to the same conditions to assess the enantiomeric excess (*ee*).
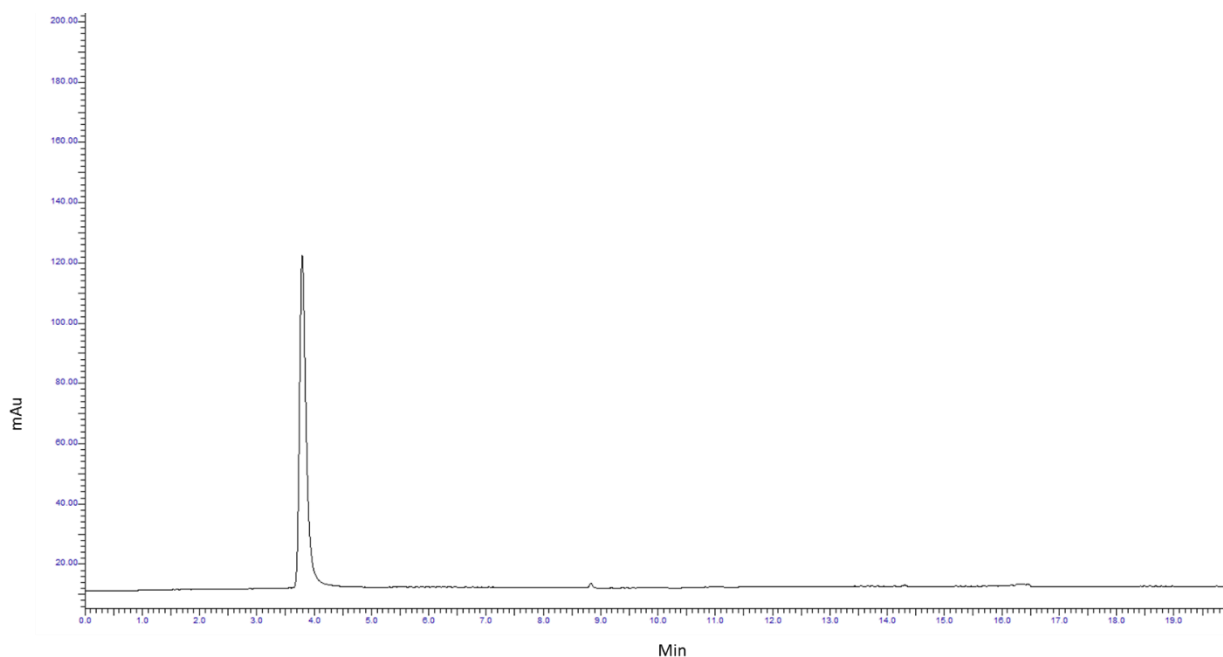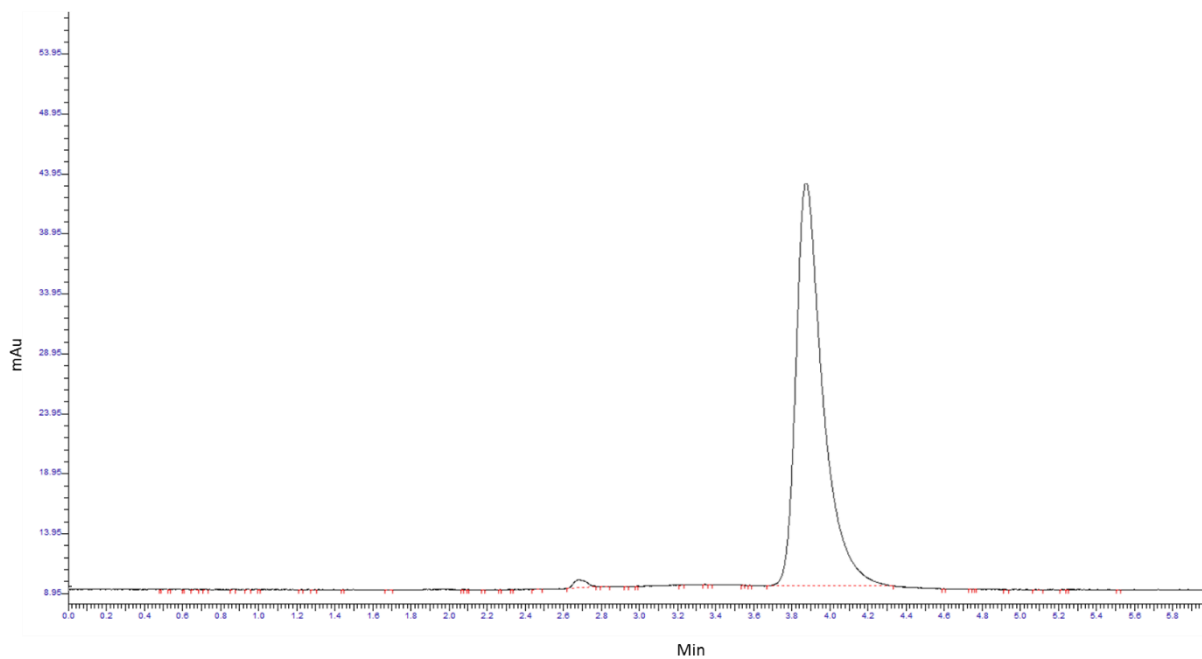
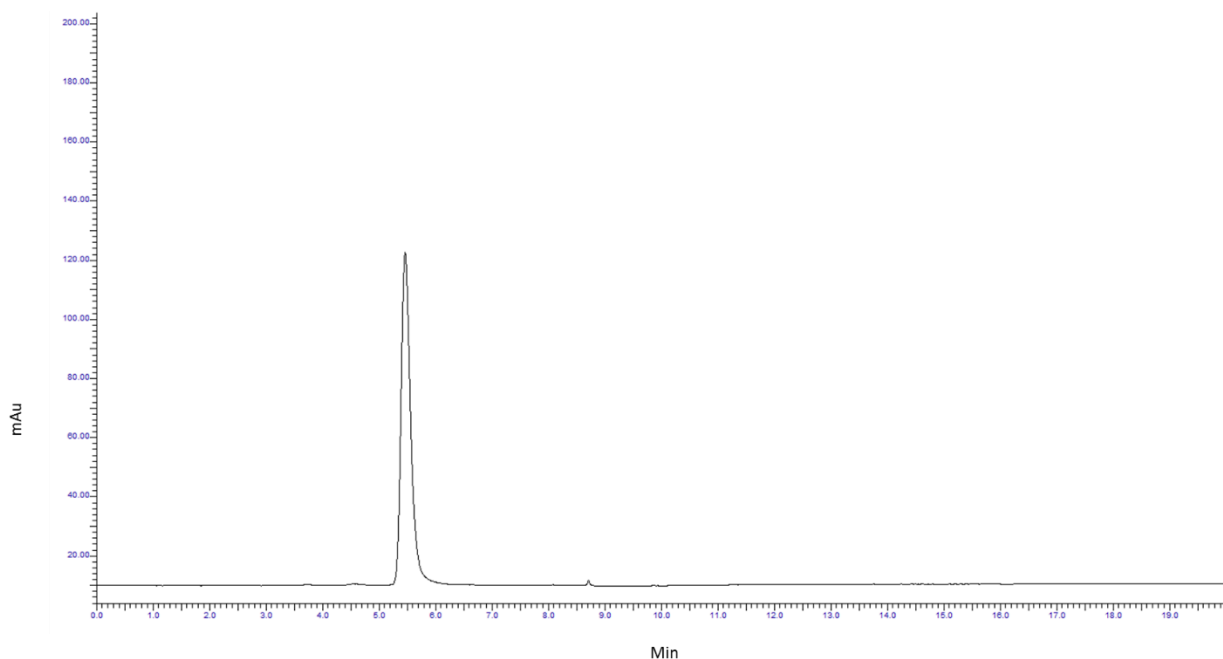**Figure 5.70**: Chromatogram of enantiomer 1 (-)-**4.1** resubmitted to the separation conditions to assess the *ee*.
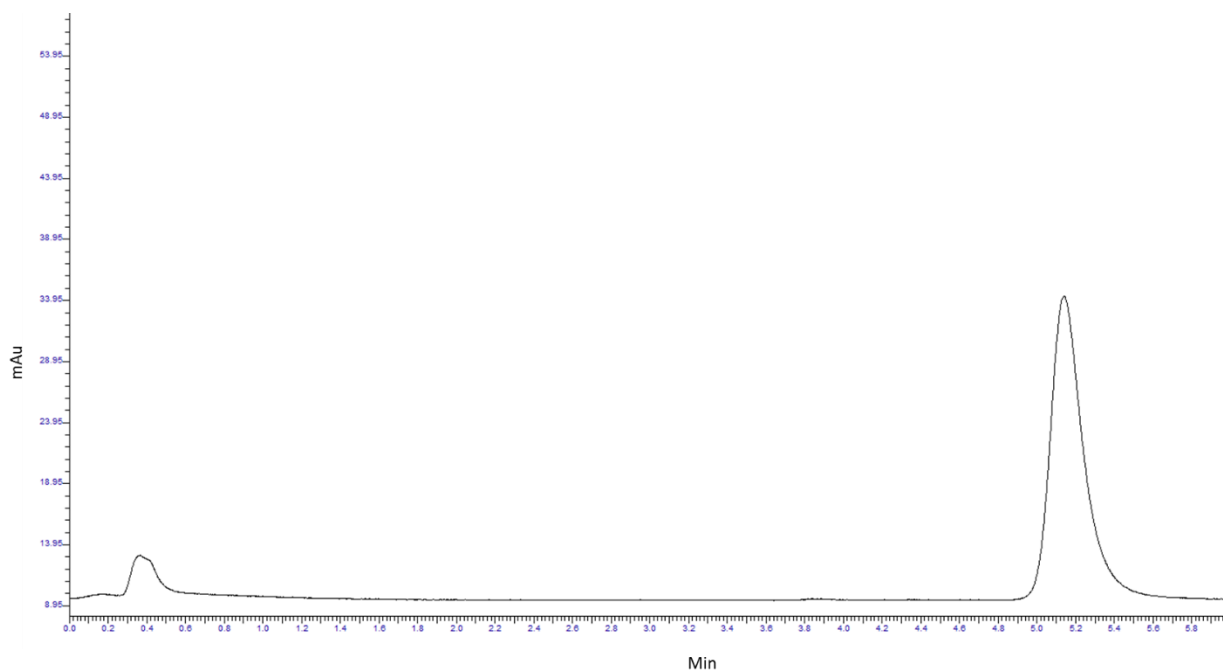
Figure 5.71: Chromatogram of enantiomer 2 (-)-**4.1** resubmitted to the separation conditions to assess the *ee*.

5.5 X-Ray Crystallography Data.

Crystal structure data for mjh150036, mjh150037 and mjh180018 were collected on a Xcalibur, Atlas, Gemini ultra diffractometer equipped with a sealed X-ray tube (λ CuKα = 1.54184 Å) and an Oxford Cryosystems CryostreamPlus open-flow N$_2$ cooling device. Analysis and structural elucidation of compounds **2.10**, **2.18** and **2.33** were performed by Dr Paul Waddell.

5.5.1 Methyl (Z)-4-((5-bromo-1*H*-pyrrol-2-yl)(5-bromo-2*H*-pyrrol-2-ylidene)methyl)benzoate (**2.10**)
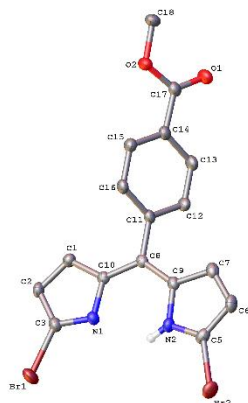
Identification code	mjh150036
Empirical formula	$C_{17}H_{12}Br_2N_2O_2$
Formula weight	436.11
Temperature/K	150.0(2)
Crystal system	monoclinic
Space group	$P2_1/c$
a/Å	11.37329(14)
b/Å	12.67359(16)
c/Å	11.57087(14)
α/°	90
β/°	98.2360(11)
γ/°	90
Volume/Å^3	1650.63(4)
Z	4
ρ_{calc}g/cm^3	1.755
μ/mm^{-1}	6.322
F(000)	856.
Crystal size/mm^3	0.4 × 0.22 × 0.18
Radiation	CuKα (λ = 1.54184)
2Θ range for data collection/°	7.854 to 133.902
Index ranges	-13≤h≤13, -14≤k≤15, -10≤l≤13
Reflections collected	11955
Independent reflections	2931 [R_{int}=0.0378, R_{sigma}=0.0272]
Data/restraints/parameters	2931/1/215
Goodness-of-fit on F^2	1.097
Final R indexes [I>=2σ (I)]	R_1 = 0.0298, wR_2 = 0.0740
Final R indexes [all data]	R_1 = 0.0326, wR_2 = 0.0762
Largest diff. peak/hole / e Å^{-3}	0.45/-0.65

Table 5.3: Crystal data and structure refinement for mjh150036

5.5.2 3-(4-(methoxycarbonyl)phenyl)-10,15-dioxa-2a^1,3a^1-diaza-10a-borabenzo[5,6]indeno[1,7-*ef*]aceanthrylen-2a^1-ium-16-uide (*N,N,O,C*-BODIPY **2.18**)
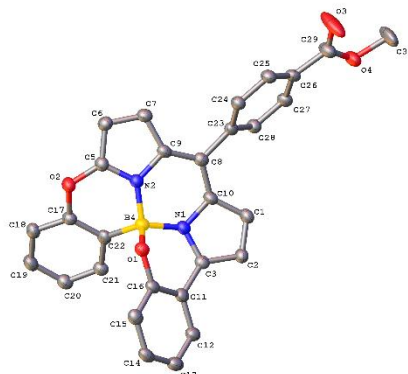
Identification code	mjh150037
Empirical formula	$C_{59}H_{39}B_2Cl_3N_4O_{8.3}$
Formula weight	1064.71
Temperature/K	150.0(2)
Crystal system	orthorhombic
Space group	Aea2
a/Å	13.62485(19)
b/Å	32.5110(5)
c/Å	11.0677(2)
α/°	90
β/°	90
γ/°	90
Volume/Å^3	4902.51(13)
Z	4
p_{calc}g/cm^3	1.443
μ/mm^{-1}	2.231
F(000)	2194.0
Crystal size/mm^3	0.39 × 0.26 × 0.15
Radiation	CuKα (λ = 1.54184)
2Θ range for data collection/°	5.436 to 133.648
Index ranges	-13≤h≤16, -36≤k≤38, -13≤l≤12
Reflections collected	17923
Independent reflections	4163 [R_{int}=0.0286, R_{sigma}=0.0191]
Data/restraints/parameters	4163/351/361
Goodness-of-fit on F^2	1.081
Final R indexes [I>=2σ (I)]	R_1 = 0.0450, wR_2 = 0.1309
Final R indexes [all data]	R_1 = 0.0467, wR_2 = 0.1334
Largest diff. peak/hole / e Å^{-3}	0.54/-0.61
Flack parameter	0.002(8)

Table 5.4: Crystal data and structure refinement for mjh150037

5.5.3 Methyl 4-(7,12-dimethyl-10,15-dioxa-2a$^1\lambda^4$,3a^1-diaza-10aλ^4-borabenzo[5,6]indeno[3,4-*ef*]aceanthrylen-3-yl)benzoate (*N,N,O,C*-BODIPY **2.33**)
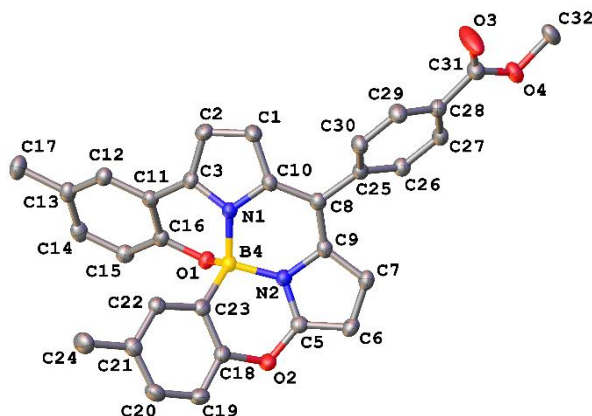
Identification code	mjh180018
Empirical formula	$C_{31}H_{23}BN_2O_4$
Formula weight	498.32
Temperature/K	150.0(2)
Crystal system	triclinic
Space group	P-1
a/Å	8.1435(3)
b/Å	8.3400(4)
c/Å	19.5670(9)
α/°	94.113(4)
β/°	93.430(4)
γ/°	111.850(4)
Volume/Å^3	1224.89(10)
Z	2
p_{calc}g/cm^3	1.351
μ/mm^{-1}	0.719
F(000)	520.0
Crystal size/mm^3	0.42 × 0.13 × 0.03
Radiation	CuKα (λ = 1.54184)
2Θ range for data collection/°	9.102 to 133.844
Index ranges	-9 ≤ h ≤ 8, -9 ≤ k ≤ 9, -23 ≤ l ≤ 23
Reflections collected	17241
Independent reflections	4319 [R_{int}=0.0368, R_{sigma}=0.0291]
Data/restraints/parameters	4319/0/347
Goodness-of-fit on F^2	1.025
Final R indexes [I>=2σ (I)]	R_1 = 0.0365, wR_2 = 0.0879
Final R indexes [all data]	R_1 = 0.0477, wR_2 = 0.0951
Largest diff. peak/hole / e Å^{-3}	0.23/-0.18

Table 5.5: Crystal data and structure refinement for mjh180018

Appendix

References

1   J. P. Riehl and F. S. Richardson, *Chem. Rev.*, 1986, **86**, 1–16.

2   H. G. Brittain, *Chirality*, 1996, 8, 357–363.

3   G. Muller, *Dalt. Trans.*, 2009, 9692–9707.

4   H. Tsumatori, T. Harada, J. Yuasa, Y. Hasegawa and T. Kawai, *Appl. Phys. Express*, 2011, **4**, 11601.

5   R. Carr, N. H. Evans and D. Parker, *Chem. Soc. Rev.*, 2012, 41, 7673–7686.

6   F. Zinna and L. Di Bari, *Chirality*, 2015, 27, 1–13.

7   J. L. Lunkley, D. Shirotani, K. Yamanari, S. Kaizaki and G. Muller, *J. Am. Chem. Soc.*, 2008, **130**, 13814–13815.

8   R. Clarke, K. L. Ho, A. A. Alsimaree, O. J. Woodford, P. G. Waddell, J. Bogaerts, W. Herrebout, J. G. Knight, R. Pal, T. J. Penfold and M. J. Hall, *ChemPhotoChem*, 2017, **1**, 513–517.

9   V. Balzani, P. Ceroni and A. Juris, *Photochemistry and Photophysics : Concepts, Research, Applications*, John Wiley & Sons, 2014.

10   M. Born and E. Wolf, *Principles of optics : electromagnetic theory of propagation, interference and diffraction of light*, Cambridge University Press, 1999.

11   K. Nakanishi, N. Berova, P. L. Polavarapu and R. W. Woody, Comprehensive Chiroptical Spectroscopy, Volume 1, Instrumentation, Methodologies, and Theoretical Simulations, John Wiley & Sons, 2013.

12   M. Schadt, *Annu. Rev. Mater. Sci.*, 1997, **27**, 305–379.

13   F. Song, G. Wei, X. Jiang, F. Li, C. Zhu and Y. Cheng, *Chem. Commun.*, 2013, **49**, 5772–5774.

14   M. Seitz, E. G. Moore, A. J. Ingram, G. Muller and K. N. Raymond, *J. Am. Chem. Soc.*, 2007, **129**, 15468–15470.

15   J. Yuasa, T. Ohno, H. Tsumatori, R. Shiba, H. Kamikubo, M. Kataoka, Y. Hasegawa and T. Kawai, *Chem. Commun.*, 2013, **49**, 4604–4606.

16   S. Furumi, *Chem. Rec.*, 2010, **10**, 394–408.

17   E. M. Sánchez-Carnerero, A. R. Agarrabeitia, F. Moreno, B. L. Maroto, G. Muller, M. J. Ortiz and S. de la Moya, *Chem. Eur. J.*, 2015, **21**, 13488–13500.

18   J. Kumar, T. Nakashima and T. Kawai, *J. Phys. Chem. Lett.*, 2015, **6**, 3445–3452.

19   C. A. Emeis and L. J. Oosterhoff, *Chem. Phys. Lett.*, 1967, **1**, 129–132.

20   H. P. J. M. Dekkers and L. E. Closs, *J. Am. Chem. Soc.*, 1976, **98**, 2210–2219.

21   P. H. Schippers, J. P. M. van der Ploeg and H. P. J. M. Dekkers, *J. Am. Chem. Soc.*, 1983, **105**, 84–89.

22   G. M. Labrador, J. Bosson, Z. S. Breitbach, Y. Lim, E. R. Francotte, R. Sabia, C. Villani, D. W. Armstrong and J. Lacour, *Chirality*, 2016, **28**, 282–289.

23   J. Bosson, G. M. Labrador, S. Pascal, F. A. Miannay, O. Yushchenko, H. Li, L. Bouffier, N. Sojic, R. C. Tovar, G. Muller, D. Jacquemin, A. D. Laurent, B. Le Guennic, E. Vauthey and J. Lacour, *Chem. Eur. J.*, 2016, **22**, 18394–18403.

24   S. Abbate, G. Longhi, F. Lebon, E. Castiglioni, S. Superchi, L. Pisani, F. Fontana, F. Torricelli, T. Caronna, C. Villani, R. Sabia, M. Tommasini, A. Lucotti, D. Mendola, A. Mele and D. A. Lightner, *J. Phys. Chem. C*, 2014, **118**, 1682–1695.

25   Y. Liu, J. Cerezo, G. Mazzeo, N. Lin, X. Zhao, G. Longhi, S. Abbate and F. Santoro, *J. Chem. Theory Comput.*, 2016, **12**, 2799–2819.

26   Y. Morisaki, M. Gon, T. Sasamori, N. Tokitoh and Y. Chujo, *J. Am. Chem. Soc.*, 2014, **136**, 3350–3353.

27   M. Gon, Y. Morisaki and Y. Chujo, *J. Mater. Chem. C*, 2015, **3**, 521–529.

28   M. Gon, Y. Morisaki and Y. Chujo, *European J. Org. Chem.*, 2015, **2015**, 7756–7762.

29   T. Kitatobe, Y. Mimura, S. Tsujimoto, N. Tajima, M. Fujiki and Y. Imai, *Tetrahedron*, 2017, **73**, 6856–6862.

30   K. Hassan, K. Yamashita, K. Hirabayashi, T. Shimizu, K. Nakabayashi, Y. Imai, T. Matsumoto, A. Yamano and K. Sugiura, *Chem. Lett.*, 2015, **44**, 1607–1609.

31   T. Kimoto, N. Tajima, M. Fujiki and Y. Imai, *Chem. - An Asian J.*, 2012, **7**, 2836–2841.

32   T. Kowada, H. Maeda and K. Kikuchi, *Chem. Soc. Rev.*, 2015, 44, 4953–4972.

33   A. Kamkaew, S. H. Lim, H. B. Lee, L. V. Kiew, L. Y. Chung and K. Burgess, *Chem. Soc. Rev.*, 2013, 42, 77–88.

34   N. Boens, V. Leen and W. Dehaen, *Chem. Soc. Rev.*, 2012, 41, 1130–1172.

35   H. Klfout, A. Stewart, M. Elkhalifa and H. He, *ACS Appl. Mater. Interfaces*, 2017, **9**, 39873–39889.

36   R. G. Clarke and M. J. Hall, in *Advances in Heterocyclic Chemistry, Volume 128*, eds. E. F. V. Scriven and C. A. Ramsden, Academic Press, 2019, p. 181.

37   A. Treibs and F. -H Kreuzer, *Justus Liebigs Ann. Chem.*, 1968, **718**, 208–223.

38   A. Loudet and K. Burgess, *Chem. Rev.*, 2007, **107**, 4891–4932.

39   G. Ulrich, R. Ziessel and A. Harriman, *Angew. Chemie - Int. Ed.*, 2008, 47, 1184–1201.

40   J. Godoy, G. Vives and J. M. Tour, *Org. Lett.*, 2010, **12**, 1464–1467.

41   C. B. Reese and H. Yan, *Tetrahedron Lett.*, 2001, **42**, 5545–5547.

42   M. Sekiya, K. Umezawa, A. Sato, D. Citterio and K. Suzuki, *Chem. Commun.*, 2009, 3047–3049.

43   R. W. Wagner and J. S. Lindsey, *Pure Appl. Chem.*, 1996, **68**, 1373–1380.

44   T. Rohand, E. Dolusic, T. H. Ngo, W. Maes and W. Dehaen, *Arkivoc*, 2007, **2007**, 307.

45   C. Tahtaoui, C. Thomas, F. Rohmer, P. Klotz, G. Duportail, Y. Mély, D. Bonnet and M. Hibert, *J. Org. Chem.*, 2007, **72**, 269–272.

46   R. I. Lerrick, T. P. L. Winstanley, K. Haggerty, C. Wills, W. Clegg, R. W. Harrington, P. Bultinck, W. Herrebout, A. C. Benniston and M. J. Hall, *Chem. Commun.*, 2014, **50**, 4714–4716.

47   M. Gupta, S. Mula, M. Tyagi, T. K. Ghanty, S. Murudkar, A. K. Ray and S. Chattopadhyay, *Chem. Eur. J.*, 2013, **19**, 17766–17772.

48   L. Li, J. Han, B. Nguyen and K. Burgess, *J. Org. Chem.*, 2008, **73**, 1963–1970.

49   M. Shah, K. Thangaraj, M.-L. Soong, L. T. Wolford, J. H. Boyer, I. R. Politzer and T. G. Pavlopoulos, *Heteroat. Chem.*, 1990, **1**, 389–399.

50   H. J. Wories, J. H. Koek, G. Lodder, J. Lugtenburg, R. Fokkens, O. Driessen and G. R. Mohn, *Recl. des Trav. Chim. des Pays-Bas*, 1985, **104**, 288–291.

51   T. Yogo, Y. Urano, Y. Ishitsuka, F. Maniwa and T. Nagano, *J. Am. Chem. Soc.*, 2005, **127**, 12162–12163.

52   G. Duran-Sampedro, A. R. Agarrabeitia, I. Garcia-Moreno, A. Costela, J. Bañuelos, T. Arbeloa, I. López Arbeloa, J. L. Chiara and M. J. Ortiz, *European J. Org. Chem.*, 2012, **2012**, 6335–6350.

53   A. Orte, E. Debroye, M. J. Ruedas-Rama, E. Garcia-Fernandez, D. Robinson, L. Crovetto, E. M. Talavera, J. M. Alvarez-Pez, V. Leen, B. Verbelen, L. Cunha Dias De Rezende, W. Dehaen, J. Hofkens, M. Van Der Auweraer and N. Boens, *RSC Adv.*, 2016, **6**, 102899-102913.

54   N. Boens, B. Verbelen and W. Dehaen, *European J. Org. Chem.*, 2015, 2015, 6577–6595.

55   T. Rohand, M. Baruah, W. Qin, N. Boens and W. Dehaen, *Chem. Commun.*, 2006, **0**, 266–268.

56   M. Baruah, W. Qin, N. Basarić, W. M. De Borggraeve and N. Boens, *J. Org. Chem.*, 2005, **70**, 4152–4157.

57   S. Rihn, P. Retailleau, N. Bugsaliewicz, A. De Nicola and R. Ziessel, *Tetrahedron Lett.*, 2009, **50**, 7008–7013.

58   M. R. Rao, S. M. Mobin and M. Ravikanth, *Tetrahedron*, 2010, **66**, 1728–1734.

59   M. Baruah, W. Qin, R. A. L. Vallée, D. Beljonne, T. Rohand, W. Dehaen and N. Boens, *Org. Lett.*, 2005, **7**, 4377-4380.

60   V. Leen, W. Qin, W. Yang, J. Cui, C. Xu, X. Tang, W. Liu, K. Robeyns, L. Van Meervelt, D. Beljonne, R. Lazzaroni, C. Tonnelé, N. Boens and W. Dehaen, *Chem. - An Asian J.*, 2010, **5**, 2016–2026.

61   C. Zhao, Y. Zhang, X. Wang and J. Cao, *J. Photochem. Photobiol. A Chem.*, 2013, **264**, 41–47.

62   T. Satoh, K. Fujii, Y. Kimura and Y. Matano, *J. Org. Chem.*, 2018, **83**, 5274–5281.

63   V. Leen, D. Miscoria, S. Yin, A. Filarowski, J. Molisho Ngongo, M. Van Der Auweraer, N. Boens and W. Dehaen, *J. Org. Chem.*, 2011, **76**, 8168–8176.

64   V. Leen, P. Yuan, L. Wang, N. Boens and W. Dehaen, *Org. Lett.*, 2012, **14**, 6150–6153.

65   T. Jiang, P. Zhang, C. Yu, J. Yin, L. Jiao, E. Dai, J. Wang, Y. Wei, X. Mu and E. Hao, *Org. Lett.*, 2014, **16**, 1952–1955.

66   N. Zhao, S. Xuan, F. R. Fronczek, K. M. Smith and M. G. H. Vicente, *J. Org. Chem.*, 2017, **82**, 3880–3885.

67   R. Maragani, M. B. Thomas, R. Misra and F. D'Souza, *J. Phys. Chem. A*, 2018, **122**, 4829–4837.

68   E. Bodio and C. Goze, *Dye. Pigment.*, 2019, **160**, 700–710.

69   C. Goze, G. Ulrich and R. Ziessel, *Org. Lett.*, 2006, **8**, 4445–4448.

70   A. Harriman, G. Izzet and R. Ziessel, *J. Am. Chem. Soc.*, 2006, **128**, 10868–10875.

71 C. Goze, G. Ulrich and R. Ziessel, *J. Org. Chem.*, 2007, **72**, 313–322.

72 R. Ziessel, C. Goze and G. Ulrich, *Synthesis (Stuttg).*, 2007, 0936–0949.

73 G. Ulrich, C. Goze, M. Guardigli, A. Roda and R. Ziessel, *Angew. Chemie - Int. Ed.*, 2005, **44**, 3694–3698.

74 C. Goze, G. Ulrich, L. J. Mallon, B. D. Allen, A. Harriman and R. Ziessel, *J. Am. Chem. Soc.*, 2006, **128**, 10231–10239.

75 S. Goeb and R. Ziessel, *Org. Lett.*, 2007, **9**, 737–740.

76 T. Rousseau, A. Cravino, T. Bura, G. Ulrich, R. Ziessel and J. Roncali, *Chem. Commun.*, 2009, **0**, 1673–1675.

77 D. Kumaresan, R. P. Thummel, T. Bura, G. Ulrich and R. Ziessel, *Chem. Eur. J.*, 2009, **15**, 6335–6339.

78 T. Rousseau, A. Cravino, E. Ripaud, P. Leriche, S. Rihn, A. De Nicola, R. Ziessel and J. Roncali, *Chem. Commun.*, 2010, **46**, 5082–5084.

79 H. Kim, A. Burghart, M. B. Welch, J. Reibenspies and K. Burgess, *Chem. Commun.*, 1999, **0**, 1889–1890.

80 Y. Kubo, Y. Minowa, T. Shoda and K. Takeshita, *Tetrahedron Lett.*, 2010, **51**, 1600–1602.

81 Y. Tomimori, T. Okujima, T. Yano, S. Mori, N. Ono, H. Yamada and H. Uno, *Tetrahedron*, 2011, **67**, 3187–3193.

82 Y. Kubo, K. Watanabe, R. Nishiyabu, R. Hata, A. Murakami, T. Shoda and H. Ota, *Org. Lett.*, 2011, **13**, 4574–4577.

83 S. Yamazawa, M. Nakashima, Y. Suda, R. Nishiyabu and Y. Kubo, *J. Org. Chem.*, 2016, **81**, 1310–1315.

84 R. B. Alnoman, S. Rihn, D. C. O'Connor, F. A. Black, B. Costello, P. G. Waddell, W. Clegg, R. D. Peacock, W. Herrebout, J. G. Knight and M. J. Hall, *Chem. Eur. J.*, 2016, **22**, 93–96.

85 Y. Gabe, T. Ueno, Y. Urano, H. Kojima and T. Nagano, *Anal. Bioanal. Chem.*, 2006, **386**, 621–626.

86 D. Gao, S. M. Aly, P. L. Karsenti, G. Brisard and P. D. Harvey, *Dalt. Trans.*, 2017, **46**, 6278–6290.

87 P. E. Doulain, C. Goze, E. Bodio, P. Richard and R. A. Decréau, *Chem. Commun.*, 2016, **52**, 4474–4477.

88 V. Bandi, S. K. Das, S. G. Awuah, Y. You and F. D'Souza, *J. Am. Chem. Soc.*, 2014, **136**, 7571–7574.

89 B. Brizet, C. Bernhard, Y. Volkova, Y. Rousselin, P. D. Harvey, C. Goze and F. Denat, *Org. Biomol. Chem.*, 2013, **11**, 7729–7737.

90 V. J. Richards, A. L. Gower, J. E. H. B. Smith, E. S. Davies, D. Lahaye, A. G. Slater, W. Lewis, A. J. Blake, N. R. Champness and D. L. Kays, *Chem. Commun.*, 2012, **48**, 1751–1753.

91 E. Deniz, M. Battal, J. Cusido, S. Sortino and F. M. Raymo, *Phys. Chem. Chem. Phys.*, 2012, **14**, 10300–10307.

92 A. M. Courtis, S. A. Santos, Y. Guan, J. A. Hendricks, B. Ghosh, D. M. Szantai-Kis, S. A. Reis, J. V. Shah and R. Mazitschek, *Bioconjug. Chem.*, 2014, **25**, 1043–1051.

93   A. L. Nguyen, P. Bobadova-Parvanova, M. Hopfinger, F. R. Fronczek, K. M. Smith and M. G. H. Vicente, *Inorg. Chem.*, 2015, **54**, 3228–3236.

94   G. Durán-Sampedro, A. R. Agarrabeitia, L. Cerdán, M. E. Pérez-Ojeda, A. Costela, I. García-Moreno, I. Esnal, J. Bañuelos, I. L. Arbeloa and M. J. Ortiz, *Adv. Funct. Mater.*, 2013, **23**, 4195–4205.

95   X. D. Jiang, J. Zhang, T. Furuyama and W. Zhao, *Org. Lett.*, 2012, **14**, 248–251.

96   T. Lundrigan and A. Thompson, *J. Org. Chem.*, 2013, **78**, 757–761.

97   T. Lundrigan, T. S. Cameron and A. Thompson, *Chem. Commun.*, 2014, **50**, 7028.

98   C. Ikeda and T. Nabeshima, *Chem. Commun.*, 2008, **0**, 721–723.

99   H. L. Kee, C. Kirmaiery, L. Yu, P. Thamyongkit, W. J. Youngblood, M. E. Calder, L. Ramos, B. C. Noll, D. F. Bocian, W. R. Scheidt, R. R. Birge, J. S. Lindsey and D. Holten, *J. Phys. Chem. B*, 2005, **109**, 20433–20443.

100   C. Bonnier, W. E. Piers, A. A. S. Ali, A. Thompson and M. Parvez, *Organometallics*, 2009, **28**, 4845–4851.

101   C. Ikeda, T. Maruyama and T. Nabeshima, *Tetrahedron Lett.*, 2009, **50**, 3349–3351.

102   M. Yamamura, S. Yazaki, M. Seki, Y. Matsui, H. Ikeda and T. Nabeshima, *Org. Biomol. Chem.*, 2015, **13**, 2574–2581.

103   Y. Gobo, R. Matsuoka, Y. Chiba, T. Nakamura and T. Nabeshima, *Tetrahedron Lett.*, 2018, **59**, 4149–4152.

104   N. Chen, W. Zhang, S. Chen, Q. Wu, C. Yu, Y. Wei, Y. Xu, E. Hao and L. Jiao, *Org. Lett.*, 2017, **19**, 2026–2029.

105   T. Rohand, W. Qin, N. Boens and W. Dehaen, *European J. Org. Chem.*, 2006, **2006**, 4658–4663.

106   V. Leen, T. Leemans, N. Boens and W. Dehaen, *European J. Org. Chem.*, 2011, **2011**, 4386–4396.

107   Z. Feng, L. Jiao, Y. Feng, C. Yu, N. Chen, Y. Wei, X. Mu and E. Hao, *J. Org. Chem.*, 2016, **81**, 6281–6291.

108   A. Savoldelli, Q. Meng, R. Paolesse, F. R. Fronczek, K. M. Smith and M. G. H. Vicente, *J. Org. Chem.*, 2018, **83**, 6498–6507.

109   M. J. Ortiz, A. R. Agarrabeitia, G. Duran-Sampedro, J. Bañuelos Prieto, T. A. Lopez, W. A. Massad, H. A. Montejano, N. A. García and I. Lopez Arbeloa, *Tetrahedron*, 2012, **68**, 1153–1162.

110   E. Palao, T. Slanina and P. Klán, *Chem. Commun.*, 2016, **52**, 11951–11954.

111   R. B. Alnoman, P. Stachelek, J. G. Knight, A. Harriman and P. G. Waddell, *Org. Biomol. Chem.*, 2017, **15**, 7643–7653.

112   V. Lakshmi and M. Ravikanth, *European J. Org. Chem.*, 2014, **2014**, 5757–5766.

113   N. Zhao, S. Xuan, B. Byrd, F. R. Fronczek, K. M. Smith and M. G. H. Vicente, *Org. Biomol. Chem.*, 2016, **14**, 6184–6188.

114   D. Frath, A. Poirel, G. Ulrich, A. De Nicola and R. Ziessel, *Chem. Commun.*, 2013, **49**, 4908–4910.

115   S. Xuan, N. Zhao, X. Ke, Z. Zhou, F. R. Fronczek, K. M. Kadish, K. M. Smith and M. G. H. Vicente, *J. Org. Chem.*, 2017, **82**, 2545–2557.

116 N. Zhao, S. Xuan, F. R. Fronczek, K. M. Smith and M. G. H. Vicente, *J. Org. Chem.*, 2015, **80**, 8377–8383.

117 S. Xuan, N. Zhao, Z. Zhou, F. R. Fronczek and M. G. H. Vicente, *J. Med. Chem.*, 2016, **59**, 2109–2117.

118 S. Kim, Y. Zhou, N. Tohnai, H. Nakatsuji, M. Matsusaki, M. Fujitsuka, M. Miyata and T. Majima, *Chem. Eur. J.*, 2018, **24**, 636–645.

119 R. Misra, B. Dhokale, T. Jadhav and S. M. Mobin, *Dalt. Trans.*, 2014, **43**, 4854–4861.

120 G. Duran-Sampedro, E. Palao, A. R. Agarrabeitia, S. de la Moya, N. Boens and M. J. Ortiz, *RSC Adv.*, 2014, **4**, 19210–19213.

121 E. Palao, G. Duran-Sampedro, S. De La Moya, M. Madrid, C. García-López, A. R. Agarrabeitia, B. Verbelen, W. Dehaen, N. Boens and M. J. Ortiz, *J. Org. Chem.*, 2016, **81**, 3700–3710.

122 G. Beer, C. Niederalt, S. Grimme and J. Daub, *Angew. Chemie - Int. Ed.*, 2000, **39**, 3252–3255.

123 A. Haefele, C. Zedde, P. Retailleau, G. Ulrich and R. Ziessel, *Org. Lett.*, 2010, **12**, 1672–1675.

124 A. Loudet, R. Bandichhor, K. Burgess, A. Palma, S. O. McDonnell, M. J. Hall and D. F. O'Shea, *Org. Lett.*, 2008, **10**, 4771–4774.

125 C. Ikeda, T. Maruyama and T. Nabeshima, *Tetrahedron Lett.*, 2009, **50**, 3349–3351.

126 A. Gossauer, F. Fehr, F. Nydegger and H. Stöckli-Evans, *J. Am. Chem. Soc.*, 1997, **119**, 1599–1608.

127 E. M. Sánchez-Carnerero, F. Moreno, B. L. Maroto, A. R. Agarrabeitia, M. J. Ortiz, B. G. Vo, G. Muller and S. D. La Moya, *J. Am. Chem. Soc.*, 2014, **136**, 3346–3349.

128 E. M. Sánchez-Carnerero, A. R. Agarrabeitia, F. Moreno, B. L. Maroto, G. Muller, M. J. Ortiz and S. De La Moya, *Chem. Eur. J.*, 2015, **21**, 13488–13500.

129 A. Gossauer, F. Nydegger, T. Kiss, R. Sleziak and H. Stoeckli-Evans, *J. Am. Chem. Soc.*, 2004, **126**, 1772–1780.

130 J. A. Schellman, *Chem. Rev.*, 1975, **75**, 323–331.

131 F. S. Richardson, *Inorg. Chem.*, 1980, **19**, 2806–2812.

132 J. I. Bruce, D. Parker, S. Lopinski and R. D. Peacock, *Chirality*, 2002, **14**, 562–567.

133 M. Wakabayashi, S. Yokojima, T. Fukaminato, K. I. Shiino, M. Irie and S. Nakamura, *J. Phys. Chem. A*, 2014, **118**, 5046–5057.

134 H. Tanaka, Y. Inoue and T. Mori, *ChemPhotoChem*, 2018, **2**, 386–402.

135 G. Zhang, M. Wang, F. R. Fronczek, K. M. Smith, M. Graç and H. Vicente, *Inorg. Chem*, 2018, **57**, 27.

136 T. Lundrigan, S. M. Crawford, T. S. Cameron and A. Thompson, *Chem. Commun.*, 2012, **48**, 1003–1005.

137 A. Burghart, H. Kim, M. B. Welch, L. H. Thoresen, J. Reibenspies, K. Burgess, F. Bergström and L. B. . Johansson, *J. Org. Chem.*, 1999, **64**, 7813–7819.

138 M. Saikawa, T. Nakamura, J. Uchida, M. Yamamura and T. Nabeshima, *Chem. Commun.*, 2016, **52**, 10727–10730.

139   A. L. Nguyen, F. R. Fronczek, K. M. Smith and M. G. H. Vicente, *Tetrahedron Lett.*, 2015, **56**, 6348–6351.

140   C. P. Ortmeyer, G. Haufe, K. Schwegmann, S. Hermann, M. Schäfers, F. Börgel, B. Wünsch, S. Wagner and V. Hugenberg, *Bioorganic Med. Chem.*, 2017, **25**, 2167–2176.

141   T. Sawazaki, Y. Shimizu, K. Oisaki, Y. Sohma and M. Kanai, *Org. Lett.*, 2018, **20**, 7767–7770.

142   Z. Wang, C. Cheng, Z. Kang, W. Miao, Q. Liu, H. Wang and E. Hao, *J. Org. Chem.*, 2019, **84**, 2732–2740.

143   F. Neese, *Wiley Interdiscip. Rev. Comput. Mol. Sci.*, 2012, **2**, 73–78.

144   Y. Nakai, T. Mori and Y. Inoue, *J. Phys. Chem. A*, 2012, **116**, 7372–7385.

145   C. Ikeda, S. Ueda and T. Nabeshima, *Chem. Commun.*, 2009, **0**, 2544–2546.

146   M. Liras, M. Pintado-Sierra, M. Iglesias and F. Sánchez, *J. Mater. Chem. A*, 2016, **4**, 17274–17278.

147   M. Yu, J. K.-H. Wong, C. Tang, P. Turner, M. H. Todd and P. J. Rutledge, *Beilstein J. Org. Chem.*, 2015, **11**, 37–41.

148   E. M. Sánchez-Carnerero, L. Gartzia-Rivero, F. Moreno, B. L. Maroto, A. R. Agarrabeitia, M. J. Ortiz, J. Bañuelos, Í. López-Arbeloa and S. De La Moya, *Chem. Commun.*, 2014, **50**, 12765–12767.

149   C. Tahtaoui, C. Thomas, F. Rohmer, P. Klotz, G. Duportail, Y. Mély, D. Bonnet and M. Hibert, *J. Org. Chem.*, 2007, **72**, 269–272.

150   J. A. Hendricks, E. J. Keliher, D. Wan, S. A. Hilderbrand, R. Weissleder and R. Mazitschek, *Angew. Chemie - Int. Ed.*, 2012, **51**, 4603–4606.

151   A. Blázquez-Moraleja, L. Cerdán, I. García-Moreno, E. Avellanal-Zaballa, J. Bañuelos, M. L. Jimeno, I. López-Arbeloa and J. L. Chiara, *Chem. Eur. J.*, 2018, **24**, 3802–3815.

152   D. Sirbu, A. C. Benniston and A. Harriman, *Org. Lett.*, 2017, **19**, 1626–1629.

153   E. Chemistry, E. Dynamics, D. Parker, R. S. Dickins, H. Puschmann, C. Crossland, J. A. K. Howard, D. Parker, R. S. Dickins, H. Puschmann, C. Crossland and J. A. K. Howard, *Chem. Rev.*, 2010, **102**, 1977–2010.

154   J. L. Lunkley, D. Shirotani, K. Yamanari, S. Kaizaki and G. Muller, *Inorg. Chem.*, 2011, **50**, 12724–12732.

155   M. Kleinschmidt, J. Tatchen and C. M. Marian, *J. Comput. Chem.*, 2002, **23**, 824–833.

156   T. Lundrigan, T. S. Cameron and A. Thompson, *Chem. Commun.*, 2014, **50**, 7028–7031.

157   J. Barbier, E. Lamy-Pitara, P. Marecot, J. P. Boitiaux, J. Cosyns and F. Verna, *Adv. Catal.*, 1990, **37**, 279–318.

158   S. P. Andrews, A. F. Stepan, H. Tanaka, S. V. Ley and M. D. Smith, *Adv. Synth. Catal.*, 2005, **347**, 647–654.

159   I. Nakamura, T. Sato and Y. Yamamoto, *Angew. Chemie - Int. Ed.*, 2006, **45**, 4473–4475.

160   US Pat., 231 142, 2015.

161   V. H. Rawal and M. P. Cava, *Tetrahedron Lett.*, 1985, **26**, 6141–6142.

162 K. M. Elbel, G. Guizzunti, M. A. Theodoraki, J. Xu, A. Batova, M. Dakanali and E. A. Theodorakis, *Org. Biomol. Chem.*, 2013, **11**, 3341–3348.

163 T. Fukuyama, S.-I. Nakatsuka and Y. Kishi, *Tetrahedron*, 1981, **37**, 2045–2078.

164 Y. Shirai, J. M. Guerrero, T. Sasaki, T. He, H. Ding, G. Vives, B. C. Yu, L. Cheng, A. K. Flatt, P. G. Taylor, Y. Gao and J. M. Tour, *J. Org. Chem.*, 2009, **74**, 7885–7897.

165 Y. Shirai, L. Cheng, B. Chen and J. M. Tour, *J. Am. Chem. Soc.*, 2006, **128**, 13479–13489.

166 V. Kolivoška, M. Mohos, I. V. Pobelov, S. Rohrbach, K. Yoshida, W. J. Hong, Y. C. Fu, P. Moreno-García, G. Mészáros, P. Broekmann, M. Hromadová, R. Sokolová, M. Valášek and T. Wandlowski, *Chem. Commun.*, 2014, **50**, 11757–11759.

167 Y. Liu, J. Kim, H. Seo, S. Park and J. Chae, *Adv. Synth. Catal.*, 2015, **357**, 2205–2212.

168 D. Sirbu, A. C. Benniston and A. Harriman, *Org. Lett.*, 2017, **19**, 1626–1629.

169 X. Zhou, C. Yu, Z. Feng, Y. Yu, J. Wang, E. Hao, Y. Wei, X. Mu and L. Jiao, *Org. Lett.*, 2015, **17**, 4632–4635.

170 B. Zeysing, C. Gosch and A. Terfort, *Org. Lett.*, 2000, **2**, 1843–1845.

171 F. Beaumard, P. Dauban and R. H. Dodd, *Synthesis (Stuttg).*, 2010, **2010**, 4033–4042.

172 J. Kurita, H. Sakai, S. Yamada and T. Tsuchiya, *ChemInform*, 1987, **18**, 285-286.

173 N. Basarić, M. Baruah, W. Qin, B. Metten, M. Smet, W. Dehaen and N. Boens, *Org. Biomol. Chem.*, 2005, **3**, 2755–2761.

174 R. Sens and K. H. Drexhage, *J. Lumin.*, 1981, **24**–**25**, 709–712.

175 D. Magde, J. H. Brannon, T. L. Cremers and J. Olmsted, *J. Phys. Chem.*

176 D. Magde, R. Wong and P. G. Seybold, *Photochem. Photobiol.*, 2002, **75**, 327–34.

177 G. E. Gaussian 09, Revision D.01, M. J. Frisch, G. W. Trucks, H. B. Schlegel, G. A. Scuseria, M. A. Robb, J. R. Cheeseman, G. Scalmani, V. Barone, B. Mennucci, J. Petersson, H. Nakatsuji, M. Caricato, X. Li, H. P. Hratchian, A. F. Izmaylov, J. Bloino, G. Zheng, J. L. Sonnenberg, M. Hada, M. Ehara, K. Toyota, R. Fukuda, J. A. Hasegawa, M. Ishida, T. Nakajima, Y. Honda, O. Kitao, H. Nakai, T. Vreven, K. N. Montgomery, Jr., J. E. Peralta, F. Ogliaro, M. Bearpark, J. J. Heyd, E. Brothers, A. Kudin, V. N. Staroverov, T. Keith, R. Kobayashi, J. Normand, K. Raghavachari, M. Rendell, J. C. Burant, S. S. Iyengar, J. Tomasi, M. Cossi, N. Rega, J. M. Millam, R. E. Klene, J. E. Knox, J. B. Cross, V. Bakken, C. Adamo, J. Jaramillo, R. Gomperts, R. L. Stratmann, O. Yazyev, A. J. Austin, R. Cammi, C. Pomelli, J. W. Ochterski, J. J. D. Martin, K. Morokuma, V. G. Zakrzewski, G. A. Voth, P. Salvador, J. C. S. Dapprich, A. D. Daniels, O. Farkas, J. B. Foresman, J. V. Ortiz and 2013 D. J. Fox, Gaussian, Inc., Wallingford CT, .

178 J. Autschbach, in *Comprehensive Chiroptical Spectroscopy*, John Wiley & Sons, Hoboken, NJ, USA, 2012, vol. 1, pp. 593–642.

179 F. M. J. Frisch, G. W. Trucks, H. B. Schlegel, G. E. Scuseria, M. A. Robb, J. R. Cheeseman, G. Scalmani, V. Barone, G. A. Petersson, H. Nakatsuji, X. Li, M. Caricato, A. V. Marenich, J. Bloino, B. G. Janesko, R. Gomperts, B. Mennucci, H. P. Hratchian, J. V., D. Lipparini, F. Egidi, J. Goings, B. Peng, A. Petrone, T. Henderson and 2016. Ranasinghe, V. G. Zakrzewski, J. Gao, N. Rega, G. Zheng, W. Liang, M. Hada, M. Ehara, K. Toyota, R. Fukuda, J. Hasegawa, M. Ishida, T. Nakajima, Y. Honda, O. Kitao, H. Nakai, T. Vreven, K. Throssell, J. A., M. Jr., J. E. Peralta, F. Ogliaro, M. J. Bearpar, .

DFT calculations of the HOMO, HOMO(-1) and LUMO *N,N,O,C*-BODIPY 2.18

To aid in the assignment of the oxidative and reductive electrochemical processes highlighted by cyclic voltammetry analysis, a series of DFT calculations were made with the intention of identifying the HOMO and LUMO of *N,N,O,C*-BODIPY **2.18** (performed by Owen Woodford). The LUMO was found to be distributed over the dipyrrin core of the BODIPY, with a minor contribution from the *meso*-aryl ring (figure AP.1). Typically, when the LUMO is distributed mostly over the dipyrrin core of a BODIPY, the electrochemistry is reversible. Therefore we can assign the reduction wave at -1.17 V as the addition of a single electron to the dipyrrin unit.
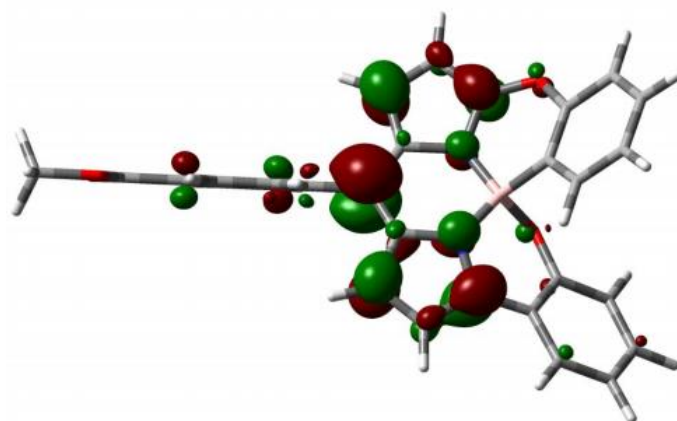
Figure AP.1: Kohn-Sham (isodensity 0.02) distribution pattern computed for the LUMO of *N,N,O,C*-BODIPY **2.18**.

Calculations of the HOMO revealed that the electron density is distributed around the dipyrrin unit, with a sizeable contribution from the directly (ie. C-C) linked phenolic ring (figure AP.2). Neither the *meso*-aryl ring nor the other phenolic ring contribute to the HOMO.
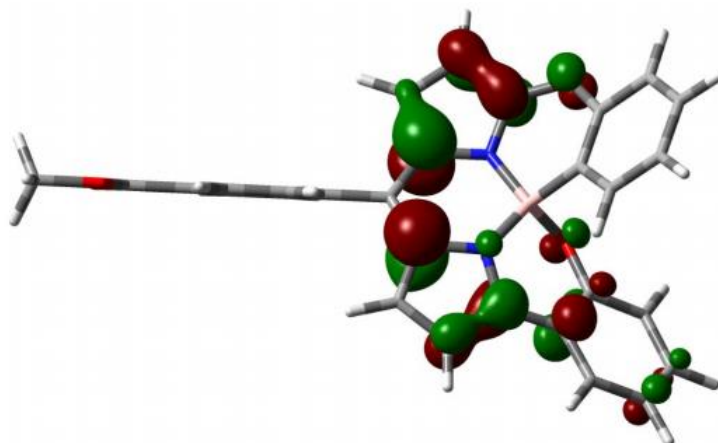
Figure AP.2: Kohn-Sham (isodensity 0.02) distribution pattern computed for the HOMO of *N,N,O,C*-BODIPY **2.18**.

Contrarily, the HOMO(-1) has the electron density distributed mostly on the phenolic rings, with only a small contribution from the BODIPY core (figure AP.3). Similar to the electronic distribution observed in the HOMO, the majority of the electron density is associated with the directly linked phenol ring, although there is considerable electron density associated with the oxygen linked phenol ring.
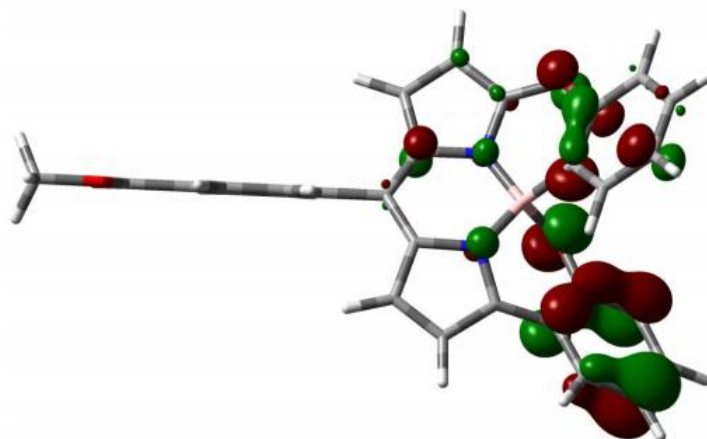
Figure AP.3: Kohn-Sham (isodensity 0.02) distribution pattern computed for the HOMO(-1) of *N,N,O,C*-BODIPY **2.18**.

Based on this information, we can assign the first oxidation peak (0.84 V) in the cyclic voltammogram of *N,N,O,C*-BODIPY **2.18** to the preferential removal of an electron from the dipyrrin unit. There is some involvement of the directly-linked phenol ring, and this might be responsible for the poor reversibility of this oxidation. As is commonly observed in BODIPY dyes, we can conclude that the optical absorption transition is primarily a HOMO-LUMO transition localised on the BODIPY core. The second oxidation process can be assigned to the removal of an electron from the boron-chelated phenol rings. On this basis, we should expect to find a charge-transfer state located slightly above the lowest energy π-π* excited-singlet state.

Structural Assignment of *N,N,O,C*-BODIPY 2.35

All NMR data was collected on a sample of *N,N,O,C*-BODIPY **2.35** in deuterated chloroform on a Bruker Avance III HD 700 MHz spectrometer by Professor William McFarlane.
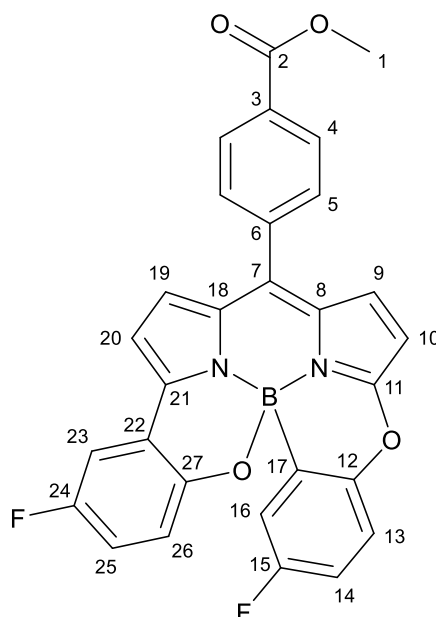
Atom	δ_C	^{1}H				^{13}C-^{1}H (HMBC)
		δ_H	Number of protons	Multiplicity	*J* (Hz)	
1	52.6	3.99	3	s	-	-
2	166.4	-	-	-	-	3.99 (**1**), 8.19 (**4**), 7.74 (**5**)
3	132.0	-	-	-	-	3.99 (**1**), 8.19 (**4**), 7.74 (**5**).
4	130.0	8.19	2	d	8.6	7.74 (**5**)
5	130.5	7.74	2	br s	-	8.19 (**4**)
6	137.8	-	-	-	-	8.19 (**4**), 7.74 (**5**), 7.03 (**9**)
7	137.5	-	-	-	-	7.74 (**5**), 7.03 (**9**)
8	127.6	-	-	-	-	7.03 (**9**), 108.5 (**10**)
9	132.3	7.03	1	d	4.6	108.5 (**10**)
10	108.5	6.44	1	d	4.6	7.03 (**9**)
11	163.6	-	-	-	-	7.03 (**9**), 108.5 (**10**)
12	152.5	-	-	-	-	7.28 (**13**), 6.89 (**14**), 6.79 (**16**)
13	118.5	7.28	1	dd	8.6, 4.0	6.89 (**14**), 6.79 (**16**)
14	114.4	6.89	1	app. td	8.6, 3.1	7.28 (**13**), 6.79 (**16**)
15	159.3	-	-	-	-	7.28 (**13**), 6.89 (**14**), 6.79 (**16**)
16	115.2	6.79	1	dd	8.0, 3.1	7.28 (**13**), 6.89 (**14**)
17	-	-	-	-	-	-
18	121.4	-	-	-	-	7.00 (**19**)
19	128.3	7.00	1	d	4.2	8.84 (**20**)

20	115.7	6.84	1	d	4.2	7.00 (**19**)
21	132.3	-	-	-	-	7.00 (**19**), 8.84 (**20**)
22	146.8	-	-	-	-	7.00 (**19**), 8.84 (**20**), 7.42 (**23**), 6.72 (**26**)
23	110.8	7.42	1	dd	8.5, 3.1	6.92 (**25**), 6.72 (**26**)
24	156.8	-	-	-	-	7.42 (**23**), 6.92 (**25**), 6.72 (**26**)
25	119.0	6.92	1	app. td	8.5, 3.9	7.42 (**23**), 6.72 (**26**)
26	121.2	6.72	1	dd	9.0, 3.9	7.42 (**23**), 6.92 (**25**),
27	150.3	-	-	-	-	7.42 (**23**), 6.92 (**25**), 6.72 (**26**)

Atom	δ_F
28	-123.1
29	-117.0

Publications

Circularly Polarised Luminescence from Helically Chiral "Confused" *N,N,O,C*-Boron-Chelated Dipyrromethenes (BODIPYs)

Rebecca Clarke,[a] Kin Lok Ho,[a] Abdulrahman Abdullah Alsimaree,[a] Owen J. Woodford,[a] Paul G. Waddell,[a] Jonathan Bogaerts,[b] Wouter Herrebout,[b] Julian G. Knight,[a] Robert Pal,[c] Thomas J. Penfold,[a] and Michael J. Hall*[a]

Chiral organic fluorophores have significant promise in the development of efficient emitters of circularly polarized light. Herein we describe a helically chiral boron dipyrromethene (BODIPY) with a hitherto unreported *N,N,O,C*-boron-chelation motif, synthesised by means of a one-pot boron metathesis, nucleophilic aromatic substitution (S_NAr), Suzuki coupling, boron chelation, cascade reaction. Resolution of the racemic BODIPY (by preparative HPLC on a chiral stationary phase) allowed examination of the chiroptical properties of the resulting enantiomers (λ_{max}(abs) = 593 nm, λ_{max}(em) = 622 nm, ε = 30 000 M^{-1} cm^{-1}, ϕ_F = 0.49, $|g_{lum}|$ = 3.7 × 10^{-3} (hexane)). This is the first example of circularly polarised emission from a non-C_2-symmetric helically chiral *N,N,O,C*-BODIPY and as such provides a valuable benchmark for future developments in this compound series.

1. Introduction

Circularly polarised luminescence (CPL) is the spontaneous differential emission of left or right circularly polarized light from an excited electronic state in the presence of a chiral field.[1] Although many highly efficient condensed phase CPL systems have been disclosed,[2] the discovery of "bright" solution-phase CPL emitters presents an ongoing challenge. To this end, chiral lanthanide complexes have been extensively studied[3] because of their high luminescence dissymmetry factors ($|g_{lum}|$ ≤ 1.38)[4,5] arising from magnetic-dipole-allowed electric-dipole-forbidden $f \rightarrow f$ transitions,[6] culminating in the development of a number of lanthanide-based CPL probes for molecular sensing.[7] However low fluorescence quantum yields (ϕ_F) for these systems can result in low overall CPL quantum efficiencies ($\phi_F \cdot |g_{lum}|$). Thus there is considerable interest in the development of homochiral small organic fluorophores capable of CPL emission (CPL-SOMs), which might provide a viable alternative to chiral lanthanide complexes.[8] To date several classes of CPL-SOMs have been investigated including those based on helicenes,[9] cyclophanes,[10] and *ortho*-oligo(phenylene)ethynylenes[11] as well as some interesting recent examples of thermally activated delayed CPL.[12] We and others have focused on the study of chiral boron-chelated dipyrromethenes (BODIPYs) due to their excellent photophysical properties (such as, high extinction coefficients (ε), fluorescence quantum yields and tuneable emission properties) and synthetic accessibility.[13] This has resulted in the disclosure of several CPL-SOM systems described as either axially[14] or helically[15] chiral BODIPYs in which the fluorophore core has been asymmetrically perturbed through the introduction of either covalent or steric restraints. However, despite these advances in homochiral BODIPY design, their CPL quantum efficiencies are still limited by low luminescence dissymmetry factors (highest reported $|g_{lum}|$ equal to 4.7 × 10^{-3} or 9 × 10^{-3} for monomeric or dimeric homochiral BODIPYs, respectively[15b,e]). Future improvement of these $|g_{lum}|$ values will require an improved understanding of the link between $|g_{lum}|$ and molecular structure in the helically chiral BODIPY series.

The luminescence dissymmetry factor ($|g_{lum}|$) is given by $4(|\mu| \cdot |m| \cdot \cos\tau)/(|\mu|^2 + |m|^2)$ where **m** and **μ** are the magnetic and electric transition dipole moment vectors, respectively, and τ is the angle between them.[6b] The relatively low $|g_{lum}|$ values arise because $|m|$ is typically three orders of magnitude smaller than $|\mu|$ for the π–π* transition of a simple homochiral organic fluorophore, such as a chiral BODIPY. Consequently, molecular design must focus upon either increasing the mag-

[a] R. Clarke, K. L. Ho, A. A. Alsimaree, O. J. Woodford, Dr. P. G. Waddell, Dr. J. G. Knight, Dr. T. J. Penfold, Dr. M. J. Hall
School of Chemistry, Bedson Building
Newcastle University
Newcastle upon Tyne, NE1 7RU (UK)
E-mail: michael.hall@newcastle.ac.uk

[b] J. Bogaerts, Prof. Dr. W. Herrebout
Department of Chemistry
University of Antwerp
Groenenborgerlaan 171, 2020 Antwerp (Belgium)

[c] Dr. R. Pal
Department of Chemistry
Durham University
South Road, Durham, DH1 3LE (UK)

Supporting Information (including two movie files) and the ORCID identification number(s) for the author(s) of this article can be found under: https://doi.org/10.1002/cptc.201700106.

netic transition dipole moment (**m**) or decreasing the electric transition dipole moment (**μ**), assuming a fixed τ value.

The transition matrix elements for the former (**m**) only operates upon the angular part of the wavefunction, and consequently can be seen as analogous to spin–orbit coupling.[16] The low angular momentum components of the light elements used herein therefore represent a limitation when compared to the $f \rightarrow f$ transitions exploited in chiral lanthanide complexes. In contrast, the electric transition dipole moment operates on the spatial part of the molecular wavefunction, and can be minimised by creating a small overlap between the initial and final state wavefunctions, that is, a charge-transfer complex.[17]

Herein, we report a new structural class of helically chiral "confused" *N,N,O,C*-boron-chelated dipyrromethenes (BODIPYs). By breaking the C_2 symmetry axis, ubiquitous amongst the reported helically chiral BODIPYs,[15] we envisaged an increase in the charge-transfer character of the emitting excited state, reducing the magnitude of electric transition dipole moment (**μ**). Chiroptical measurements in combination with computational and electrochemical analysis has allowed us to rationalize the impact of this structural change on the observed $|g_{lum}|$ value, providing an insight into the link between the molecular structure and the chiroptical properties in helical BODIPY CPL-SOMs.

2. Results and Discussion

While investigating improved methods for the synthesis of *N,N,O,O*-boron-chelated dipyrromethenes,[18] we examined the Suzuki coupling of **1a** (see Scheme 1 for the structure of **1a**) with 2-hydroxyphenolboronic acid.[19] Surprisingly, alongside the expected BODIPY (*rac*)-**2**, we observed the formation, in 8% yield, of an unsymmetrical helically chiral BODIPY **3** containing a previously unreported tetradentate "confused" *N,N,O,C*-boron-chelation motif, in which the binding of one of the 3,5-*ortho*-phenolic substituents is inverted in comparison to that of the parent compound **2**.[20–22] Switching the starting material to the potential more reactive 3,5-dibromo-BODIPY **1b** resulted an improved 36% yield of (*rac*)-**3**. We propose that (*rac*)-**3** is formed through a complex series of reaction steps involving: Metathesis of the BF$_2$ group with the boron of (2-hydroxyphenyl)boronic acid, nucleophilic aromatic substitution (S$_N$Ar) of aryl bromide by the phenolic hydroxy group, Suzuki coupling with a second equivalent of (2-hydroxyphenyl)boronic acid and finally chelation of the boron by the free phenolic hydroxy group (Scheme 1).

Crystallization of (*rac*)-**3** provided material suitable for single-crystal X-ray analysis, revealing an orthorhombic space group (*Aea*2) in which two pairs of enantiomers occupy the unit cell. Analysis of the crystal structure confirmed that the 3,5-*ortho*-phenolic substituents did indeed induce a twist into the fluorophore; a twist angle of approximately 7.7° being observed between the two planes as defined by the two pyrrolic rings (Figure 1).[23]

Preliminary computational modelling of (*rac*)-**3** also showed an increase in excited-state charge-transfer character and ab-
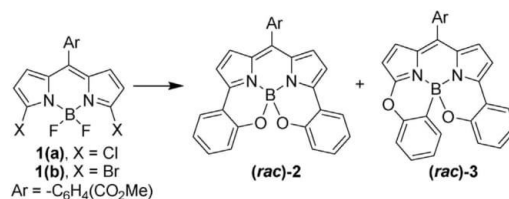
Scheme 1. Synthesis of (*rac*)-**2** and (*rac*)-**3**. Conditions: **1a**: X=Cl, (2-hydroxyphenyl)boronic acid, Na$_2$CO$_3$, [Pd(PPh$_3$)$_4$] (5 mol%), toluene, 1,4-dioxane, 90 °C, 24 h, yields **2**=63%, **3**=8%; **1b**: X=Br, (2-hydroxyphenyl)boronic acid Na$_2$CO$_3$, [Pd(PPh$_3$)$_4$] (5 mol%), toluene, 1,4-dioxane, 90 °C, 80 min, yields **2**=43%, **3**=36%.
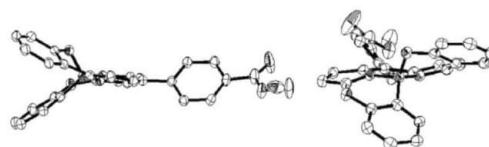

Figure 1. Two views of a molecule in the crystal structure of (*rac*)-**3** illustrating the asymmetry in the fluorophore core (H atoms are omitted for clarity; *M*-isomer shown).

sorption and emission spectra were consistent with those of a highly fluorescent red-shifted BODIPY dye (λ_{max}(abs)=593 nm, λ_{max}(em)=622 nm, $\varepsilon=30\,000$ M^{-1}cm^{-1} and $\phi_F=0.49$ in hexane). This serendipitous discovery of a stable, highly fluorescent, non-C_2-symmetric, helically chiral BODIPY provided the opportunity to examine the impact of this structural change on the chiroptical properties of the molecule.

Resolution by semi-preparative HPLC on a chiral stationary phase gave the dextro- and levorotatory enantiomers (+)-**3** and (−)-**3** respectively by retention time. Mirror-image electronic circular dichroism spectra (ECD) were recorded for the two enantiomers, showing good alignment to the UV/Vis absorption spectra of (*rac*)-**3** (Figure 2a). Boltzmann-weighted ECD spectra for the postulated enantiomer were then obtained from TD-DFT calculations at the cam-B3LYP/6-311++ G(3df,2pd) level for the *M* enantiomer of **3** (Figure 2b), allowing the assignment of (+)-**3** as *M* and thus (−)-**3** as *P* (see the Supporting Information). CPL measurements for (*M*)-(+)-**3** and (*P*)-(−)-**3** also gave mirror-image spectra with a $|g_{lum}|=3.7\times10^{-3}$, which when combined with the fluorescence quantum yield ($\phi_F=0.49$) gave an overall CPL quantum efficiency ($|g_{lum}|\cdot\phi_F$) of 1.8×10^{-3} in hexane (Figure 2).

Cyclic voltammetry of (*rac*)-**3** was carried out to provide supporting evidence for the involvement of charge transfer in the excited state. Oxidative scans revealed an irreversible one-electron wave with a peak potential of 0.84 V vs. Ag/Ag$^+$, which can be assigned as a preferential removal of an electron from the dipyrrin unit, with a second irreversible oxidation at 1.01 V vs. Ag/Ag$^+$ suggesting the removal of an electron from the boron-chelated phenoxy rings. This suggests that the observed optical absorption transition is primarily a HOMO–LUMO transition localised on the BODIPY core with a charge-transfer state
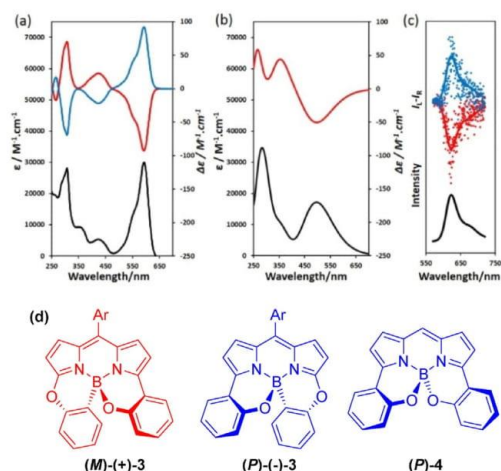
CHEMPHOTOCHEM
Articles

Figure 2. a) Experimental ECD spectra [red = (+)-**3**, blue = (−)-**3**] and UV/Vis absorption spectra [black = (*rac*)-**3**]. b) Calculated Boltzmann-weighted spectra, ECD [red = postulated (*M*)-**3** (wavelength uncorrected)] and UV/Vis absorption spectra [black = postulated (*M*)-**3** (wavelength uncorrected)]. c) Normalised CPL [$I_L - I_R$] [red = (+)-**3**, blue = (−)-**3**] and fluorescence spectra, [black = (*rac*)-**3**]. d) Structures of (*M*)-(+)-**3**, (*P*)-(−)-**3** and (*P*)-**4**.

located slightly above the lowest-energy π–π* excited-singlet state (see the Supporting Information).

Unfortunately this increase in charge-transfer character had not increased the observed $|g_{lum}|$ of **3** as desired, in comparison to the maximum values previously observed for a monomeric *N,N,O,O*-boron-chelated dipyrromethene (such as **4**, $|g_{lum}| = 4.7 \times 10^{-3}$; Figure 2).[15b] To better understand this result, the excited states of both (*P*)-**3** and *N,N,O,O*-boron-chelated dipyrromethene (*P*)-**4** were calculated using DFT(PBE0) with a def2-TZVP basis set (Table 1) as implemented within the

Table 1. Calculated electric (**μ**) and magnetic (**m**) transition dipole moments, the angle between them (τ) and $|g_{lum}|_{calc}$ in comparison with $|g_{lum}|_{exp}$ for (*P*)-**3** and (*P*)-**4**.

Compound	μ [au]	m [au]	τ [°]	$|g_{lum}|_{calc}$	$|g_{lum}|_{exp}$[a]
3	6.0×10^{-1}	7.3×10^{-4}	70	2×10^{-3}	3.7×10^{-3}
4	7.6×10^{-1}	1.4×10^{-3}	65	3×10^{-3}	4.7×10^{-3}

[a] $|g_{lum}|_{exp}$ given at the respective $\lambda max_{(em)}$ value, measured in hexane.

ORCA quantum chemistry package.[24] Comparison of these two related molecular systems confirmed the presence of charge-transfer character in the excited state of **3** along with the consequential decrease in electric transition dipole moment (**μ**).

However any resultant increase in $|g_{lum}|$ had been offset by both a reduction in the magnetic transition dipole moment (**m**) and an unanticipated detrimental change in angle (τ) between the two transition dipole moments (from 65° in **4** to 70° in **3**). The decrease in the former (**m**), is larger than that ob-

served for the electric transition dipole moment (**μ**), due to a reduction in both wavefunction overlap in the case of (*P*)-**3** compared to (*P*)-**4** and in the change in the orbital angular momentum between the ground and excited state. The decrease in **m** of ≈ 50 % and change in τ value combine to give an overall decrease in both the calculated and experimental $|g_{lum}|$ of circa 20 %. Interestingly, examination of the calculated electric (**μ**) and magnetic (**m**) transition dipole moments of **3** and **4** shows that **m** aligns with the helical axis whilst **μ** aligns with the π system in both molecules, in line with the previously observed orientation of both **μ** and **m** in the carbo[*n*]helicenes series (for an animated graphical representation of the direction of both **μ** and **m** with respect to the structures of **3** and **4**, see the Supporting Information).[25] Based on these results we propose that the $|g_{lum}|$ value in a CPL-emissive helically chiral BODIPY maybe indeed be tuneable through the use of synthetic design to dictate both the magnitude and relative direction of **μ** and **m** through simultaneous control of both the helical pitch and the extent of π conjugation in the molecule. Thus, the focus of our current research is to apply these new design principles to the synthesis of helically chiral dipyrromethenes with improved chiroptical properties.

3. Conclusions

We have synthesised the first example of a resolved helically chiral "confused" *N,N,O,C*-boron-chelated dipyrromethene and investigated its properties in the context of an efficient small organic molecular emitter of red-shifted circularly polarised light. Despite exhibiting a reduction in their electric transition dipole moment these systems exhibit an overall reduction in $|g_{lum}|$ value, arising as a consequence of the delicate and complex interplay between **μ**, **m** and τ parameters. In this case the use of charge-transfer states has been shown to be of limited value as the desired decrease in **μ** is intrinsically coupled to an undesirable decrease in **m**. Through our comparative investigation of the calculated and experimentally measured chiroptical properties of *N,N,O,C*-boron-chelated dipyrromethene **3**, we have demonstrated the need to control **μ**, **m** and τ in future attempts to maximise CPL efficiency in CPL-SOMs.

Conflict of interest

The authors declare no conflict of interest.

[1] a) J. P. Riehl, F. S. Richardson, *Chem. Rev.* **1986**, *86*, 1–16; b) J. P. Riehl, G. Muller, in *Comprehensive Chiroptical Spectroscopy, Vol. 1* (Eds.: N. Berova, P. L. Polavarapu, K. Nakanishi, R. W. Woody) Wiley, Hoboken, **2012**.

[2] For selected condensed-phase CPL emission, see: a) E. Peeters, M. P. T. Christiaans, H. P. Janssen, H. F. Schoo, H. P. J. M. Dekkers, E. W. Meijer, *J. Am. Chem. Soc.* **1997**, *119*, 9909–9910; b) H. Tsumatori, T. Nakashima, T. Kawai, *Org. Lett.* **2010**, *12*, 2362–2365; c) W. Zhang, K. Yoshida, M. Fujiki, X. Zhu, *Macromolecules* **2011**, *44*, 5105–5111; d) M. Fujiki, A. J. Jalilah, N. Suzuki, M. Taguchi, W. Zhang, M. M. Abdellatifd, K. Nomurad, *RSC Adv.* **2012**, *2*, 6663–6671; e) J. Liu, H. Su, L. Meng, Y. Zhao, C. Deng, J. C. Y. Ng, P. Lu, M. Faisal, J. W. Y. Lam, X. Huang, H. Wu, K. S. Wong, B. Z. Tang, *Chem. Sci.* **2012**, *3*, 2737–2747; f) B. A. San Jose, S. Matsushita, K. Akagi, *J. Am. Chem. Soc.* **2012**, *134*, 19795–19807; g) D. Lee, Y.-J. Jin, H. Kim, N. Suzuki, M. Fujiki, T. Sakaguchi, S. K. Kim, W.-E. Lee, G. Kwak, *Macromolecules* **2012**, *45*, 5379–5386; h) J. Kumar, T. Nakashima, H. Tsumatori, T. Kawai, *J. Phys. Chem. Lett.* **2014**, *5*, 316–321; i) B. A. San Jose, J. Yan, K. Akagi, *Angew. Chem. Int. Ed.* **2014**, *53*, 10641–10644; *Angew. Chem.* **2014**, *126*, 10817–10820; j) Z. Shen, T. Wang, L. Shi, Z. Tang, M. Liu, *Chem. Sci.* **2015**, *6*, 4267–4272; k) J. Kumar, H. Tsumatori, J. Yuasa, T. Kawai, T. Nakashima, *Angew. Chem. Int. Ed.* **2015**, *54*, 5943–5947; *Angew. Chem.* **2015**, *127*, 6041–6045; l) J. R. Brandt, X. Wang, Y. Yang, A. J. Campbell, M. J. Fuchter, *J. Am. Chem. Soc.* **2016**, *138*, 9743–9746; m) J. Kumar, B. Marydasan, T. Nakashima, T. Kawai, J. Yuasa, *Chem. Commun.* **2016**, *52*, 9885–9888.

[3] a) D. Parker, R. S. Dickins, H. Puschmann, C. Crossland, J. A. K. Howard, *Chem. Rev.* **2002**, *102*, 1977–2010; b) R. Carr, N. H. Evans, D. Parker, *Chem. Soc. Rev.* **2012**, *41*, 7673–7686; c) F. Zinna, L. Di Bari, *Chirality* **2015**, *27*, 1–13.

[4] Luminescence dissymmetry factor $g_{lum}(\lambda) = 2(I_L - I_R)/(I_L + I_R)$, in which I_L and I_R are the intensity of left and right circularly polarized emissions, respectively.

[5] a) J. L. Lunkley, D. Shirotani, K. Yamanari, S. Kaizaki, G. Muller, *J. Am. Chem. Soc.* **2008**, *130*, 13814–13815; b) J. L. Lunkley, D. Shirotani, K. Yamanari, S. Kaizaki, G. Muller, *Inorg. Chem.* **2011**, *50*, 12724–12732; c) S. Di Pietro, L. Di Bari, *Inorg. Chem.* **2012**, *51*, 12007–12014.

[6] a) J. A. Schellman, *Chem. Rev.* **1975**, *75*, 323–331; b) F. S. Richardson, *Inorg. Chem.* **1980**, *19*, 2806–2812; c) J. I. Bruce, D. Parker, S. Lopinski, R. D. Peacock, *Chirality* **2002**, *14*, 562–567; d) M. Wakabayashi, S. Yokojima, T. Fukaminato, K. Shiino, M. Irie, S. Nakamura, *J. Phys. Chem. A* **2014**, *118*, 5046–5057.

[7] a) C. P. Montgomery, E. J. New, D. Parker, R. D. Peacock, *Chem. Commun.* **2008**, 4261–4263; b) C. P. Montgomery, B. S. Murray, E. J. New, R. Pal, D. Parker, *Acc. Chem. Res.* **2009**, *42*, 925–937; c) G. Muller, *Dalton Trans.* **2009**, 9692–9707; d) D. M. Dias, J. M. C. Teixeira, I. Kuprov, R. J. New, D. Parker, C. F. G. C. Geraldes, *Org. Biomol. Chem.* **2011**, *9*, 5047–5050; e) S. J. Butler, L. Lamarque, R. Pal, D. Parker, *Chem. Sci.* **2014**, *5*, 1750–1756; f) G. Pescitelli, L. Di Bari, N. Berova, *Chem. Soc. Rev.* **2014**, *43*, 5211–5233.

[8] a) E. M. Sánchez-Carnerero, A. R. Agarrabeitia, F. Moreno, B. L. Maroto, G. Muller, M. J. Ortiz, S. de la Moya, *Chem. Eur. J.* **2015**, *21*, 13488–13500; b) J. Kumar, T. Nakashima, T. Kawai, *J. Phys. Chem. Lett.* **2015**, *6*, 3445–3452.

[9] For selected CPL-SOMs based on helicenes, see: a) S. Abbate, G. Longhi, F. Lebon, E. Castiglioni, S. Superchi, L. Pisani, F. Fontana, F. Torricelli, T. Caronna, C. Villani, R. Sabia, M. Tommasini, A. Lucotti, D. Mendola, A. Mele, D. A. Lightner, *J. Phys. Chem. C* **2014**, *118*, 1682–1695; b) H. Sakai, S. Shinto, J. Kumar, Y. Araki, T. Sakanoue, T. Takenobu, T. Wada, T. Kawai, T. Hasobe, *J. Phys. Chem. C* **2015**, *119*, 13937–13947; c) P. E. Reyes-Gutiérrez, M. Jirásek, L. Severa, P. Novotná, D. Koval, P. Sázelová, J. Vávra, A. Meyer, I. Císařová, D. Šaman, R. Pohl, P. Štěpánek, P. Slavíček, B. J. Coe, M. Hájek, V. Kašička, M. Urbanová, F. Teplý, *Chem. Commun.* **2015**, *51*, 1583–1586; d) Y. Yamamoto, H. Sakai, J. Yuasa, Y. Araki, T. Wada, T. Sakanoue, T. Takenobu, T. Kawai, T. Hasobe, *J. Phys. Chem. C* **2016**, *120*, 7421–7427; e) H. Sakai, T. Kubota, J. Yuasa, Y. Araki, T. Sakanoue, T. Takenobu, T. Wada, T. Kawai, T. Hasobe, *J. Phys. Chem. C* **2016**, *120*, 7860–7869; f) I. Hernández Delgado, S. Pascal, A. Wallabregue, R. Duwald, C.

[10] Besnard, L. Guénée, C. Nançoz, E. Vauthey, R. C. Tovar, J. L. Lunkley, G. Muller, J. Lacour, *Chem. Sci.* **2016**, *7*, 4685–4693; g) S. Pascal, C. Besnard, F. Zinna, L. Di Bari, B. Le Guennic, D. Jacquemin, J. Lacour, *Org. Biomol. Chem.* **2016**, *14*, 4590–4594.

[10] For selected CPL-SOMs based on cyclophanes, see: a) Y. Morisaki, M. Gon, T. Sasamori, N. Tokitoh, Y. Chujo, *J. Am. Chem. Soc.* **2014**, *136*, 3350–3353; b) M. Gon, Y. Morisaki, Y. Chujo, *J. Mater. Chem. C* **2015**, *3*, 521–529; c) M. Gon, Y. Morisaki, R. Sawada, Y. Chujo, *Chem. Eur. J.* **2016**, *22*, 2291–2298; d) Y. Morisaki, R. Sawada, M. Gon, Y. Chujo, *Chem. Asian J.* **2016**, *11*, 2524–2527.

[11] S. P. Morcillo, D. Miguel, L. Á. de Cienfuegos, J. Justicia, S. Abbate, E. Castiglioni, C. Bour, M. Ribagorda, D. J. Cárdenas, J. M. Paredes, L. Crovetto, D. Choquesillo-Lazarte, A. J. Mota, M. C. Carreño, G. Longhi, J. M. Cuerva, *Chem. Sci.* **2016**, *7*, 5663–5670.

[12] a) T. Imagawa, S. Hirata, K. Totani, T. Watanabe, M. Vacha, *Chem. Commun.* **2015**, *51*, 13268–13271; b) S. Feuillastre, M. Pauton, L. Gao, A. Desmarchelier, A. J. Riives, D. Prim, D. Tondelier, B. Geffroy, G. Muller, G. Clavier, G. Pieters, *J. Am. Chem. Soc.* **2016**, *138*, 3990–3993.

[13] a) G. Ulrich, R. Ziessel, A. Harriman, *Angew. Chem. Int. Ed.* **2008**, *47*, 1184–1201; *Angew. Chem.* **2008**, *120*, 1202–1219; b) A. Loudet, K. Burgess, *Chem. Rev.* **2007**, *107*, 4891–4932; c) H. Lu, J. Mack, Y. Yanga, Z. Shen, *Chem. Soc. Rev.* **2014**, *43*, 4778–4823; d) H. Lu, J. Mack, T. Nyokong, N. Kobayashi, Z. Shen, *Coord. Chem. Rev.* **2016**, *318*, 1–15.

[14] a) E. M. Sánchez-Carnerero, F. Moreno, B. L. Maroto, A. R. Agarrabeitia, J. Bañuelos, T. Arbeloa, I. López-Arbeloa, M. J. Ortiz, S. de la Moya, *Chem. Commun.* **2013**, *49*, 11641–11643; b) E. M. Sánchez-Carnerero, L. Gartzia-Rivero, F. Moreno, B. L. Maroto, A. R. Agarrabeitia, M. J. Ortiz, J. Bañuelos, Í. López-Arbeloab, S. de la Moya, *Chem. Commun.* **2014**, *50*, 12765–12767; c) R. I. Lerrick, T. P. L. Winstanley, K. Haggerty, C. Wills, W. Clegg, R. W. Harrington, P. Bultinck, W. Herrebout, A. C. Benniston, M. J. Hall, *Chem. Commun.* **2014**, *50*, 4714–4716; d) T. Bruhn, G. Pescitelli, S. Jurinovich, A. Schaumlöffel, F. Witterauf, J. Ahrens, M. Bröring, G. Bringmann, *Angew. Chem. Int. Ed.* **2014**, *53*, 14592–14595; *Angew. Chem.* **2014**, *126*, 14821–14824; e) E. M. Sánchez-Carnerero, F. Moreno, B. L. Maroto, A. R. Agarrabeitia, M. J. Ortiz, B. G. Vo, G. Muller, S. de la Moya, *J. Am. Chem. Soc.* **2014**, *136*, 3346–3349; f) S. Kolemen, Y. Cakmak, Z. Kostereli, E. U. Akkaya, *Org. Lett.* **2014**, *16*, 660–663; g) T. Bruhn, G. Pescitelli, F. Witterauf, J. Ahrens, M. Funk, B. Wolfram, H. Schneider, U. Radius, M. Bröring, *Eur. J. Org. Chem.* **2016**, 4236–4243; h) J. F. Kögel, S. Kusaka, R. Sakamoto, T. Iwashima, M. Tsuchiya, R. Toyoda, R. Matsuoka, T. Tsukamoto, J. Yuasa, Y. Kitagawa, T. Kawai, H. Nishihara, *Angew. Chem. Int. Ed.* **2016**, *55*, 1377–1381; *Angew. Chem.* **2016**, *128*, 1399–1403; i) F. Zinna, T. Bruhn, C. A. Guido, J. Ahrens, M. Bröring, L. Di Bari, G. Pescitelli, *Chem. Eur. J.* **2016**, *22*, 16089–16098; j) J. Jiménez, L. Cerdán, F. Moreno, B. L. Maroto, I. García-Moreno, J. L. Lunkley, G. Muller, S. de la Moya, *J. Phys. Chem. C* **2017**, *121*, 5287–5292.

[15] a) A. Gossauer, F. Nydegger, T. Kiss, R. Sleziak, H. Stoeckli-Evans, *J. Am. Chem. Soc.* **2004**, *126*, 1772–1780; b) R. B. Alnoman, S. Rihn, D. C. O'Connor, F. A. Black, B. Costello, P. G. Waddell, W. Clegg, R. D. Peacock, W. Herrebout, J. G. Knight, M. J. Hall, *Chem. Eur. J.* **2016**, *22*, 93–96; c) Y. Gobo, M. Yamamura, T. Nakamura, T. Nabeshima, *Org. Lett.* **2016**, *18*, 2719–2721; d) C. Ray, E. M. Sánchez-Carnerero, F. Moreno, B. L. Maroto, A. R. Agarrabeitia, M. J. Ortiz, I. López-Arbeloa, J. Bañuelos, K. D. Cohovi, J. L. Lunkley, G. Muller, S. de la Moya, *Chem. Eur. J.* **2016**, *22*, 8805–8808; e) M. Saikawa, T. Nakamura, J. Uchida, M. Yamamura, T. Nabeshima, *Chem. Commun.* **2016**, *52*, 10727–10730; f) M. Toyoda, Y. Imai, T. Mori, *J. Phys. Chem. Lett.* **2017**, *8*, 42–48.

[16] M. A. El-Sayed, *Acc. Chem. Res.* **1968**, *1*, 8–16.

[17] T. J. Penfold, *J. Phys. Chem. C* **2015**, *119*, 13535–13544.

[18] H. Kim, A. Burghart, M. B. Welch, J. Reibenspies, K. Burgess, *Chem. Commun.* **1999**, 1889–1890.

[19] **1a** was prepared based on a modified procedure: X. Zhou, C. Yu, Z. Feng, Y. Yu, J. Wang, E. Hao, Y. Wei, X. Mu, L. Jiao, *Org. Lett.* **2015**, *17*, 4632–4635.

[20] For related non-chiral *N,N,O,C*-BODIPYs, see: a) T. W. Hudnall, T.-P. Lin, F. P. Gabbai, *J. Fluorine Chem.* **2010**, *131*, 1182–1186; b) Z. Li, T.-P. Lin, S. Liu, C.-W. Huang, T. W. Hudnall, F. P. Gabbai, P. S. Conti, *Chem. Commun.* **2011**, *47*, 9324–9326; c) A. L. Nguyen, F. R. Fronczek, K. M. Smith, M. G. H. Vicente, *Tetrahedron Lett.* **2015**, *56*, 6348–6351.

[21] For related chiral *N,N,O,C*-BODIPYs, see: a) C. Ikeda, T. Maruyama, T. Nabeshima, *Tetrahedron Lett.* **2009**, *50*, 3349–3351; b) M. Yamamura, S.

222

Yazaki, M. Seki, Y. Matsui, H. Ikeda, T. Nabeshima, *Org. Biomol. Chem.* **2015**, *13*, 2574–2581.

[22] For related chiral *N,N,O,F*-BODIPYs, see: D. Sirbu, A. C. Benniston, A. Harriman, *Org. Lett.* **2017**, *19*, 1626–1629.

[23] CCDC 1488164 and 1488165 contains the supplementary crystallographic data for this paper. These data can be obtained free of charge from The Cambridge Crystallographic Data Centre.

[24] F. Neese, *WIREs Comput. Mol. Sci.* **2012**, *2*, 73–78.

[25] Y. Nakai, T. Mori, Y. Inoue, *J. Phys. Chem. A* **2012**, *116*, 7372–7385.

223